8-2017

Regulation of haplid phenotypes in Ustilago maydis by ammonium transporters and components of the b mating locus.

Rena Margaret Wallen
University of Louisville

REGULATION OF HAPLOID PHENOTYPES IN *USTILAGO MAYDIS* BY AMMONIUM TRANSPORTERS AND COMPONENTS OF THE *b* MATING LOCUS

By

Rena Margaret Wallen
M.Sc., Biology, University of Louisville, 2012

Dissertation
Submitted to the Faculty of the
College of Arts and Sciences of the University of Louisville in
Partial Fulfillment of the Requirements for the Degree of

Doctor of Philosophy in Biology

Department of Biology,
Division of Molecular, Cellular and Developmental Biology,
College of Arts and Sciences
University of Louisville
Louisville, Kentucky

August 2017

REGULATION OF HAPLOID PHENOTYPES IN *USTILAGO MAYDIS* BY AMMONIUM TRANSPORTERS AND COMPONENTS OF THE *b* MATING LOCUS

By

Rena Margaret Wallen
M.Sc., Biology, University of Louisville, 2012

A Dissertation Approved on

August 4, 2017

By the following Dissertation Committee:

_____
Dr. Michael H. Perlin, Principal Advisor

_____
Dr. James Graham

_____
Dr. Carolyn Klinge

_____
Dr. David Schultz

_____
Dr. Deborah Yoder-Himes

ACKNOWLEDGMENTS

First and foremost, I would like to that Dr. Michael H. Perlin for his endless supply of encouragement and faith in my endeavors as a scientist, as a mother, and as a human. His mentorship, both in science and in life, has been invaluable, delivered with the utmost kindness, always focused on the most high quality science, not necessarily the most flashy results. His lab has been my home away from home for the better part of 8 years and he has markedly influenced by development both as a scientist and as a human being.

Second, I would like to thank the other four members of my dissertation committee, Dr. David Schultz, Dr. Deborah-Yoder Himes, Dr. James Graham, and Dr. Carolyn Klinge. Their individual expertise and vast experience have provided perspectives I had not considered and advice I could not replace. All of them have been willing to help with various aspects of my research and have continuously made their skill set and knowledge available to me when I found myself in rough spots. Although not a member of my committee, I am deeply indebted to Dr. Michelle Barati for the countless hours she spent assisting me with microscopy and images of my biofluorescently labeled mutants.

My project would never have been completed without the support of my Goat Lab mates and my team of faithful science sidekicks, the Land Sharks. Thank you to Jinny Paul for beginning the work that led to the formation of my project. I am indebted to Su San Toh for her patience in teaching me the finer

points of RNA extraction. Michael Cooper taught me many of the basic techniques involved in working with *U. maydis.* Current members of the Goat Lab have helped me celebrate my successes and troubleshoot my failures. Swathi Kuppireddy always provided an endless supply of competent cells. Sunita Khanal kindly supplied basic items that I was often too scatterbrained to remember to prepare myself. Lalu Krishna has contributed to countless plant infections. William Beckerson, Ming-Chang Tsai (Nelson) and Joseph Angermeier have provided insight and encouragement even when things were rough.

My group of merry scientists, the Land Sharks, has included countless undergraduate and graduate students, without whom my productivity would have been much less and my science would not have been nearly as much fun. Madison Furnish, the longest standing member, spent all four years of her undergraduate career with me, and often surpassed my teaching in her ability to complete protocols. Current graduate students that I am fortunate enough to call Land Sharks, Kirsten Richardson and Hector Mendoza, have been able to carry the science torch for my project while I labor away at the more mundane task of writing and submitting papers. Founding members of the Land Sharks, Brad Clark, Allison Dentinger, Victoria Mosely, and Madeline Shelton, taught me about leadership while I was teaching them about science. Other past members, including Joshua French, Nick Roller, and Hannah Mizano, Eliana Zamora, have left the Goat Lab to pursue their own graduate degrees, hopefully taking some of our teachings with them and furthering their own goals. Each one of the Land

Sharks contributed to the successful completion of my project and making the lab a fun and productive place of science.

Science, sadly, is not free and we have been fortunate to receive funding from a variety of sources, including the National Science Foundation and the University of Louisville. Without the access to resources these monies provided, it would have been difficult to complete the experiments we did.

I would also like to thank my parents, Ed and Rena Wallen, and brother, Matthew Wallen, who believed in me even when I struggled to believe in myself, and provided love and encouragement when I doubted my own abilities to persevere. I'm sure after more than 5 years they were hoping they I would have found the cure for cancer or at least solved world hunger. I failed in that endeavor but hopefully they are at least proud that I made fungus glow.

Finally, I would like to thank my partner Brad and my son Braxton. Brad has made sacrifices to care for our son while I have found myself lost in dissertation writing and before we had Braxton, dealt with the demanding schedule of a graduate student consumed by research and writing. Braxton has been as understanding as a 2-year-old can be of the time that I spend locked in the basement analyzing data and writing. Hopefully one day I will be able to share my experiences with him so that he understands hard work and perseverance.

ABSTRACT

REGULATION OF HAPLOID PHENOTYPES IN *USTILAGO MAYDIS* BY AMMONIUM TRANSPORTERS AND COMPONENTS OF THE *b* MATING LOCUS

Rena Margaret Wallen

August 4, 2017

Fungi that can switch from budding to a filamentous infectious state have evolved mating type loci. *Ustilago maydis*, the maize pathogen, must mate with compatible partners possessing different alleles at two mating type loci for successful host infection. The *a* locus encodes pheromones and receptors, while the *b* locus encodes subunits of a heterodimeric transcription factor that regulates expression of virulence genes. Mating is triggered by environmental signals, including nutrient deprivation. My goal was to determine the fate of nitrogen starved haploid cells without a compatible mating partner.

On solid low ammonium media, wild-type *U. maydis* filaments. I examined the roles of the *b* mating locus, and Ump2, the high affinity ammonium transporter, in this phenotype. Expression of *ump2* increases under low ammonium, while deletion of *b* or *ump2* results in loss of filamentation. Deleting *b* did not affect the induction of *ump2,* but deletion of *ump2* altered expression from the *b* locus. In my model of filamentation on low ammonium, *ump2* senses

nitrogen availability and, in a *b*-dependent manner, upregulates targets canonically involved in mating but, without a partner, functions in filamentation.

The *b* locus contains two genes, *bE* and *bW,* but the heterodimer does not form in haploid cells. I found evidence that *bE* and *bW* function independently in haploids to regulate gene expression. Partial deletion of *b* also results in loss of filamentation in media depleted of ammonium. Although *ump2* overexpression in a *b* deletion background rescues the loss of filamentous phenotype, this phenomenon is absent when *bE* remains. This suggests *bW* regulates transcription of mating and pathogenicity targets in a similar manner to *ump2*, while *bE* does so in the opposite direction.

Finally, through biofluorescent labelling I visualized the rearrangement of the actin cytoskeleton in response to low ammonium. I also investigated via qRT-PCR several targets, including actin and its regulators, and cell wall remodeling enzymes. Although these targets showed dynamic expression levels in the mutants, no pattern emerged explaining the varied filamentous phenotypes. As such, changes of the actin cytoskeleton upon exposure to low ammonium are not regulated at the transcription level.

TABLE OF CONTENTS

LIST OF TABLES

LIST OF FIGURES

CHAPTER I

AN OVERVIEW OF THE EVOLUTION, THE FUNCTION, AND THE MAINTENANCE OF SEXUAL REPRODUCTION IN DIMORPHIC FUNGI

Fungi, due to their ease of manipulation in a laboratory setting and short generation time, provide excellent model organisms for studying the development of eukaryotic-specific processes, such as sexual reproduction. Unlike most higher eukaryotes, members of this group also reproduce asexually. The maintenance of both strategies of reproduction within a single organism allows the study of both why a mechanism such as sexual reproduction may have evolved as well as why asexual reproduction may have been maintained. Fungi have generally been classified into phyla based on the type of sexual reproduction a particular species uses as well as the amount of time they spend in the sexual reproductive stage. A 2007 reclassification of fungal phylogeny integrated newly available molecular and genetic data to rearrange the fungal portion of the tree of life. Based on molecular data, the Kingdom fungi was divided into seven phyla and one subkingdom, *Dikarya* (Hibbett et al., 2007). The subkingdom *Dikarya* contains *Ascomycota* and *Basidiomycota* based on the presence of dikaryotic hyphae in both, putatively a characteristic of the most recent common ancestor of the two groups (Hibbett et al., 2007). These two

groups, including industrially essential organisms such as baker's yeast and brewer's yeast, as well as many agriculturally important pathogens such as rusts and smuts are potentially the most highly studied among fungi. These organisms comprise the dimorphic fungi, which can switch between a yeast phase and a hyphal phase based on environmental conditions. Because of the high volume of molecular data available for these organisms as well as the differences in lifestyle amongst the two groups, *Ascomycota* and *Basiodiomycota*, comparing the evolution of sexual reproduction within the two groups provides insight into the reason this lifestyle evolved in eukaryotes.

Genetic Components of Sexual Reproduction

Unlike higher eukaryotes (with a few exceptions), single-celled fungi that reproduce sexually do not exist as male and female phenotypes. Rather, they exist as one of multiple mating types that are generally indistinguishable except at a molecular level. In order to have multiple mating types, there are a few essential genetic ingredients. First, an organism needs a mechanism by which to identify a member of its species of different mating type. This mechanism may be as simple as a pheromone produced by one mating type that is recognized by a member of a different mating type, or it may involve more complex mechanisms. Second, an organism needs a mechanism by which to express other genes specific to its mating type, which is usually accomplished by specialized transcription factors. By looking for evidence of these components within various members of the Ascomycetes and Basidiomycetes and

considering the complexity of the mating system with respect to other aspects of life style, such as whether or not the organism is a pathogen and requires a host to complete its lifecycle, or is a free living organism, the function of sexual reproduction for fungi can be better understood.

The Ascomycetes

The phylum *Ascomycota* or sac fungus contains a variety organisms including plant, insect, and mammalian pathogens, as well as unicellular yeast, saprotrophs and mutualistic symbiotes. These fungi form meiotic spores called ascospores enclosed in a special sac called an ascus. As a group, sexual reproduction is more common in plant pathogens than in human pathogens and mating type (MAT) loci are comparatively small, encoding only transcription factors while pheromone and pheromone receptors are located elsewhere in the genome (Morrow & Fraser, 2009), but evidence of the genetic components for sexual reproduction exists in all members. Evidence of the genetic requirements for mating coupled with the lifestyle of the organism can provide insight into the reason for the use (or lack of use) of sexual reproduction.

Saccharomyces cerevisiae

Saccharomyces cerevisiae, or brewer's yeast, is potentially the most studied eukaryotic organism. As early as the 1940s, long before molecular genetic techniques were available, scientists realized that different haploid cells of this yeast were able to mate with cells of opposite mating type (Lindegren,

1945). Not until the 1980s was the molecular mechanism of this mating more fully understood. Mating type in *S. cerevisiae* is determined by a single locus, the mating type locus defined as either *MATa* or *MATα*, based on the resident sequence. However, it was discovered that haploid cells of one mating type (either a or α) could produce progeny of the opposite mating type during mitosis (Hicks, Strathern, & Klar, 1979). These findings led the development of the "cassette model" of mating type switching, in which "silent" copies of the alternate mating type resided in another location within the genome (Hicks et al., 1979). Haploid cells of mating type a, for example, were found to contain all the genetic elements to be mating type α, but the genetic material was contained in a transcriptionally non-active region within the genome (Hicks et al., 1979).

The genetic regions at either *MATa* or *MATα* were later characterized and the function of the resulting proteins analyzed. The two regions are not the same length, with *MATa* being shorter than *MATα*, and encode regulatory proteins that control α-specific or a-specific genes *(*Astell, Ahlstrom-Jonasson, & Smith, 1981). They share little homology and so, are not true alleles, but rather "idiomorphs" (Crow & Dove, 1990). In fact, all of the proteins encoded by the MAT locus are DNA binding proteins which define one of three cell types (haploid *MATα* or *MATa,* or diploid) by directing other gene expression (Dranginis, 1990). The activity of products of the *MATα* locus determines whether the cell exhibits α or a phenotype. MATα encodes two genes, α1 and α2. MATα1 controls expression of α-specific genes, while MATα2 suppresses a-specific genes that would otherwise be expressed constitutively (Astell et al., 1981; Dranginis, 1990). The

MATa locus encodes a single protein, a1, which is dispensable for mating, but acts with α2 to control gene expression after mating has occurred in the diploid state (Astell et al., 1981). In the diploid, α2 and a1 form a DNA-binding heterodimer. The α2 protein contains a homeodomain region plus an additional sequence at the C terminus while the a1 contains only the homeodomain motif, suggesting that a1 mediates both DNA binding and interaction with α2 (Phillips, Stark, Johnson, & Dahlquist, 1994). In a/α diploid cells, the heterodimer represses expression of haploid specific genes (Dranginis, 1990).

In addition to the genetic requirement to have a set of genes specific to mating type, *S. cerevisiae* also has a system by which to identify cells of the opposite mating type in the form of a pheromone/pheromone receptor system. While in this organism as is typical with other Ascomycetes, the pheromone/ pheromone receptor system is not part of the mating type locus, products of the mating type locus can affect expression of the pheromone and receptor genes. Cells that exhibit the a phenotype express a-factor (either Mfa1 or Mfa2), a polypeptide hormone, that interacts with α cells to cause cell cycle arrest and other physiological changes associated with the mating response (Michaelis & Herskowitz, 1988). In α haploid cells, α-factor, a pheromone, is produced which also interacts with a haploid cells to arrest the cell cycle prior to DNA synthesis (Bucking-Throm, Duntze, Hartwell, & Manney, 1973). This arrest in cell cycle synchronizes haploid cells in preparation for conjugation (Wilkinson & Pringle, 1974). Haploid cells also produce receptors that recognize the pheromones from haploids of opposite mating type. In α haploid cells, *ste3* encodes the receptor

for a-factor. It is required for mating only in α cells and its transcription only occurs in α cells (Hagen, McCaffery, & Sprague, 1986). Moreover, a-factor is able to induce the production of its receptor in α cells (Hagen & Sprague, 1984). In a haploid cells, *ste2* encodes the receptor for α-factor.

Exposure to the pheromone of the opposite mating type not only arrests the cell cycle but also changes expression of a variety of genes. For example, when exposed to α-factor, *MATa* haploids show decreased expression of genes related to vegetative growth and increased expression of genes related to the mating process (Stetler & Thorner, 1984). Additionally, while the pheromone/ pheromone receptor system is not physically part of the mating type loci in *S. cerevisiae*, the activity of the products of the MAT can affect their expression level. MATα1 activates transcription of α-specific structural genes and a-factor receptor genes while MATα2 represses a specific structural genes and α-factor receptor genes (Bender & Sprague, 1989).

Despite the presence of all the genetic requirements necessary for a sexual reproduction system, outcrossing in *S. cerevisiae* in wild populations is relatively rare. Genetic analysis of several wild isolates estimates that this yeast mates approximately once every 50,000 divisions (Ruderfer, Pratt, Seider, & Kruglyak, 2006). The same study estimated that any two strains have undergone approximately 16 million cell divisions since their last common ancestor with only 314 outcrossing events (Ruderfer et al., 2006). Why would an organism maintain such an intricate system of sexual reproduction that is so infrequently used?

Because *S. cerevisiae* generally are saprophytic and require no interaction with a live host, the maintenance of a mating system is not driven by the need to create variability in the population to evolve along with the host's ability to rid itself of the invading pathogen. However, the yeast nonetheless requires the ability to respond to changes in its environment and mating may provide the means by which to do so. Diploid *S. cerevisiae* cells, resulting from mating, can undergo changes in cell shape as well as patterns of cell division leading to formation of long, thin pseudohyphae that grow away from the central colony (Gimeno, Ljungdahl, Styles, & Fink, 1992). In the lab, mating and subsequent dimorphic changes in the cells can be induced by starving the cells for nitrogen. This phenomenon is only observed in diploid cells and does not happen with haploid cells (Gimeno et al., 1992). The main function of sexual reproduction in all organisms is DNA repair and production of higher quality offspring (Horandl, 2009). Nutrient starvation, such as nitrogen starvation, can induce damage to an organism's DNA. By evolving a mechanism for sexual reproduction, *S. cerevisiae* become simultaneously able to repair damage caused by starvation and to create structures that allow for "scavenging" of nutrients in the form of elongated hyphal structures.

Neurosporra crassa

A saprophytic bread mold, *Neurosporra crassa*, also provides evidence for the close relationship between nutrient availability and mating. Before the elements of the mating type locus and developmental program of this Asomycete

were fully understood, researchers recognized that in order to induce mating, this organism required low nitrogen, low light and low temperature (Perkins & Berry, 1977), all conditions unfavorable to vegetative growth. Subsequent research demonstrated that the physiological changes necessary for mating, such as production of the female mating structures, protoperithecia and trichogynes, and vegetative spores or conidia, also happened under depleted environmental conditions (Staben & Yanofsky, 1990). The fusion of the trichogynes to conidia of opposite mating type initiates sexual reproduction and maturation of sexual structures, and these processes are governed by components of the mating type locus (Staben & Yanofsky, 1990). Trichogynes adjust their growth pattern in the direction of conidia of opposite mating type, also governed by products of the mating type locus (Bistis, 1981)

Like other Ascomycetes, the mating type locus contains genetic elements that allow for recognition of a cell of the opposite mating type and for expression of mating type specific genes. They also control entry into the sexual cycle and prevent formation of mixed heterokaryons during the vegetative phase (Glass, Grotelueschen, & Metzenberg, 1990). The mating types in *N. crassa* are termed A and a. The A mating type locus contains sequences responsible for recognizing cells of opposite mating type and a region with a high degree of amino acid similarity to MATα1 of *S. cerevisiae* (Glass et al., 1990). The a region contains at least two functional segments, one of which is responsible for maturation of sexual structures and the other of which specifies mating identity and induction of mating (Staben & Yanofsky, 1990).

Like *S. cerevisiae*, *N. crassa* has pheromones and pheromone receptors that function in mating but are not part of the mating type locus. The putative pheromone precursor, Mfa-1 (mating factor a-1) shows many structural similarities to other fungal pheromone precursors and is found in greatest abundance when cells are starved for nutrients (Kim, Metzenberg, & Nelson, 2002). Unlike pheromone precursors in *S. cerevisiae*, products of this gene may function in both mating types, attracting trichogynes of mating type A but also functioning in the development of female structures in both mating types as well as in vegetative growth (Kim et al., 2002). The mating type A pheromone precursor, *ccg-4*, has also been shown to accumulate under low nitrogen conditions (Bobrowicz, Pawlack, Correa, Bell-Pedersen, & Ebbole, 2002). Pheromone receptors have also been identified with sequence similarity to those in *S. cerevisiae* and mating type specific expression (Kim & Borkovich, 2004). While *N. crassa* provides additional evidence for the link between starvation for nutrients, specifically nitrogen, and the induction of mating in Ascomycetes, examination of another saprophytic organism indicates both starvation and DNA repair as being intrinsically tied to mating pathways.

Schizosaccharomyces pombe

Another closely related Ascomycete provides additional evidence for the concept of sexual reproduction evolving as a mechanism of response to low nutrient availability. *Schizosaccaharomyces pombe*, or fission yeast, is also a saprophytic yeast, requiring dead or decaying organic matter, but not a live host,

and exists in two mating types h+ and h-. *Sc. pombe*, like *S. cerevisiae*, has a relatively simple life cycle consisting of a haploid and diploid state (Kelly, Burke, Smith, Klar, & Beach, 1988). The two requisite groups of genetic elements, transcription factors to express mating type specific genes and a pheromone receptor system are also present. The mating type region of *Sc. Pombe* consists of three components, *mat1*, *mat2-P* and *mat3-M* (Kelly et al., 1988). Cell type is determined by alternate alleles present at the *mat1* locus, either P in h+ cells or M in h- cells. The P region contains two open reading frames Pc and Pi. The predicted product of Pi contains regions homologous to homeobox sequences and is therefore believed to encode DNA binding proteins that regulate the expression of other genes (Kelly et al., 1988). The M region also contains two open reading frames Mc and Mi, and Mc also appears to have homeobox like sequences (Sugimoto, Iino, Maeda, Watanabe, & Yamamoto, 1990). As with *S. cerevisiae*, not all products of the mating type locus are necessary for both haploid and diploid cell types. Pc and Mc alone were necessary to produce h+ and h- phenotypes, respectively, in haploid cells but all four, Pc, Pi, Mc, and Mi were required for gene expression in the diploid.

Like *S. cerevisae*, haploid *Sc. pombe* cells secrete pheromones that are recognized by cells of the opposite mating type. Haploid h+ cells secrete P factor and h-cells respond to this pheromone in a physiological manner (Imai & Yamamoto, 1994). Similarly, haploid h- cells secrete M factor to which h+ cells respond (Davey, 1991). Like budding yeast, fission yeast also respond to pheromone stimulation with cell cycle arrest. Interestingly, in this system, it was

originally believed to be nutrient starvation that arrested cell cycle, not response to pheromones (Imai & Yamamoto, 1994).

While nutrient starvation is not directly responsible for cell cycle arrest, the responsiveness of mating-related genes to nutrient starvation provides additional evidence for the evolution and maintenance of mating system as a response to nutrient starvation. While Pc and Mc are expressed from the mating type locus at a low basal level, expression of both is greatly induced in nitrogen-free media and expression of Pi and Mi is only detectable under conditions of nitrogen starvation (Kelly et al., 1988). Furthermore, nutritional starvation also leads to decreased levels of cAMP, an essential signaling component in mating pathways (Mochizuki & Yamamoto, 1992). Although nitrogen starvation seemed to induce transcription from mating type alleles, the response to starvation of all nutrients was not the same. Glucose-depleted but nitrogen-replete media did not result in the same induction of *mat* transcripts (Kelly et al., 1988). Additionally, another protein, Ste11, is induced in response to nitrogen starvation and decreased cAMP levels. Like Ste11 in *S. cerevisiae*, the *Sc. pombe* protein is essential for sexual development. Ectopic exposure causes uncontrolled mating and sporulation in *Sc. pombe*. Unlike the protein of the same name in *S. cerevisiae*, which is a protein kinase, *Sc. pombe* Ste11 encodes an HMG-box protein and regulates transcription of *matP* and *matM*. While not part of the mating type loci, this *Sc. pombe* protein represents another tie between nitrogen starvation and sexual reproduction.

Further evidence for sexual reproduction as a means of DNA repair also comes from the increased mating response of *Sc. pombe* to oxidative stress. Exposure of fission yeast to hydrogen peroxide increases sexually reproducing cells, a response that would be expected if mating and subsequent meiosis have evolved as a DNA repair mechanism in response to stress (Bernstein & Johns, 1989). While *S. cerevisiae, Sc. pombe*, and *N. crassa* live without a host, they all demonstrate mating in response to low nutrient conditions and provide evidence for the evolution of sexual reproduction as a response to such environments. Examination of other Ascomycetes that do require hosts adds an additional layer of understanding of sexual reproduction in fungi.

Candida albicans

As the most prevalent fungal pathogen of humans, *Candida albicans* provides such an example of an ascomycete with the requirement for a host. Interestingly, it was long believed that this organism did not undergo any type of sexual cycle. Evidence of the genetic components for a sexual reproduction system prompted researchers to investigate further. Not until the late 1990s was it determined that *C. albicans* did in fact contain regions with similarity to mating type loci in *S. cerevisiae.* These regions, named MTLa and MTLα, both encode regulatory sequences similar to those found in the corresponding regions of *S. cerevisiae*, although spanning a larger area within the genome (Hull & Johnson, 1999). Within these regions several similarities were found to the MAT loci of other fungi, including the presence of transcriptional regulators, the general

organization of the loci, and conserved position of introns within various coding regions (Hull & Johnson, 1999). In addition to the presence of transcriptional regulators, pheromone and pheromone receptor genes were also discovered within the genome (Bennett, Uhl, Miller, & Johnson, 2003). In fact, response to pheromone of the opposite mating type induces the expression of many genes whose homologs in *S. cerevisiae* are known to be involved in mating (Bennett et al., 2003). So with all the requisite components, why was there no evidence of meiosis and mating in these fungi?

The answer seems to lie within the specific relationship this pathogen has with its host. In a lab setting, *C. albicans* cells can grow as white or opaque colonies, regardless of mating type. Interestingly, the switch from white to opaque is controlled by homeodomain proteins within the mating type locus (Miller & Johnson, 2002). The switch from white to opaque is relatively rare. Infrequent mating observed in clinical populations seems to be a result of the relationship between virulence and mating efficiency; that is, the type of cells that establish the most robust infection are those least suited to mate (Hull & Johnson, 1999).

Generally speaking, *C. albicans* exists as a diploid, but genes from the mating type loci exist in only a single copy (Hull & Johnson, 1999). However, the most commonly studied lab strain exists as a heterozygote at the mating type locus, possessing both mating type alleles. Strains were genetically manipulated to create single mating-type diploids to allow the study of the response of the two cell types to each other (Miller & Johnson, 2002). Like *S. cerevisiae*, these

mating types were termed a and α. These strains both produced superficially opaque colonies, although the parental diploid strain did not (Miller & Johnson, 2002). Opaque cells of α type secreted pheromones that cause opaque cells of a type to form projections toward the α type cells. This phenomenon was only observed in opaque cells of a type and not α type indicating the response was mating type-specific (Bennett et al., 2003; Miller & Johnson, 2002). Opaque cells are 10^6 times more efficient at mating than white cells, while white cells are generally the phenotype found in mammalian infections (Miller & Johnson, 2002). While a human pathogen must be able to survive inside its host and respond dynamically to the host's immune system, ascospores are highly antigenic so sexual reproduction inside the host may inadvertently lead to a greater and more effective immune response (Forche et al., 2008).

C. albicans has, as a result, evolved what has been termed a parasexual life cycle. This form of reproduction allows for some of the genetic variation created by recombination and none of the undesirable host attention attendant with switching to opaque cell type or producing ascospores. In this system, tetraploid strains become unstable and start losing chromosomes to generate diploid strains (Forche et al., 2008). Genetic recombination happens at a lower rate than in a normal meiotic cycle but sufficient to generate some variation within the population (Forche et al., 2008). While imprecise, parasexual reproduction does help to increase diversity and explains the maintenance of the mating-related genes within *C. albicans* despite the lack of obvious meiosis.

As a mammalian pathogen, *C. albicans* represents an extreme example of evolution of sexual reproduction as a response to host specificity. Because the host immune response is more intense to the phenotype of cells required for mating and for the products of mating, selection has been in favor of a parasexual reproductive life cycle that avoids both. An examination of pathogens with plant hosts further elucidates how interaction with hosts can favor different changes in fungal sexual reproduction.

Magnaporthe grisea

The *Magnaporthe grisea* and *Magnaporthe oryzae* species complex are the causative agents of rice blast disease and have a huge economical impact on the agricultural industry. Like other members of the Ascomycetes, a region within the genome have been identified as the mating type locus, distinguishing the two mating types, Mat1-1 or Mat1-2. Similar to what has been found in other fungi, these regions are idiomorphs with relatively no sequence similarity (Kang, Chumley, & Valent, 1994). Additionally, pheromone precursors have been identified within the genome. While genes for both pheromone precursors are present in the genomes of both mating types, they are expressed in a mating-type specific manner. *MF1-1* is expressed by Mat1-1 strains while *MF1-2* is expressed by Mat1-2 strains (Shen, Bobrowicz, & Ebbole, 1999). What is more interesting still, these pheromones are not expressed under low nutrient availability as is seen in other ascomycetes but under relatively replete media conditions (Shen et al., 1999).

The infectious process of the *Magnaporthe* complex may offer some insight into this deviation from normal induction of pheromone expression level. Rice blast infection begins with an asexual spore forms an appressorium and is able to penetrate plant tissue, develop, and establish infection inside the host. While many of the pathways governing this development and infection are canonical signaling pathways involved in mating in other fungi, such as cAMP/PKA pathway and MAPK pathways, there appears to be no requisite for mating in order for this organism to form an appressorium and enter the host (Choi & Dean, 1997; Zhao, Kim, Park, & Xu, 2005). While strains of opposite mating type can mate in a laboratory setting, most field isolates from rice are relatively infertile, although isolates from different hosts demonstrate different degrees of fertility (J. Li et al., 2016). Moreover, appressorium formation seems to be repressed by the presence of mating pheromones. In response to *S. cerevisae* α-factor, *M. grisea* Mat1-2 does not form appressoria even in typically inducing environmental conditions and this lack of morphological response to be due to the interaction of the pheromone with the pheromone receptor. Although it was not demonstrated to specifically be the Mat1-1 pheromone, culture filtrates from Mat1-1 had the same effect on Mat1-2 appressorium formation (Beckerman, Naider, & Ebbole, 1997).

Like *C. albicans*, *M. grisea* represents an extreme example of change in sexual reproduction strategies as a result of host interactions. Mating is a costly process and potentially may reduce the ability of the organism to infect its host plant. This fungus has been able to circumvent the need for mating altogether,

while maintaining the pathways involved in other mating systems. Despite the evolution of a mating system potentially in response to DNA damage, successful infection without mating has been maintained in the population as the selective pressure in favor of infection outweighs that in favor of whatever positives can be gained from mating. While *Magnaporthe* species represent an extreme strategy of sexual reproduction (or lack thereof) to produce successful infection, other plant pathogen members of *Ascomycota* that also reproduce primarily asexually have evolved other means of using components of the mating pathway for interaction with their plant hosts.

Fusarium oxysporum

A species complex causing vascular wilt disease in over 100 different plants, *Fusarium oxysporum*, is an asexually reproducing Ascomycete. Because the fungus dwells in the soil and enters the plant through the root, there is some evidence indicating that the fungus can sense the host plant and grow in that direction (Turra, El Ghalid, Rossi, & Di Pietro, 2015). Despite its asexual lifestyle, *F. oxysporum* still has the mating type locus components found in all Ascomycetes. There are two idiomorphs present at the mating type locus, either MAT1-1 or MAT1-2. Although their function in an asexual fungal system is largely known, the MAT1-2 idiomorph does encode a protein with an HMG-box domain, like other ascomycetes (Arie et al., 2000).

What is particularly interesting with the species complex, in the context of understanding the evolution of MAT loci, is the possibility of the pheromone

receptor system in sensing chemical signals from potential host plants. Growth of the fungal hyphae towards the host plant is directly in response to a specific type of peroxidase secreted by the plant (Turra et al., 2015). Moreover, exposing microconidia to glutamate results in increased production of germ tubes (Turra et al., 2015), indicating that nitrogenous nutrients can illicit a chemotrophic response as well. This response was specific to only some amino acids and nitrogen sources, indicating that it was not a general response to any nitrogen. While no sexual cycle as been found in *F. oxysporum*, putative pheromone precursors are found in the genome, and exposure to either these pheromones or pheromones from *S. cerevisiae* resulted in a similar chemotrophic response (Turra et al., 2015). With respect to canonical mating pathway components, this chemotrophic response was found to be mediated by a MAPK cascade as well as the *F. oxysporum* Ste2, a functional homolog of the protein of the same name is *S. cerevisiae* that is one of the pheromone receptors (Turra et al., 2015). While exposure to pheromone can cause morphological changes in a responding cell, in a similar fashion, signals received by the pheromone receptor can change the growth of the fungal hyphae in the direct of a potential host. Although the pheromone receptor may no longer have a role in sexual development, it is vital to the fungal ability to sense a suitable host in its environment.

An analysis of the components of the mating type loci in Ascomycetes provides an understanding of potential reasons for sexual reproduction to have evolved in fungi (See Figure 1 for a schematic of representative Ascomycete mating loci). While all members of this group produce the genetic components

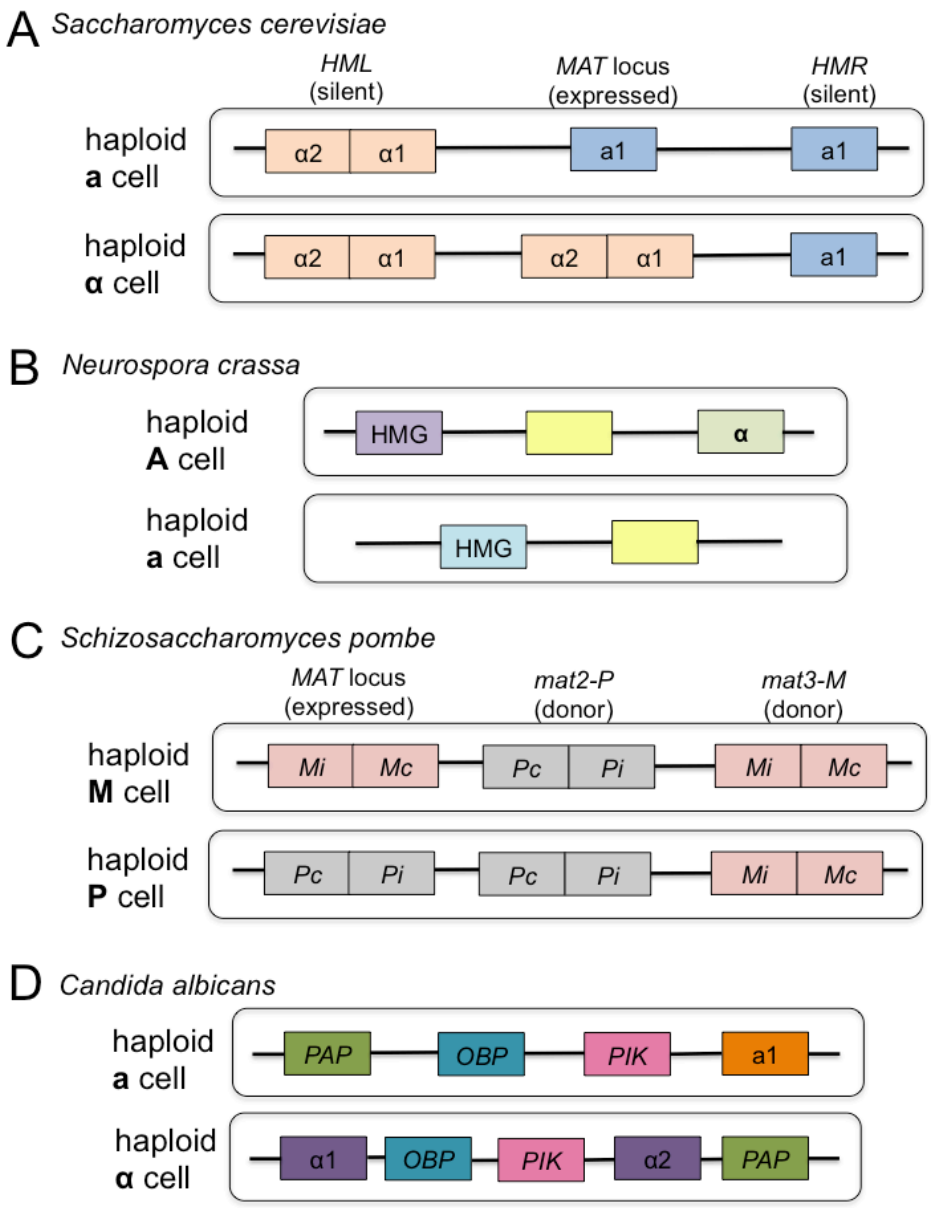

Figure 1: Mating type loci from sample Ascomycetes.
A) *Saccharomyces cererivisae* is the model organism for the group and the MAT for these species contains several transcriptional regulations. B) Like *S. cerevisiae*, *Neurospora crassa* contains transcriptional regulations (HMG and α) as well as proteins of unknown function that are important in mating type determination (yellow boxes). C) *Schizosaccharomyces pombe*, like *S. cerevisiae*, contains one region from which expression determines mating sites and two donor regions that allow for mating type switching. D) *Candida albicans* typically exists as diploid cells but haploid cells do exist. Their MAT also contain regions that encode proteins (a and α) that regulation transcription of mating type specific genes.

necessary for sexual reproduction, not all of them use it, and those that do seem to use it infrequently in wild populations. Most likely as a means of DNA repair, sexual reproduction evolved as a method to right the wrongs created by nutrient starvation or exposure to other potentially damaging agents. For strictly saprophytic organisms like *S. cerevisiae* and *Sc. pombe*, sexual reproduction still occurs, albeit infrequently, in wild populations and can be induced synthetically through nitrogen starvation. In infectious organisms, the ability to sexually reproduce is even more rarely seen in field isolates, either due to the loss of fitness as an infecting agent in the case of *C. albicans* or due to a loss of necessity of mating in the case of *M. grisea* or *F. oxysporum*. The selective pressure in favor of successful infection of a host far outweighs any benefit gained from sexual reproduction. However, as is seen in *F. oxysporum*, the components of the mating pathway remain vital to the fungus, particular in the case of *F. oxysporum*, as a means of host interaction. An examination of the other members of *Dikarya*, the Basidomycetes, provides further evidence of the interconnectivity of sexual reproduction and selective fitness for both nonpathogenic and pathogenic fungal members. Most of these fungi engage in sexual reproduction and in the context of lifestyle, different selective pressures have resulted in evolution within the mating locus and with process of mating.

The Basidiomycetes

The phylum *Basidiomycota* can be divided into three major lineages: mushrooms, rusts and smuts. The most recent attempt at phylogenetic

classification based on available molecular data resulted in the formation of three subphyla: *Agaricomycotina* (mushrooms), *Pucciniomycotina* (rusts), and *Ustilaginomycotina* (smuts), and two other classes outside of these subphyla, *Wallemiomycetes* and *Entorrhizomycetes* (Hibbett et al., 2007). In general, these organisms reproduce sexually and produce specialized spores as the result of meiosis called basidiospores. The tetrapolar mating system, where both the homeodomain portion of the locus and the pheromone/pheromone receptor portion of the mating type locus are physically unlinked, is unique to this group, although not all members use this system. Analysis of various organisms of this phylum provides further understanding of the function of the mating type loci in the formation and maintenance of each organism's ecological niche.

Coprinopsis cinerea

Potentially one of the most well studied mushroom species, *Coprinopsis cinerea*, also called *Coprinus cinereus*, is a saprophytic species of mushrooms, known to be an important ecological decomposer. As in most mushroom systems, mating between compatible mating partners results in the formation of a dikaryon on which mushroom fruiting bodies develop (Asante-Owusu, Banham, Bohnert, Mellor, & Casselton, 1996). There are two groups of mating type genes in *C. cinerea*, A mating-type genes and B mating-type genes. A and B independently regulate different steps in dikaryon development and allow self versus non-self recognition (Kues et al., 1992). The A mating-type genes encode several genes that can be characterized as one of two classes of homeodomain

proteins, HD1 or HD2 (Asante-Owusu et al., 1996). Seven A genes have been identified, four of which encode homeodomain proteins, and these four genes determine mating type specificity (Kues et al., 1992). In a compatible mating partner, only one of these alleles must be different between the two partners and one heteroallelic combination in the mated pair is sufficient to trigger A-regulated development (Kues et al., 1992). Different combinations of these four A-specific alleles generate the many different mating types in nature (Kues et al., 1992).

Compatible mating partners bring together different versions of homeodomain proteins that can heterodimerize, generating active transcription factors that leads to sexual development (Asante-Owusu et al., 1996). This heterodimerization mediated by the N terminus of these homeodomain proteins is an essential component of self versus non-self recognition (Asante-Owusu et al., 1996). Different A genes seem to be responsible for clamp cell formation (Asante-Owusu et al., 1996). In addition to this aspect of mating partner recognition, the B mating locus encodes pheromones and pheromone receptors that also serve in identification of potential mates and govern adjacent cell fusion during mating (Asante-Owusu et al., 1996). The B mating locus encodes peptide pheromones and corresponding 7-transmembrane helix receptors for their recognition (O'Shea et al., 1998). A single B mating type locus may contain genes for as many as three receptors and six pheromone precursors (O'Shea et al., 1998). As with the A mating locus, a single different pheromone precursor gene or pheromone receptor gene in another cell is sufficient for mating compatibility (O'Shea et al., 1998).

This mushroom species clearly has benefitted from the generation of variability through sexual reproduction. Due to the multiallelic state of both the pheromone and pheromone receptor-containing locus as well as the homeodomain protein-containing locus, this system generates a potential for outcrossing of greater than 50% (O'Shea et al., 1998). In nature, this translates to both the increased probability of encountering a compatible mating partner as well as the generation of great genetic variability within a population due to the numerous possibilities of outcrossing. For this organism, sexual reproduction is an essential element of niche formation by increasing fitness through successful mating. Also of note, genes induced in this species by meiosis are more highly conserved than genes not induced by meiosis in Asomycetes like *S. cerevisiae* and *Sc. pombe,* despite the divergence of these species between 500 and 900 million years ago (Burns et al., 2010). Examination of another mushroom species indicates just how many different mating types can be generated with multiallelic mating loci.

Schizophyllum commune

Another well studied mushroom, *Schizophyllum commune*, is found in many diverse environments and typically as a wood rot fungus. Like *C. cinerea*, *S. commune* has two multiallelic mating locus regions. The A mating type region, containing Aα or Aβ regions, encodes homeodomain proteins to regulate A-dependent sexual development. There are at least three Aα mating types, Aα1, Aα3, and Aα4. Aα3 and Aα4 both encode two polypeptides, Y and Z, while Aα1

encodes a single polypeptide Y (Stankis et al., 1992). The Z and Y polypeptides are homeodomain proteins, and the Y product also has a putative DNA binding domain (Stankis et al., 1992). In a compatible mating pair, the Y from one partner interacts with the Z from another partner to regulate Aα-regulated development (Stankis et al., 1992). The Aβ loci are functionally redundant with the Aα loci, and there have been at least 32 different variations of Aβ loci identified in wild populations (Specht, 1995).

The B mating type region also contains two tightly linked loci, Bα and Bβ, and, like their A counterparts, they are functionally redundant, both encoding pheromone and pheromone receptors that govern self vs non-self recognition (Wendland et al., 1995). While the two loci are functionally redundant, receptors from Bβ do not respond to Bα pheromones (Wendland et al., 1995). Differences at either Bα or Bβ between a mated pair of individuals is sufficient to initiate B-dependent sexual development (Vaillancourt, Raudaskoski, Specht, & Raper, 1997). An analysis of the Bα1 locus found it contains three pheromone precursors and one pheromone receptor (Vaillancourt et al., 1997). The Bβ1 locus also contains the genes that function with Bβ specificity. Comparison of the DNA sequence of Bα1 and Bβ1 suggest they may be the result of a duplication event (Vaillancourt et al., 1997).

As with the *C. cinerea* system, the A and B mating loci are responsible for different parts of sexual development through transcriptional regulation. A-dependent regulation results in the upregulation of genes having to do with the cell cycle and the down regulation of genes related to metabolism, while B-

dependent genes include those for cell wall and membrane metabolism, stress response, and the redox state of the cell (Erdmann et al., 2012). Because of the redundancy of function of Aα and Aβ genes, as well as Bα and Bβ genes, a compatible mating partner does not have to have different alleles at all four loci. At least 28,000 different mating types of *S. commune* exist because of the different number of alleles at these four loci, and any individual mating type can mate with all but three of the others (Specht, 1995). Selective pressure on this system has strongly favored increased variation through mating and diversity at the mating type loci to increase the possible mating partners available.

The other two major lineages of *Basidiomycota* are pathogens, requiring a host to complete their lifecycle. As the pathogen and the host tend to evolve together, different selective pressures apply to these organisms that saprophytic organisms do not encounter. For these organisms, mating serves as both of mechanism of self versus non-self recognition as well as in some cases a means by which to enter the specific host. Increasing host specificity as well as intraspecies recognition are different selective pressures that have shaped the evolution of the mating type loci in these organisms. Human pathogens represent the extreme example within the *Basidomycetes*, where the sexual cycle is not implicated in the infection process.

Malassezia globosa

A resident of the human host, typically associated with dandruff, *Malassezia globosa* is closely related to *Ustilago maydis*. This organism and

other closely related *Malassezia* species are part of the normal human epidermal flora but some may become infectious during periods of dense growth that lead to the human symptoms of dandruff and seborrheic dermatitis. *M. globosa* has a small genome compared to other free living fungi, with only 9 megabase pairs, and appears to be haploid because there are very few polymorphisms within the genome (Xu et al., 2007). The genome contains components similar to the *a* and *b* loci of *U. maydis*, with an arrangement more like that of *U. hordei*, with the genes encoding the pheromone/pheromone receptor system and the homeodomain proteins physically linked to each other (Xu et al., 2007). Additionally, several orthologs for components of the MAPK pathway in *S. cerevisiae* have been identified (Xu et al., 2007). While no sexual cycle has been observed, there are several reasons to believe that this organism is capable of sexual reproduction, including the isolation of strains that appear to be hybrids of other known strains (Saunders, Scheynius, & Heitman, 2012). Sexual reproduction in a human pathogen, if discovered, would be unique to this organism, as others, such as *C.albicans*, do not reproduce sexually within the host because of the immune response to the products of mating. Another human pathogen that does have a known sexual cycle provides additional evidence that mating may be possible but not necessary for invasion of a human host.

Cryptococcus neoformans

The causative agent of fungal infections in both healthy and immunocompromised individuals, *Cryptococcus neoformans* is primarily a

resident of the human lung, although it can cause fungal meningitis. The infectious particle is not the yeast cell itself but an asexual basidiospore produced during haploid budding (Wickes, Mayorga, Edman, & Edman, 1996). While sexual reproduction for this organism does not occur within the host, it has been observed. Under suitable environmental conditions, fusion between cells of opposite mating type occurs, producing dikaryotic hyphae characteristic of the Basidiomycetes (Wickes et al., 1996). Mating type, either a or α, is defined by the genetic components of the mating type locus in this organism's bipolar mating system (Kwon-Chung, 1976). Several pheromone precursors and pheromone precursor genes have been identified in the genome but unlike model fungal genomes, such as those from *U. maydis* or *S. commune*, these genes are not tightly linked but instead are dispersed throughout the mating type locus (Lengeler et al., 2002). A novel homeodomain protein has been identified within the α mating type alleles but not within the a mating type alleles, and this novel protein does show a high degree of homology with the *b* locus of *U. maydis* and *U. hordei* (Lengeler et al., 2002). Other orthologs of mating-related genes have been identified within the α mating type locus that are also dispersed through a large genomic region (Karos et al., 2000). The evolution of the α mating type locus appears to be similar to that of mammalian sex chromosomes, involving large chromosomal rearrangements and recombination suppression, resulting in a large sex-determining region of generally unlinked genes (Fraser et al., 2004).

While there is no physiological difference between a and α cells, they do behave differently and are represented in different proportions within clinical

isolates (Wickes et al., 1996). Almost all clinical isolates are α mating type, and a mating type cells do not undergo haploid filamentation resulting in the production of spores (Brefort, Muller, & Kahmann, 2005; Wickes et al., 1996). While this organism is capable of sexual reproduction, the independent evolution of mating loci within the two mating types has resulted in one mating type of the organism that can establish infection independently of the other. In fact, mating between two α mating type cells has been observed, to the extent that meiosis and recombination occur (Lin, Hull, & Heitman, 2005). In this way, within the host, the organism reaps all the benefits of sexual reproduction, such as DNA repair to damage caused by the host response, without the bother of finding a compatible mating partner. This evolution of the mating type locus represents an extreme example of the accumulation of components of canonical mating type components within a single mating type of a species to the extent that all the benefits of mating can be obtained, creating a nearly clonal population. The move toward sex chromosomes, not just mating type locus, can also be found in other members of the *Basidiomycota.*

Microbotryum lychnidis-dioicae

Previously called *Microbotryum violaceum* and *Ustilago violaceum*, *Microbotryum lychnidis-diociae* is the causative agent of anther smut in *Silene latifolia* and a member of *Pucciniomycotina*. This fungus is a unique system to study because it acts as a sexually transmitted disease and is capable of changing the gender of its host. This fungus infects its host and replaces the

pollen on anthers with diploid teliospores that are then carried to a new host by bees and other pollinators. Once on the new host, the teliospores germinate, undergo meiosis, and produce haploid sporidia. If sporidia of compatible mating type encounter each other, they form conjugation tubes and mating, producing dikaryotic hyphae that can grow inside plant tissue. The infection becomes systemic, eventually leading to the production of teliospores in the place of pollen and the cycle continues (Giraud, Yockteng, Lopez-Villavicencio, Refregier, & Hood, 2008).

The mating type loci of *M. lychnidis-diociae* is the first example of sex chromosomes encountered in fungi (M.E. Hood, 2002). The two mating types of *M. lychnidis-diociae*, A1 and A2, are both defined by the different alleles at loci for homeodomain proteins and for pheromone/pheromone receptor systems. The two mating type chromosomes show divergence over 90% of the length flanked by pseudoautosomal regions on either end (M. E. Hood, Petit, & Giraud, 2013). The sex chromosomes are among the largest in this organism's genome, with A2 being larger than A1 (M.E. Hood, 2002). A2 has two genes encoding pheromone precursors, while A1 contains a single locus (Badouin et al., 2015). While the two chromosomes seem to be the result of a duplication event by the number of syntenic blocks, extensive rearrangements in the form of inversions have occurred resulting in the gene order present (Badouin et al., 2015). There is significant repression of recombination in the mating chromosomes, resulting in linkage of the pheromone/pheromone receptors and homeodomain protein-encoding genes (Badouin et al., 2015).

Before the nature of the genetic material governing compatible mating partners in this organism was fully elucidated, it was discovered that different environmental factors, including low temperature and nutrient availability activated mating type alleles. As regulators of the developmental switch between three pathways of development, vegetative budding, conjugation, and sexual differentiation, mating type allele activity results in different responses to different environmental conditions. In high temperatures and nutrient levels, cells of this fungus bud vegetatively; however, in correct environmental conditions and upon exposure to the products of cells of opposite mating type (presumably pheromones), cells of a single mating type become blocked in G1 and develop conjugation tubes (Day, 1979). Cells carrying both mating type alleles exposed to similar environmental conditions also could not exit G1 and differentiated into spores (Day, 1979).

Later research also indicated that not only did environmental conditions activate mating, but also governed how the products of mating would act. The promycelium is the product of teliospore germination in this fungus. Generally speaking, the promycelium contains three cells but at low nutrient and temperature conditions, it may only contain two (M. E. Hood & Antonovics, 1998). An extensive study of promycelia under different environmental conditions revealed different results based on nutrient availability and temperature. After the first meiotic event within the promycelia, the daughter nuclei are separated immediately by septation. After the second meiotic division, one of the proximal nuclei migrates back into the teliospore; however, based on nutrient availability,

the fate of the two distal nuclei can be different (M. E. Hood & Antonovics, 1998). At ideal temperature and nutrient levels, the two distal nuclei are separated by a second septation event resulting in a three celled promycelium, each of which is uninucleated. At low temperature and nutrient availability, the second septation event does not occur resulting in a two-celled promycelium, with one single nucleated cell and one cell with two nuclei, both of the same mating type, as a result of the two components of the mating type locus being linked (M. E. Hood & Antonovics, 1998). As the number of heterokaryons that can be formed from a two-celled promycelium versus a three-celled promycelium is different, this environmental response allows flexibility of the mating system to either produce more heterokaryons or more infectious units (M. E. Hood & Antonovics, 1998).

Because of the complete linkage of the two components of the mating locus, mating between products of the first meiotic division is possible (M. E. Hood & Antonovics, 2000), which ensures the flexibility of the response in promycelia of different number of cells. As such, the mating system of *M. lychnidis-diociae* tends toward mating within the tetrad, ultimately reducing variation in the population and maintenance of deleterious alleles, with rare outcrossing events (M. E. Hood & Antonovics, 2000). This rapid intratetrad mating allows the organism to form infectious units to gain access to the host plant in response to environmental conditions such as low nutrient availability without having to encounter another cell of different mating type on the surface of the plant. Other Basidiomycete pathogens require mating with a compatible partner not part of a meiotic tetrad in order to invade their host of preference.

Ustilago maydis

The fungal tree of life remains a dynamic entity, particularly with the increased availability of molecular and genomic data. While there is some uncertainly as to the exact placing of many plant pathogens within a fungal phylogentic tree, the conservation of many aspects of the mating type locus remains indisputable. *Ustilago maydis*, the causative agent of corn smut, is potentially the most well studied Basidiomycete, and many would argue a better model organism for eukaryotes than *S. cerevisiae*. It has become the standard against which other mating type loci of this group are analyzed. In nature, *U. maydis* is found as haploid sporidia (Figure 2). When sporidia of opposite mating

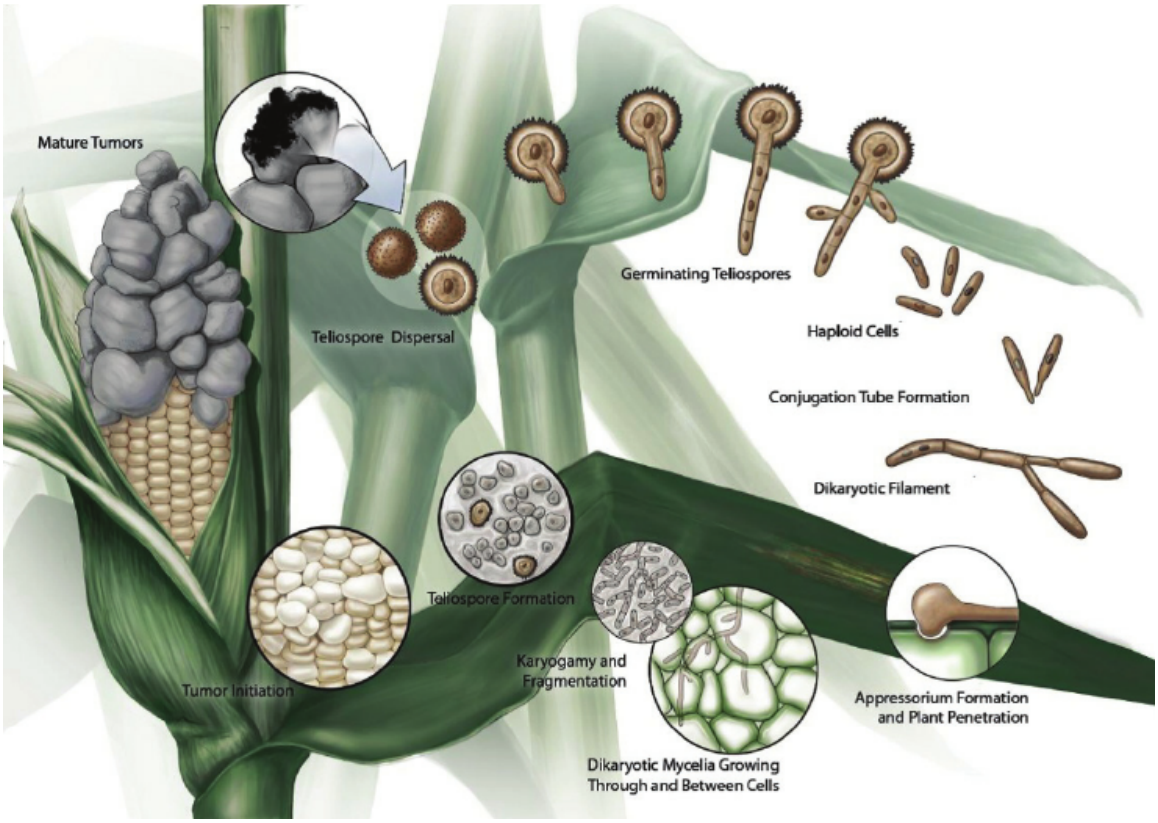

Figure 2: The life cycle of *Ustilago maydis.*
(Saville, Donaldson, & Doyle, 2012)

type recognize each other, they form conjugation tubes and the resulting dikaryon is able to penetrate the host plant. Inside the plant, numerous diploid teliospores are formed inside galls or tumors, giving rise to the characteristic smut appearance of the plant. These teliospores germinate, producing haploid sporidia and the cycle continues.

The mating type locus in *U. maydis* has been studied extensively and includes two genomic regions on different chromosomes (Figure 3). The a

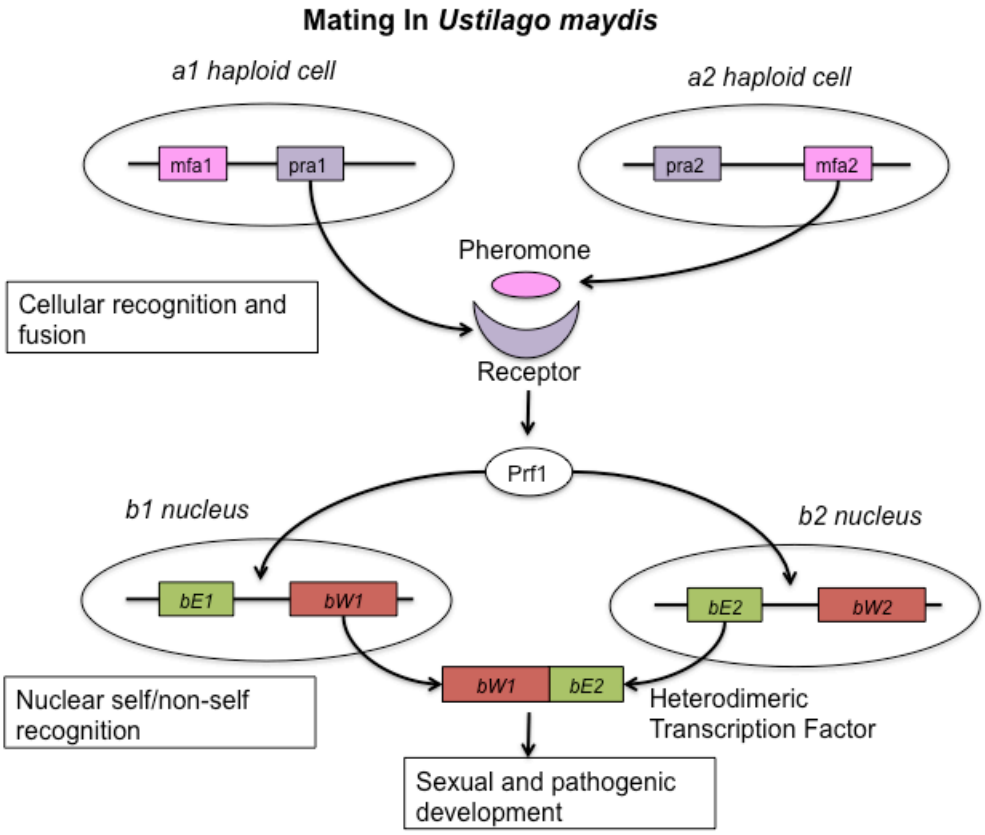

Figure 3: Mating between haploid cells of *Ustilago maydis.*

mating type locus of *U. maydis* encodes the pheromone and pheromone receptor system. The allele at the a locus is identified as either a1 or a2. Molecular analysis of the a alleles reveals that the a1 allele is smaller, at 4.5 kb while the a2

allele is larger at 8 kb (Bolker, Urban, & Kahmann, 1992). The sequences show no homology to each other and are absent in strains of the opposite mating type; *i.e.*, the a1 allele is specific to a1 strains (Bolker et al., 1992). Thus, technically they are not true alleles and, as was seen in *S. cerevisiae*, the two different forms are commonly referred to as idiomorphs (Crow & Dove, 1990). The genes *mfa1* and *mfa2* encode pheromone precursors in their respective mating types and are the only pheromone precursors. Mutants deleted for *mfa1*, for example, are unable to fuse to haploid cells of the opposite mating type (Bolker et al., 1992). The pheromone receptors are encoded by the *pra1* and *pra2* genes, and are very similar to the *S. cerevisiae* Ste3 receptor gene (Bolker et al., 1992). The receptors are located on the cell surface and bind to a secreted pheromone from a cell of the opposite mating type, resulting in a cellular response leading to preparation for mating (Bolker et al., 1992).

The *b* locus of *U. maydis* contains two unrelated homeodomain proteins that are most different in the N terminal region (Kamper, Reichmann, Romeis, Bolker, & Kahmann, 1995). The two proteins are either b-East (bE) or b-West (bW), and there have been at least 25 different alleles identified from wild isolates (Kronstad & Leong, 1990). Deletion of a gene encoding a single homeodomain protein has no affect on phenotype (Gillissen et al., 1992), suggesting a redundancy of function. Self/non-self recognition is mediated by dimerization of two homeodomain proteins from different mating types, for example bE1 with bW2 (Kamper et al., 1995). The heterodimer acts as a transcription factor for genes necessary to establish the infectious dikaryon and

proliferate within the host (Kronstad & Leong, 1989). Any combination of different alleles from the *b* locus can cause the dimorphic switch from yeast-like to infectious filamentation and trigger the pathogenic program (Schulz et al., 1990). It is possible to form haploid infectious strains simply by introducing homeodomain proteins at the *b* locus that are capable of forming a heterodimer (Kronstad & Leong, 1989). While in nature, b proteins derived from the same allele cannot dimerize, synthetic fusions of bE2 and bW2, for example, result in pathogenic development when introduced into haploid strains deleted for the native *b* locus (Romeis, Kamper, & Kahmann, 1997).

The *b* locus seems to be more involved in the development of pathogenicity than the *a* locus, as diploids that are heterozygous for *a* but homozygous for *b* grow in a yeast-like manner and fail to establish infection in host plants (Schlesinger, Kahmann, & Kamper, 1997). Heterozygosity at the *a* locus is not required for pathogenicity, and diploids homozygous for *a* but heterozygous for *b* form similar tumors in host plants as mated haploid strains. However, in nature, the function of both the *a* locus and the *b* locus in a multiallelic incompatibility system functions to limit inbreeding and increase variability within the population (Yee & Kronstad, 1993). Also in the synthetic setting of the lab, organisms must be deprived of nutrients, specifically ammonium, in order to see the mating phenotype. Similarly, in nature, mating occurs during appropriate environmental conditions. In this system, mating and sexual reproduction is vital to plant infection. Only synthetically made laboratory haploid strains are able to infect the host corn plant, and in nature, mating and

formation of the infectious dikaryon is paramount to establishing infection inside the host, gaining access to the resources inside the host, and proliferating the species. Because of the intrinsic connection between nutrient limitation and induction of mating, it is likely that invasion of the host gives the organism access to nutrients that are needed for survival. Successfully accessing necessary nutritional components by invading the plant can only be accomplished by being able to recognize a suitable mate, mediated by the mating type loci. Examination of another closely related species reveals how slight modifications to the maturation process of mating competent cells can further guarantee the recognition of the correct compatible mating partner.

Ustilago hordei

Recent molecular genomic analysis has placed *Ustilago hordei* and *Ustilago maydis* as more distant relatives than their genus name would suggest. However, the conservation of genetic material with the mating type locus between these two species is undeniable. *U. hordei* infects barley and like *U. maydis*, forms large masses of black teliospores within the host plant. Like all smuts, the two fungal pathogens share many life cycle features, including a yeast-like stage and an infectious dikaryon arising from the fusion of two haploid cells (Bakkeren et al., 1992). Unlike the *U. maydis* mating system which is tetrapolar, the *a* and *b* loci being on different chromosomes, *U. hordei* has a bipolar mating system in which the *a* and *b* loci are physically linked on the same chromosome and designated as one of two mating types, MAT-1 or MAT-2

(Bakkeren & Kronstad, 1993). In the *U. hordei* bipolar system, every fusion event mediated by the *a* locus will guarantee that the *b* locus will also be of opposite mating type and the resulting fusion will form an infectious dikaryon (Bakkeren & Kronstad, 1994).

Like the *U. maydis* mating locus, the *a* locus in *U. hordei* contains the pheromone precursors and pheromone receptor genes, with a high degree of similarity to the sequences contained within the *U. maydis* locus (Bakkeren & Kronstad, 1994). Also similar to the other smut, the *b* locus contains two homeodomain proteins that during mating dimerize to create a transcription factor to regulate expression of mating-related genes (Bakkeren, Kamper, & Schirawski, 2008). Interestingly, there is a high degree of sequence similarity between the *U. hordei* mating type locus and MAT loci of other closely related organisms, including *U. maydis* and *S. cerevisiae (*Bakkeren et al., 1992). In fact, If the homeodomain of "opposite mating type" from *U. maydis* is expressed in *U. hordei*, and vice versa, there is a positive mating reaction on charcoal plates, although pathogenicity in corn is markedly reduced, resulting in no teliospores and only weak symptoms of infection (Bakkeren & Kronstad, 1996). Analyzing of the morphological changes that occur upon induction of the mating reaction in *U. hordei*, it seems that to ensure mating with a member of the same species, the conjugation tubes of this fungus develop at a later time than those of *U. maydis*, for example, so that even if the two organisms were to encounter each other, unproductive mating is unlikely to occur because the timing of conjugation tubes would not occur appropriately (Bakkeren et al., 2006).

Another interesting characteristic of the *U. hordei* mating type locus is the similarities it shares with sex chromosomes. While the mating type locus is located within a chromosome, not as an entity unto itself as is the case in *M. lychnidis-diociae*, it is unusually large compared to other smuts and has an accumulation of repetitive DNA and retrotranspons, few of which are found in *U. maydis* (Bakkeren et al., 2006). In addition to the presence of pheromone precursors, pheromone receptors and homeodomain proteins regulating mating and virulence, the *U. hordei* also contains 47 other genes, most of which have homologs in *U. maydis* but are not physically linked to the mating type locus (Bakkeren et al., 2006). Because the mating type locus in *U. hordei* brings along much of the necessary genetic information for successful mating, variability in this region has not been favored by selection; and, by having a specially timed mating program, this fungus has become quite specialized to parasitizing cereal grasses (Bakkeren & Kronstad, 1994). Although *U. hordei* lacks the variation in the mating type locus seen in other closely related smuts, because encountering a compatible mating partner guarantees successful mating due to the physical linkage of the pheromone/pheromone receptor complex and the homedomain proteins and the unique timing of the formation of conjugation tubes in this organism, variability is not necessary for successful parasitism within the group and linkage of other genes required for infection to the mating locus ensures that they segregate in a way that is favorable to allow the fungus to gain access to its host. Examination of another basidiomycete biotrophic fungus reveals that host specificity is mediated by the organism's ability to respond to the host's immune

response, and that while interspecies mating may occur, only mates from compatible haploids of the same species result in teliospore formation on the host and successful passage of genetic material to future generations.

Sporisorium reilianum

Another smut fungus similar to *U. maydis*, *Sporisorium reilianum*, exists in two varieties based on host specificity, one that infects maize (SRZ) and one that infects sorghum (SRS) (Zuther et al., 2012). Like some other closely related smuts, the mating type locus is composed of two unlinked genomic regions, *a* and *b*, which code for a pheromone and pheromone receptor and homeodomain proteins, respectively. The genetic material within and around these loci shows a high degree of synteny with *U. maydis (Schirawski, Heinze, Wagenknecht, & Kahmann, 2005)*. The *b* locus exists in at least five different alleles and encodes two subunits of a heterodimeric homeodomain transcription factor (Schirawski et al., 2005). In contrast to *U. maydis* which has only two alleles, the *a* locus of *S. reilianum* can be one of three alleles all containing two pheromone precursors (Schirawski et al., 2005). These different versions, designated a1, a2, and a3 are idiomorphs, Each idiomorph encodes different pheromones and pheromone receptors. The pheromones for a particular receptor have identical sequence even if they exist in a different allele; that is, the pheromones from a1 and a3 that bind to the receptor from a2 have the same sequence (Schirawski et al., 2005). Two of these pheromones, those binding to the receptors of a1 and a2, show a high degree of homology to the same genes in *U. maydis*; the third set, binding to

the receptor from a3, while they are identical to each other, are only weakly related to other fungal pheromone precursors (Schirawski et al., 2005). This arrangement of two pheromone precursors and one pheromone receptor in each *a* allele appears to have arisen from a recombination event within the locus itself and serves to increase the number of mating types within the species (Schirawski et al., 2005).

Interestingly enough, despite the narrow host range of the two varieties of *S. reilianum*, there is remarkable similarity between the pheromones of the two (Radwan, 2013), and therefore the possibility that the two subspecies could potentially mate in natural populations. However, despite the similarity of the genetic material within the mating type loci, SRS is only successfully able to produce teliospores within sorghum and SRZ is only able to do the same in maize. In its respective host species, each is able to resist the attempts of the plant to clear the infection, while in the opposite species, the fungal succumbs to the plant's defense mechanisms. In this case, selection has most likely not favored variation within the mating type locus to reduce promiscuity between different species but instead has favored the maintenance of other specific genes that allow proliferation within the host despite the plant's attempt to rid the infection. Like other basidiomycetes such as the mushrooms, more allelic versions of the *a* locus allows for more mating types and greater variation within the natural populations. Successful matings only within appropriate hosts guarantees that offspring only carry parental DNA from organisms that are able to establish infection in the host.

As with the Ascomycetes, there are examples of Basidiomycetes that have the genetic components for mating but, due to their interaction with their specific hosts, do not typically mate in natural populations. Such a system could develop for one of two reasons. Either the organism can bypass the metabolically costly process of mating and still establish effective infection or the products of mating may trigger an immune response from the host that make the organism less able to establish infection. Whichever the case, the maintenance of the mating type loci within these organisms indicates that mating is an important part of the evolutionary history of this group of fungi.

This review of the mating type loci components and functions of several fungi reveals the diversity of strategies that have evolved to allow each organism to persist and carve out very specific ecological niches. In saprophytic free-living organisms like *S. cerevisiae* and *Sc. pombe*, the components necessary for sexual reproduction are present in all cells, although the occurrence of mating in natural populations is rare. The selective pressure in favor of ability to mate, and therefore respond to adverse environments such as nutrient limitation which may damage DNA, has been maintained because of the advantage it gives the organism to create offspring that are more viable than their parents. Other ascomycetes, specifically pathogens, also have the ability to mate, but the occurrence in natural populations is even more rare. *C. albicans* exists as a diploid and has a parasexual lifecycle, as to not invoke a response from the human host immune system, while *M. grisea* in wild populations is virtually sterile because the organism has been able to evolve mechanisms to establish infection

within the host plant without the need for mating. Species like *F. oxysporum*, while not mating sexually, use the components of the mating system, specifically the pheromone receptors, to sense the presence of a suitable host. For all of these parasitic organisms, the mating type locus is maintained, although its function in the lifecycle of the organism varies as to make it to the most suitable pathogen for its host species.

In Basidiomycetes, the evolution of the mating type locus has served a variety of purposes to enhance the ability of the organism to survive and pass genetic material to future generations (See Figures 4 and 5 for schematics of Basidiomycete mating loci). Meiosis can also cause variation within haploids and loss of deleterious alleles (Horandl, 2009). For mushrooms like *C. cinerea* and *S. commune*, the variation of alleles within the mating type locus has allowed for the evolution of thousands of mating types which has created enormous diversity within wild populations and the ability to colonize many environments. For plant pathogens, like the rusts and smuts, mating is a necessary part of host invasion and evolution within the mating type locus has dictated more precise mechanisms of identifying self versus non-self even within closely related organisms to ensure successful mating and invasion and subsequent passage of genetic material to future generations. As seems to be the case with Ascomycete human pathogens, Basidomycete human pathogens have developed other means of colonization without mating to avoid the host immune response, although the genetic material found within the mating type locus continues to play a vital role in the organisms development and infection.

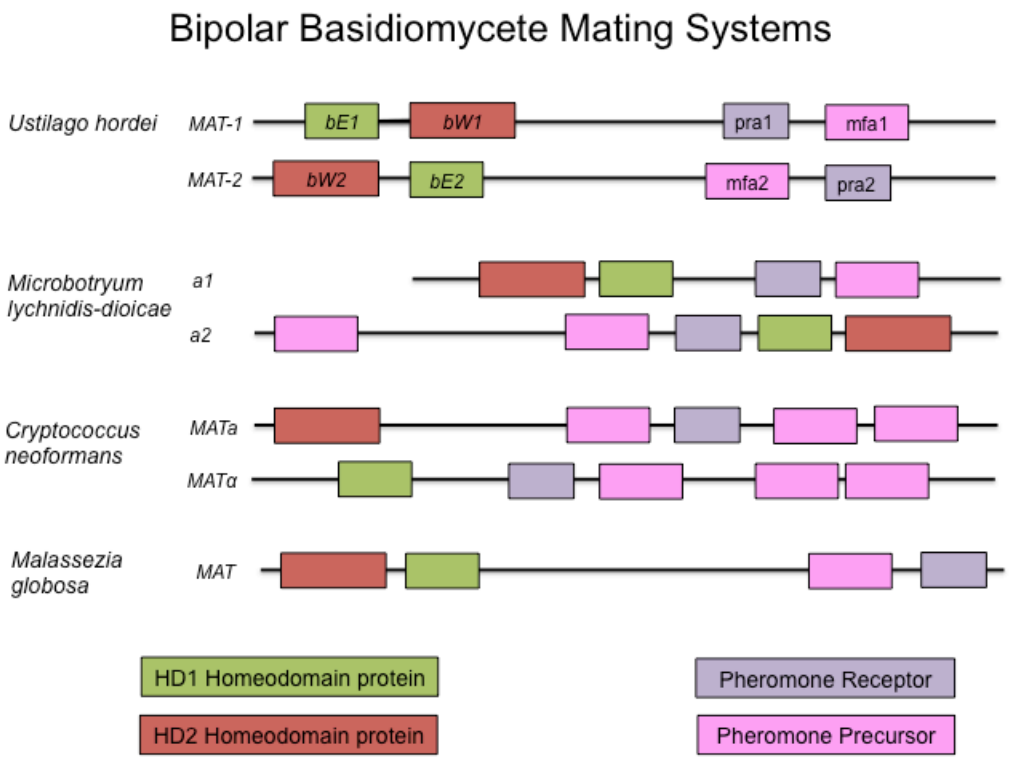

Figure 4: Bipolar Basidiomycete Mating Systems.
Basidiomycetes that use a bipolar mating system have MAT that encode homeodomain proteins and pheromone / pheromone receptor systems that are physically linked on the same chromosome.

Although the mechanism by which the function of the mating type locus differs within fungal species is not well understood, it is clear that the ability to reproduce sexually gave the organism a selective advantage to repair DNA damage that an asexually reproducing organism would not possess. Moreover, it is also apparent that nutrient limitation, specifically nitrogen, plays an important role in inducing mating in most fungi. The purpose of the current work is to investigate the interplay between genes regulating response to nitrogen availability and those regulating mating in the model organism, *Ustilago maydis.*

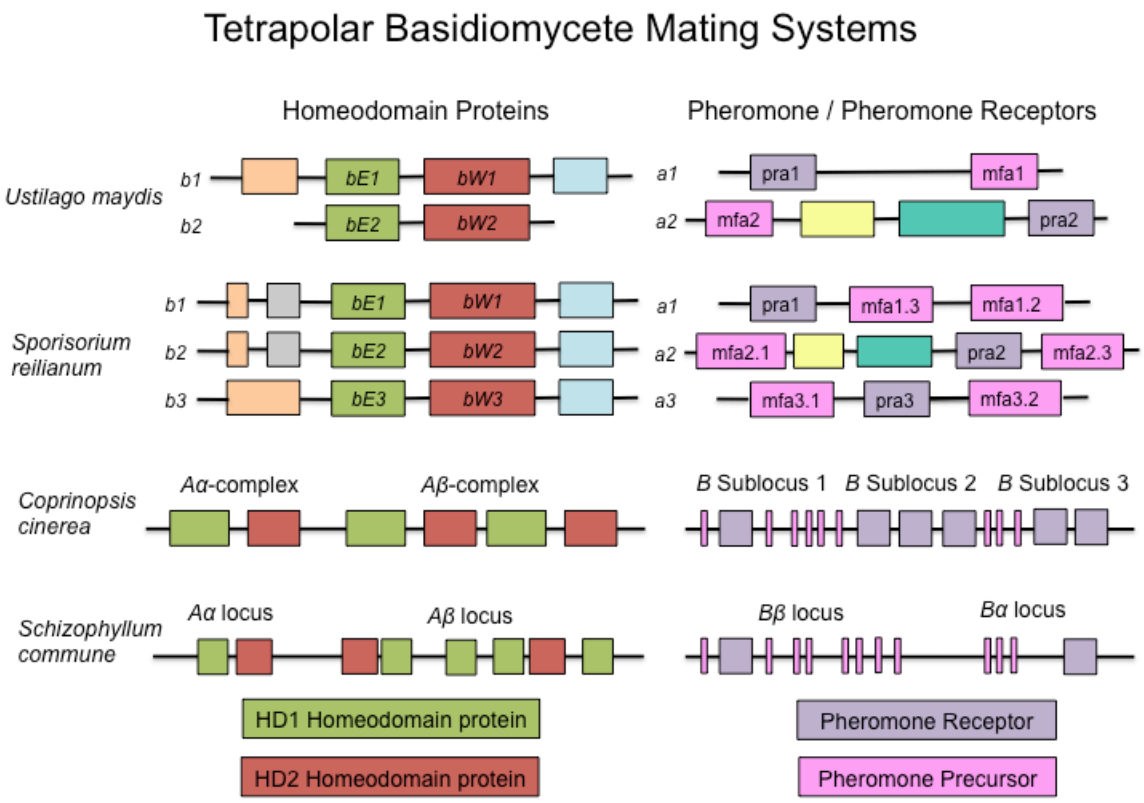

Figure 5: Tetrapolar Basdiomycete Mating Systems.
Basidiomycetes that use a tetrapolar mating system have two genetic regions that comprise the MAT loci, one endocing homeodomain proteins, and the other encoding the pheromone / pheromone receptor system. Other regions (unlabeled boxes) show a high degree of homology across related species.

As many plant pathogens, *U. maydis* secretes effectors once inside their host to mediate establishment of infection; moreover, the same set of effector genes can be induced by limiting nitrogen availability (Bolton & Thomma, 2008). Many of these effectors are expressed as a result of regulation by the heterodimer produced by the homeodomain proteins encoded within the *b* mating type locus. While the induction of mating and subsequent development of infection mediated by the *b* mating type locus is well understood, the role that these genes play in a haploid, unmated cell, has not been well elucidated. Genes from the *b* locus are

expressed at basal levels in haploid strains; additionally, haploid cells have a characteristic filamentation response to low ammonium, a phenotype which is lost in the absence of an intact *b* locus.

Biological Questions

In Chapter 2, the relationship between nitrogen availability and expression mediated by the protein products of the *b* locus is examined. Nitrogen limitation results in a change in gene expression in wild-type haploid organisms, including upregulation of ammonium transporters, Ump2 and Ump1, in *Ustilago maydis*. The homolog for Ump2 in *S. cerevisiae*, Mep2*,* is known to act as a transceptor, both physically moving ammonium across the cell membrane as well as sensing the availability within the environment. In other organisms, homologs of Ump2 are expressed during infection (Donofrio et al., 2006), supporting the hypothesis that Ump2 may play a role in infection as well as ammonium transportation. Moreover, Ump2 homologs, such as Mep2p in *C. albicans*, are required for filamentation in response to low ammonium (K. Biswas & Morschhauser, 2005). In this chapter, the possibility of Ump2 acting in a similar manner is examined, as well as how different expression levels of *ump2* can affect the mating program.

In Chapter 3, the effect of each of the two components of the *b* mating locus, b-East and b-West, is examined in more detail. While these two homeodomain proteins are not normally able to dimerize in a haploid cell, it is hypothesized that they may play individual roles in other ways within the haploid cell. The response of the haploid lacking either bE or bW is examined within the

context of nitrogen availability, both phenotypically and at the level of gene expression. Moreover, the expression level of *ump2* in strains missing either bE or bW is further examined to determine if the affect is different based on the genetic material present at the *b* locus.

In Chapter 4, various microscopy techniques are employed to examine regulation of *ump2* expression and the role of the actin cytoskeleton in the formation of filaments in response to low ammonium conditions. Expression levels of potential actin regulatory proteins and cell wall modification proteins are also examined to further elucidate the role of these proteins in the formation of filamentous colonies from haploid strains of *U. maydis*.

Finally, Chapter 5 serves as an overall Conclusion to the dissertation, in order to summarize the important “take-home” lessons from this work.

CHAPTER II

COORDINATE REGULATION OF *USTILAGO MAYDIS* AMMONIUM TRANSPORTERS AND GENES INVOLVED IN MATING AND PATHOGENICITY

Chapter Overview

The dimorphic switch from budding to filamentous growth is an essential morphogenetic transition many fungi utilize to cause disease in the host. Although different environmental signals can induce filamentous growth, the developmental programs associated with transmitting these different signals may be the same at one or more levels. Here, we explore the relationship between filamentation and expression levels of ammonium transporters (AMTs) that also sense low ammonium for *Ustilago maydis*, the pathogen of maize. Overexpression of the high affinity ammonium transporter, Ump2, under normally non-inducing conditions, results in filamentous growth. Further examination of AMT expression levels and their influence on signal transduction pathway genes revealed that *ump2* expression levels are correlated with expression of genes involved in the mating response pathway and in pathogenicity; expression of these genes was further affected by deletion of the *ump1* gene, encoding the low affinity ammonium transporter. Ump1 and Ump2 transcription levels also tracked expression of genes normally up-regulated during either filamentous growth or during growth of the fungus inside the host. Interestingly, haploid strains deleted

for the *b* mating-type locus, like those deleted for *ump2*, failed to filament on low ammonium; they also shared some alterations in gene expression patterns with cells deleted for *ump2* or over-expressing this gene. Deletion of *ump2* either in both mating partners or in a solopathogenic haploid strain resulted in a dramatic reduction in disease severity for infected plants, suggesting some importance of this transceptor in the pathogenesis program.

Introduction

Many fungi have the ability to switch from budding growth to filamentous growth, and several pathogenic fungi utilize this ability to cause disease. One of the cues for such a dimorphic switch is the availability of nutrients. In the presence of abundant carbon and nitrogen, fungal cells (like *Saccharomyces cerevisiae* and *Ustilago maydis*) grow by budding. However, under conditions of nitrogen limitation, the cells undergo pseudohyphal or filamentous growth. Ammonium transporter (AMT) genes encode proteins that are essential for uptake of ammonium as a nitrogen source and are conserved across a wide variety of taxa. AMT proteins in the different fungal species are essential for a variety of processes: *e.g.,* initiation of the dimorphic transition required for completion of the sexual life cycle in some, pathogenicity where the filamentous form is infectious, or foraging for nutrients. (K. Biswas & Morschhauser, 2005; Lo et al., 1997; Lorenz & Heitman, 1998; Smith, Garcia-Pedrajas, Gold, & Perlin, 2003). The high affinity AMT proteins of *S. cerevisiae*, *U. maydis* and *Candida*

albicans are required for filamentous growth under low ammonium conditions (S. Biswas, Van Dijck, & Datta, 2007; Lorenz & Heitman, 1998; Smith et al., 2003). While only the haploid invasive growth in *Schizosaccharomyces pombe* and *S. cerevisiae* on low ammonium is dependent on these ammonium permeases, both mating and haploid invasive growth in *Cryptococcus neoformans* are induced by ammonium limitation and specifically require the high affinity ammonium transporter (Mitsuzawa, 2006; Rutherford, Lin, Nielsen, & Heitman, 2008).

Mutational studies conducted on the high affinity AMT, Mep2, in *S. cerevisiae* and *C. albicans* reveal that Mep2 not only has a transport function but also has an independent role for the induction of filamentous growth. An additional function attributed at least to the *S. cerevisiae* Mep2 is the function of a transceptor, activating the cAMP dependent PKA pathway after the addition of ammonium to starved cells (Van Nuland et al., 2006). Although the exact connection between Mep2 signaling and the signal transduction pathway is not known, epistasis studies suggest RAS-cAMP being a downstream target of Mep2 (Lorenz & Heitman, 1998; Rutherford, Chua, Hughes, Cardenas, & Heitman, 2008) In *S. cerevisiae*, Mep2 dependent pseudohyphal growth is not restricted to low ammonium conditions but is dependent on the expression level of Mep2 (K. Biswas & Morschhauser, 2005; Rutherford, Chua, et al., 2008) In *S. cerevisiae*, the expression level of Mep2 is important for its regulatory functions, whereby induction of Mep2 leads to pseudohyphal growth under non-limiting ammonium conditions. This led the authors to hypothesize a role for Mep2 interacting with signal transduction pathway(s) to activate downstream effectors to lead to

changes in phenotype of haploid cells. The study revealed differential expression of genes predicted to be involved in pseudohyphal growth, and presented evidence for differential activation of the MAPK pathway in a Mep2-dependent manner.

Although many different signals can induce filamentous growth, the strategy for responding to these extracellular signals by cellular differentiation has been proposed to be conserved among fungi, *i.e.*, induction of comparable developmental pathways (Sánchez-Martínez & Pérez-Martín, 2001) In *Ustilago maydis*, the pathogen of maize, the growth form of wild-type cells and pathogenicity on maize are inextricably linked because the filamentous, dikaryotic stage is the natural pathogenic cell type. The haploid strains of the fungus are saprophytic, budding cells. Cell fusion is controlled by the *a* mating-type locus, encoding pheromone precursors and receptors, similar to those of yeast. The *b* mating-type locus encodes two homeodomain proteins, bE and bW, that interact when produced from different alleles. Heterozygosity at the multiallelic *b* locus is required for the production and maintenance of a stable filamentous dikaryon, and for pathogenicity (Flora Banuett & Herskowitz, 1994). The *b* heterodimer controls post cell fusion events required for the production of a stable filamentous dikaryon and regulates the transcription of a set of target genes controlling morphogenetic transitions and pathogenicity (Flora Banuett & Herskowitz, 1994). However, little is known about the genes directly involved in the transition from budding to filamentous growth, though it clearly is influenced by the control exerted by the *b* locus, in addition to environmental conditions

(e.g., lipids, including corn oils; low pH; and nitrogen availability (R Kahmann, Basse, & Feldbrugge, 1999; Klosterman, Perlin, Garcia-Pedrajas, Covert, & Gold, 2007)) that can lead to a similar filamentous morphology *in vitro*, even in the absence of a mating partner. Global gene expression differences for each cell type have been observed (Andrews, Garcia-Pedrajas, & Gold, 2004; Babu, Choffe, & Saville, 2005; Garcia-Pedrajas & Gold, 2004), strengthening the idea that elucidating the developmental programs triggered by the morphogenetic transition in response to various signals *in vitro* may reveal normal interactions between the pathogen and host *in vivo* (Sánchez-Martínez & Pérez-Martín, 2001)

For *U. maydis*, phenotypic changes in response to low ammonium require only one of the ammonium transporters, Ump2. Deletion of *ump1* (encoding the other, low affinity ammonium transporter) does not yield any discernible difference in phenotype from the wild-type (*i.e.*, filamentous growth under ammonium limiting conditions). In contrast, cells deleted for *ump2* (encoding the high affinity ammonium transporter) were unable to produce filaments under similar growth conditions (Smith et al., 2003). In *S. cerevisiae* transcriptional control of ammonium permeases occurs in response to a particular nitrogen source and this ensures expression of appropriate pathways (Cooper, 2002). Such control of *ump2* expression similarly could be the case in *U. maydis*. MAPK and cAMP-dependent PKA signaling pathways are both implicated in affecting filamentous growth in *U. maydis*, but their role in affecting filamentation in response to low nitrogen availability, specifically ammonium, mediated by *ump2*, has yet to be fully elucidated. Earlier investigations hypothesized that the

connection of *ump2* to the PKA signaling pathway occurs at multiple levels. More recently, Ump2 has been found to interact physically with Rho1 (Paul, Barati, Cooper, & Perlin, 2014), a small G protein required for viability in haploid *U. maydis* cells (Pham et al., 2009). This provides additional evidence for a role of the Ump2 protein in coordinating with signaling pathways (See Figure 6 for a diagram of the current model of the mating pathway).

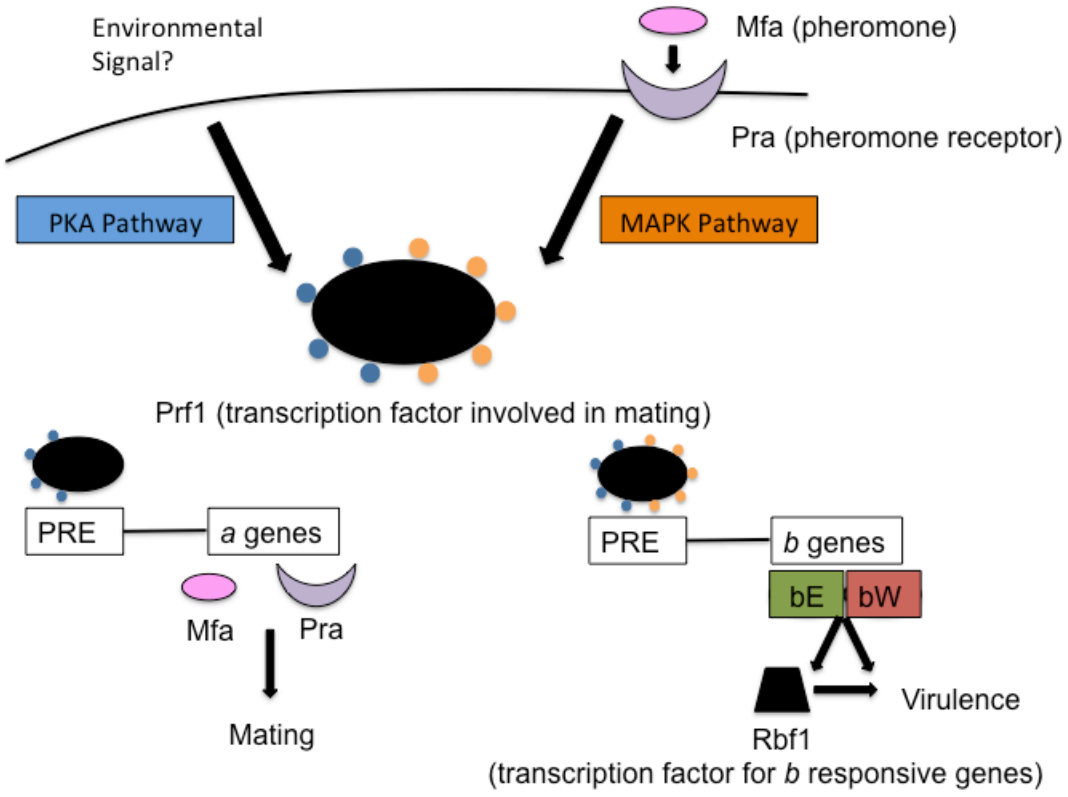

Figure 6: Cross-talk between PKA Pathway and MAPK Pathway in *Ustilago maydis* result in mating and virulence.

In the current study, we address the role of *ump2* in modulating global transcription to initiate the appropriate morphogenetic response. We show that filamentation facilitated by *ump2* can occur on nitrogen-replete media and this is

dependent on the expression levels of *ump2* as seen in the case of *S. cerevisiae*, suggesting that ammonium limitation as such might not be solely responsible for induction of the filamentous response by *ump2.* The results of the transcriptional profiling revealed that AMT proteins affect transcription of genes shown to be essential in causing disease on the host. Moreover, haploid cells deleted for the *b* mating-type locus, similar to *ump2* deletion mutants, lost their ability to filament on low ammonium, and shared some transcriptional alterations with the *ump2* mutant. Finally, our study also reveals the requirement for AMT proteins in causing disease on the host.

Methods

Strains and Growth Conditions

U. maydis cells were grown at 30^{o}C on Array Medium [AM] (6.25% Holliday Salt Solution (Holliday, 1974), 1% glucose, 30 mM Glutamine/50 µM Ammonium sulfate and 2% agar) and Array Medium [AM] with low ammonium (6.25% Holliday Salt Solution, 1% glucose, 50 µM ammonium sulfate and 2% agar) for 48 hrs. In order to assure that any filamentation observed on the latter medium was not due to acidification of the media, the strains were also tested on AM with low ammonium that had been buffered with Tris-HCl, pH 7.0; filamentation was comparable in all cases to what was observed on unbuffered AM low ammonium plates. *U. maydis* strains used are listed in Table 1. All mutants were generated in either the FB1 background (F. Banuett & Herskowitz, 1989), or the SG200 background (Kamper et al., 2006).

Table 1: *U. maydis* strains used for Chapter 2.

Strain	Genotype	Reference
FB1 WT	*a1b1*	(F. Banuett & Herskowitz, 1989)
FB2 WT	*a2b2*	(F. Banuett & Herskowitz, 1989)
SG200	*a1mfa2 bW2bE1*	(Smith et al., 2003)
SG200 *Δump2*	*a1mfa2 bW2bE1 ump2::hyg^R*	This study
FB1 *ump2^{Otef}*	*a1b1 P$_{otef}$-ump2, cbx^R*	This study
FB1 *Δump2*	*a1b1 ump2::hyg^R*	This study
FB1 *Δump1*	*a1b1 ump1::cbx^R*	This study
FB1 *Δump2c*	*a1b1 ump2::hyg^R P$_{otef}$-ump2, cbx^R*	This study
FB2 *Δump2*	*a2b2 ump2::hyg^R*	This study
FB2 *Δump2c*	*a2b2 ump2::hyg^R P$_{otef}$-ump2, cbx^R*	This study
FB1 *Δb*	*a1b1 bE/W::hyg^R*	This study
FB1 *Δb c*	*a1b1 bE/W::hyg^R , b, cbx^R*	This study

Primer Design

Primers, other than for the Real Time PCR, were designed using the Primer 3 program available at [http://frodo.wi.mit.edu/primer3/] (Rozen & Skaletskey, 2000). Primers were obtained from Eurofins MWG Operon [Huntsville, AL].

PCR

PCR reactions were run on a PTC100 thermal controller [MJ Research Inc., San Francisco, CA] and a DNA Engine thermal cycler [BioRad Laboratories, Hercules, CA]. PCR cycling conditions utilized an initial denaturation

temperature of 94°C for 4 minutes, followed by 34 cycles of a three-step process of denaturation at 94°C for 30 seconds, annealing at 60°C for 30 seconds and extension at 72°C for 1 minute per 1 kb of anticipated product length. A final extension at 72°C for 10 minutes was used to complete all products. For most reactions Ex-Taq™ Hot Start DNA polymerase (Takara, Madison,WI) or Apex DNA polymerase [Genesee Scientific, San Diego, CA] was used. For high fidelity reactions, Phusion DNA polymerase [Finnzymes, Lafayette, CO] was used.

Genetic Manipulation and Vector Construction

Deletion and overexpression of *ump2* in *U. maydis* were obtained by homologous recombination as described previously (Brachmann, Konig, Jullus, & Feldbrugge, 2004). The *ump2* deletion construct was created using a 6 kb PCR product from strain um2h-2, *Δump2 a1b1* (Smith et al., 2003) generated using primers Ump2KOup5' (GGCAAGACAAGACGAGAAGA) and Ump2_Dn_TapR (TGCGTGTCTCAAACTCCTCT). The *ump2* overexpression construct was produced by amplifying the *ump2* ORF from the plasmid pUmp2 303 using the Ump2_CGO5' (ATTAACCGCGGAAATGGTTAACGCCAGCTAC) and Ump2_CGO3' (TGATTGCGGCCGCTTAGACAGCAGTAGGCTG) primers and cloning the product into pCR2.1 TOPO (Invitrogen) (Smith et al., 2003). To provide constitutive expression, the *ump2* ORF was cloned after the P*otef* promoter between the *SacII* and *NotI* sites of the p123 vector (Otef expression vector) (Weber, Abmann, Thines, & Steinberg, 2006). The Otef expression vector was linearized using the restriction enzyme *Ssp1* before transforming *U. maydis*

to select for recombinants at the *ip* locus, providing carboxin resistance (Brachmann, Weinzieri, Kamper, & Kahmann, 2001). The construct for making the *b* gene deletion in *U. maydis* strain FB1 (*a1 b1*) was obtained from Dr. J. Kämper (Kämper, 2004) Complementation of *ump2* similarly used the ORF cloned with or without its native promoter into the Otef expression vector. Complementation of the *b* deletion mutant was achieved by cloning both ORFs (and promoter regions) from the wild-type *b* mating locus into the Otef expression vector. This construct was introduced into *b* deletion mutants as previously described.

RNA Isolation and Expression Analysis

U. maydis cells were grown on AM-glutamine high ammonium and AM-low ammonium plates for 48 hours. RNA isolation for the transcriptional profile was as described previously (Perlin et al., 2015). These cells were further processed using the RNeasy plant mini kit [Qiagen, Valencia, CA] or the Quick-RNA™ MiniPrep Plus (Zymo Research, Irvine, CA) following the manufacturer's instructions. The integrity of the RNA samples was checked using an Agilent Bioanalyser 2100. The RNA samples were treated with DNaseI [New England Biolabs, Ipswich, MA] before proceeding to the preparation of the cDNA samples. The double stranded cDNA samples were prepared with Super Script III [Invitrogen, Carlsbad, CA] using 25 mg of RNA as the starting material and following manufacturer's instructions. 10 mg of cDNA was sent to Nimblegen [Rejkavik, Iceland] for hybridization experiments on a custom *U. maydis*

oligonucleotide microarray (Robledo-Briones & Ruiz-Herrera, 2013) representing all predicted ORFs and positive and negative control genes. Data from two biological replicates were analyzed for each condition examined, using Ingenuity [Qiagen, Redwood City, CA] and R (Bioperl; http://bioperl.org/wiki/Main_Page). Genes of interest were initially picked as those with p-value <0.1. Microarray data files and analyses from R are available upon request but have not been deposited, as they did not meet statistical significance requirements for the two biological replicates and thus served only as an indicator of candidate genes for comparison with RNA-Seq and to examine further via qRT-PCR.

For Real-Time PCR experiments, RNA was isolated from *U. maydis* strains using the TRIzol reagent protocol from Invitrogen, with modifications. *U. maydis* cells were grown on AM-glutamine, AM-ammonium and AM-low ammonium agar plates for 48 hours. The cells were scraped off the plates and homogenized under liquid nitrogen in a mortar and pestle. Roughly 100 mg of the homogenate was treated with 1 ml of TRIzol and processed further for RNA extraction. 5 µg of total purified RNA samples were treated with Turbo DNase [Ambion Inc., Foster City, CA] before being used for synthesizing cDNA using the cDNA synthesis kit [Superscript II, Invitrogen]. The cDNA was used as a template for RT-PCR and real-time qRT-PCR.

For Illumina Next Generation Sequencing (RNA-Seq), the total RNAs from one biological sample of each strain treatment were subsequently sent to BGI-Americas (Davis, CA) for cDNA library construction, sequencing, and initial bioinformatic analyses. The cDNA library format was a 140-160 bp insert library

(Truseq library prep) for each sample, with Read length Paired-end 100 bp and Data output of 4 Gb clean data per sample. These data have been deposited at the Gene Expression Omnibus (GEO) at ncbi. (http://www.ncbi.nlm.nih.gov/geo; GSE64993 and GSM1585543-GSM1585550) and provide quality scores and statistical significance measures. RNA-Seq data from different conditions were processed using the Trinity pipeline (Grabherr et al., 2011; Haas et al., 2013), and RNA-Seq reads from each sample were aligned using bowtie (Langmead, Trapnell, Pop, & Salzberg, 2009) against protein coding sequences extracted based on annotation. Fungal gene expression levels were estimated by RSEM (B. Li & Dewey, 2011), and edgeR with TMM normalization (Kadota, Nishiyama, & Shimizu, 2012; Robinson, McCarthy, & Smith, 2010) was used to identify differentially expressed genes (DEGs) between each pair of conditions with a corrected p-value cutoff of 0.001; for these analyses, RPKM measurements were used to calculate log2-fold changes. Assessment of overlapping sets of differentially-expressed genes relative to wild-type FB1 grown on AM-high ammonium was made using the online version of VENNY (http://bioinfogp.cnb.csic.es/tools/venny/index.html; (Oliveros, 2007-2015). Functional category enrichment was determined using the FunCat database available at http://mips.helmholtz-muenchen.de/funcatDB/ and enrichment was considered to be those categories with $p<0.001$.

To further evaluate differences in expression levels of a subset of genes suggested by microarray data or RNA-Seq, real time quantitative RT-PCR (qRT-PCR) was employed. Primers for the different genes (Table 2) were designed

using the ABI Primer Express software version 3.0, ensuring that all the primer sets investigated had the same amplification efficiency. The generated cDNA was diluted 5-20 fold depending on the starting concentration of RNA that was used for making cDNA. All real-time PCR reactions were performed in a 62.4 µl mixture containing 1/10 volume of the diluted cDNA preparation, 1X Power SYBR green PCR master mix [Applied Biosystems, Foster City, CA, USA], 1.6 µl each of the 2.5 µM forward and reverse primers, making up the reaction volume to 62.5 µl with dH_2O. Quantifications of RNA expression levels were performed in an Applied Biosystems Step-One thermocycler using the following PCR conditions: 95^{o}C for 10 mins followed by 95^{o}C for 15 secs and 60^{o}C for 1 min for 40 cycles. Melting curve analysis was performed at the end of each cycle to ensure specificity of the reaction. The concentration was determined by the comparative CT method (threshold cycle number at the cross point between amplification plot and threshold) and values were normalized to expression of the constitutively expressed gene, *eif2B* (unchanged in RNA-Seq analysis), encoding the translation initiation factor eIF2. Changes in the gene expression are averages of at least three biological replicates (except for the FB1 *Δump1* mutant, for which one biological replicate was tested) and are displayed as log2-fold changes relative to expression of wild-type FB1 under high ammonium condition or as a comparison of the mutant at high and low ammonium.

For statistical analysis of qRT-PCR results, first the transcript level of each target for each mutant in low vs high ammonium conditions was compared, using Kruskal Wallis (Daniel, 1990), as we do not except the transcript level to vary

Table 2: Genes and the Primers used for qRT-PCR for Chapter 2

Gene Name	Primers	Sequences (5' → 3')
guanine nucleotide exchange factor	rt-eIF-2B-F new	ATCCCGAACAGCCCAAAC
	rt-eIF-2B-R new	ATCGTCAACCGCAACCAC
ump1 (um04523)	rt-Ump1-F	CGGTCTCACCTGGATGTTCCT
	rt-Ump1-R	AGCCAACGACGGACCACTT
ump2 (um05889)	rt-Ump2-F	TGGGTCCCGTTCTCATTTTC
	rt-Ump2-R	AGGCGATGGGATTGTAGACAA
prf1 (um02713)	rt-Prf1-F new	TCGGTAGAACGAGCTGTGATG
	rt-Prf1-R new	CTGTTGGACGATGTTGGAGTTG
mfa1 (um02382)	rt-Mfa1-F	ATGCTTTCGATCTTCGCTCAG
	rt-Mfa1-R	TAGCCGATGGGAGAACCGT
bE (um00577)	b2Elft164	CTACCCGAACTTTTCCCTCAC
	b2Ert451	TTCAAGGCTTTGCTTGTGTCT
bW (um00578)	b1Wlft1559	TCGAGTCTGCCTCAATTCCT
	b1Wrt1827	CTCTCCTATGCTGGCTCCAC
kpp6 (um02331)	rt-Kpp6-F new	GGTACCGTGCTCCGGAGATT
	rt-Kpp6-R new	CATCCGACTGCCCATACAT
actin (um11232)	rt-Actin-F	CTCGGGTGACGGTGTTACG
	rt-Actin-R	AGTGCGGCAGCGAGTAACC
rep1 (um03924)	rt-Rep1-F	TGGTCTCGAAGAACTCGAACAA
	rt-Rep1-R	CCGAAAAGACCGTCCAGGAT
egl1 (um06332)	rt-Egl1-F	TGCAGCAAACTGCCCAAA
	rt-Egl1-R	TCCGAGAAGCGCCACTTG
mig2-6 (um06126)	rt-Mig2-6-F	GGCCAGTTGCAAGTTCCAA
	rt-Mig2-6-R	GCTGCCGCCGTGTTCTAC
pten (um3760)	rt-PTEN-F	CGGACGTACGGGTGTCAAG
	rt-PTEN-R	CACCCTGCAGAGGCAATGT
probable *hxt5*-hexose transporter (um02037)	rt-Hxt5-F new	TCTCGTCGGGTATCGGAAAG
	rt-Hxt5-R new	CGTAACCGAGAATGAAGAAGCA
chitin deacytelase (um01788)	rt-01788-F	TCATCCCTCAAGCGGTCAAC
	rt-01788-R	AGTGCGGGATCCGCTGTA
conserved hypothetical (um03116)	rt-03116-F	AGAGGCAGATCTTTGGAAACGT
	rt-03116-R	TGGTTGAACGAAGCAGAAGCT
related to polyketide synthase (um04095)	rt-04095-F	TGGCCCGCGGATGAT
	rt-04095-R	TGCCGGGCTCGTTGTC
chitinase (um06190)	rt-06190-F	CGCACGTCCACGAATAAGCT
	rt-06190-R	GAGTCGAGGCTGTCCAATCC
probable high affinity glucose transporter (um11514)	rt-11514-F	TGCTGGCCGAGTACCATGA
	rt-11514-R	GCCTTCGCCAGAGCTCTCT

normally. Second, the absolute transcript level for each mutant under each conditions was compared to that for FB1 wild-type under the same condition. So, all the mutants on high ammonium were compared to wild-type on High ammonium and then all the mutants on low ammonium were compared to the wild-type on low ammonium. This analysis again used Kruskal-Wallis, as we assume these do not vary normally. Third, analysis of covariance on all of the changes for high to low ammonium. This analysis corrects for any variations within biological replicates of each mutant and sets the "control" (in our case High Ammonium) to zero, and then looks at the absolute increase or decrease in transcript level based on these corrections. Values obtained with RNA-Seq and with qRT-PCR were normalized against those obtained for FB1 (wild-type) grown on nitrogen-replete medium. From those baseline values all other relevant comparisons could be made among the remaining strains and conditions.

Mating Assay and Plant Pathogenesis

Cell densities of liquid cultures were measured spectrophotometrically. Liquid overnight cultures were diluted in fresh media to obtain an Absorbance at 600 nm (A600) of 0.1. The newly inoculated culture was allowed to grow for an additional 4 hrs to obtain an A600 between 0.5 - 0.7 (exponential growth phase). Mating assays were performed using 10^7 cells / ml and spotting 10 µl onto PDA charcoal as previously described (F. Banuett & Herskowitz, 1989; Gold, Brogdon, Mayorga, & Kronstad, 1997). Plant infection using 8-10 day old Golden Bantam corn seedlings [Bunton Seed Co., Louisville, KY and W. Atlee Burpee & Co.,

Warminster, PA] was performed with a cell density of 10^8 cells / ml for pre-mixed haploid strains of opposite mating type or for the solopathogenic SG200 strain as previously described (Gold et al., 1997) and virulence was rated by a disease index (DI) on a scale of 0 to 5 (Gold et al., 1997). Statistical analysis of the disease index measures was performed using a Kruskal-Wallis Test with a Multiple Comparison Test in R (Daniel, 1990).

Results

Filamentation in response to ammonium is correlated with transcription level of the *ump2* gene.

In *C. albicans*, higher concentrations of ammonium blocked filamentation, even when the high affinity transporter was over-expressed (K. Biswas & Morschhauser, 2005). In contrast, studies in *S. cerevisiae* revealed that increasing the expression of the corresponding high affinity ammonium transporter (Mep2) led to pseudohyphal growth, even under non-inducing conditions (Rutherford, Chua, et al., 2008). Thus, we explored the role of *ump2* expression in affecting filamentation in *U. maydis*. Similar to increasing expression levels *mep2* in *S. cerevisiae*, overexpression of *ump2* caused filamentous growth of haploid cells of *U. maydis* under nutrient rich conditions. This is in contrast to wild-type cells that grow by budding (yielding smooth colonies) under similar nutrient rich conditions (Figure 7a). When grown in low ammonium (AM-low ammonium media), cells carrying the *ump2* overexpression construct showed extensive filamentous growth within 48 hours as opposed to the wild-type cells that display filamentous growth only after 3 days (Figure 7a).

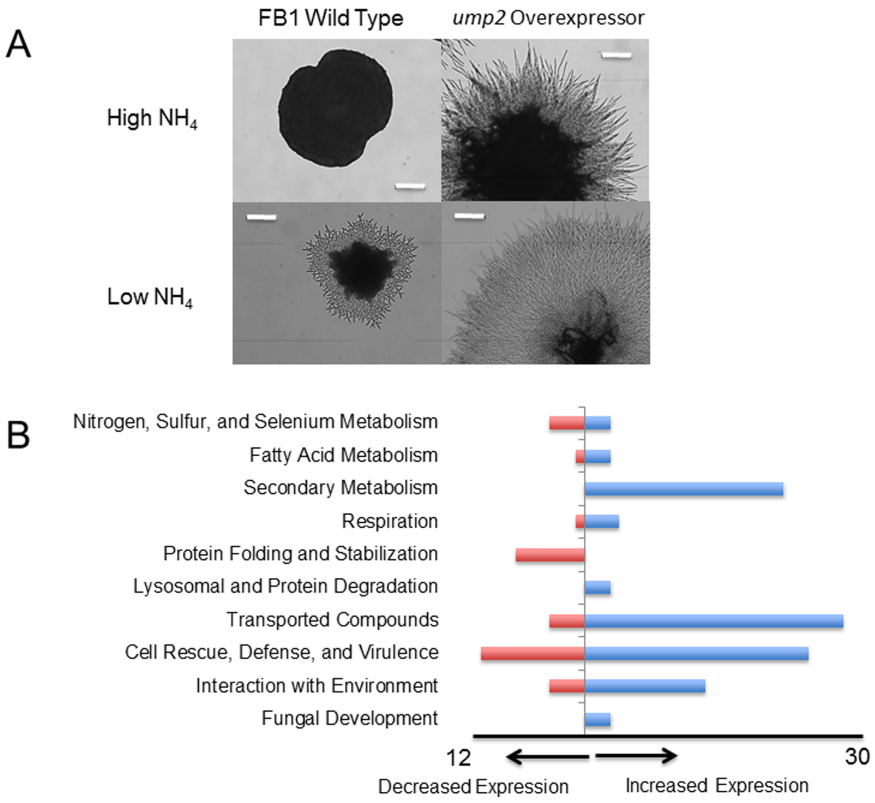

Figure 7: Overexpression of *ump2* leads to phenotypic and global genes expression changes.
(A) Haploid cells wild-type FB1 and *ump2* overexpressor strain (FB1 *ump2*^{otef}) were grown on AM high ammonium (AM, Array Medium (6.25% Holliday Salt Solution [20], 1% glucose, 30 mM Glutamine/50 µM Ammonium sulfate and 2% agar)). Cells overexpressing *ump2* showed filamentous growth in this nitrogen and carbon replete medium. On AM-low ammonium (50 mM NH_4) for 48 hrs, the *ump2* overexpressor showed hyper-filamentation relative to wild-type FB1. Size bars, 200 µm. (**B**), Functional categories enriched in both the *ump2* overexpressor on high ammonium and FB1 wild-type on low ammonium. Red bars represent the number of genes per category with decreased expression and blue bars represent the number of genes per category with increased expression. Functional category enrichment was determined using the FunCat database available at http://mips.helmholtz-muenchen.de/funcatDB/ and enrichment was considered to be those categories with $p<0.001$. Differential expression as determined from RNA-Seq data (log2 fold change>1 and $p<0.001$).

This suggests that ammonium limitation per se might not be the only trigger for filamentous response mediated by *ump2*.

Overexpressing *ump2* in replete medium mimics part of the low ammonium response in wild-type.

Filamentation due to ammonium levels is only observed on solid media (*i.e.*, agar plates) and usually begins by 48 hours. Thus, for all expression experiments, cells were harvested at 48 hours. For RNA-Seq (and later, for qRT-PCR), after RPKM calculations, all data were then normalized against those for FB1 wild-type, grown on AM-high ammonium medium (high). This provides the opportunity to make all other comparisons for expression.

The first biological question we sought to investigate was which genes were expressed or altered in gene expression during the filamentation we observed for haploid *U. maydis* cells. In the *ump2* overexpressor strain (FB1 *ump2*^{otef}), filamentation under non-inducing conditions was accompanied by a change in global gene expression (see Figure 8). According to RNA-Seq data (see Table S2 for RSEM/edgeR analyses of differentially expressed genes (DEGs), overexpressing *ump2* resulted in differential expression of 627 genes under replete (*i.e.*, high) ammonium conditions (log2 fold>|1|, *i.e.*, >2-fold change; $p<.001$; and FDR<0.001), nearly 10% of the predicted *U. maydis* transcriptome. Of the genes differentially expressed, 238 also corresponded to genes that were differentially expressed in the wild-type under low ammonium conditions (Figure 8a and 8b). Of this group, 238, or approximately 67%, were differentially expressed in the same direction and with similar magnitude in the *ump2* overexpressor on replete media and the wild-type strain under low ammonium conditions. These genes corresponded to proteins of various functions (Figure 7b). Since *ump2* is typically induced under low ammonium

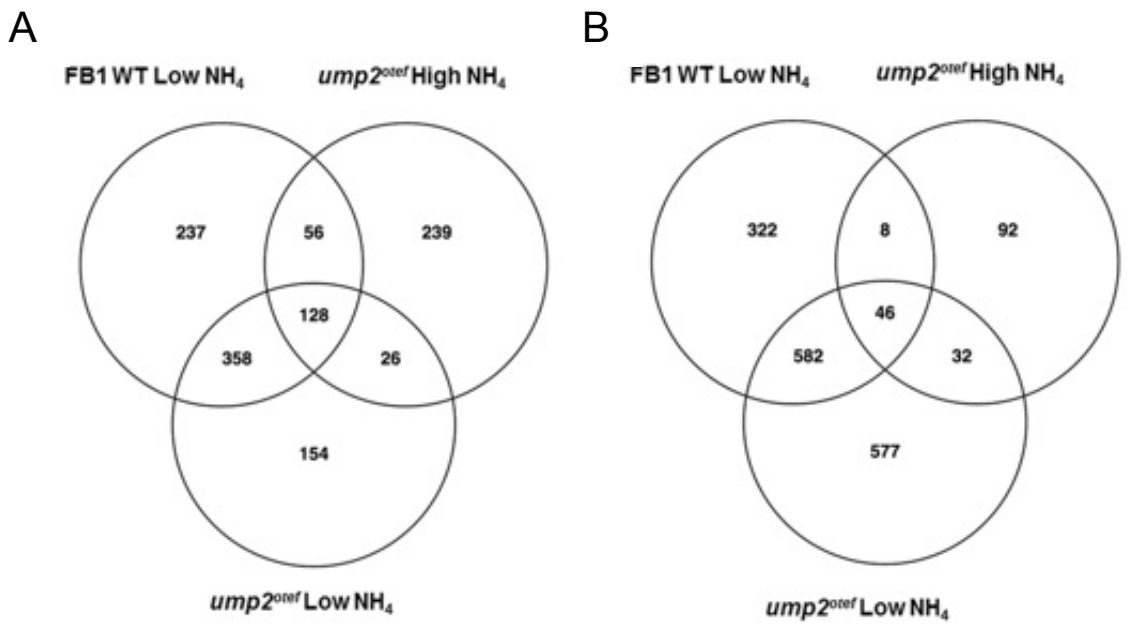

Figure 8: Venn diagram of RNA-Seq identified differentiall expressed genes for the *ump2* overexpressor compared to wild-type FB1 on low ammonium.
Genes identified by RSEM/edgeR analysis of RNA-Seq data were used to select a pool of differentially expressed genes for each strain/condition, with minimum 1 log2-fold fold change, p-value<0.001, and FDR (False Discovery Rate)<0.001. **(A)** Up-regulated genes; **(B)** Down-regulated genes. FB1 WT Low NH_4, FB1 wild-type strain on AM-low ammonium; *ump2*^{otef} High NH_4, *ump2* overexpressor strain FB1 *ump2*^{otef}*,* grown on AM-high ammonium; *ump2*^{otef} Low NH_4, *ump2* overexpressor strain FB1 *ump2*^{otef}*,* grown on AM-low ammonium.

conditions in the wild-type strain, it is not surprising that some of the genes differentially expressed related to metabolism of nitrogen, as well as other compounds such as carbohydrates and fatty acids. Other functional categories also enriched included cellular transport, cell rescue and defense (including detection of nutrient depletion), interaction with environment, and fungal cell development. These data also suggest that, in general, *ump2* overexpression on nitrogen-replete medium up-regulates expression, as the vast majority of genes that were differentially expressed had increased expression levels.

Overexpression of *ump2* under low ammonium conditions also results in changes in global gene expression.

Since we wanted to identify genes that were differentially expressed in strains that exhibited filamentation, we again compared the *ump2* overexpressor strain, which hyperfilaments in low ammonium, with the FB1 wild-type strain, exhibiting normal filamentation. RNA-Seq showed that overexpressing *ump2* under low ammonium conditions resulted in differential expression of 1903 genes (almost 30% of the genome) as normalized against the wild-type FB1 strain under replete ammonium conditions (Figure 8). Of this subset of genes, also under low ammonium conditions, FB1 wild-type had 486 genes (or roughly 25%) similarly upregulated (Figure 8a) and 628 genes (or roughly 33%) down regulated (Figure 8b). As such, 789 (almost 40%) of those genes differentially regulated in the *ump2* overexpressor on low ammonium were not differentially expressed in wild-type. Of this set of genes, only 58 (about 8%) were also differentially regulated when *ump2* was overexpressed under replete ammonium conditions, meaning that the differential regulation of the rest was specific to overexpressing *ump2* under low ammonium conditions. Of particular note, we found differential expression for the genes encoded in the *b* mating locus, *um00577* (*bE1*) and *um00578* (*bW1*). To differing degrees, both these genes were down-regulated in the *ump2* overexpressor on low ammonium medium.

The vast majority (577) of the 789 genes uniquely differentially regulated in the FB1 *ump2* overexpressor on low ammonium were down regulated. Enriched functional categories as determined by FunCat analysis include various types of metabolism, e.g., nucleotides, chitin, fatty acid, isoprenoid, and energy

reserves, as well as G1/S transition of the mitotic cell cycle, cell cycle-dependent cytoskeleton reorganization of both actin and microtubules, and DNA topology. Additionally, many gene expression categories were functionally enriched, including RNA synthesis and processing, splicing, and regulation of transcription factors. Several protein regulatory functional categories were also enriched, including protein synthesis, ribosome biogenesis, translation, modification by ubiquitination, and regulation by modification. Finally, cell growth and morphogenesis functional categories were also enhanced (Figure 9).

There were 497 genes (184 upregulated and 313 down regulated) that were differentially expressed in the FB1 wild-type under low ammonium that were not differentially expressed by the overexpression strain (FB1 *ump2*^{otef}) under the same conditions (Figure 8; Figure 9b). Enriched functional categories in this subset of genes included amino acid metabolism, assimilation of ammonia, carbohydrate metabolism, secondary metabolism, and transported substrates. Additionally, regulation of protein functional categories were enriched such as protein folding and stabilization, protein targeting, sorting, and translocation, and proteolytic protein processing. Several regulatory functional categories were also enriched, including calcium mediated signal transduction, transmembrane signal transduction, and receptor mediated signaling. Interestingly, in the wild-type on low ammonium conditions, several genes related to cell wall biogenesis, microtubule cytoskeleton, and cell type differentiation were differentially regulated, while in the *ump2* overexpressor on low ammonium, the expression of these genes was comparable to the wild-type on replete media conditions.

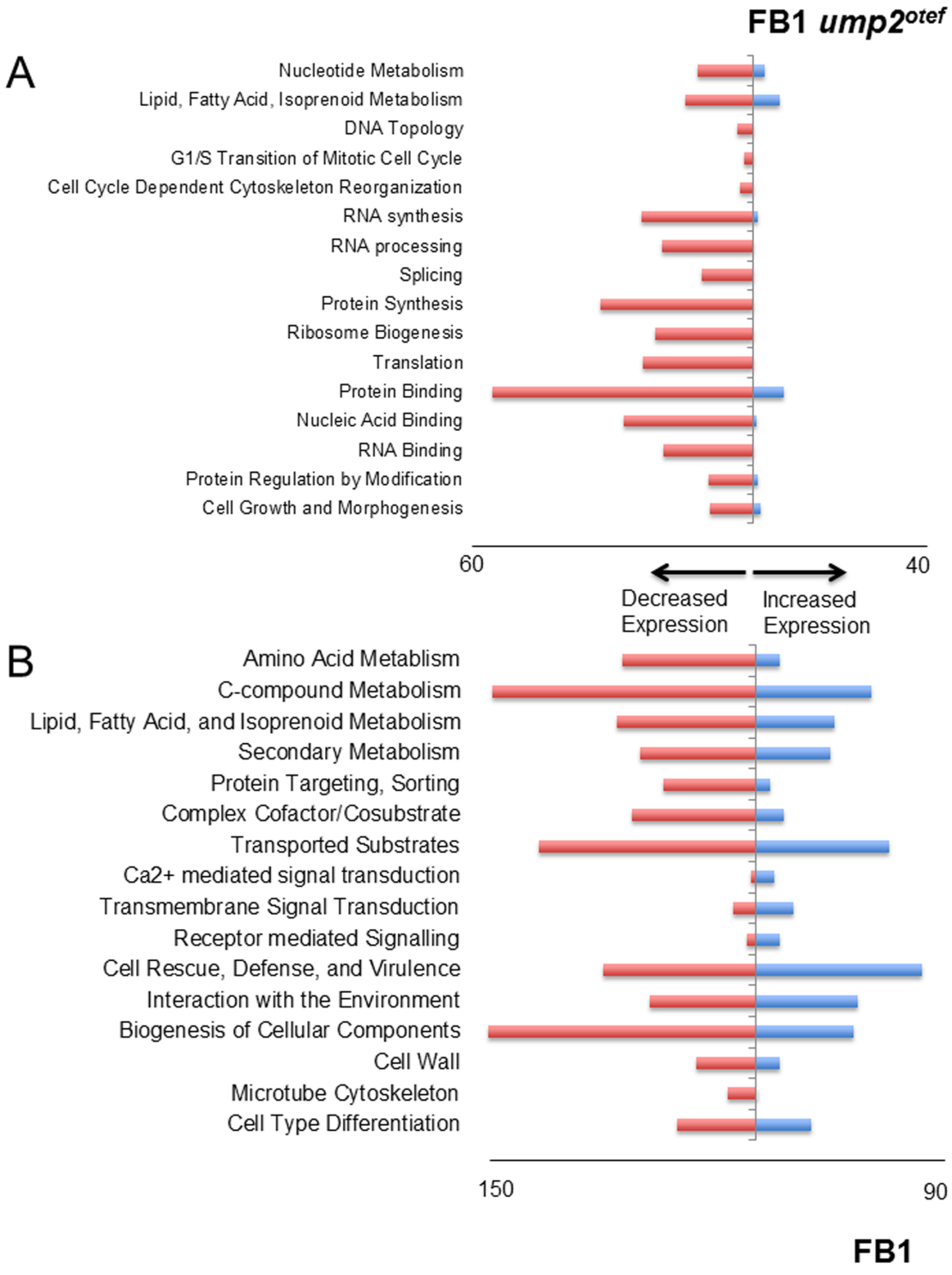

Figure 9: Functional Category Analysis of DEGS in *ump2* overexpressor. **(A)** Functional categories enriched in the *ump2* overexpressor (FB1 *ump2* ^{otef}) but not in the FB1 wild-type under low ammonium conditions. **(B)** Functional categories of genes differentially expressed in FB1 wild-type on low ammonium but not differentially expressed in an *ump2* overexpressor under similar ammonium availability.

Overall, there was an overlap of 128 genes up-regulated in common among the wild-type FB1 grown on low ammonium and the *ump2* overexpressor grown on either high or low ammonium medium; similarly, there were 46 genes in common among these strains/treatments that were down-regulated (See Figure 8a and b, respectively). Since all three conditions produced filamentous growth (in contrast to wild-type on high ammonium) these genes are candidates for those involved in the filamentation process. The magnitude of differential expression was the same for the majority of genes upregulated in common among FB1 grown on low ammonium and the *ump2* overexpressor grown on either high or low ammonium medium. Seven of the 128 were more highly expressed in FB1 *ump2*^{otef} on high ammonium compared with FB1 on low ammonium; five of these were expressed at the same levels in both wild-type and FB1 *ump2*^{otef} on low ammonium. The remaining two were also more highly expressed in FB1 *ump2*^{otef} than in wild-type on low ammonium (um01949 - uncharacterized protein; um03402 - indole–3-acetaldehyde dehydrogenase). There were an additional eight genes upregulated in FB1 *ump2*^{otef} on low ammonium compared with FB1 on low ammonium, one of which was, unsurprisingly, *ump2.* Of the remaining, five were predicted to encode uncharacterized proteins, while one (um01796) encoded the effector family protein, eff-1. The final gene, um04309, encodes a probable alpha-L-arabinofuranosidase precursor and was downregulated in *a1 ump2*^{otef} on high ammonium compared with FB1 on low ammonium.

Moreover, of the 46 genes downregulated in common, seven genes encoded as-yet-uncharacterized proteins whose expression was more greatly reduced in FB1 *ump2*^{otef} on low ammonium than in wild-type FB1 under the same conditions. Thus, although the hyper-filamentation of the *ump2* overexpressor under low ammonium conditions is the product of unique differential gene regulation in the strain, different from that of the FB1 wild-type under the same conditions, it is difficult to attribute obvious responsibility for the differences in filamentation since most of the genes just mentioned are annotated as “uncharacterized proteins”.

Deletion of *ump2* in the FB1 background results in loss of filamentation under low ammonium conditions, decreased mating phenotype on charcoal, and attenuated virulence.

Expression differences for the mating-type genes among the wild-type and the overexpression AMT mutant led us to examine the effect of the loss of this gene various phenotypes. Deletion of *ump2* resulted in the loss of filamentation under low ammonium conditions (Figure 10a). Constitutive expression of *ump2* rescued this loss of phenotype (Figure 10a).

We next examined the effect on the mating efficiency of these strains, measured by the formation of aerial hyphae “fuzz” and thus, *b* locus-dependent filaments, on charcoal agar plates (F. Banuett & Herskowitz, 1989). When compatible haploid mutant partners (*i.e.*, FB1 *Δump2* and FB2 *Δump2*) were mixed and spotted onto charcoal plates, a sharp reduction in fuzz was observed compared with the corresponding wild-type combination (see Figure 10b). When

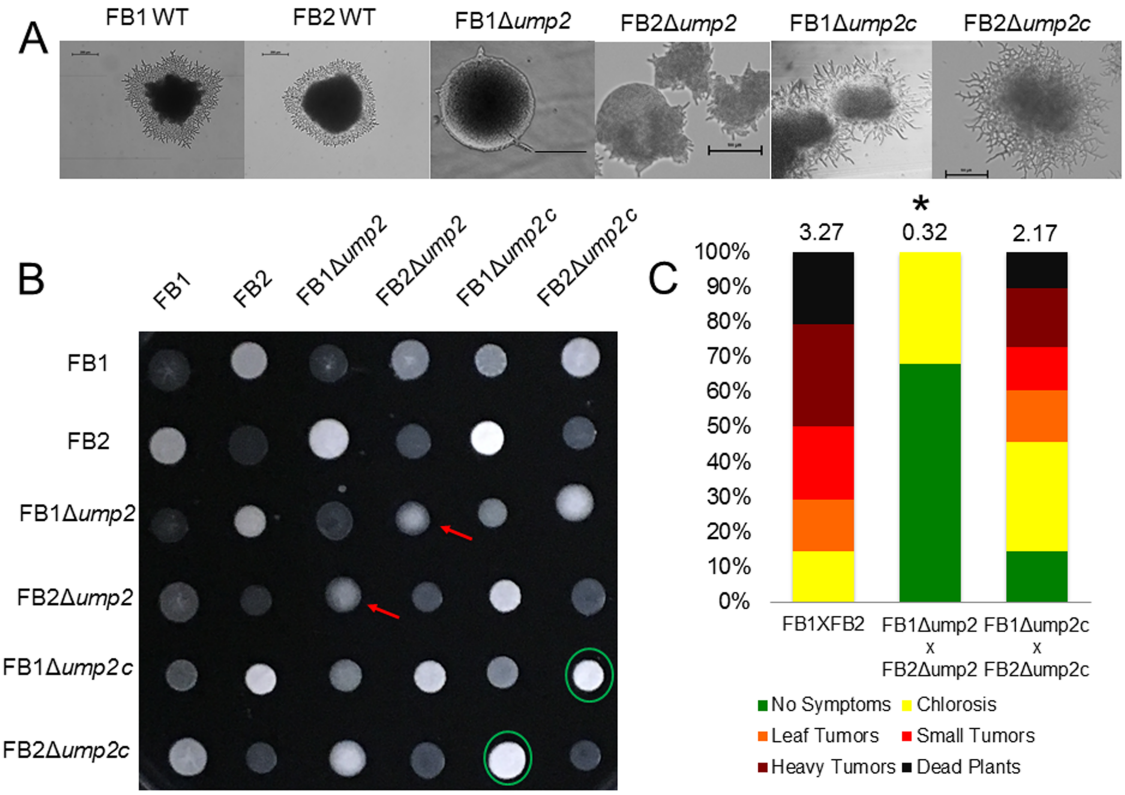

Figure 10: Phenotype changes related to deletion of *ump2.*
Deletion of *ump2* in a haploid strain eliminates filamentation due to low ammonium, but also the fuzz phenotype in matings on charcoal, and is associated with loss of virulence on maize. **(A)** Size bars, 100 µm. Complemented *ump2* deletion strains, filament on AM-low ammonium, as do their wild-type progenitors; size bar, 100 µm. **(B)** Plate mating assay on PDA charcoal medium for wild-type FB1 and FB2, the corresponding *ump2* deletion mutants, and these mutants complemented with a wild-type copy of the gene. Equal mixtures of haploid strains of opposite mating type background were plated onto PDA plates containing activated charcoal and were grown for 24 hrs. A positive mating reaction produced a white "fuzz" phenotype of aerial hyphae production. Red arrows indicate the reduced "fuzz" reaction of the *Δump2* mutants co-spotted with compatible *Δump2* mating partner. Green circles indicate wild-type levels of fuzz with matings that paired complemented strains **(C)** Disease symptom formation in the various *U. maydis* mutant strains. Plants were inoculated with one paired background, indicated on the X axis. The graphs display the percentage of plants with specific symptoms of infection 12 days post in fection. The infections where both partners bore the *ump2* deletion strain displayed reduced pathogenicity. Numbers above bar graphs are Disease Indices (DI) as calculated previously (Gold et al., 1997); * indicates significant compared to FB1 (a1 b1) x FB2 (a2 b2) and to FB1*Δump2c* x FB2*Δump2c* , Kruskal-Wallis Test with a Multiple Comparison Test with p value < 0.05.

experiments as it allows infectious filament formation and successful completion both mutants were complemented, the mating reaction was comparable to that of wild-type partners (Figure 10b).

Since an effect on mating was observed in mutants lacking the *Δump2* gene, we next examined possible effects of this mutation on virulence. The role of ammonium transporters in virulence was determined by mixing and co-injecting compatible mutant strains of opposite mating type, or by injecting solopathogenic SG200 or its derivatives (see below), into 8-10 day old maize seedlings and following virulence at regular intervals. The virulence for each infection was measured by a disease index, where the severity of the disease was assessed on a scale of 0-5. The results presented in Figure 10c indicate that infections in which both partners contained the *Δump2* mutation had significantly reduced virulence compared to the wild-type dikaryon (Figure 10c). The strains complemented with a wild-type copy of *ump2* gene displayed virulence comparable to that of the wild-type matings (Figure 10c).

Deletion of *ump2* in a solopathogenic strain eliminates filamentation on low ammonium, fuzz on charcoal medium, and pathogenicity.

Given the effects of deletion of *ump2* on filamentation on low ammonium or on pathogenicity, we wanted to examine whether these effects would be recapitulated in a haploid strain whose pathogenicity does not require mating and fusion of compatible haploids. When the *ump2* deletion mutant was produced in the solopathogenic haploid strain SG200 (Kamper et al., 2006), this strain also failed to filament on low ammonium. (Figure 11a). The SG200 strain (Kamper et

al., 2006) is a solopathogenic strain commonly used for plant pathogenicity experiments as it allows infectious filament formation and successful completion

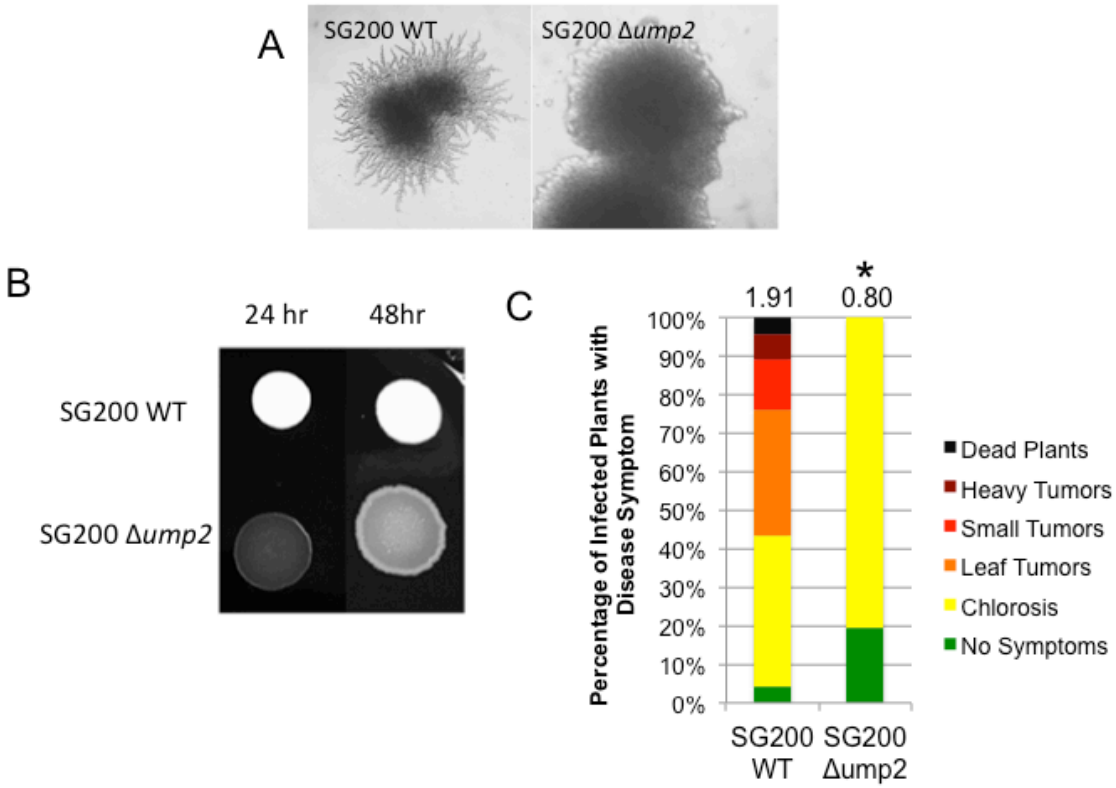

Figure 11: Phenotypes associated with *ump2* deletion in SG200. Deletion of *ump2* in a solopathogenic haploid strain eliminates filamentation due to low ammonium, but also the fuzz phenotype on charcoal, and is associated with loss of virulence on maize. (**A)** SG200, SG200*Δump2* strains. On AM low ammonium, for 48 h. Size bars, 200 µm. **(B)** Approximately 10^6 cells from mid-log phase cultures of either SG200 or SG200*Δump2* mutant were spotted onto PDA charcoal medium and allowed to grow for 24 h and 48 h at 26 ^{o}C. **(C)** Disease symptom formation in the *U. maydis* SG200 mutant strains. All strains were rated at 10 days post-infection. Plants were inoculated with one background, indicated on the X axis. A disease index (DI; (Gold et al., 1997)) was used initially to rate virulence of each infection, with 0 = no symptoms/ healthy plants, 1= chlorosis and / or anthocyanin production, 2 = small leaf galls, 3 = small leaf and stem galls, 4 = large galls and 5 = plant death. Diseases rating for the plants were obtained 12 days post infection (dpi) and the disease indices for each strain were averaged to get a DI measure per strain. The graphs display the percentage of plants with specific symptoms of infection. Above each bar is the DI; * indicates significant compared to SG200, Kruskal-Wallis Test with a Multiple Comparison Test with p value < 0.05, (Daniel, 1990)

of the lifecycle *in planta*. This strain normally produces the “fuzz” reaction on charcoal media. Surprisingly, when the *ump2* gene was deleted in this background, the resulting strain failed to display aerial hyphae on charcoal plates (Figure 11b).

In SG200, defects in pathogenicity due *ump2* could be assessed independently of the initial mating process. The results are presented in a percent of symptom formation graph (Lovely, Aulakh, & Perlin, 2011) (Figure 11c). Significantly more healthy plants survived at the end of the study in the group that was infected with the SG200 *Δump2* mutant and in most of the plants (~63-83%), the fungus was only able to progress in infection to stage 1 (chlorosis) (Figure 11c).

Deletion of the *b* locus or *ump2* eliminates filamentation due to low ammonium and leads to changes in global gene expression in response to nitrogen limitation.

Only two biological replicates were used in microarray experiments, and statistical significance for differences observed was not accurately obtained; thus, we also later examined most of the same strains (except *Δump2*) using RNA-Seq. Although only one biological replicate was used for each strain/condition in the RNA-Seq experiments, statistically significant differences were determined, with the caveat that greater power and confidence in the differences observed would be obtained through inclusion of additional biological replicates in the future. The results from both experiments were used to suggest candidates to investigate via qRT-PCR (quantitative real-time PCR).

Based on the *in vitro* expression data, we wanted to determine if reduced expression of the *b* locus (*bE* or *bW*) affected filamentation associated with low ammonium in haploid cells. Unlike wild-type FB1 and similar to what had been previously observed with deletion of *ump2* (Smith et al., 2003), *U. maydis* strains with the deletion of the entire *b* locus were unable to grow filamentously under low ammonium conditions (Figure 12a); this defect was rescued in the strain where the mutation was complemented with the wild-type *b* locus (Figure 12a). This suggests a role for the gene products of the *bE* and *bW* genes in filamentation associated with nutritional requirements such as low ammonium; this is in contrast to the role of the bE/bW heterodimer in dikaryotic filamentation associated with pathogenicity following mating. RNA-Seq (again normalized against FB1 on nitrogen-replete medium as a standard) allowed us to characterize both global changes in transcription associated with ammonium levels and those due to deletion of the *b* locus (Figure 13).

When FB1 wild-type *U. maydis* was grown on solid media with limited ammonium, 1675 genes (approximately 25% of the genome) were differentially expressed. In the *b* deletion mutant, on replete media (*i.e.*, abundant nitrogen), only 493 genes were differentially expressed compared to wild-type on similar media, suggesting a limited role for the *b* locus under nitrogen-replete conditions. However, on low ammonium conditions, 1977 genes were differentially expressed in the *b* mutant, indicating a combined effect due to mutant, discussed below) did not filament on low ammonium, we sought to identify changes in gene expression in the non-filamenting mutants compared to wild-type. An additional

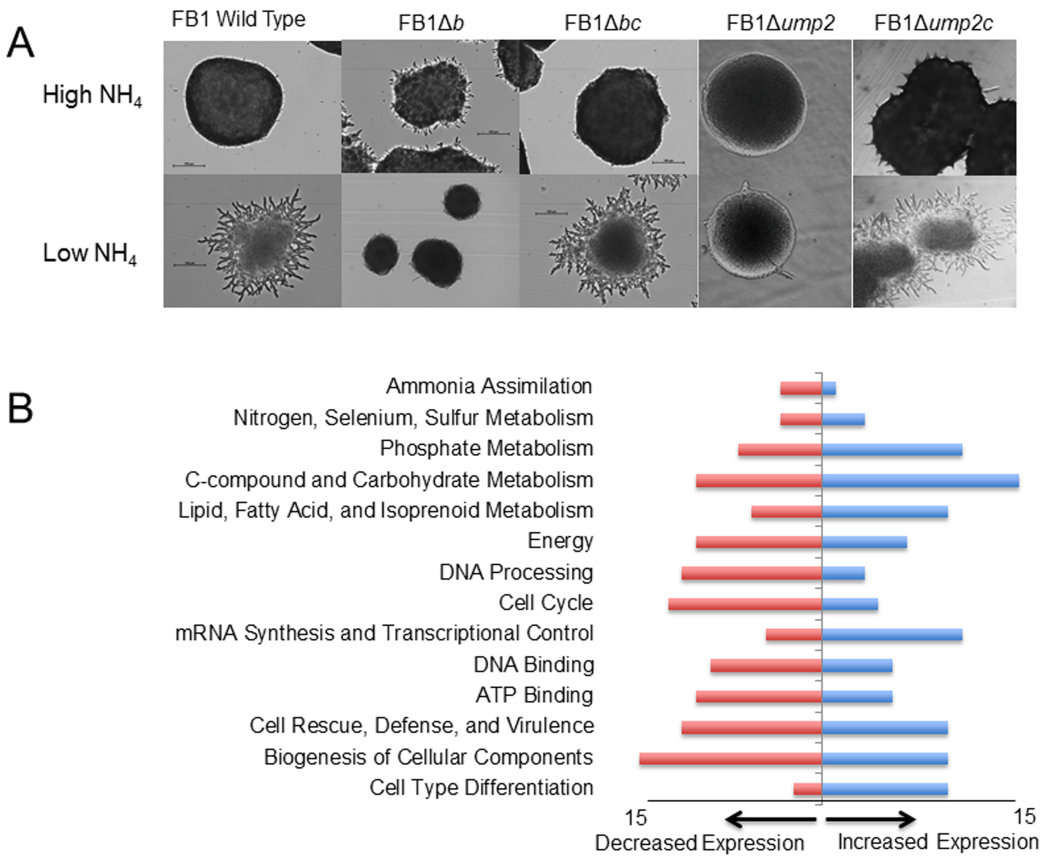

Figure 12: Phenotypes associated with *b* deletion.
As seen with disruption of *ump2*, haploid cells with deletion of the *b* locus grow by budding as compared to the wild-type when grown on AM-low ammonium plates. **(A)** Size bars, 100 µm. Complementation of FB1 *ump2* deletion strain with a functional copy of *ump2* locus results in filamentation on AM-low ammonium plates; similarly, complemented *b* deletion strain, complemented with a functional copy of *b* locus, filaments on AM-low ammonium; size bar, 100 µm. (**B)** Functional categories enriched in those genes differentially expressed in FB1 wild-type under low ammonium conditions but not differentially expressed in mutants completely deleted for the *b* locus or *ump2* under similar nitrogen availability. Red bars represent the number of genes per category with decreased expression and blue bars represent the number of genes per category with increased expression. Functional category enrichment was determined using the FunCat database available at http://mips.helmholtz-muenchen.de/funcatDB/ and enrichment was considered to be those categories with $p<0.05$. Differential expression as determined from RNA-Seq data (log2fold change>1 and $p<0.05$).

376 genes were differentially regulated in the wild-type on low ammonium, but the *b* mutant had expression levels equivalent to the wild-type under replete ammonium conditions. Enriched functional categories included a variety of regulatory and metabolic pathways, as well as biogenesis of cell wall components, and specifically, actin cytoskeleton, which may account for the loss of filamentous phenotype (Figure 12b).

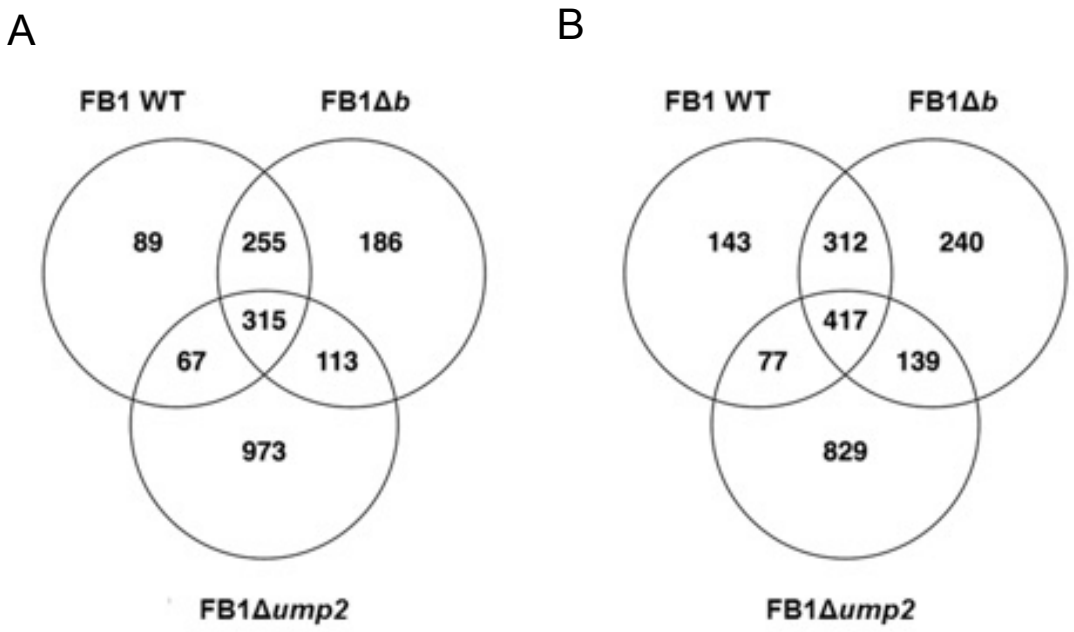

Figure 13: Venn diagram of DEGs for the *b* and *ump2* deletion strains grown on low ammonium compared to wild-type FB1 on low ammonium. For FB1 wild-type and *Δb* mutant, genes identified by RSEM/edgeR analysis of RNA-Seq data were used to select a pool of differentially expressed genes (DEGs) for each strain/condition, with minimum 1 log-fold fold change, p-value<0.001, and FDR (False Discovery Rate)<0.001. For the *Δump2* mutant, genes identified from microarray were used to select a pool of differentially expressed genes (DEGs) with minimum p-value<0.1. **(A)** Up-regulated genes; **(B)** Down-regulated genes. FB1 WT, FB1 wild-type strain on AM-low ammonium; FB1*Δb*, *Δb* mutant of FB1; FB1*Δump2*, *Δump2* mutant of FB1.

Comparing Figure 13a and 13b, only 1299 of these differentially regulated genes were also differentially regulated in FB1 wild-type on ammonium-limited

media (e.g., the Nar1 nitrate reductase and Nir1, the putative nitrite reductase, with the latter being even more highly up-regulated in the *Δb* mutant than wild-type); in contrast, the remaining 678 did not demonstrate differential expression in the wild-type under similar nitrogen availability (Figure 13).

Deletion of the *ump2* locus also resulted in changes in global gene expression, both under replete ammonium conditions and nitrogen limiting conditions, as measured by microarray. Because of the similarity of phenotype between the FB1 *Δump2* mutant and one lacking the *b* locus, we investigated what changes in gene expression the two mutants have in common to further elucidate the loss of filamentation phenotype in depleted ammonium conditions.

In comparing differential gene expression of the two deletion mutants and wild-type on low ammonium conditions, 232 (89 upregulated and 143 downregulated) genes in the FB1 wild-type strain on low ammonium were not differentially expressed in the two deletion mutants under these conditions (Figure 13). These represent potential genes whose expression is required for filamentation. FunCat analysis revealed that functional categories enriched in this subset of genes included, broadly, metabolism, energy production, DNA processing, cell cycle regulation, biogenesis of cellular components, and cell type differentiation. More narrowly, these functional categories included assimilation of ammonia, cell wall and microtubule cytoskeleton biogenesis, budding, cell polarity, and filament formation (Figure 12b).

qRT Analysis indicates that an intact b locus is necessary for the positive regulatory effect ump2 expression has on canonical mating genes even in haploid cells.

qRT-PCR provides the opportunity for targeted investigation of differential gene expression. Moreover, for these purposes, it allowed the comparison of transcription levels of target genes of one strain across low and high ammonium conditions as well as the comparison of all mutants to the FB1 wild-type on replete media (See Figure 6 for various pathways involving target genes). Low ammonium resulted in differential expression of a multitude of genes in the wild-type strain, particularly those involved in the mating and pathogenicity programs. Although in the RNA-Seq data, neither *bE* nor *bW*, showed significant differential expression in wild-type on low ammonium, they were investigated further using qRT-PCR. For wild-type FB1, just as the *ump2* and *ump1* genes were up-regulated, both *bE1*and *bW1*, as well as *prf1*, *mfa1*, and *rbf1* genes were all upregulated under low ammonium conditions, *i.e.*, where filamentation would normally be observed (qRT-PCR data found in Table 3 reported as average of three biological replicates plus/minus standard error; Figure 14a). The observation that filamentation occurs in the *ump2* overexpression strain (FB1 $ump2^{otef}$) under nutrient rich conditions led us to investigate the role of *ump2* expression in altering that of genes upregulated in wild-type FB1 under low ammonium. On replete ammonium media, overexpression of *ump2* led to lower expression levels of all targets examined as compared to wild-type FB1 under low ammonium conditions, indicating that while the overexpressor was able to filament on high ammonium, it was not as a result of differential regulation of

Table 3: Subset of Differentially Expressed Genes of Interest[a] from qRT-PCR Experiments

Target	WT Low[b]	P_{otef} *ump2* High[b]	P_{otef} *ump2* Low[b]	*Δump2* High[b]	*Δump2* Low[b]
ump2 (um05889)	5.89±0.81	4.46±0.48	8.58±1.48	No amp[c]	No amp[c]
ump1 (um04523)	4.04±1.56	-3.91±0.55	1.31±0.44	0.01±0.50	-1.67±1.27
bE1 (um00577)	2.64±1.82	-5.81±1.10	-1.19±0.91	1.16±0.82	-4.72±0.58
bW1 (um00578)	1.68±1.37	-3.21±0.81	-2.21±0.86	2.35±0.92	0.79±0.47
prf1 (um02713)	1.76±0.98	-2.98±0.22	-2.63±0.24	-1.28±0.50	-2.89±1.17
mfa1 (um02382)	4.33±0.59	-0.58±0.25	2.02±0.51	-6.81±0.16	No amp[c]
rbf1 (um03172)	4.02±0.52	-1.01±0.50	1.39±0.32	5.35±0.33	-0.75±0.71

Target	*Δb* High[b]	*Δb* Low[b]	*Δump1* High[b,d]	*Δump1* Low[b,d]
ump2 (um05889)	-1.75±0.51	4.59±1.19	1.32	6.89
ump1 (um04523)	2.20±0.28	2.04±1.21	No amp[c]	No amp[c]
bE1 (um00577)	No amp[c]	No amp[c]	n.t.[e]	n.t.[e]
bW1 (um00578)	No amp[c]	No amp[c]	n.t.[e]	n.t.[e]
prf1 (um02713)	-1.74±0.13	-2.12±1.10	-0.384	10.2
mfa1 (um02382)	0.68±0.29	1.54±0.42	3.86	6.38
rbf1 (um03172)	4.14±0.23	0.37±0.07	1.54	5.83

[a]qRT-PCR log2 fold changes, normalized and expressed relative to FB1 WT on rich medium (High); negative values reflect decreased expression, whereas positive values represent increased expression
[b]WT, wild-type FB1; P_{otef} *ump2*, FB1 with *ump2* over-expressed from constitutive P_{otef} promoter; *Δump2*, FB1 with entire ump2 gene deleted; *Δb*, FB1 deleted for entire *b* mating-type locus; *Δump1*, FB1 deleted for the entire *ump1* gene coding region; High, 30 mM NH_4 medium, Low, 50 μM NH_4
[c]No amp, no amplification detected
[d]Only one biological replicate tested
[e]n.t., not tested

these targets in a similar manner to the wild-type on low ammonium (Table 3). Strains overexpressing *ump2* on low ammonium hyper-filament, creating colonies with longer filaments and larger portions of the colonies covered by filamentous growth as compared to wild-type FB1 under similar conditions. Hence, we examined the same set of mating-related targets in the overexpressor on low ammonium to determine if differential expression of these targets could account for this phenotype. Overexpression of *ump2* on low ammonium resulted in decreased absolute transcript level from the *b* locus, *um00577* (*bE1*) and *um00578* (*bW1*) relative to FB1 wild-type under the same conditions. However, in comparing growth on low vs. high ammonium for the overexpressor strain, expression of both genes increased significantly (Figure 14b). This was true for the rest of the targets examined, with the exception of *prf1* which had a similar expression level on low and high ammonium (Table 3; Figure 14b). *ump1* also showed an interesting pattern of expression. Here, overexpression of *ump2* led to decreased *ump1* transcription relative to wild-type in both replete and low ammonium media, although an increased expression level in the same mutant on low ammonium versus high ammonium conditions (see Table 3). Based on these observations, filamentation under replete media conditions and hyper-filamentation under low ammonium conditions by the *ump2* overexpressor were not a product of differential regulation of these targets.

Because mutants deleted for the *b* mating type locus or the *ump2* ammonium transporter share a loss of filamentous phenotype under low ammonium, we examined expression levels of the same set of targets to

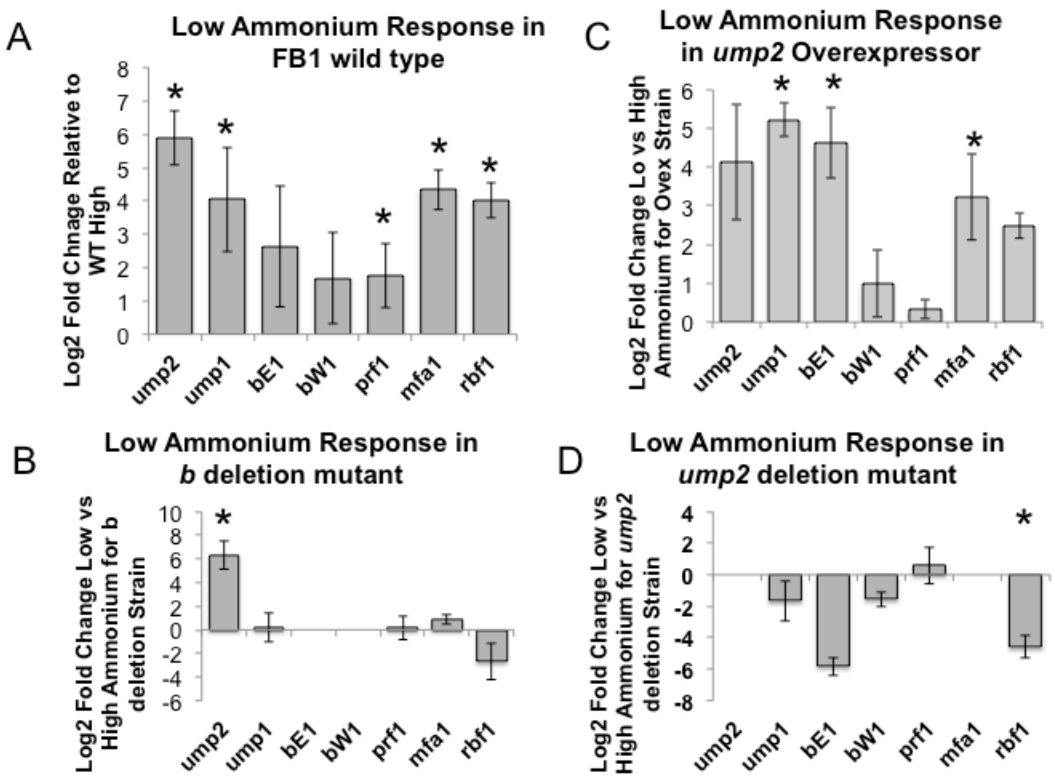

Figure 14: Relative expression of wild-type and mutant strains on replete and low ammonium media.
(A) wild-type FB1; **(B)** P_{otef} *ump2*, FB1 with *ump2* over-expressed from constitutive P_{otef} promoter; **(C)** *Δump2*; **(D)** *Δb*. Log2 Fold changes for qRT-PCR on AM-low, normalized and expressed relative to the same strain on AM-high; negative values reflect decreased expression, whereas positive values represent increased expression. Bars represent averages of biological triplicates and standard errors are indicated in the graphs. High, 30 mM NH_4 medium, Low, 50 mM NH_4. The transcript level of each target for each mutant, comparing AM-low ammonium vs. AM-high ammonium, was compared using Kruskal Wallis (Daniel, 1990); stars on the graph indicate significance, all at $p<0.05$.

determine if these mutants share similar impairments in expression. An inability to express *ump2* cannot be the only reason for the loss of filamentation phenotype. While *ump2* deletion mutants have no measurable *ump2* transcription regardless of ammonium availability, *b* mutants do not share this defect; yet, neither mutant filaments under low ammonium. Under replete

ammonium conditions, *b* mutants had a slightly reduced level of *ump2* expression as compared to wild-type FB1 under similar nutrient conditions; however, under low ammonium conditions *b* mutant expression level of *ump2* was comparable to wild-type in the same condition (Table 3).

Moreover, *ump1* expression levels did not seem to be responsible for the lack of filamentation phenotype. Under replete ammonium conditions, the *ump2* deletion mutant had comparable *ump1* expression levels to the wild-type FB1under the same conditions, while the *b* mutant had slightly increased levels of *ump1* expression. On low ammonium media, the *ump2* mutant and the *b* mutant both had lower levels of *ump1* than wild-type under the same conditions (Table 3). Deletion of the *ump1* ammonium transporter does not result in a loss of filamentation under low ammonium conditions (Smith et al., 2003), so again this shared defect cannot fully explain the shared lack of phenotype. Patterns of expression for *ump2*, as well as *prf1*, *mfa1*, and *rbf1* were examined in mutants lacking *ump1*, and while the magnitude of expression varied, *ump1* mutants showed increased levels of all of these targets under low ammonium conditions as was the case for FB1 wild-type (Table 3).

In contrast, *b* and *ump2* deletion mutants shared expression changes in targets related to mating, specifically *prf1*, *mfa1*, and *rbf1*. While all of these genes show increased expression level in the wild-type under conditions of low ammonium, both the *b* and *ump2* deletion mutants showed lower transcript levels of these targets under the same conditions (Table 3). Additionally, while these mutants had different expression levels of *prf1*, *mfa1*, and *rbf1* on high

ammonium as compared to the wild-type strain, neither demonstrated the ability to induce expression of these targets under low ammonium (*i.e.*, the expression level on low was comparable or lower to expression level in the same mutant on high ammonium) (Table 3, Figure 14c and 14d). In fact, when compared to itself on high ammonium, the *ump2* mutant showed a markedly decreased level of *rbf1* (Figure 14c). Expression levels of *mfa1* were undetectable in the *ump2* mutant under low ammonium conditions, indicating a more dramatic reduction (Table 3).

While deletion of the *b* locus did not dramatically alter the organism's ability to induce expression of *ump2* under low ammonium conditions (Figure 14d), deletion of *ump2* did result in changed expressed from the *b* mating type locus for both *bE1* and *bW1.* FB1 wild-type under low ammonium conditions demonstrated increased expression from both genes of the *b* locus, although of different magnitudes. Under low ammonium conditions, deletion of *ump2* decreased expression from both genes (Table 3, Figure 14c), indicating that wild-type *ump2* expression levels are require for normal induction of *b* expression under low ammonium conditions.

Most of this analysis focuses on the response of a strain to low ammonium conditions and as such we compared within the same strain the transcript level on low ammonium media to that of the same mutant on high ammonium. Due to the variability of expression levels of a particular target even within biological replicates, we wanted to ensure that the changes we saw in expression level were actual increases or decreases of a particular target, not an artifact of the expression level of a target within a specific mutant being affected regardless of

ammonium availability. To this end, a one-way analysis of covariance (ANCOVA, (Lowry, 1999-2000)) was used to compare induction of each target across the three mutants (FB1Δ*b*, FB1Δ*ump2*, and FB1 *ump2*^{Potef}) to the induction in the FB1 wild on reduced ammonium as compared to replete media (Figure 15). This analysis accounted for the variability of expression level within a particular mutant as well as differences in expression levels for the strains on high ammonium. The ΔC_T values from qRT-PCR experiments (the change in threshold cycle between the target of interest and the endogenous control, *eif-2B*) of three biological replicate for each target was used to calculate variation within and between strains (Yuan, Reed, Chen, & Steward, 2006). An ANCOVA analysis allowed recalculations of inductions (or decreases) or each target by resetting the levels for each target in a particular mutant to the start point on high ammonium. Confirming our previously analysis, *ump2* induction (in strains with functional copies of the gene) was not different across the mutant strains, but induction of other targets, including *bE1*, *prf1*, *mfa1*, and *rbf1* was significantly different in some of the mutants as compared to the FB1 wild-type.

Because *ump2* expression levels seemed to directly affect *b* locus expression, we examined additional targets relating to pathogenicity. To confirm some additional preliminary predictions from microarrays and RNA-Seq, we chose a set of 12 genes for qRT-PCR analysis from the different functional categories (Table 4). For *kpp6*, a MAPK gene essential for pathogenicity on the host, the mutants only differed from wild-type under replete conditions, with the *ump2* overexpressor slightly elevated and the *Δump2* slightly reduced.

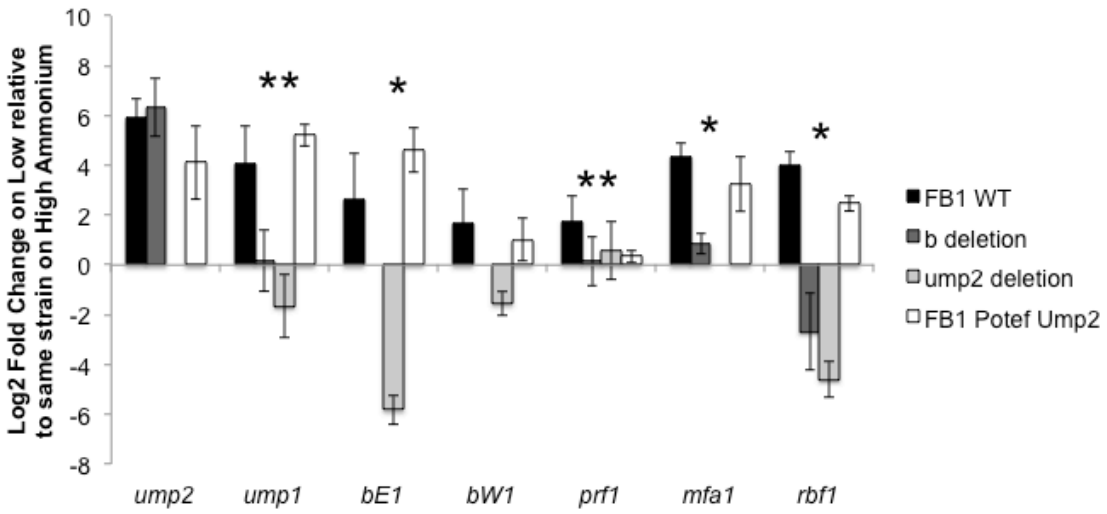

Figure 15: Comparison of induction of each target within strain on Low Ammonium as compared to High Ammonium.
Bars represent average of three biological replicates with standard error. ** is significant at $p<0.01$ and * is significant at $p<0.05$. For deletion strains, null data was not including in analysis. Post-hoc analysis (ANCOVA, (Lowry, 1999-2000)) revealed the following target differences: 1) *ump1* induction is equivalent in FB1 WT and the *ump2* overexpressor but different in the two deletion mutants. 2) *bE1* expression induction is equivalent in the FB1 WT and *ump2* overexpressor; it is decreased in the *ump2* deletion mutant as compared to both. 3) *prf1* expression in all three mutants is different from FB1 WT. 4) *mfa1* induction is equal in FB1 WT and *ump2* overexpressor, reduced in *b* deletion mutant. 5) *rbf1* induction is equivalent and FB1 WT and the *ump2* overexpressor and reduced in the two deletion mutants. FB1 WT, FB1 wild-type; b deletion, FB1 *Db*; ump2 deletion, FB1 *Dump2*; FB1 Potef Ump2, FB1 $ump2^{otef}$.

Additionally, the *mig* genes, encoding small, secreted, cysteine-containing proteins, are normally highly up-regulated upon penetration into host tissue (Farfsing, Auffarth, & Basse, 2005). Here, we found expression of *mig 2-6* on low ammonium was dramatically reduced for FB1 wild-type and FB1*Δump2* compared to their growth on nitrogen-replete medium, while expression for the *ump2* overexpressor was even further reduced (see Table 4); moreover, the mutants also had reduced expression in replete medium relative to wild-type.

Table 4: DEGs [a] related to pathogenicity from qRT-PCR Experiments

Gene	WT Low[b]	*P_{otef} ump2* High[b]	*P_{otef} ump2* Low[b]	*Δump2* High[b]	*Δump2* Low[b]
Signal Transduction					
kpp6 (um02331)	-1.03±0.73	1.28±0.46	-0.55±0.26	-1.25±0.49	-0.87±0.42
pten (um3760)	2.27±0.13	-0.86±0.14	0.76±0.44	0.22±0.22	0.86±0.68
Secretory Pathway					
rep1 (um03924)	-8.00±0.03	-0.62±0.13	-7.45±0.39	-1.96±0.15	-8.45±0.18
egl1 (um06332)	1.35±0.96	5.43±0.39	3.72±0.31	1.20±2.35	1.75±0.90
mig2-6 (um06126)	-9.97±0.07	-3.61±0.28	-9.74±0.32	-6.68±3.06	-10.4±0.06
Metabolism, Interaction with the Environment					
chitin deacytelase (um01788)	0.65±0.62	1.46±1.35	-4.87±0.49	0.24±0.21	-0.37±0.57
chitinase (um06190)	-4.03±3.08	2.71±1.36	-5.88±0.12	0.33±0.82	-7.12±0.31
Transporters					
probable *hxt5*-hexose transporter (um02037)	-0.04±1.33	2.14±0.32	0.69±0.53	0.70±0.43	0.19±0.14
probable high affinity glucose transporter (um11514)	-0.13±0.06	2.48±0.01	-2.61±0.27	-0.68±0.28	-3.20±0.17
Miscellaneous Proteins					
actin (um06217)	-5.50±1.29	-0.51±2.28	-3.05±0.01	-2.78±0.84	-4.08±0.13
related to polyketide synthase (um04095)	-1.15±0.22	6.70±1.81	2.24±1.29	4.46±0.41	-3.57±0.60
conserved hypothetical (um03116)	-1.30±3.19	6.91±2.26	3.61±1.02	4.64±0.57	-0.95±0.57

[a]log2 fold change relative to wild-type on High

[b]High, array medium containing 30 mM glutamine/50 μM ammonium sulfate; Low, array medium containing 30 mM glutamine/50 mM ammonium sulfate

Discussion

In the basidiomycete fungus, *U. maydis*, the dimorphic transition, from yeast-like growth to filamentous growth, changes the life style of the fungus from saprophytic to pathogenic. This transition occurs in response to sensing different environmental conditions (Hartmann, Kruger, Lottspeich, & Kahmann, 1999). Nutrient limitation, specifically for nitrogen, is one of the factors responsible for the transition. One of the most preferred sources of nitrogen is ammonium and in *U. maydis* under conditions of low ammonium, the yeast-like cells differentiate to form filaments. The filamentous growth of haploid cells observed in response to low ammonium is functionally distinct from filaments formed by mating followed by the formation of dikaryon. Therefore, it is unclear whether the developmental program associated with filamentous growth under ammonium limiting conditions in the laboratory is of any functional importance with respect to the ability of *U. maydis* to be pathogenic.

On the other hand, the observation that genes induced during infection were also induced under nitrogen limiting conditions led Snoeijers et al. (Snoeijers, Vossen, Goosen, Van den Broek, & De Wit, 1999) to propose that a plant pathogen would face similar growth conditions in the host. Furthermore, in *Colletotrichum lindemuthianum*, there was reduction in pathogenicity and in *M. grisea* reduction in the expression of the pathogenesis genes, due to mutations in genes controlling nitrogen metabolism (Lau & Hamer, 1996; Pellier, Lauge, Veneault-Fourrey, & Langin, 2003). This led Ho et al. to suggest the importance of characterizing genes involved in nitrogen metabolism and its control for a more

complete understanding of *U. maydis* pathogenicity (Ho, Cahill, & Saville, 2007). In different fungi developmental processes such as filamentous growth, invasive growth and mating in response to low ammonium are dependent on the AMT family of ammonium permeases. For example, haploid invasive growth in response to low ammonium in *S. pombe*, *S. cerevisiae* and *C. neoformans* and mating response in *C. neoformans* are dependent on ammonium transporters (Mitsuzawa, 2006; Rutherford, Chua, et al., 2008; Rutherford, Lin, et al., 2008) The two ammonium permeases of *U. maydis* are involved in transporting ammonium into the cell and an additional 'sensor of ammonium' function is assigned to the high affinity ammonium transporter (Ump2). In the current study, we have presented evidence expanding the role of *ump2* in differentiation associated with coordinate expression of several possible direct or indirect target genes, including those associated with virulence.

We found that a dikaryon produced from mating partners deleted for both *U. maydis* AMTs was severely reduced in virulence (Figure 10). The use of the solopathogenic strain SG200 and its mutant derivatives suggests further, that the presence of at least *ump2* is required for full pathogenicity even in the absence of mating (see Figure 11), as these mutants were also severely impaired in disease production.

Similar to the findings in *S. cerevisiae* and *C. albicans,* we were able to link the ability of *U. maydis* to grow filamentously to the expression levels of the high affinity ammonium transporter (K. Biswas & Morschhauser, 2005; Rutherford, Chua, et al., 2008). Increased expression of *ump2* made the cells

filament faster under low ammonium conditions, within 48 hours, and surprisingly, it triggered filamentous growth under nutrient rich conditions. This suggests a possible role of *ump2* in dimorphic transition normally linked to ammonium availability, but also dependent on *ump2* levels even when ammonium is not limiting.

Overexpression of *ump2* in nitrogen-replete conditions results in global gene expression that, in some ways, mimics the low ammonium response of wild-type. Thus, it is likely that the filamentation phenotype observed from *ump2* overexpression is due to the change in expression level of these genes. In this regard, induction of *ump2* seems to correspond to perception of low ammonium availability and the resulting filamentous phenotype observed under low ammonium conditions. Since not all of the genes differentially expressed in wild-type under low ammonium conditions were similarly differentially expressed by the *ump2* overexpressor under replete media conditions, Ump2 levels may be only part of the ammonium availability sensing process. However, since deletion of *ump2* results in the loss of the filamentous phenotype under low ammonium conditions, *ump2* expression must be essential for normal filamentation in response to low ammonium. Moreover, *ump2* is essential for induction of other nitrogen-sensing related genes, such as *ump1*, as is demonstrated by the lack of induction of *ump1* under low ammonium conditions in an *ump2* deletion mutant. In *U. maydis* it is proposed that mating is induced in response to nutrient deprivation under the control of cAMP-PKA pathway, which represses hyphal growth and induces the mating pathway (Sánchez-Martínez & Pérez-Martín,

2001). However, in the absence of a compatible mating partner, the cells undertake filamentous growth under similar growth condition (Regine Kahmann, Basse, & Feldbrügge, 1999; Sánchez-Martínez & Pérez-Martín, 2001). Nitrogen starvation also induces the formation of conjugation tubes and true filaments, although, the formation of the former is dependent on the presence of partners with compatible *a* mating loci and the latter is dependent on active *a* and *b* loci (Flora Banuett & Herskowitz, 1994). *U. maydis* Prf1 is a transcription factor that controls the expression of genes involved in mating and dikaryon formation, particularly those of the *a* and *b* locus (Hartmann et al., 1999), integrating the environmental signals and affecting the morphological outcomes of *U. maydis* development. However, the role of *prf1* for filamentous growth in haploid cells is unclear (Sánchez-Martínez & Pérez-Martín, 2001). Changes in the expression of the ammonium transporters were associated with expression levels of *prf1*. Our expression analysis of *prf1* reveals that this gene, normally induced under low ammonium conditions, shows reduced expression for all mutant strains on low ammonium (except FB1*Δump1*), although there was essentially no change in the *prf1* levels for the *ump2* overexpressor observed comparing its growth on high with that on reduced ammonium. Similarly, *mfa1* expression is substantially affected by *ump2* expression level, and is greatly induced under low ammonium conditions in the overexpression strain, as is typical of the low ammonium response in wild-type. Further, whereas *bE1* and *bW1* were induced under low ammonium conditions in the wild-type (see Table 3), to differing degrees both were reduced in the FB1*Δump2* and *ump2* overexpressor strains. We

hypothesize that the up-regulation in expression of *mfa1* could normally be associated with the absence of a compatible mating partner under conditions of low ammonium, perhaps so that increased concentrations of pheromone might increase the probability of encountering a distant partner; however, deletion of *ump2*, which in turn reduces expression from *prf1*, may disrupt normal *mfa1* up-regulation. The corresponding strong reduction in wild-type of *bE1* and *bW1* gene products would suggest the role of the *b* locus in the normal filamentation phenotype of haploid cells on low ammonium in the absence of a mating partner.

Based on the expression data we propose a role for ammonium transporter expression in transmitting information to the developmental programs, in order to help decide the fate of the cells under nutrient limiting conditions (Figure 16). *ump2* and the *b* locus are tied together at the level of transcriptional regulation and normal low ammonium response. Ump2 is necessary for induction of *ump1* as well as other targets that occur during the low ammonium response, such as *prf1* and *rbf1.* While deletion of the *b* locus does not directly affect the *ump2* expression level under low ammonium conditions, the expression level of *ump2* is no longer able to induce other targets such as *ump1* and the others listed above. Additionally, deletion of *ump2* also results in the lack of induction of *ump1* and other targets under low ammonium conditions. Although overexpression of *ump2* results in decreased levels of *b* locus expression as compared to FB1 wild-type, the overexpression of the Ump2 high-affinity ammonium transporter does increase expression from the *b* locus when compared to itself on low ammonium. Presence and expression from the *b*

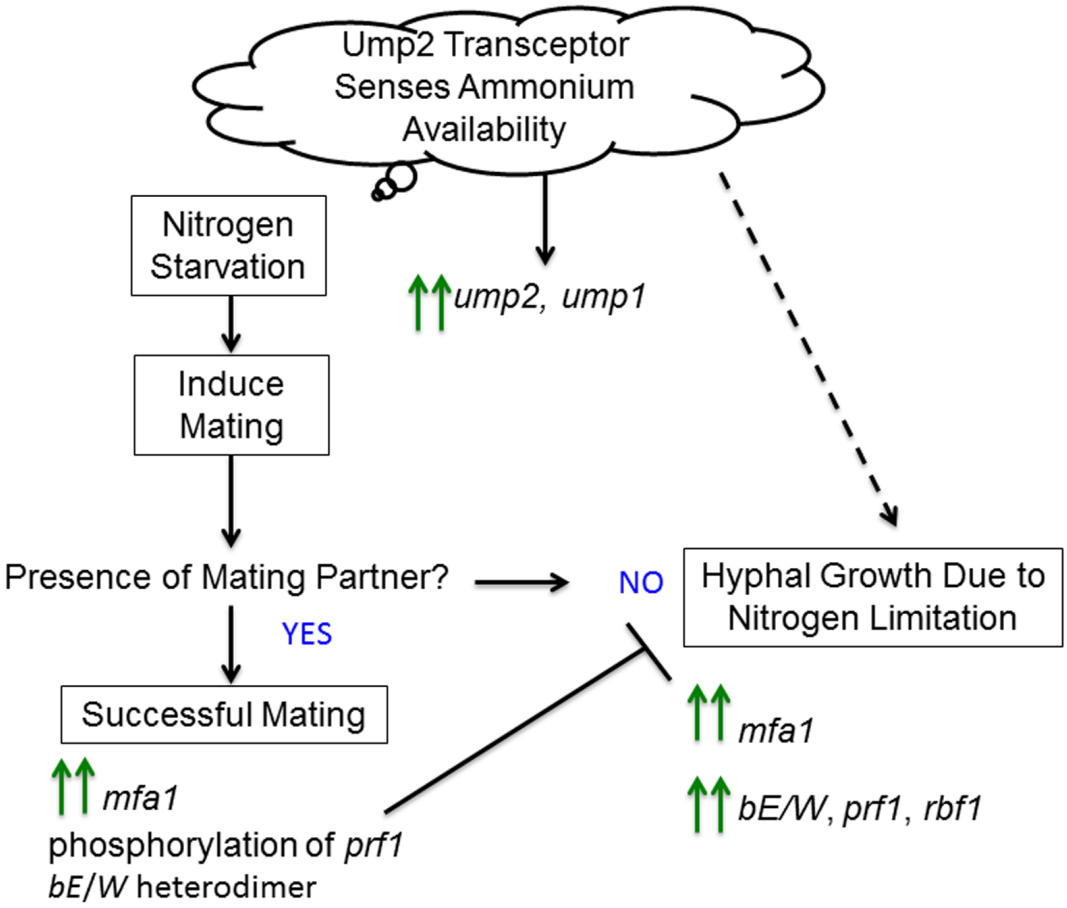

Figure 16: Model for the role of Ump2 in determining the developmental fate of the cells.
Nutrient limiting condition is sensed by Ump2 which relays signal to downstream effectors to induce mating. Cells sense the presence or absence of a mating partner. In the presence of a mating partner the cells undergo successful mating but in the absence of a mating partner, the haploid cells undertake filamentous growth in response to low nitrogen.

locus and the *ump2* gene are necessary for the normal induction of expression associated with the low ammonium response. Our data suggest that the same elements canonically involved in the mating pathway may also be functioning in the low nutrient response in haploid cells.

While expression from the *b* locus has been demonstrated to halt cell cycle in the G2 phase, our data suggest that overexpression of *ump2* may halt

the cell cycle earlier, in G1. As such, deletion of the entire *b* locus or deletion of the Ump2 transceptor may result in similar phenotype but not a complete overlap of transcriptional profiles. Preliminary data (Wallen et al., unpublished) also suggest that overexpressing *ump2* in a mutant that is deleted for the entire *b* locus, rescues the loss of filamentation phenotype, indicating that while *b* is necessary for normal induction through *ump2*, Ump2 overexpression may allow for changes in gene expression that result in the return of the filamentation phenotype independent of the *b* mating locus.

Altering ammonium transporter expression also affects expression of other transporter proteins and expression of genes coding for secreted enzymes. Some of these secreted proteins are expressed during growth of the fungus inside the host, while others are expressed specifically during filamentous growth (Doehlemann et al., 2009; Horst et al., 2010; Schauwecker, Wanner, & Kahmann, 1995; Wosten et al., 1996). This would suggest that ammonium transporters might play a role in assessing the nutrient situation inside the host during infection and then transmitting this signal to the pathogen for effective colonization and progression inside the host. Then, in the absence of the AMTs, ineffective disease progression could be due to the resultant dysregulation. In conclusion, AMTs play a role in determining the morphogenetic fate of the cells in low ammonium by affecting more than one signaling pathway at multiple levels.

CHAPTER III

DIFFERENT ROLES FOR *bE* AND *bW,* THE PRODUCTS OF THE *b* MATING TYPE LOCUS*,* IN THE LOW AMMONIUM RESPONSE OF HAPLOID *USTILAGO MAYDIS* CELLS

Chapter Overview

Mating in dimorphic fungi is often a response to adverse environmental conditions, particularly nitrogen starvation. In *Ustilago* maydis, a biotrophic pathogen of maize, the mating program itself is governed by products of the *a* and *b* mating type loci. Moreover, the high affinity ammonium transporter, Ump2, acts to sense the availability of environmental ammonium and is essential for successful infection. In the absence of a mating partner, haploid cells form characteristic filamentous colonies on low ammonium media, which is also dependent on *ump2* expression. To provide clearer understanding of possible interplay between these two programs, targeted gene expression studies were undertaken for haploid cells, in the absence of a mating partner, under depleted ammonium conditions. The *b* mating type locus is required for this filamentation phenotype, and deletion of either *bE1* or *bW1* encoded by this locus resulted in the loss of the normal response to low ammonium. Partial or complete deletion of the *b* mating type locus led to an inability to respond to low ammonium by inducing gene expression of various mating-related targets, including Prf1*,* a

transcription factor involved in mating, Mfa1, a pheromone precursor, and Rbf1, the master regulator of *b*-responsive gene expression. Of interest, overexpression of *ump2* was able to rescue the loss of filamentation on low ammonium in the absence of the entire *b* locus and in the absence of *bE1* alone, but not in the absence of *bW1*. These observations taken together indicate different and non-synonymous roles of *bE1* and *bW1* in the nitrogen starvation response of haploid *U. maydis* cells, including opposing or supporting expression induced by Ump2.

Introduction

Ustilago maydis is a dimorphic, biotrophic fungal pathogen of maize. Like other basidiomycete plant pathogens, ability to penetrate a potential host is mediated by the organism's ability to mate. In nature, *U. maydis* may exist as haploid cells. Given appropriate nutrient and other environmental signals and a compatible partner, the haploid cells are able to fuse and form an infectious dikaryon, penetrate plant tissue and initiate the rest of the organism's life cycle.

Similar to other basidiomycetes, mating in *U. maydis* is governed by a self versus non-self recognition program in the form of pheromones and pheromone receptors, and homedomain proteins that control sexual development and infection, and also mediates the switch from a budding-yeast like state to an infectious filamentous stage. As is the case with many other basidiomycetes, this mating system is tetrapolar, with two physically unliked genetic regions housing the mating type loci. In *U. maydis*, these two regions are referred to as

the *a* and *b* loci. The genetic components at both of these loci determine the mating type for an individual organism. Two *a* loci have been found and characterized (Bolker et al., 1992), while nearly 30 different variations of the *b* mating type loci have been found in natural populations (Kronstad & Leong, 1990). The combination of the specific genetic material at each of these mating loci defines an individual organism's mating type.

The function and regulation of these genes involved in mating have been well studied and characterized. The *a* mating type locus encodes the genetic information for the production of pheromones and pheromone receptors, and defines the mating type of any particular cell as either *a1* or *a2*. The *a1* and *a2* mating type versions are of different sizes (4.5 kb and 8 kb, respectively) and have no sequence homology, and are thus referred to as "idiomorphs" (Bolker et al., 1992). The pheromones, Mfa1 and Mfa2, are produced as precursors which are posttranscriptionally and posttranslationally modified and then secreted, while the pheromone receptors, Pra1 and Pra2, are located on the cell surface (Bolker et al., 1992). When a pheromone binds to its receptor, an intracellular response is activated that leads to mating competence and mediates fusion of the two cells of opposite mating type (Bolker et al., 1992).

The *b* mating type locus encodes two unrelated homeodomain proteins, bE and bW, that mediate a secondary component of self-versus non-self recognition. Any combination of different alleles between two mating cells at this locus can contribute to pathogenic development (Schulz et al., 1990). Long before molecular genetic analysis had been developed, it was hypothesized that

bE and bW of opposite mating types fuse to form a heterodimer which then functions to activate transcription leading to pathogenicity, a system parallel to other basidiomycetes, particularly mushrooms (Gillissen et al., 1992). Later experiments have since demonstrated that these two homeodomain proteins dimerize through their N-terminal domains, provided that the two proteins are from alleles from different mating types (Kamper et al., 1995).

The regulation of expression from the two mating type loci has also been thoroughly studied in *U. maydis*. A transcription factor, Prf1, which is phosphorylated by components of two different pathways serves as the master regulator for mating type locus genes (Kaffarnik, Muller, Leibundgut, Kahmann, & Feldbrugge, 2003). Prf1 functions to both provide high levels of pheromone and pheromone receptor during mating and maintain expression of *b* genes during pathogenic development (Hartmann et al., 1999). The extent to which phosphorylation of this protein is from either the MAPK pathway or the PKA pathway determines the extent to which either the *a* locus genes or *b* locus genes are expressed (Kaffarnik et al., 2003) (For a schematic of the mating program in *U. maydis*, see Figure 6, Chapter 2).

While the regulation and participation of all of these proteins has been well studied in mating cells, the goal of the current research is to determine the role, if any, these proteins may have in haploid cells. In nutrient-restricted conditions, *U. maydis* haploid cells would prefer to find a compatible mating partner and penetrate a host plant, but what is the fate of these cells and what genetic determinants are involved when no mating partner is available? Haploid wild-

type cells grow in colonies with characteristic a filamentation phenotype that is different from the dikaryotic filamentation seen in fused haploids (Smith et al., 2003). It has already been determined that without synthetic linkage, bE and bW derived from alleles in the same mating type locus cannot form a functional heterodimer in nature (Gillissen et al., 1992; Kamper et al., 1995; Romeis et al., 1997). However, these two proteins, bE and bW, differ in their structure and potentially in their function, as well. For example, bW carries a transcriptional activation domain similar to those found in yeast that bE does not possess (Kamper et al., 1995). Additionally, bW has found to have additional interaction partners during mating that bE does not have, such as Clp1, resulting in down regulation of *a* dependent genes once mating has been initiated (Heimel, Scherer, Schuler, & Kamper, 2010).

Moreover, it has also been determined that proteins functioning in transport of nutrients, particularly the high affinity ammonium transporter, Ump2, play a role in the filamentation phenotype, as the disruption of the *ump2* gene leads to the loss of this characteristic colony growth under low ammonium conditions (Smith et al., 2003). Complete deletion of the *b* mating type locus and deletion of *ump2* both result in the loss of filamentation under low ammonium conditions, while deletion of the *b* locus does not equate a loss of induction of *ump2* expression under low ammonium condtions (Chapter 2). Here we investigate a possible coordinated role between *ump2* expression level and different components of the *b* mating type locus in the filamentation phenotype seen in ammonium-starved haploid cells.

Methods

Strains and Growth Conditions

U. maydis cells were grown at 30°C on Array Medium [AM] (6.25% Holliday Salt Solution (Holliday, 1974), 1% glucose, 30 mM Glutamine/50 µM Ammonium sulfate and 2% agar) and Array Medium [AM] with low ammonium (6.25% Holliday Salt Solution, 1% glucose, 50 µM ammonium sulfate and 2% agar) for 48 hrs. *U. maydis* strains used are listed in Table 5.

Primer Design

Primers, other than for the Real Time PCR, were designed using the Primer 3 program available at [http://frodo.wi.mit.edu/primer3/] (Rozen & Skaletskey, 2000). Primers were obtained from Eurofins MWG Operon [Huntsville, AL].

PCR

PCR reactions were run on a PTC100 thermal controller [MJ Research Inc., San Francisco, CA] and a DNA Engine thermal cycler [Bio Rad Laboratories, Hercules, CA]. PCR cycling conditions utilized an initial denaturation temperature of 94°C for 4 minutes, followed by 34 cycles of a three-step process of denaturation at 94°C for 30 seconds, annealing at 60°C for 30 seconds and extension at 72°C for 1 minute per 1 kb of anticipated product length. A final extension at 72°C for 10 minutes was used to complete all products. For most reactions Ex-Taq™ Hot Start DNA polymerase (Takara, Madison,WI) or Apex

Table 5: *U. maydis* strains used for Chapter 3.

Strain	Genotype	Reference
FB1 WT	*a1 b1*	(F. Banuett & Herskowitz, 1989)
FB2 WT	*a2 b2*	(F. Banuett & Herskowitz, 1989)
FB1Δ*b*	*a1 b1 bE/W::hyg*^{R}	Chapter 2
FB1 *ump2*^{Otef}	*a1 b1 P*$_{otef}$*ump2, cbx*^{R}	Chapter 2
FB1Δ*b ump2*^{Otef}	*a1 b1 bE/W::hyg*^{R} *P*$_{otef}$*ump2, cbx*^{R}	This Study
RK1607	*a1 bE1 bW1::hyg*^{R}	(Gillissen et al., 1992)
RK1661	*a2 bE2 bW1::hyg*^{R}	(Gillissen et al., 1992)
RK1722	*a2 bW2 bE2::hyg*^{R}	(Gillissen et al., 1992)
RK1725	*a1 bW1 bE1::hyg*^{R}	(Gillissen et al., 1992)
RK1607 *ump2*^{Otef}	*a1 bE1 bW1::hyg*^{R} *P*$_{otef}$*ump2, cbx*^{R}	This Study
RK1725 *ump2*^{Otef}	*a1 bW1 bE1::hyg*^{R} *P*$_{otef}$*ump2, cbx*^{R}	This Study

DNA polymerase [Genesee Scientific, San Diego, CA] was used. For high fidelity reactions, Phusion DNA polymerase [Finnzymes, Lafayette, CO] was used.

Genetic Manipulation and Vector Construction

Complete *b* deletion strain

The construct for making the *b* gene deletion in *U. maydis* strain FB1 (a1 b1) was obtained from Dr. J. Kämper (Kämper, 2004). The *b* mating locus in this construct is replaced by the hygromycin resistance cassette. The fragment was amplified using PCR, purified from agarose gel, and used to transform competent

U. maydis cells. Putative mutants were first selected for hygromycin resistance and then screened by PCR for lack of the *b* locus.

bE1 and *bW1* deletion stains

The *bE1* deletion strain (RK1725) and *bW1* deletion strain (RK1607) were graciously provided by Regine Kahmann. RK1725 was made by deleting the entire *b* locus and replacing it with a construct containing the *bW1* allele and the hygromycin resistance cassette in the place of *bE1* in FB1 (Gillissen et al., 1992). RK1607 was derived by deleting the entire *b* locus and replacing it with a construct containing the hygromycin cassette disrupting the *bW1* locus and the coding region for bE1 in FB6b (Gillissen et al., 1992). FB6b, like FB1, was derived from teliospores resulting from the cross of *Ustilago maydis 521* and *Ustilago maydis 518* (F. Banuett & Herskowitz, 1989). Before modification, at the mating type loci, FB6b is *a1b2*. With the above insertion, RK1725 exhibits *b1* mating type specificity (Gillissen et al., 1992).

Construction of the *ump2* overexpression strains

A detailed description of construction of this vector was described in Chapter 2. The Otef expression vector was linearized using the restriction enzyme *Ssp*I before transforming *U. maydis* to select for recombinants at the *ip* locus, providing carboxin resistance (Brachmann et al., 2001). The construct for making the *b* deletion in *U. maydis* strain FB1 (*a1 b1*) was obtained from Dr. J. Kämper (Kämper, 2004)

RNA Isolation and Expression Analysis

U. maydis cells were grown on AM-glutamine, AM-ammonium and AM-low ammonium plates for 48 hours. RNA isolation for the transcriptional profile was as described previously (Perlin et al., 2015). For Illumina Next Generation Sequencing (RNA-Seq), the total RNAs were subsequently sent to BGI-Americas (Davis, CA) for cDNA library construction, sequencing, and initial bioinformatic analyses. The cDNA library format was a 140-160 bp insert library (Truseq library prep) for each sample, with Read length Paired-end 100 bp and Data output of 4 Gb clean data per sample. RNA-Seq data from different conditions were processed using the Trinity pipeline (Grabherr et al., 2011; Haas et al., 2013) , and RNA-Seq reads from each sample were aligned using bowtie (Langmead et al., 2009) against protein coding sequences extracted based on annotation. Fungal gene expression levels were estimated by RSEM (B. Li & Dewey, 2011), and edgeR with TMM normalization (Kadota et al., 2012; Robinson et al., 2010) was used to identify differentially expressed genes between each pair of conditions with a corrected p-value cutoff of 0.001; for these analyses, RPKM measurements were used to calculate log2-fold changes. Assessment of overlapping sets of differentially-expressed genes was made using the online version of VENNY (http://bioinfogp.cnb.csic.es/tools/venny/index.html; (Oliveros, 2007-2015). To verify differences in expression levels of a subset of genes identified by RNA-Seq, real time quantitative RT-PCR (qRT-PCR) was employed. Primers for the different genes (Table 6) were designed using the ABI Primer Express software version 3.0, ensuring that all the primer sets investigated had

the same amplification efficiency, since comparison of gene expression using real-time PCR assay assumes that the efficiency of amplification for all the primer pairs is equal. Additional details of the qRT-PCR reactions are provided in Supplemental Materials Additional Methods. Differences in expression level were analyzed using the nonparametric Kruskal-Wallis Test (Lovely et al., 2011) and ANCOVA one directional analysis of covariance (Lowry, 1999-2000).

Mating Assay and Plant Pathogenesis.

Cell densities of liquid cultures were measured spectrophotometrically. Liquid overnight cultures were grown to an Absorbance at 600 nm between 0.5 - 0.7 (exponential growth phase). Mating assays were performed using 10^7 cells / ml and spotting 20 µl onto PDA charcoal as previously described (F. Banuett & Herskowitz, 1989). Plant infection using 8-10 day old Golden Bantam corn seedlings [Bunton Seed Co., Louisville, KY and W. Atlee Burpee & Co., Warminster, PA] was performed with a cell density of 10^8 cells / ml for pre-mixed haploid strains of opposite mating type as previously described (Gold et al., 1997) and virulence was rated by a disease index (DI) on a scale of 0 to 5 (Gold et al., 1997). Statistical analysis of the disease index measures were performed using a Kruskal-Wallis Test with a Multiple Comparison Test in R (Daniel, 1990; Lovely et al., 2011).

Table 6: Genes and the Primers used for qRT-PCR for Chapter 3

Gene Name	Primers	Sequences (5' → 3')
guanine nucelotide exchange factor (um04869)	rt-eif-2B-F	CAAATGCGATCCCGAACAG
	rt-eif-2B-R	GGGACACCACTTGTCAAGCA
ump1 (um04523)	rt-Ump1-F	CGGTCTCACCTGGATGTTCCT
	rt-Ump1-R	AGCCAACGACGGACCACTT
ump2 (um05889)	rt-Ump2-F	TGGGTCCCGTTCTCATTTTC
	rt-Ump2-R	AGGCGATGGGATTGTAGACAA
prf1 (um02713)	rt-Prf1-F	CAGCACCAAGGTGGAAAGGT
	rt-Prf1-R	GAATTGCCACGTGTTTGCAA
mfa1 (um02382)	rt-Mfa1-F	ATGCTTTCGATCTTCGCTCAG
	rt-Mfa1-R	TAGCCGATGGGAGAACCGT
bE1 (um00577)	b1E1ft123	GCAACAAAAGATACCCAACGA
	b1E1rt334	TTCGACACCCTACATCAGGAC
bW1 (um00578)	b1W1ft1559	TCGAGTCTGCCTCAATTCCT
	b1W1rt1827	CTCTCCTATGCTGGCTCCAC
rbf1 (um03172)	RT Rbf1 F	AGGGTGTGGCAAATCGTTCT
	RT Rbf1 R	TCGGCATCAGCATGGTTTC
pra1 (um02383)	Pra1 qrt F	ACTCGATGGTCTGGTGGAAG
	Pra1 qrt R	CTCACGCTCAATTCGCAATA

Results

Deletion of the entire *b* locus results in loss of filamentation of haploid cells in response to low ammonium.

FB1 wild-type (WT) cells show a characteristic filamentation phenotype when exposed to low ammonium. Deletion of the entire *b* locus in this background resulted in the loss of this phenotype (Figure 17a). RNA-Seq data indicated that deleting the *b* locus resulted in a change in global gene expression in response to low ammonium; a portion of these transcriptomic changes were not observed FB1 WT was exposed to the same conditions. Based on qRT-PCR analysis, exposure to low ammonium resulted in a characteristic change in gene

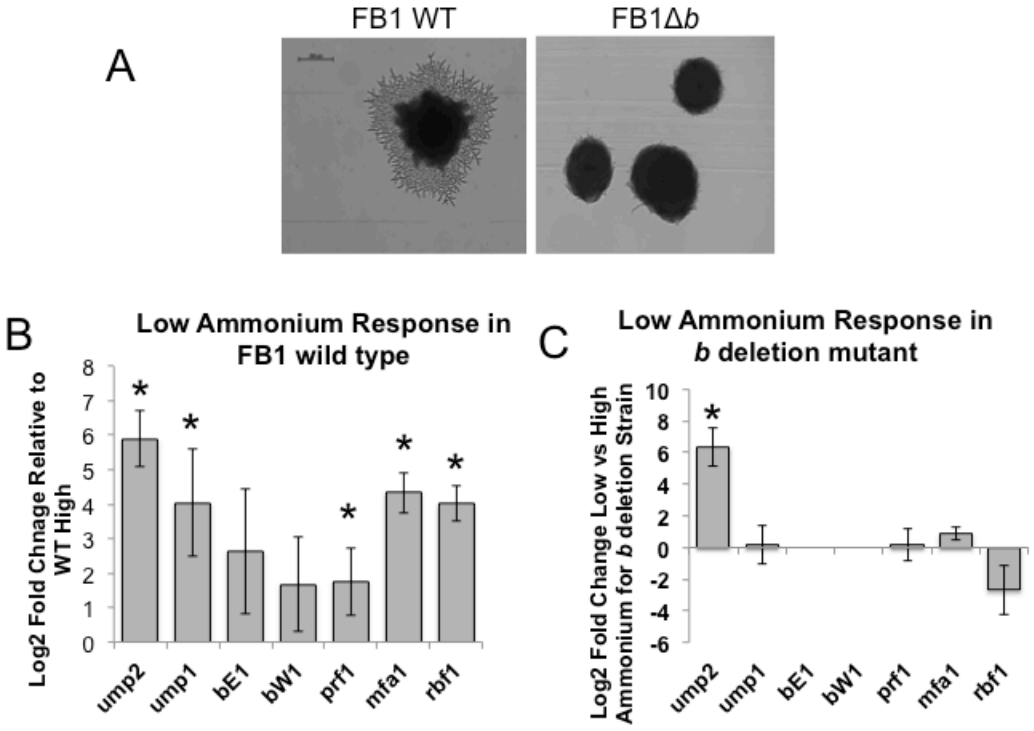

Figure 17: Deletion of the *b* locus results in loss of filamentation under low ammonium conditions and changes in gene expression levels with response to low ammonium.
(A) Haploid cells of wild-type FB1 (FB1 WT) and the FB1Δ*b* strain were grown on Low ammonium (50 μM NH_4). FB1 WT colonies display filamentous colony morphology after 4 days, while FB1Δ*b* colonies lack this phenotype. Size bars, 200 μm. **(B) (C)** Log2 Fold changes for qRT-PCR on Low, normalized and expressed relative to the same strain on High for FB1 WT (B) and FB1Δ*b* (C). Negative values reflect decreased expression, whereas positive values represent increased expression. Bars represent averages of biological triplicates and standard errors are indicated in the tables and graphs. High, 30 mM NH_4 medium, Low, 50 mM NH_4. Stars indicate significant change in expression level ($p<0.05$) as determined by Kruskal-Wallis (Daniel, 1990).

expression of several targets related to ammonium transport and the mating pathway in FB1 wild-type organisms, including the upregulation of *ump2*, the high affinity ammonium transporter, *ump1*, the low affinity ammonium transporter, as well as *bE1*, *bW1*, *mfa1*, *prf1*, and *rbf1* (Figure 17b). A similar analysis of

mutants deleted for the entire *b* locus revealed that while *ump2* was still upregulated, the expression level of the other targets did not change in response to low ammonium (Figure 17c). The goal of the current study is to examine whether an individual component of the mating type locus, either *bE1* or *bW1*, play a different role in this loss of gene upregulation and filamentation phenotype.

Deletion of either *bE1* or *bW1* also results in loss of filamentation of haploid cells in response to low ammonium, but no loss of function as a mating partner.

Strains deleted for only one part of the *b* locus, either *bE1* or *bW1*, have a similar phenotype to those deleted for the entire *b* locus. After 4 days under low ammonium conditions, RK1725 and RK1607 lacked filamentation on low ammonium much like the FB1 *b* deletion strain, while FB1 WT colonies had a filamentous appearance (Figure 18a.). However, when mixed together in equal amounts with a compatible mating partner (FB2 WT *a2b2*), both mutant strains exhibited normal fuzz morphology on charcoal agar (Figure 18b). When each mutant was mixed with a compatible mating partner bearing only the compatible portion of the *b* allele, fuzz morphology was still observed although to a lesser degree (Figure 18b). *In planta*, again using each mutant paired with the compatible FB2 wild-type, both were able to establish similar infection with similar

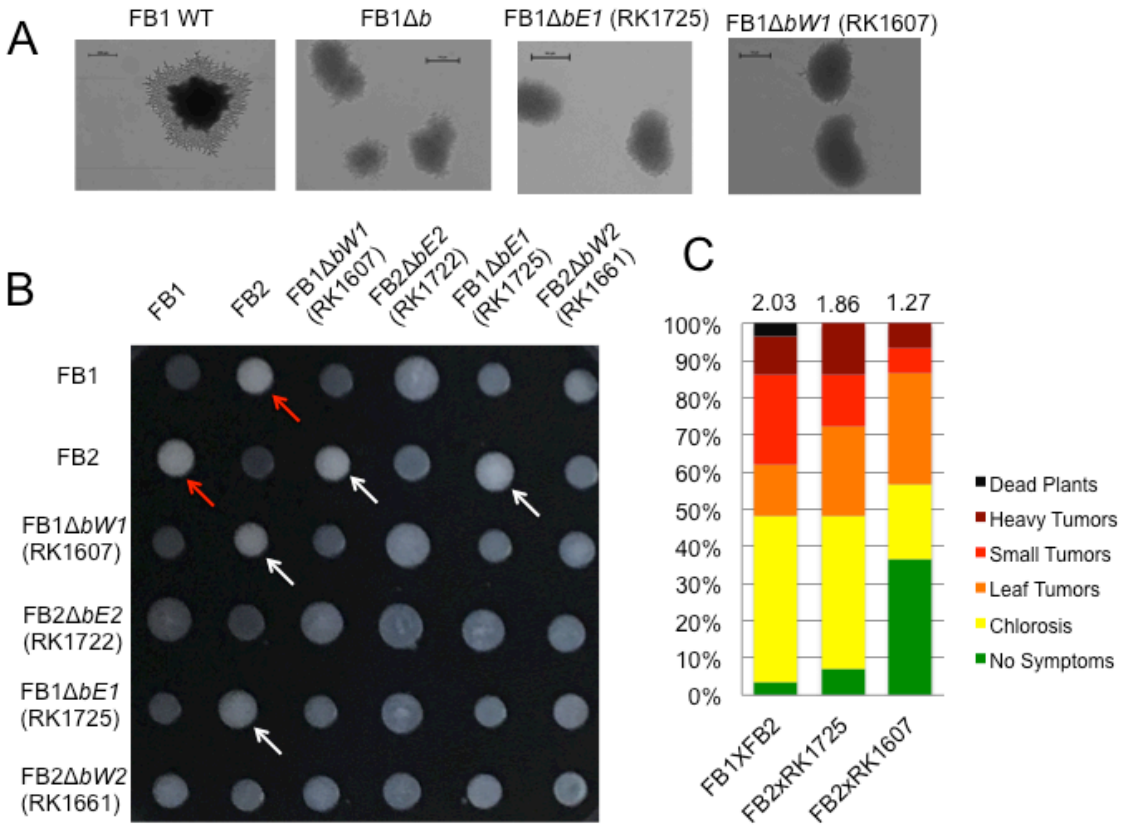

Figure 18: Strains deleted for either *bE1* or *bW1* show a defect in filamentation under low ammonium conditions but not in mating assays or infection when in the presence of a compatible mating partner.
(A) Haploid cells of wild-type FB1 (FB1 WT), FB1Δ*b* strain, RK1607, and RK1725 were grown on Low ammonium (50 μM NH_4). FB1 WT colonies display filamentous colony morphology after 4 days, while the three mutants colonies lack this phenotype. Size bars, 200 μm for FB1 WT and 100 μm for the other three. **(B)** When mixed with a compatible wild-type mating partner, FB2, RK1607 and RK1725 display fuzz phenotype on charcoal mating plates. Red arrows indicate FB1 WT x FB2 WT. White arrows indicate partial *b* mutants in FB1 background crossed with FB2. **(C)** *In planta* infection assays with either partial *b* mutant in the FB1 background crossed with FB2 wild-type resulted in similar disease indices as those with the FB1 WT crossed with FB2 WT. Bars represent percentage of plants infected with disease symptoms and diseases indices are indicated at the top of the bar graphs. No statistical significance as assessed by Kruskal Wallis (Daniel, 1990)

virulence to the FB1xFB2 wild-type cross (Figure 18c). As such, these strains showed attenuation of phenotype relating to growth as haploid cells only.

Overexpression of *ump2* in the *b* deletion strain rescues the loss of filamentation in response to low ammonium and changes global gene expression.

Overexpression of *ump2* from a constitutive promoter in FB1*Δb* resulted in filamentation on low ammonium that was indistinguishable from the filamentation observed with FB1 wild-type colonies (Figure 19). In addition to the restoration of the characteristic filamentation phenotype, overexpression of the high affinity ammonium transporter in the FB1*Δb* background changed global gene

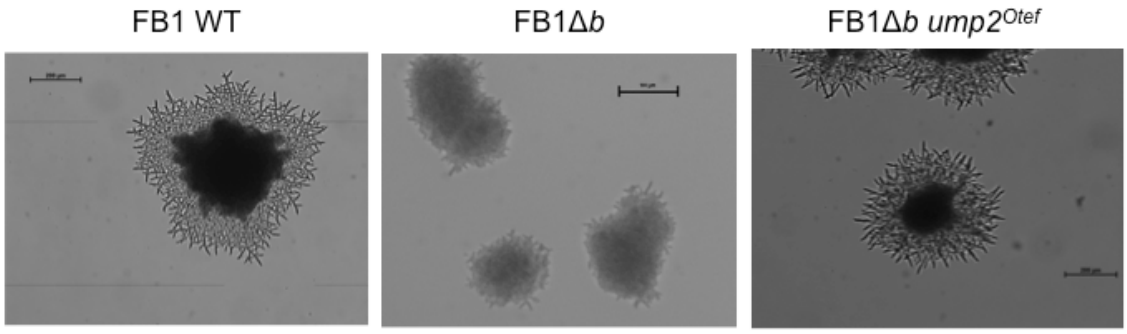

Figure 19: Overexpression of *ump2* rescues the loss of filamentation phenotype under low ammonium conditions in the FB1Δ*b* strain.
Haploid cells of FB1 wild-type (FB1 WT), FB1Δ*b*, and FB1Δ*b* *ump2*^{Potef} were grown on Low ammonium (50 μM NH_4). Wild-type colonies and FB1Δ*b* *ump2*^{Potef} filament, while the FB1Δ*b* mutant does not. Size bars, 200 μm for FB1 WT and FB1Δ*b* *ump2*^{Potef}, 100 μm for FB1Δ*b*.

expression. According to RNA-Seq data, there are 169 genes that are upregulated in the FB1 wild-type strain under low ammonium conditions but not in the FB1*Δb* under the same nutrient limitation (see Chapter 2, Figure 13). Overexpressing *ump2* in the *b* deletion background resulted in the upregulation of 63 or approximately 40% of these genes (Figure 20a). A functional analysis of these 63 genes revealed that a few pertinent categories are enriched, including metabolism, specifically of ammonia and related compounds, cellular transport,

cell rescue, defense, and virulence, and cell growth (Figure 20c). Similarly, there are 218 genes that are down regulated in the FB1 wild-type strain under low ammonium conditions but not in the FB1Δ*b* under the same conditions.

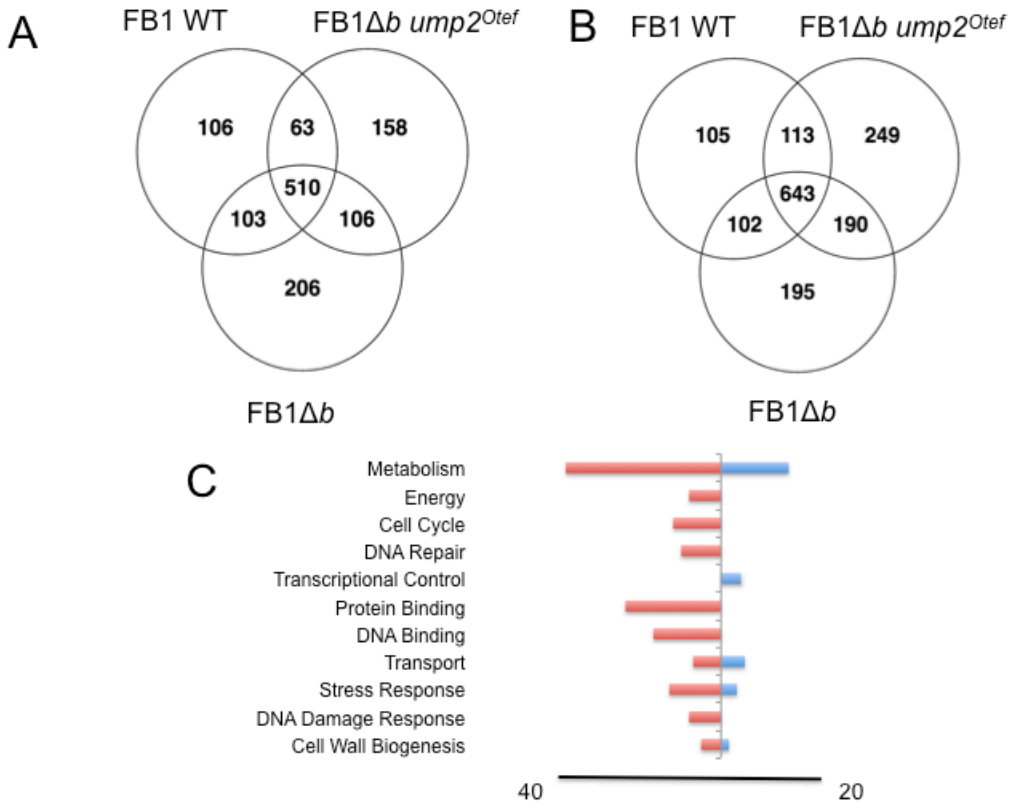

Figure 20: Overexpression of *ump2* in the FB1Δ*b* strain results in changes in global gene expression on low ammonium.
(A) Low ammonium conditions results in the upregulation of several genes in FB1 WT. Some of these genes are not differentially regulated in the FB1Δ*b* mutant but overexpression of *ump2* in the FB1Δ*b* background results in the upregulation of these genes. **(B)** A similar phenomenon is observed for genes that are typically down regulated in the FB1 WT but not down regulated in the FB1Δ*b* mutant. **(C)** Functional analysis of the genes that are correctly differentially regulated when *ump2* is overexpressed in the FB1Δ*b* background. Functional category enrichment was determined using the FunCat database available at http://mips.helmholtz-muenchen.de/funcatDB/ and enrichment was considered to be those categories with $p<0.05$. Differential expression as determined from RNA-Seq data (log2fold change>1 and $p<0.05$). Red bars indicate decreased expression; blue bars indicate increased expression.

Overexpressing *ump2* in the FB1*Δb* background resulted in down regulation of 113 of these genes, or more than 50% (Figure 20b). Enriched functional categories included metabolism, particular of C-compounds and their derivatives, energy related categories like gluconeogenesis, cell cycle and DNA processing, and biogenesis of cellular components (Figure 20c).

Quantitative Real Time PCR (qRT-PCR) analysis was also done for several targets related specifically to canonical mating genes and those related to ammonium transport in these backgrounds. Expression levels of *ump2*, the high affinity ammonium transporter, were generally increased under low ammonium conditions in the FB1 WT. Low ammonium exposure also resulted in the significant induction of *ump1*, the low affinity ammonium transporter, *mfa1*, *prf1*, and *rbf1* ($p<0.05$), all known to be functional in the mating pathway or infection (Figure 17b). Transcript levels of *bE1* and *bW1* were also increased in FB1 WT under low ammonium conditions, although not at the same significance level. In the FB1*Δb* mutant, while the characteristic induction of *ump2* was still observed, the other listed targets did not increase in the mutant under low ammonium conditions (Figure 17c). On replete ammonium media, overexpression of *ump2* from a constitutive promoter in an FB1*Δb* background resulted in significantly increased *ump2* expression ($p<0.05$) and expression of *ump1* as well, but not to the same degree of statistical significance ($p=0.0863$) (qRT-PCR data found in Table 7 reported as average of three biological replicates plus/minus standard error, Figure 21a). Under low ammonium

conditions, overexpressing *ump2* constitutively in the *b* deletion background increased *ump1* and *mfa1* expression ($p<0.05$) (Figure 21b).

Deletion of only *bE1* results in the loss of filamentation under low ammonium conditions but a different gene expression profile than with the complete *b* deletion.

RK1725 possesses only a functional copy of *bW1*, as *bE1* has been replaced by the hygromycin resistance cassette. After 4 days under low ammonium conditions, like FB1*Δb*, this mutant was unable to filament under low ammonium conditions (Figure 18a). QRT-PCR analysis of changes in gene

Table 7: Subset of Differentially Expressed Genes of Interest[a] from qRT-PCR Experiments with complete *b* deletion mutants and their derivatives

Target	WT Low[b]	*Δb* High[b]	*Δb* Low[b]	FB1Δ*b* ump2^{Otef} High[b]	FB1Δ*b* *ump2*^{Otef}*Low*[b]
ump2 (um05889)	5.89±0.81	-1.75±0.51	4.59±1.19	4.23±1.10	5.46±0.40
ump1 (um04523)	4.04±1.56	2.20±0.28	2.04±1.21	5.36±1.07	3.97±0.33
bE1 (um00577)	2.64±1.82	No amp	No amp	No amp	No amp
bW1 (um00578)	1.68±1.37	No amp	No amp	No amp	No amp
prf1 (um02713)	1.76±0.98	-1.74±0.13	-2.12±1.12	-1.56±0.35	2.59±0.56
mfa1 (um02382)	4.33±0.60	0.68±0.29	1.54±0.42	0.87±1.04	5.17±1.45
pra1 (um02383)	-0.77±1.24	0.97±2.03	0.53±2.45	-3.58±1.37	1.95±0.89
rbf1 (um03172)	4.02±0.52	4.14±0.235	0.37±0.07	3.00±1.33	0.99±0.60

[a]qRT-PCR log2 fold changes, normalized and expressed relative to FB1 WT on rich medium (High); negative values reflect decreased expression, whereas positive values represent increased expression
[b]WT, wild-type FB1; *Δb*, FB1 deleted for entire *b* mating-type locus; FB1*Δb* *ump2*^{Otef} FB1 deleted for entire *b* mating-type locus with *ump2* over-expressed from constitutive P_{otef} promoter; High, 30 mM NH_4 medium, Low, 50 µM NH_4
[c]No amp, no amplification detected

expression of the targets listed above revealed that despite the expression of *bW1* under high ammonium conditions, there was no detectable expression of *bW1* under low ammonium conditions (qRT-PCR data found in Table 8 reported as average of three biological replicates plus/minus standard error). On media replete for ammonium, deletion of *bE1* actually changed expression level of several targets examined as compared to the mutant deleted for the entire *b* locus. Expression levels of *ump2* and *mfa1* were increased, while expression levels of *ump1* and *rbf1* decreased ($p<0.05$) (Figure 22a). Under depleted

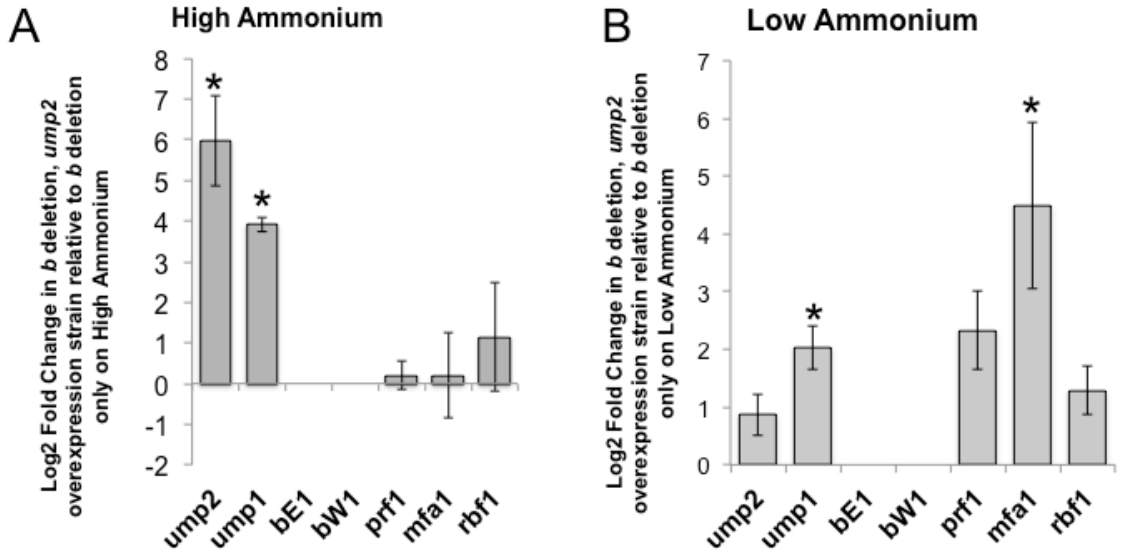

Figure 21: Overexpression of *ump2* in the FB1Δ*b* strain results in changes in expression levels of targets related to ammonium transport and mating. **(A)** High Ammonium conditions, overexpression of *ump2* in the FB1Δ*b* background significantly increased expression levels of *ump2* and *ump1* as compared to the FB1Δ*b* mutant on similar media. **(B)** Low ammonium conditions, overexpression of *ump2* in an FB1Δ*b* background resulted in significantly increased expression of *ump2, ump1,* and *mfa1*, and increased *prf1* expression, with a trend towards significance. Negative values reflect decreased expression, whereas positive values represent increased expression. Bars represent averages of biological triplicates and standard errors are indicated. High, 30 mM NH_4 medium, Low, 50 μM NH_4. Stars indicate significant change in expression level ($p<0.05$), as determined by Kruskal-Wallis (Daniel, 1990).

ammonium conditions, RK1725 had similar expression levels of *ump2* and *ump1* as the complete *b* deletion mutant. Expression levels of *prf1*, *mfa1*, and *rbf1* increased ($p<0.05$) (Figure 22b). When examining expression levels of targets in this *bE1* deletion strain from low to high ammonium, the expression profile was similar to that of FB1 WT under similar conditions, with *ump2*, *ump1*, *prf1*, and *rbf1* all being significantly increased ($p<0.05$). One notable difference was the lack of increase of *mfa1* (Figure 22c); in fact, expression was decreased in low ammonium relative to replete medium.

Table 8: Subset of Differentially Expressed Genes of Interest[a] from qRT-PCR Experiments with RK1725 and its derivatives

Target	WT Low[b]	RK1725 High[b]	RK1725 Low[b]	RK1725 *ump2*^{Otef} *High*[b]	RK1725 *ump2*^{Otef} *Low*[b]
ump2 (um05889)	5.89±0.81	1.32±0.77	3.84±1.12	4.35±0.61	9.05±0.49
ump1 (um04523)	4.04±1.56	-2.21±0.23	0.89±1.30	-0.81±0.78	4.76±0.88
bE1 (um00577)	2.64±1.82	No amp	No amp	No amp	No amp
bW1 (um00578)	1.68±1.37	0.56±0.83	No amp	3.81±0.40	0.65±0.05
prf1 (um02713)	1.76±0.98	-3.94±0.65	2.30±0.92	-0.89±0.79	1.66±0.15
mfa1 (um02382)	4.33±0.60	4.41±0.09	4.12±1.17	0.78±0.41	5.014±0.67
pra1 (um02383)	-0.78±1.24	2.13±0.41	0.42±2.58	3.16±1.25	1.15±2.12
rbf1 (um03172)	4.02±0.52	-2.02±1.28	3.01±0.89	1.90±0.12	3.36±0.05

[a]qRT-PCR log2 fold changes, normalized and expressed relative to FB1 WT on rich medium (High); negative values reflect decreased expression, whereas positive values represent increased expression
[b]WT, wild-type FB1; RK1725, *bE1* deletion in FB1 background; RK1725 *ump2*^{Otef}, RK1725 with *ump2* over-expressed from constitutive; High, 30 mM NH_4 medium, Low, 50 µM NH_4
[c]No amp, no amplification detected

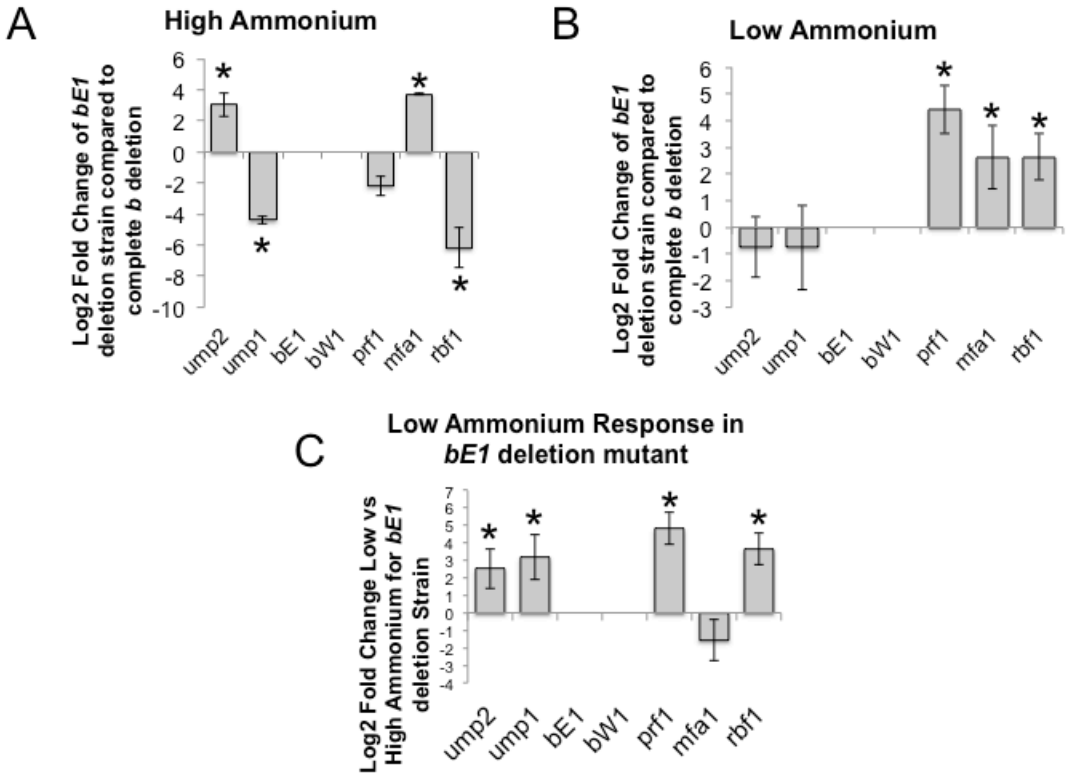

Figure 22: Deletion of *bE1* results in a different pattern of gene expression of the targets examined under high and low ammonium conditions, and a different response of the *bE1* deletion mutant to low ammonium.
(A) On replete ammonium conditions, deletion of only *bE1* results in higher *ump2* and *mfa1* expression than the complete *b* deletion, and lower *ump1* and *rbf1* expression levels. **(B)** On low ammonium conditions, while the expression levels in the *bE1* deletion strain are comparable to the complete *b* deletion strain for *ump2 and* ump1*, mfa1*, *prf1*, and *rbf1* are all upregulated in the partial *b* deletion strain as compared to the complete *b* deletion strain. (**C)** The FB1Δ*bE1* demonstrates regulation of targets examined more like the FB1 WT than the complete *b* deletion strain in response to low ammonium, with the notable exception of *mfa1*. Negative values reflect decreased expression, whereas positive values represent increased expression. Bars represent averages of biological triplicates and standard errors are indicated. High, 30 mM NH_4 medium, Low, 50 μM NH_4. Stars indicate significant change in expression level ($p<0.05$), as determined by Kruskal-Wallis (Daniel, 1990).

Overexpression of *ump2* in a mutant deleted for *bE1* restores the filamentation phenotype and changes gene expression profile in response to low ammonium.

Overexpression of *ump2* from the *Potef* constitutive promoter in the *bE1* deletion background resulted in filamentation after 4 days on low ammonium media (Figure 23a). On replete ammonium media, overexpression of *ump2* in the FB1*ΔbE1* background resulted in significantly increased expression of *ump2*, *ump1*, *prf1*, and *rbf1* ($p<0.05$) and increased *bW1* expression, with a trend towards significance ($p=0.863$) (Figure 23b). Under low ammonium conditions, constitutive overexpression of *ump2* resulted in increased *ump1* and *ump2* expression ($p<0.05$). Expression levels of *prf1*, *mfa1*, and *rbf1* were essentially identical for the FB1*ΔbE1* and FB1*ΔbE1 ump2* overexpression strain (Figure 23c). Also of note, while the expression level of *bW1* was undetectable in FB1*ΔbE1* under low ammonium conditions, in the FB1*ΔbE1 ump2* overexpressor, levels of *bW1* were detectable. While there is no mathematical way to quantitatively calculate the change in expression level as one mutant has an undetectable level of expression, it is of note that overexpressing *ump2* in an FB1*ΔbE1* background resulted in increased *bW1* expression as compared to the FB1*ΔbE1* mutant alone.

Deletion of only *bW1* results in the loss of filamentation under low ammonium conditions but a different gene expression profile than with the complete *b* deletion.

RK1607 possesses only a functional copy of *bE1*, as *bW1* has been replaced by the hygromycin resistance cassette. After 4 days under low ammonium conditions, this mutant, like FB1*Δb*, was unable to filament under low

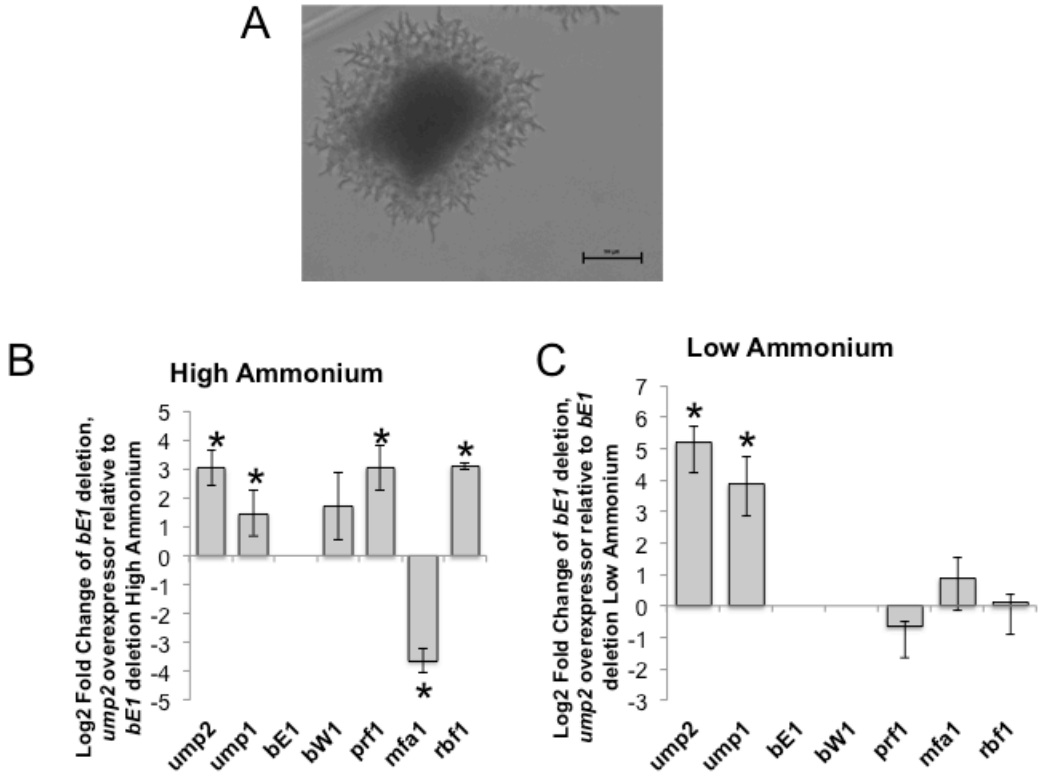

Figure 23: Overexpression of *ump2* in the FB1Δ*bE1* background results in filamentation on low ammonium.
(A) FB1Δ*bE1* strains also overexpressing *ump2* show characteristic filamenation on low ammonium after four days. Size bar, 100 µm. **(B)** Overexpression of *ump2* in the FB1Δ*bE1* results in a change in gene expression level of several targets, including upregulation of *ump2*, *ump1*, *prf1*, and *rbf1*, as compared to the FB1Δ*bE1* mutant on high ammonium. **(C)** Overexpression of *ump2* in the FB1Δ*bE1* results in a change in gene expression level of several targets, including upregulation of *ump2* and *ump1*, as compared to the FB1Δ*bE1* mutant on low ammonium. Negative values reflect decreased expression, whereas positive values represent increased expression. Bars represent averages of biological triplicates and standard errors are indicated. High, 30 mM NH_4 medium, Low, 50 µM NH_4. Stars indicate significant change in expression level ($p<0.05$), as determined by Kruskal-Wallis (Daniel, 1990).

ammonium conditions (Figure 18a). QRT-PCR analysis revealed that under replete ammonium conditions, targets examined were differentially expressed in the *bW1* deletion mutant as compared to the complete *b* deletion mutant.

Transcript levels of *ump1* were significantly decreased, while *prf1* and *mfa1* were all significantly increased ($p<0.05$) (qRT-PCR data found in Table 9 reported as average of three biological replicates plus/minus standard error, Figure 24a). Under low ammonium conditions, the expression levels of *ump2* and *ump1* were similar between the *bW1* deletion mutation and the complete *b* deletion mutant. However, *mfa1* was expressed at a significantly higher level in the *bW1* deletion mutant as compared to the complete *b* deletion mutant and *prf1* and *rbf1* showed a similar pattern ($p<0.05$) (Figure 24b). The *bW1* deletion mutant when compared to itself in low versus high ammonium only showed a significant induction for *ump2* and *ump1* (Figure 24c). It is important to note in this case

Table 9: Subset of Differentially Expressed Genes of Interest[a] from qRT-PCR Experiments with RK1607 and its derivatives

Target	WT Low[b]	RK1607 High[b]	RK1607 Low[b]	RK1607 *ump2*^{Otef} *High*[b]	RK1607 *ump2*^{Otef} *Low*[b]
ump2 (um05889)	5.89±0.81	-0.57±0.49	3.72±0.91	7.10±0.75	9.97±2.12
ump1 (um04523)	4.04±1.56	-4.20±0.304	3.12±0.99	0.66±0.74	3.15±1.24
bE1 (um00577)	2.64±1.82	2.25±0.14	1.60[d]	0.01±0.74	0.98±0.98
bW1 (um00578)	1.68±1.37	No amp[c]	No amp[c]	No amp[c]	No amp[c]
prf1 (um02713)	1.76±0.98	1.41±0.18	0.55±0.72	0.07±0.47	-3.58±1.49
mfa1 (um02382)	4.33±0.60	9.79±0.85	4.50±0.16	7.31±0.12	3.33±0.84
pra1 (um02383)	-0.77±1.24	0.12±0.39	0.43[d]	1.36±0.43	0.25±0.89
rbf1 (um03172)	4.02±0.52	1.89±0.57	2.67±0.61	2.84±1.31	0.72±0.50

[a]qRT-PCR log2 fold changes, normalized and expressed relative to FB1 WT on rich medium (High)
[b]WT, wild-type FB1; RK1607, *bW1* deletion in FB6b background; RK1607 *ump2*^{Otef}, RK1607 with *ump2* over-expressed from constitutive; High, 30 mM NH_4 medium, Low, 50 µM NH_4
[c]No amp, no amplification detected
[d]No amplification in two out of three biological replicates.

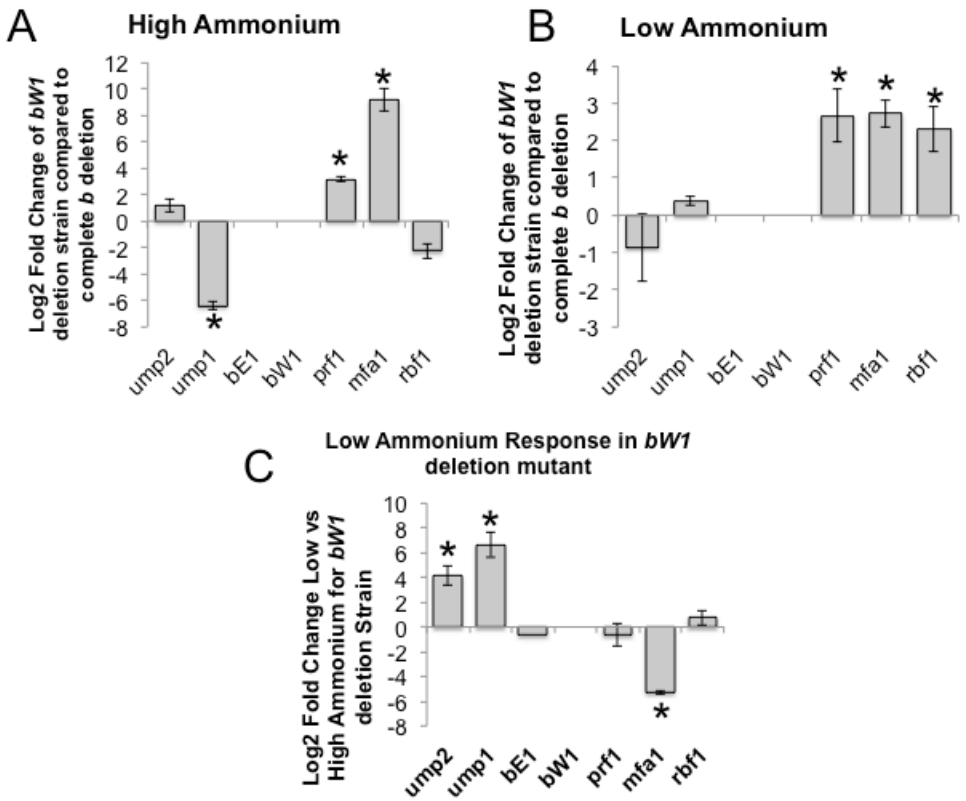

Figure 24: Deletion of only *bW1* results in a different pattern of gene expression of the targets examined under high and low ammonium conditions, and a different response than that of the *bE1* deletion mutant to low ammonium.

(A) On replete ammonium conditions, deletion of only *bW1* results in highly increased *mfa1* expression compared with *mfa1* expression by the complete *b* deletion strain, and lower *ump1* expression levels. **(B)** On low ammonium conditions, while the expression levels in the *bW1* deletion strain are comparable to the complete *b* deletion strain for *ump2* and *ump1, mfa1*, *prf1*, and *rbf1* are all upregulated in the partial *b* deletion strain as compared to the complete *b* deletion strain. **(C)** The FB1Δ*bW1* regulates the targets examined more like the complete *b* deletion strain in response to low ammonium, with the notable exception of *ump1*. Exposure to low ammonium does not result in upregulation of *ump1* in response to low ammonium. Negative values reflect decreased expression, whereas positive values represent increased expression. Bars represent averages of biological triplicates and standard errors are indicated. High, 30 mM NH_4 medium, Low, 50 μM NH_4. Stars indicate significant change in expression level ($p<0.05$), as determined by Kruskal-Wallis (Daniel, 1990).

that *mfa1* levels in the mutant under replete ammonium conditions were comparable to those found in FB1 WT under low ammonium conditions, so while there was no induction in response to low ammonium, the absolute transcript levels were comparable.

Overexpression of *ump2* in a mutant deleted for *bW1* does not restore the filamentation phenotype but does changes gene expression profile in response to low ammonium.

Overexpression of *ump2* from the *Potef* constitutive promoter in the *bW1* deletion background did not result in filamentation after 4 days on low ammonium media (Figure 25a). In fact, the colonies resembled the parental RK1607 colonies under the same depleted ammonium conditions. While there was no visible phenotypic difference in the RK1607 *bW1* deletion strain and the same background with *ump2* constitutively expressed, there were changes in gene expression levels for various targets examined. Under replete ammonium conditions, overexpression of *ump2* in the *bW1* deletion background significantly increased both *ump2* and *ump1* expression ($p<0.05$). Expression levels were decreased for *bE1* and *mfa1*, although the reduction only showed a trend toward statistical significance ($p=0.0863$) (Figure 25b). When grown on low ammonium media, overexpression of *ump2* resulted in significantly increased *ump2* expression in the *bW1* deletion background, but the other targets showed comparable levels to those of the deletion strain alone (Figure 25c).

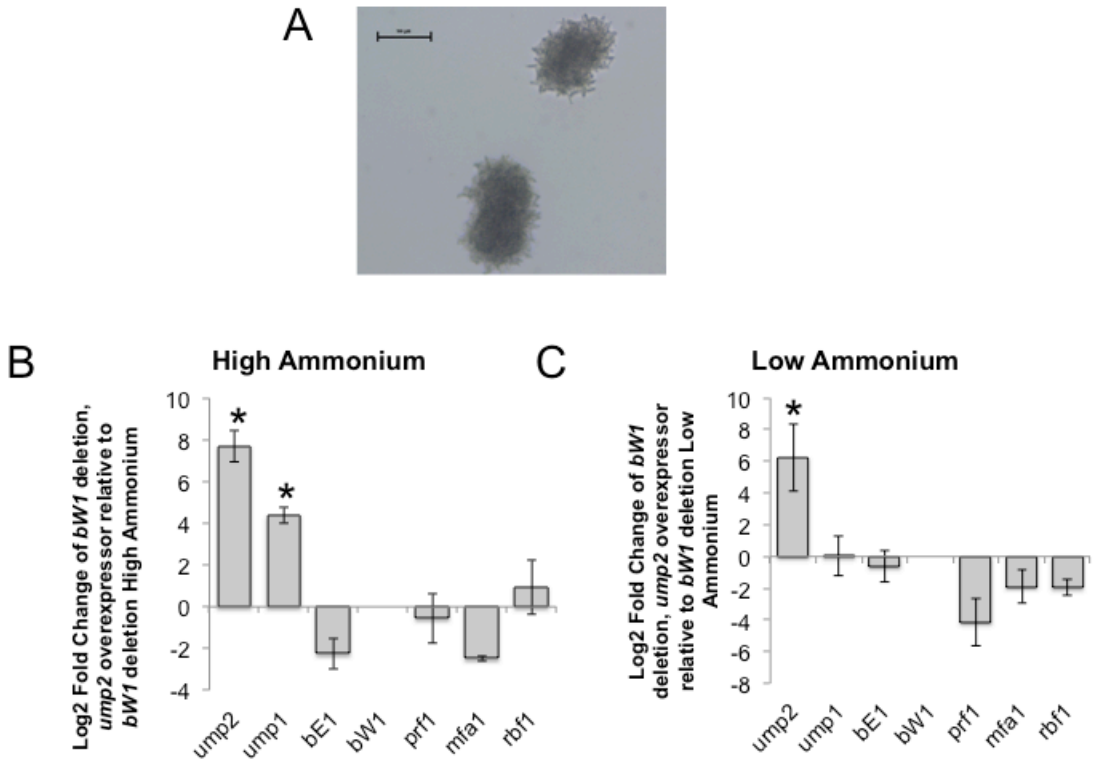

Figure 25: Overexpression of *ump2* in the FB1Δ*bW1* background does not result in filamentation on low ammonium.
(A) FB1Δ*bW1* strain also overexpressing *ump2* lacks characteristic filamentation on low ammonium after four days. Size bar, 100 μm. **(B)** Overexpression of *ump2* in the FB1Δ*bW1* results in a change in gene expression levels of a few targets, including upregulation of *ump2* and *ump1*, as compared to the FB1Δ*bW1* mutant on high ammonium. **(C)** Overexpression of *ump2* in the FB1Δ*bW1* results in a change in gene expression level of only one target, *ump2*, as compared to the FB1Δ*bW1* mutant on low ammonium. Negative values reflect decreased expression, whereas positive values represent increased expression. Bars represent averages of biological triplicates and standard errors are indicated. High, 30 mM NH_4 medium, Low, 50 μM NH_4. Stars indicate significant change in expression level ($p<0.05$), as determined by Kruskal-Wallis (Daniel, 1990).

bW1 and *bE1* affect transcription levels of different targets related to ammonium transport and mating under replete media conditions.

On high ammonium conditions, the presence of *bE1* (RK1607) or *bW1* (RK1725) alone had different regulatory effects on gene expression level. To

compare these transcript levels to both the wild-type on replete ammonium conditions and the complete *b* deletion mutant, a Kruskal Wallis multiple comparisons test was used to determine significant differences in transcript level relative to FB1 WT on replete ammonium conditions (Daniel, 1990; Yuan et al., 2006). Deletion of the entire *b* locus resulted in changes in gene expression of tested targets as compared to FB1 WT on high ammonium. For example, expression level of *ump2* was decreased in the complete *b* deletion mutant as compared to the FB1 WT under these conditions. Deletion of *bW1* resulted in a similar pattern of transcript levels (See Table 7, 8, and 9 for qRT-PCR data, Figure 26). However, deletion of only *bE1*, leaving *bW1* functional, resulted in increased expression levels of *ump2* as compared to the complete deletion strain and were comparable to transcript levels in FB1 WT (Figure 26).
Transcript levels of *rbf1* were regulated in a similar pattern, different in each of the partial deletions as compared to the complete deletion of the *b* mating type locus. Deletion of the entire locus resulted in increased expression of *rbf1* under replete ammonium conditions although RK1607 and RK1725 showed comparable levels of expression to the FB1 WT under the same conditions (Figure 26).

Deletion of the entire *b* locus resulted in slightly (although significantly) increased expression of *ump1* in this background as compared to the FB1 WT on replete ammonium media. However, deletion of either *bW1* or *bE1* resulted in dramatically decreased expression levels of *ump1* in both mutants as compared to the complete *b* deletion and FB1 WT. Similarly, although in a different

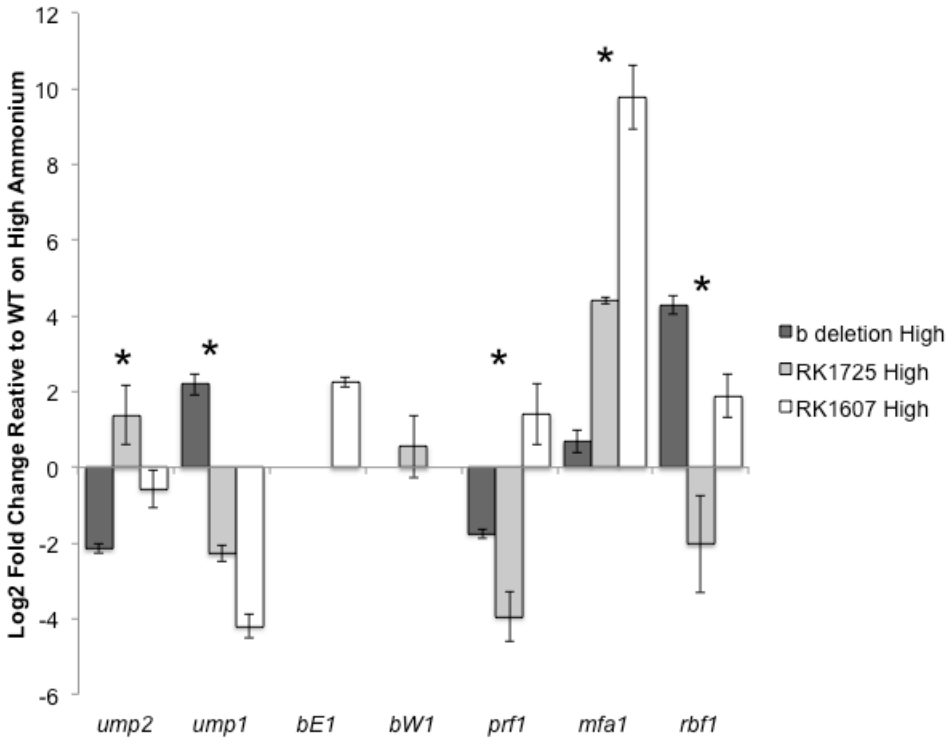

Figure 26: Comparison of transcript levels of various targets in the three variations of *b* deletion to FB1 WT on High Ammonium.
Stars indicate significant difference in expression levels across the three mutants ($p<0.05$). Negative values reflect decreased expression, whereas positive values represent increased expression. Bars represent averages of biological triplicates and standard errors are indicated in the table and graphs. High, 30 mM NH_4 medium, Low, 50 μM NH_4. Stars indicate significant difference amongst the mutants in expression level ($p<0.05$), as determined by Kruskal Wallis (Daniel, 1990).

direction, deletion of the entire *b* locus resulted in relatively little change in expression level of *mfa1*, but RK1607 and RK1725 both show markedly increased expression levels of *mfa1* under replete ammonium conditions (Figure 26).

Finally the presence of only one half of the *b* mating type locus may have a different effect on transcript level than deletion of the entire locus, but in a

manner specific to either *bE1* or *bW1*. Deletion of the entire *b* mating type locus or *bW1* alone resulted in relatively little change in the transcript level of *prf1*. However, deletion of *bE1* resulted in decreased expression levels of this target (Figure 26). While deletion of *bE1* seems to have no effect on expression of *bW1*, the *bW1* deletion mutant showed increased transcript levels of *bE1* under replete ammonium conditions (Figure 26).

bW1 and *bE1* affect transcription levels of different targets related to ammonium transport and mating under low ammonium conditions.

On media with low ammonium, mutants with partial *b* deletions showed different patterns of gene expression as compared to the mutant with the entire *b* mating locus deleted. Again, Kruskal Wallis with multiple comparisons was used to compare differences in transcript levels as compared to FB1 WT under the same media conditions (Daniel, 1990; Yuan et al., 2006). In some instances, this change made the expression level in the partial deletion strain more comparable to that of FB1 WT under similar nutrient conditions than to that of the complete *b* deletion strain (See Tables 7, 8, and 9 for qRT-PCR data). Transcript level of *ump1* was typically induced in the FB1 WT under low ammonium conditions. In the complete *b* deletion mutant, while there was increased *ump1* expression, the induction was not significant. In RK1725 (the *bE1* deletion mutant), there was no induction of *ump1*, although RK1607 (the *bW1* deletion mutant) showed a similar increased expression level to that of the FB1 WT under the same nutrient conditions (Figure 27). Exposure of FB1 WT to low ammonium also resulted in an increase in *prf1* transcript level. This induction was lost in the complete *b*

deletion strain. RK1725 showed similar induction levels to the FB1 WT, while RK1607 had no induction of this target in low ammonium (Figure 27).

For both *mfa1* and *rbf1* transcript levels, the FB1 WT grown in low ammonium had increased expression as compared to the same strain grown under high ammonium conditions. In both cases, the FB1*Δb* strain had no induction of these targets under low ammonium conditions; however, both RK1725 and RK1607 show increased expression levels of these targets as compared to the FB1 WT on high ammonium (Figure 27).

Since there was no expression seen for either *bE1* or *bW1* in the complete *b* deletion mutant, a statistical analysis for the expression level differences could not be done in this case. However, it is of note that FB1 WT under low ammonium conditions had higher transcript levels of both as compared to the same strain grown under high ammonium conditions. In the RK1725 (*bE1* deletion) strain, levels of *bW1* were undetectable in low ammonium conditions; however, in the *bW1* deletion strain (RK1607), transcript levels of *bE1* were increased under low ammonium conditions.

None of the *b* mutants filament on low ammonium media as a result of their lack of response to this condition.

While the partial *b* deletion mutants had more similar absolute expression levels of the targets analyzed as compared to FB1 WT than the complete *b* deletion, none of the *b* mutants displayed the characteristic filamentation

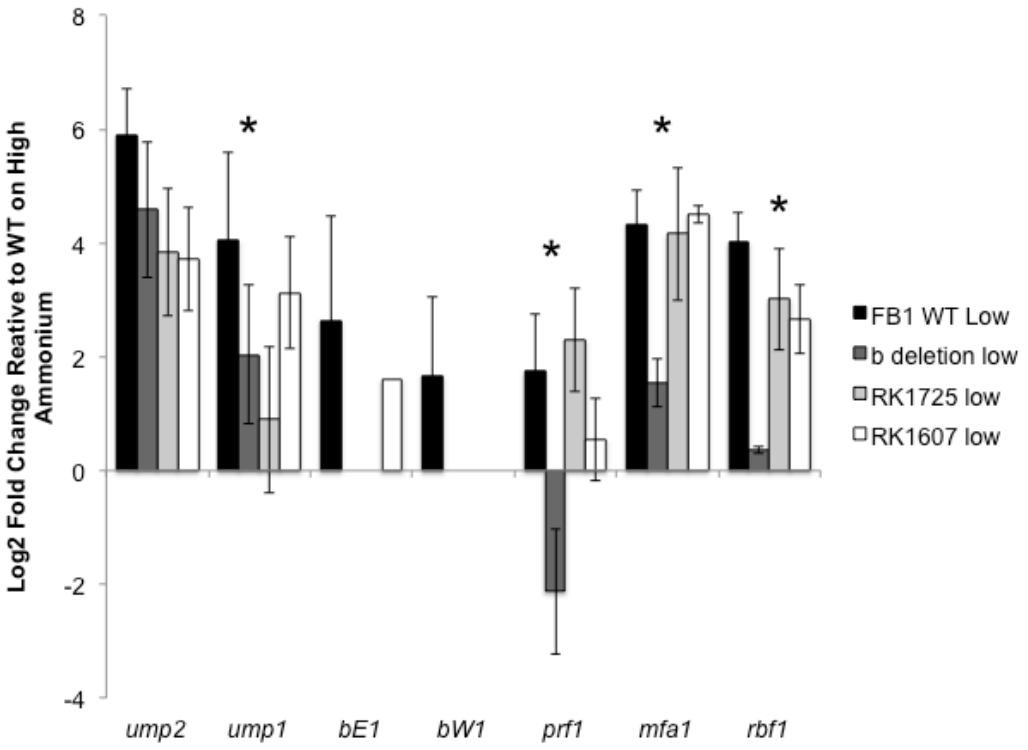

Figure 27: Comparison of transcript levels of various targets FB1 WT and *b* mutants under low ammonium conditions to transcript levels of FB1 WT on high ammonium.
Negative values reflect decreased expression, whereas positive values represent increased expression. Bars represent averages of biological triplicates and standard errors are indicated in the table and graphs. High, 30 mM NH_4 medium, Low, 50 μM NH_4. Stars indicate significant difference amongst the mutants in expression level ($p<0.05$), as determined by Kruskal Wallis (Daniel, 1990)

phenotype under low ammonium conditions. Because the targets involved are either confirmed or presumed regulatory proteins, it is also important to examine the changes in expression level within each strain, as well as compared to the FB1 WT response (Figure 28). While a specific mutation with the *b* locus may change absolute transcript level for a particular target, all of the *b* mutants showed markedly reduced ability to respond to low ammonium by changing the levels of these targets as compared to the FB1 WT (See Tables 7, 8, and 9 for qRT-PCR data). To determine if the response to low ammonium was different

between mutants, an ANCOVA was used to eliminate any variation caused by the initial expression level of each target under replete ammonium conditions (Lowry, 1999-2000). Each mutant, FB1Δ*b*, RK1725, and RK1607 had different impairments in gene induction as compared to the FB1WT; yet, they all shared the inability to induce expression levels of *mfa1* under low ammonium conditions ($p<.001$). (Figure 28).

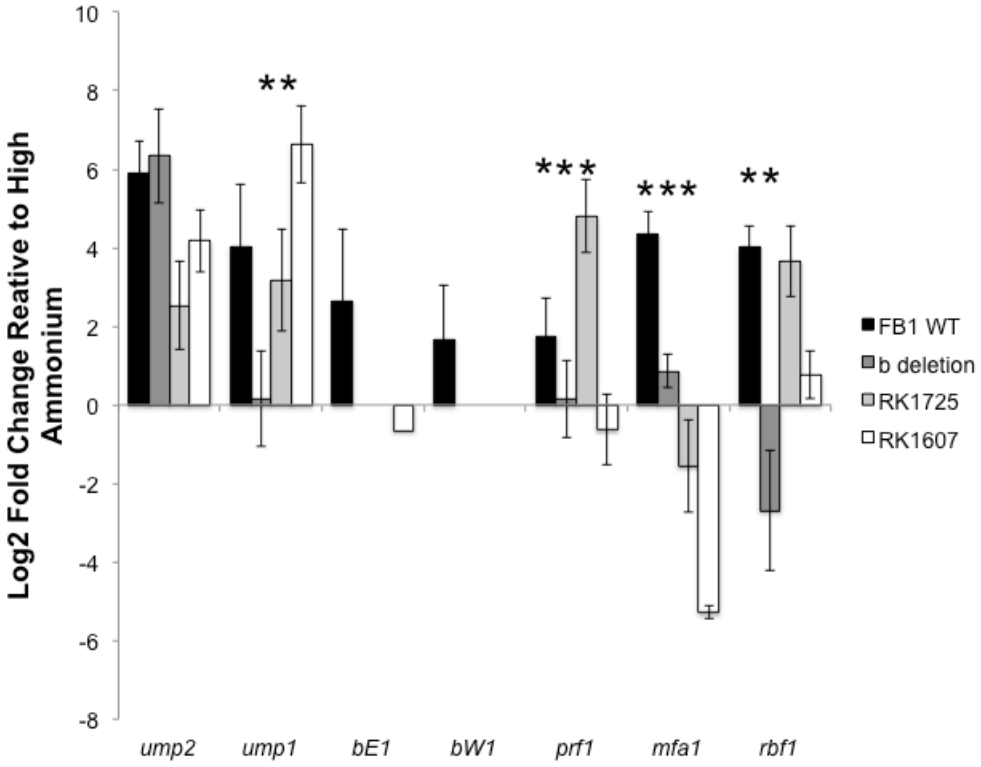

Figure 28: Response measures by transcript level change of targets analyzed in FB1 WT and *b* mutants in response to low ammonium.
Note, all three *b* mutants fail to induce *mfa1* expression, a marked difference from wild-type. Bars represent averages of biological triplicates and standard errors are indicated in the graphs. High, 30 mM NH_4 medium, Low, 50 μM NH_4. **($p<0.01$) and ***($p<.001$), as determined by ANCOVA (Lowry, 1999-2000).

Overexpression of *ump2* is able to rescue the loss of filamentation phenotype in some of the *b* mutants by rescuing the lack of transcript level responsiveness to low ammonium conditions.

Overexpression of *ump2* was able to rescue the loss of filamentation in the complete *b* deletion mutant and in RK1725, the *bE1* deletion mutant, under low ammonium conditions (Figures 19, 23a), although not in RK1607*,* the *bW1* deletion mutant (Figure 25a). To determine if the induction (or reduction) of transcript level was due to a difference in the expression level of a particular target on replete ammonium media or due to the actual change in transcript level on low ammonium for a particular mutant, an ANCOVA was used to eliminate any initial variation (Lowry, 1999-2000; Yuan et al., 2006). In both the complete *b* deletion mutant and RK1725, overexpression of the high affinity ammonium transporter resulted in the organism's ability to increase *mfa1* expression under low ammonium conditions, an ability lost in both mutants without *ump2* overexpression (Figure 29). Moreover, the *bE1* deletion mutant with overexpression of *ump2* also showed a dramatic decrease in other mating targets, such as *rbf1*, and *prf1* on low ammonium as compared to the FB1 WT and the other two mutants, also overexpressing *ump2* (Figure 29).

Because filamentation phenotype seemed to directly correlate to the ability to induce expression of *mfa1* under low ammonium conditions, expression levels of *pra1*, the pheromone receptor and other component of the *a* mating type locus, were examined to determine if the induction applied to the *a* locus as a whole, or if it was specific to *mfa1*. As was the case with the *b* mating type locus, expression levels of the two components of the *a* locus were not equivalent.

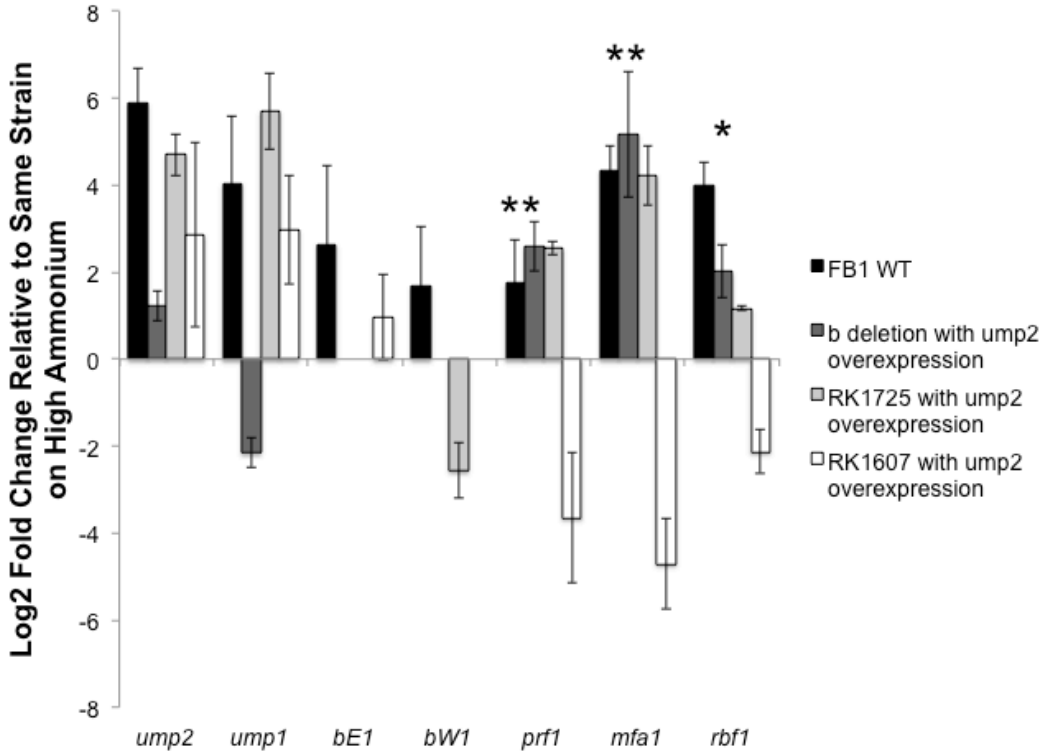

Figure 29: Response of various *b* mutants to low ammonium when the strains are also overexpressing *ump2*.
Overexpression of *ump2* changes the response of FB1Δ*b* and FB1Δ*bE1* (RK1725) to low ammonium by upregulating targets not observed in the mutants without *ump2* overexpression, while overexpression in the FB1Δ*bW1* (RK1607) background results in a decrease of several targets related to mating in response to low ammonium. Bars represent averages of biological triplicates and standard errors are indicated in the graphs. High, 30 mM NH_4 medium, Low, 50 μM NH_4. *(p<.05) and **(p<.01), as determined by ANCOVA (Lowry, 1999-2000).

Expression level of *pra1* does not seem to play a role in filamentation phenotype.

Unlike *mfa1*, *pra1* was not induced in the FB1 WT under low ammonium conditions (Tables 7, 8, and 9; Figure 30a and 30b). While increased expression level of *mfa1* under low ammonium conditions correlated with ability to filament under low ammonium conditions, there was no pattern of induction or loss of induction across the complete *b* deletion mutant, the partial *b* deletion mutants,

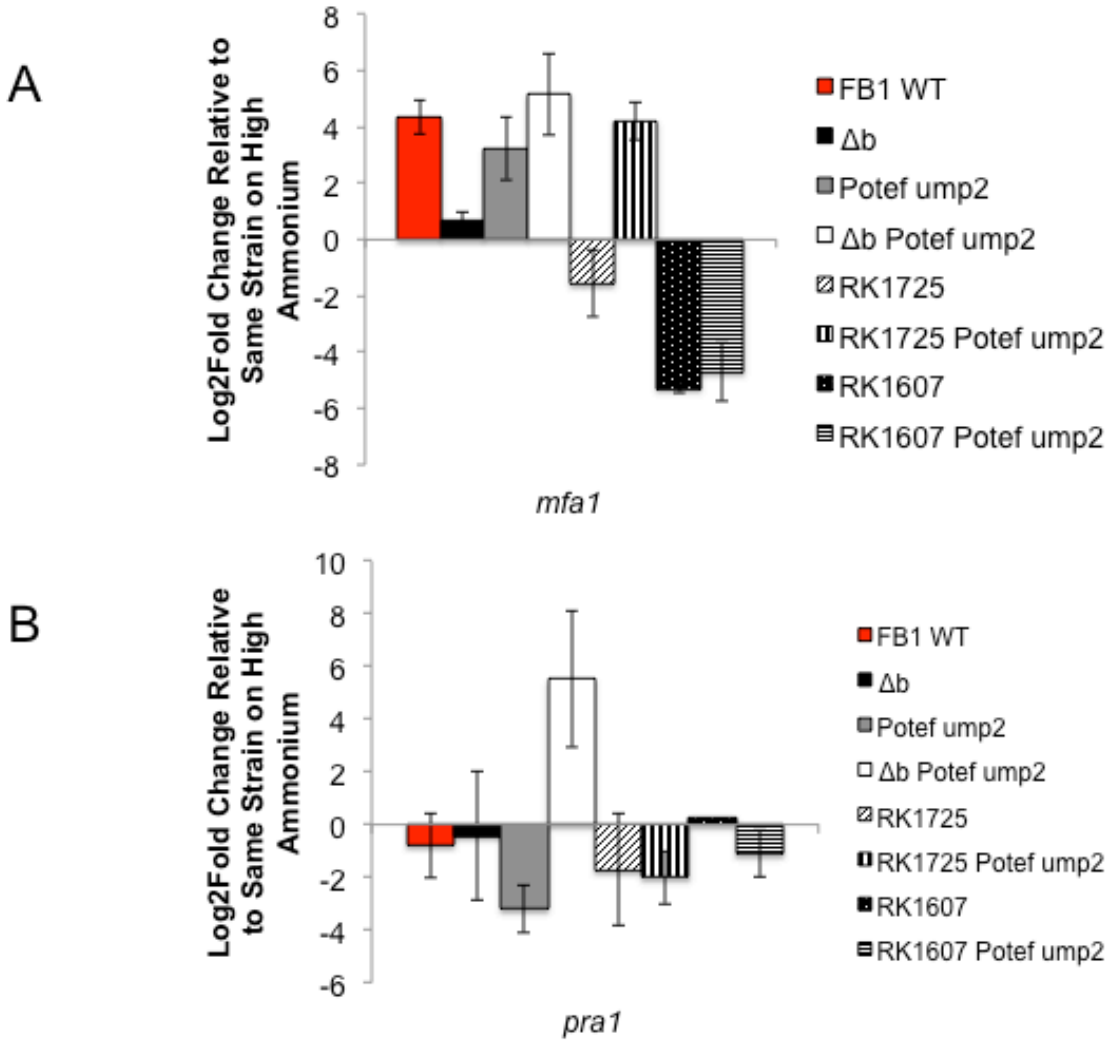

Figure 30: Changes in expression levels of *mfa1* and *pra1* in various mutants on low versus high ammonium.
(A) *mfa1* and **(B)** *pra1* expression levels in the mutants examined in this study. Bars represent averages of biological triplicates and standard errors are indicated in the graphs. High, 30 mM NH_4 medium, Low, 50 μM NH_4.

or the *b* mutants over expressing *ump2* with regards to *pra1* that correlated with the change in phenotype (Figure 30b). As such, it appears that the filamentation of haploid cells does not require increased expression from the entire *a* mating locus, but just *mfa1.* It is of note that overexpression of *ump2* in a complete *b* deletion background resulted in higher induction of *pra1* than any of the other mutants analyzed. Similarly, this same mutant demonstrated increased levels of

mfa1 expression as compared to the *b* deletion strain alone. Moreover, over expressing *ump2* in the wild-type background (*i.e.*, with the *b* mating locus intact) increased *mfa1* expression under low ammonium conditions, while decreasing *pra1* expression by approximately the same magnitude. A similar pattern emerges for expression levels of the two components of the *a* mating locus in the *bE1* deleted mutant (RK1725) overexpressing *ump2*. Conversely, when *ump2* is overexpressing in the *bW1* deletion mutant (RK1607), *mfa1* expression is dramatically reduced under low ammonium conditions and *pra1* expression remains unchanged from high to low ammonium in this mutant. While the expression levels of *pra1* do not correlate with the filamentation phenotype, it is interesting that while *ump2* overexpression can have a positive regulatory affect on both components of the *a* mating type locus under low ammonium conditions when the entire *b* mating locus is absent.

Discussion

bE1 and *bW1* have different effects on transcriptional levels of various targets related to ammonium metabolism and mating under replete ammonium conditions.

Under low ammonium conditions, wild-type *U. maydis* cells typically show a filamentous colony morphology. Deletion of the entire *b* mating locus led to loss of this phenotype. Partial deletions of the *b* locus, either of *bE1* or *bW1*, leaving the remaining allele intact and functional, also resulted in the loss of filamentous phenotype.

Deleting the entire *b* mating type locus resulted in changes in gene expression of several targets examined as compared to FB1 WT when the

strains were on grown under replete ammonium conditions. Most notable, *prf1* expression was decreased as were expression levels of *mfa1* and *rbf1*, although to a lesser extent. Deletion of only *bE1* resulted in decreased *ump1* expression, a phenomenon not observed in the complete *b* deletion. Moreover, while *prf1*, *mfa1*, and *rbf1*, were expressed at lower levels in the complete *b* deletion, their expression levels remained largely unchanged in the *bE1* deletion. Conversely, *a bW1* deletion strain showed no defect in *ump1* expression, but had reduced *prf1* expression, similar to the complete *b* deletion strain. This observation implies that under replete ammonium conditions, the absence of *bE1* is more influential on *ump1* expression levels than the presence of *bW1*, in a way that *bE1* may have a negative regulatory effect, albeit it either indirect or using other components to provide the effect, on *ump1* expression levels.

In a similar vein, the complete deletion of the *b* mating locus resulted in reduction of *prf1* expression under replete ammonium conditions as did the deletion of *bW1*, while the *bE1* deletion mutant had an expression level similar to that of FB1 WT, implying that *bW1* presence is more important for *prf1* expression than *bE1*, having a positive regulatory effect.

_bE1_ and _bW1_ regulate gene expression differently in response to low ammonium.

Under low ammonium conditions, the complete *b* deletion mutant was incapable of inducing *ump1* expression; that is, the expression level in this mutant was the same on low and high ammonium. However, the presence of either *bE1* or *bW1* resulted in induction under low ammonium similar to that of

FB1 WT under the same nutrient conditions, indicating that either is sufficient for normal *ump1* induction.

The complete *b* deletion mutant also was defective in induction of *prf1*, *mfa1*, and *rbf1* expression under low ammonium conditions. RK1725, the *bE1* deletion mutant, displayed induction levels of *rbf1* comparable to those of FB1 WT and, in fact, increased levels of *prf1.* On the other hand, RK1607*,* the *bW1* deletion mutant, was unable to induce either other these targets, indicating that *bW1* is sufficient for induction of these targets under the same nutrient limiting conditions. None of the three *b* mutants increased *mfa1* expression, which correlated to an inability to filament on depleted nutrient conditions.

bE1 and bW1 contribute to regulation of gene expression differently upon overexpression of _ump2_ under low ammonium conditions.

Overexpression of *ump2* in either a complete *b* deletion background or a *bE1* deletion background resulted in restoration of both the filamentation phenotype and the ability to induce *mfa1* expression under low ammonium conditions. The same overexpression in the *bW1* deletion background restored neither. Additionally, while overexpression of *ump2* in the FB1 wild-type background generally increased *mfa1* expression and decreased *pra1* expression, when overexpressed in the complete *b* deletion background, both components of the *a* mating locus were upregulated under depleted ammonium availability. The pattern of increasing *mfa1* and decreasing *pra1* was also seen when ump2 was overexpressed in the *bE1* deleted background (RK1725) on low ammonium, while a different pattern emerges for overexpression of *ump2* in the

bW1 deleted background, again suggesting interplay between these two regulators at the level of transcription.

Expression level of *ump2* may be part of a signaling pathway that leads to filamentation. If regulation by *ump2* under limited ammonium availability in the absence of a mating partner favors filamentation, it would follow that the pheromone receptor, *pra1* would be downregulated, as it would be useless to make receptors with the absence of pheromone. Moreover, *mfa1* upregulation under low ammonium conditions appears to be a prerequisite for filamentation, as all the mutants who are able to filament when grown on depleted ammonium media demonstrate an induction of *mfa1* in this condition. The presence of *bW1* favors regulation in a positive manner, while presence of *bE1* may block the organism's ability to upregulate *mfa1* in this manner by targeting an upstream regulator of *mfa1* under low ammonium conditions. In the complete *b* deletion mutant, where neither *bE1* or *bW1*, *ump2* overexpression was able to increase *mfa1* expression. Because this phenomenon was observed without either portion of the *b* mating locus, *bW1* was not essential for this induction to occur. Similarly, in RK1725 where *bE1* is missing, the same induction occurred. However, in RK1607, the presence of *bE1* prevented this induction from happening.

Filamentation is a haploid cell's response to low ammonium conditions, in the absence of a mating partner. In the presence of both components of the *b* mating locus, as is the case with FB1 WT, the combined regulatory processes of *bE1* and *bW1* resulted in filamentation and induction of *mfa1* transcript level

under low ammonium conditions. RK1607 showed markedly increased *mfa1* expression levels as compared to both the complete *b* deletion and RK1725 on high ammonium (Figure 26). On low ammonium, *mfa1* transcript levels in the two partial *b* deletion strains were approximately equal (Figure 27), although the change in absolute transcript level was the same in the RK1607 from high to low ammonium. The complete *b* deletion mutant had comparable *mfa1* expression levels on replete media, with no significant change in expression levels of this gene on low ammonium. In this instance, transcriptional regulation by *bW1* allows for the response to low ammonium, in this case increased *mfa1* expression as compared to the same strain under replete ammonium conditions. Additionally, the presence of *bE1* without *bW1* also down regulates targets related to mating, specifically *prf1* and *rbf1*, in the presence of *ump2* overexpression (Figure 29). It is unlikely that *mfa1* expression is directly responsible for the filamentation phenotype, but rather upregulation of *mfa1* is the byproduct of another pathway that *ump2* overexpression is able to influence in the absence of *bE1.*

Another interesting observation from this study has been the lack of necessity of *ump1* expression for the filamentation phenotype under low ammonium conditions. While overexpression of *ump2* rescued the loss of filamentation phenotype in the complete *b* deletion mutant, it was not through increased expression levels of *ump1*. Overexpression of *ump2* in this background did not dramatically change the expression level of *ump1* from high to low ammonium, meaning that while overall expression levels of *ump1* are

higher than in the *b* deletion mutant under both high and low ammonium conditions, there was no induction in the FB1*Δb ump2* overexpression mutant from high to low ammonium (Figure 29).

Furthermore, absence of one portion of the *b* mating type locus did not seem to dramatically affect the transcript level of the remaining allele. In both RK1725 and RK1607, expression level of the intact portion of the *b* locus was not dramatically altered in a way that could clearly explain the phenomenon observed. In the absence of one half of the *b* mating type locus, expression of the other allele was comparable to expression level in the FB1 WT on high ammonium. On low ammonium, *bW1* was virtually undetectable under low ammonium conditions, but its expression level was not high to begin with under replete ammonium conditions in RK1725. For the *bW1* deletion mutant, *bE1* expression was virtually the same under high and low ammonium conditions.

Under low ammonium conditions, a haploid cell would prefer to mate, penetrate a host, and access nutrients in that manner. The haploid cell in response to low ammonium attempts to respond in a way that will both guarantee survival of the cell should a compatible mating partner not be found and prepares the cell for mating in the event that a compatible mating partner is detected. The two components of the *b* mating type locus may serve to modulate these responses in opposite directions. In response to low ammonium, *bW1* serves to increase *prf1* and *rbf1* expression level, both of which play essential roles in mating. Conversely, *bE1* serves to modulate transcription levels of these targets

in response to low ammonium, in a way to preserve metabolic energy in the absence of a compatible mating partner.

Expression levels of *ump2* not only are the result of low ammonium conditions but also indicate to the organism the lack of nutrients in their environment. Previous work has demonstrated that deleting *ump2* also resulted in loss of filamentation phenotype under low ammonium conditions and the reduction of expression levels of mating-related targets, particularly *mfa1* (Chapter 2). In this manner, overexpression of *ump2* is interpreted as a severe case of nutrient deprivation and the response of transcript level regulated by the components of the *b* mating type locus is a more extreme version of the typical response to low ammonium. In this instance, *bE1* regulation serves to block even more transcription of mating-related genes, such as *mfa1*, *prf1*, and *rbf1*. Similarly, *bW1* ramps up its transcriptional efforts to prepare for the presence of a mating partner by increasing these targets. In the absence of both components of the *b* locus, these targets are still upregulated as their expression level is not dependent on *bW1*; however, whatever regulation is able to increase their expression level is unable to operate in the presence of *bE1* without *bW1.*
To this end, the current work demonstrates that *bE1* and *bW1* play different roles in transcriptional regulation in haploid cells, particularly in response to low ammonium. The expression levels of *ump2* also serve to regulate the response to low ammonium, partially in coordination with *bE1* and *bW1* regulation (Figure 31). Overexpression of *ump2* was able to change gene expression levels of targets related to mating in the absence of the entire *b* mating locus, indicating

that the regulation by *ump2* expression level is not completely dependent on the *b* mating type allele. Furthermore, presence of *bE1* without *bW1* was able to abolish the effect of increased *ump2* expression levels, indicating that while regulation of *mfa1*, *prf1*, and *rbf1* by *ump2* and *bW1* may serve to increase expression in response to low ammonium, regulation by *bE1* serves to prevent an induction of expression under low ammonium.

This may be the first example of the ability of homeodomain proteins from basidiomycetes acting independently of normal binding partners (which are not present in haploid cells). Moreover, this work indicates that the ability to sense

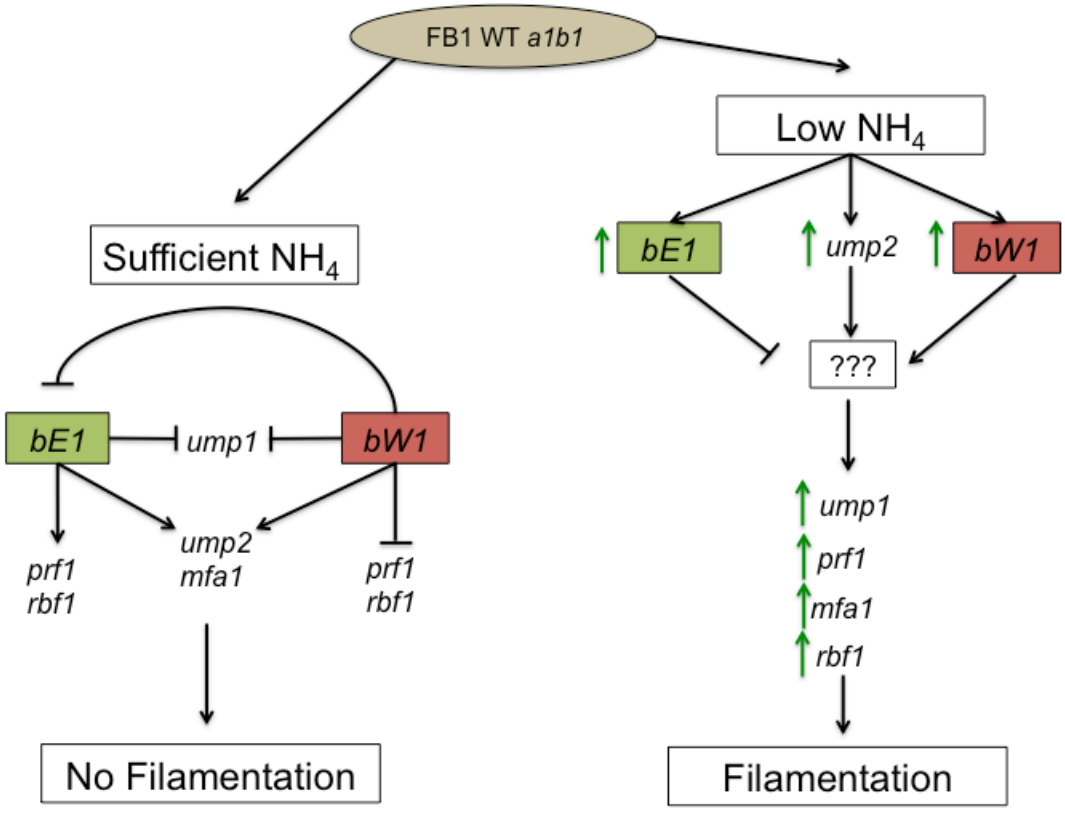

Figure 31: Proposed model for *bE1* and *bW1* under high and low ammonium conditions.

nitrogen availability through *ump2* expression levels is directly tied to the mating program, before induction of mating by a compatible mating partner. The expression level of *mfa1* has been previously demonstrated to be responsive to the cAMP pathway, as well as to *prf1* and the PKA pathway (Hartmann et al., 1999). The expression level of *ump2* may serve as the conduit for the environmental signal necessary in a haploid cell that results in activation of the cAMP pathway and summarily upregulation of both *prf1* and *mfa1.* Further investigation of genes directly responsive to *ump2* expression level will be necessary to understand clearly by what pathway this signal is translated into gene expression levels and alternative cellular phenotypes.

CHAPTER IV

PROTEIN-LEVEL INVESTIGATION OF *USTILAGO MAYDIS* HAPLOID PHENOTYPES

Chapter Overview

In order to infect its host plant, *Ustilago maydis* must undergo a dimorphic change from a budding yeast-like state to a filamentous dikaryon. In wild populations, this switch is mediated by first initiating mating. In the absence of a mating partner, haploid cells also undergo phenotypic changes when grown in nitrogen-limited solid media. Mutants deleted for either the *b* mating locus or the *ump2* high affinity ammonium transporter are unable to mate or to establish infection in the host and are similarly unable to filament when exposed to low ammonium conditions as haploid cells. The goal of the current set of experiments was to find targets not related to mating and pathogenicity that may be differentially regulated as a result of these mutations so as to further elucidate the loss of filamentation in haploid cells. While rearrangement of the actin cytoskeleton is paramount for this filamentous response, differential regulation of actin expression and the actin regulatory proteins investigated can be excluded as the reason for the observed phenotypes. Moreover, while different *ump2* and *b* mutants show differing abilities to survive adverse environmental conditions potentially encountered during infection, differential regulation of targets related

to cell wall integrity, budding, polarity, and cell wall modification cannot fully explain the observed filamentous phenotype on low ammonium medium. As such, the regulation that brings about this change in phenotype is not at the level of transcription.

Introduction

Ustilago maydis, the biotrophic pathogen of maize, undergoes a dimorphic switch from a budding yeast-like state to a dikaryotic infectious state in order to infect its host and complete its lifecycle. This switch is mediated by environmental signals, such as nutrient starvation, and the activation of the mating pathway. In nature, the dikaryotic infectious state is the product of mated haploid cells, although in the laboratory setting, haploid mutants have been constructed that are solopathogenic as a result of containing opposite alleles of mating type locus genes. Moreover, in the absence of a mating partner, wild-type haploid strains also show other phenotypic switches when nutrients are depleted, particularly nitrogen in the form of ammonium. Wild-type strains form colonies with a characteristic filamentation phenotype surrounding the central colony area (see Chapter 2, Figure 7). Our attempt at understanding this phenotype thus far has focused on genes related to mating and nitrogen assimilation at a transcript level. We sought to further elucidate the change in colony morphology by examining changes at a protein level, as well as identifying other potential targets that are differentially regulated in strains with mutations in genes related to mating and nitrogen assimilation.

In Chapter 2, we examined the role of *ump2* overexpression in changing the colony morphology of *U. maydis* strains. While FB1 WT cells only form filamentous colonies in depleted nitrogen environments, overexpression of *ump2* resulted in filamentation under replete ammonium conditions and hyperfilamentation under low ammonium conditions. From RNA-Seq data, it appeared that transcript level of *ump2* was exponentially higher in the *ump2* overexpressor on low ammonium than the wild-type under similar media conditions, leading us to hypothesize that protein product from the overexpression construct was having an impact on the native locus. To this end, we fluorescently tagged *ump2* expressed from the native locus with YFP to allow us to determine if overexpressing *ump2* would increase protein coming from gene products of this locus, in the hopes of having a protein-level explanation of the hyperfilamentation phenotype.

In addition to seeking an understanding of the hyperfilamentation phenotype associated with overexpression of *ump2* under limited nitrogen availability, we also wanted to explore other proteins more directly involved in the response than the regulatory proteins previously analyzed. Low ammonium availability can be thought of as one of many environmental stresses a haploid *U. maydis* cell may encounter in the natural environment. To fully understand if our group of mutants were responding differently to environmental stress, we examined their viability in other conditions known to evoke the stress response. Upon entry into its host plant, *U. maydis* encounters a variety of unfavorable conditions, including changes in osmolarity, to which it must be able to effectively

respond to establish an infection (Salmeron-Santiago et al., 2011). A similar situation can be simulated in the lab by growing *U. maydis* on media supplemented with high concentrations of either sorbitol or sodium chloride (NaCl). We used these conditions to assess if any of our mutants were attenuated in the ability to respond to this type of stress, potentially explaining their inability to establish infection.

Moreover, in order to create the filaments seen in haploid colonies under low ammonium conditions, we hypothesized that the organism must be able to rearrange its cell wall. To test this hypothesis, we examined the effect of Congo Red, a known cell wall stressor, on the viability of our group of mutants. Congo Red can affect cell wall assembly by binding directly to chitin and inhibiting enzymes that link macromolecules to β-1,3-glucan and β-1,6-glucan, ultimately weakening the cell wall (Ram & Klis, 2006). Susceptibility to Congo Red can be used to detect mutants with an inability to maintain their cell wall integrity and mutants with more chitin in their cell walls seem to be more susceptible (Ram & Klis, 2006).

We also hypothesized that the ability to create these filaments seen around colonies of haploid *U. maydis* cell involved rearrangement or modification to the actin cytoskeleton. Actin is abundant and highly conserved across all eukaryotes (Berepiki, Lichius, & Read, 2011). Globular actin polypeptides can assemble into filaments and two filaments can form a double-helix known as a microfilament (Berepiki et al., 2011). Assembly into these structures changes often and rapidly, allowing for cellular organization and shape of an individual cell

(Berepiki et al., 2011). Actin filaments are bundled by tropomyosin and other components to allow for transportation of vesicles essential for cell survival (Berepiki et al., 2011) (Figure 32). To visualize changes in the actin cytoskeleton in the growth of filaments around colonies of haploid cells responding to low ammonium, we used fluorescently tagged elements related to actin and examined the expression level of actin regulatory proteins.

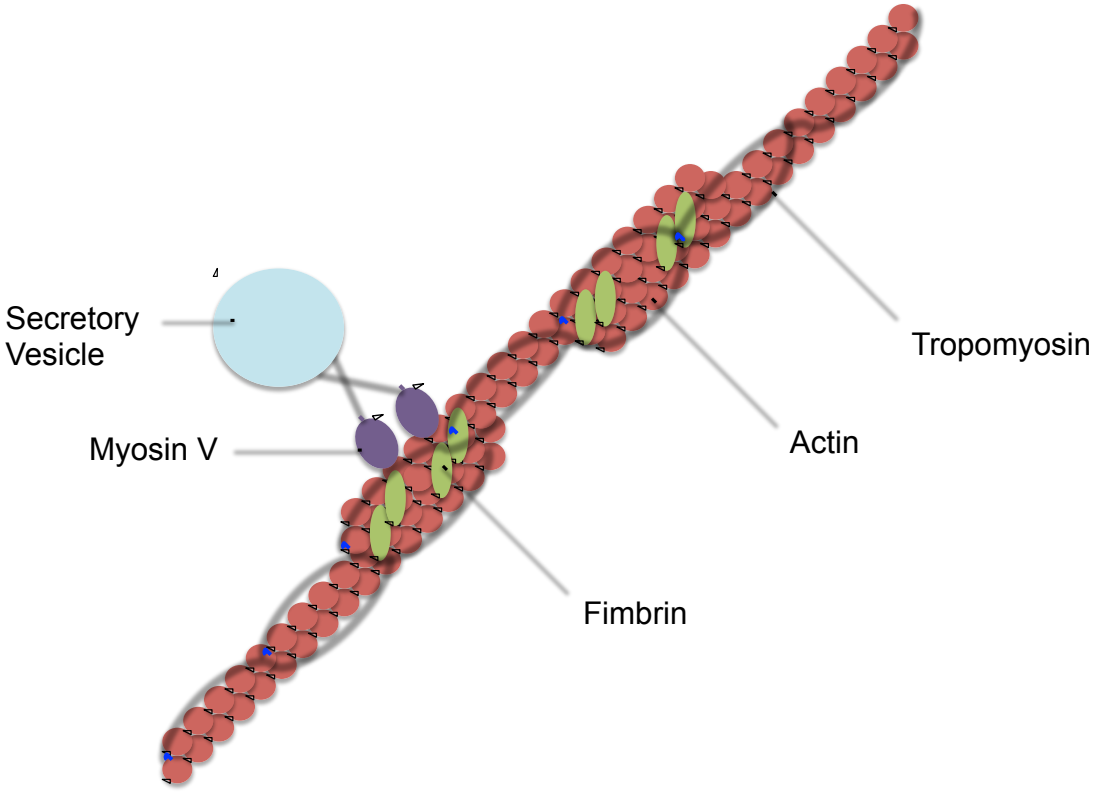

Figure 32: Diagram of Fungal Actin Microfilament Wrapped with Tropomyosin.

As a group, these experiments allow us to examine the formation of filaments in response to low ammonium at a protein level and at the targets more closely related to cell morphogenesis. Here we provide evidence that not only are protein products of the *b* mating locus and the *ump2* high affinity ammonium

transporter able to change the regulation of other genes involved in mating and pathogenicity, but also regulation by these elements changes the organism's ability to survive adverse conditions and respond to these adverse conditions through modification of the cell wall and actin cytoskeleton.

Methods

Strains and Growth Conditions

U. maydis cells were grown at 30^{o}C on Array Medium [AM] (6.25% Holliday Salt Solution (Holliday, 1974), 1% glucose, 30 mM Glutamine/50 µM Ammonium sulfate and 2% agar) and Array Medium [AM] with low ammonium (6.25% Holliday Salt Solution, 1% glucose, 50 µM ammonium sulfate and 2% agar) for 48 hrs. *U. maydis* strains used are listed in Table 10.

Stress Media Conditions

For stress tests, *U. maydis* cells were grown in YPS (1% yeast extract, 2% peptone, 2% sucrose) liquid media overnight and diluted to an Absorbance of 0.500 at 600 nm ($O.D._{600}$). The diluted culture was then further serially diluted in water 10x, 100x, and 1000x. Cell suspension were spotted on respective stress test plates in 20 µL drops and incubated at 30°C. Images were taken at 24 and 48 hours incubation.

Growth for stress tests was compared to the same strains and dilutions plated in a similar fashion in YPS solid media (1% yeast extract, 2% peptone, 2% sucrose, 2% agar). Strains were grown on YPS media supplemented with

another compound to induce stress. 1 M Sorbitol and 1 M NaCl were used to test osmotic stress, and 130 µM Congo Red was used to test cell wall integrity.

Table 10: *Ustilago maydis* Strain List for Chapter 4

Strain	Genotype	Reference
FB1 WT	*a1 b1*	(F. Banuett & Herskowitz, 1989)
FB1Δ*b*	*a1 b1 bE/W::hyg*^{R}	Chapter 2
FB1 *Δump2*	*a1 b1 ump2::hyg*^{R}	Chapter 2
FB1 *ump2*^{Otef}	*a1 b1* P_{otef}*ump2, cbx*^{R}	Chapter 2
FB1Δ*b ump2*^{Otef}	*a1 b1 bE/W::hyg*^{R} P_{otef}*ump2, cbx*^{R}	Chapter 3
FB1 Δ*ump2c*	*a1 b1 ump2::hyg*^{R} P_{otef}*ump2, cbx*^{R}	Chapter 2
RK1607	*a1 bE1 bW1::hyg*^{R}	(Gillissen et al., 1992)
RK1725	*a1 bW1 bE1::hyg*^{R}	(Gillissen et al., 1992)
RK1607 *ump2*^{Otef}	*a1 bE1 bW1::hyg*^{R} P_{otef}*ump2, cbx*^{R}	Chapter 3
RK1725 *ump2*^{Otef}	*a1 bW1 bE1::hyg*^{R} P_{otef}*ump2, cbx*^{R}	Chapter 3
FB1 GFP-*Tropo*^{Tropo}	*a1 b1* P_{Tropo}*Tropo-GFP, cbx*^{R}	This Study
FB1 *ump2*-YFP	*a1 b1 ump2-YFP hyg*^{R}	(Paul et al., 2014)
FB1 *ump2*-YFP *ump2*^{Otef}	*a1 b1 ump2-YFP hyg*^{R} P_{otef}*ump2, cbx*^{R}	This Study

Primer Design

Primers, other than for the Real Time PCR, were designed using the Primer 3 program available at [http://frodo.wi.mit.edu/primer3/] (Rozen & Skaletskey, 2000). Primers were obtained from Eurofins MWG Operon [Huntsville, AL].

PCR

PCR reactions were run on a PTC100 thermal controller [MJ Research Inc., San Francisco, CA] and a DNA Engine thermal cycler [Bio Rad Laboratories, Hercules, CA]. PCR cycling conditions utilized an initial denaturation temperature of 94 ^{o}C for 4 minutes, followed by 34 cycles of a three-step process of denaturation at 94 ^{o}C for 30 seconds, annealing at 60 ^{o}C for 30 seconds and extension at 72 ^{o}C for 1 minute per 1 kb of anticipated product length. A final extension at 72 ^{o}C for 10 minutes was used to complete all products. For most reactions Ex-Taq™ Hot Start DNA polymerase (Takara, Madison,WI) or Apex DNA polymerase [Genesee Scientific, San Diego, CA] was used. For high fidelity reactions, Phusion DNA polymerase [Finnzymes, Lafayette, CO] was used.

Genetic Manipulation and Vector Construction

Complete *b* deletion strain

The construct for making the *b* gene deletion in *U. maydis* strain FB1 (a1 b1) was obtained from Dr. J. Kämper (Kämper, 2004). The *b* mating locus in this construct is replaced by the hygromycin resistance cassette. The fragment was amplified using PCR, purified from agarose gel, and used to transform competent *U. maydis* cells. Putative mutants were first selected for hygromycin resistance and then screened by PCR for lack of the *b* locus and the presence of the hygromycin cassette in the correct genomic location.

bE1 and *bW1* deletion stains

The *bE1* deletion strain (RK1725) and *bW1* deletion strain (RK1607) were graciously provided by Dr. Regine Kahmann. RK1725 was made by deleting the entire *b* locus and replacing it with a construct containing the *bW1* allele and the hygromycin resistance cassette in the place of *bE1* in FB1 (Gillissen et al., 1992). RK1607 was derived by deleting the entire *b* locus and replacing it with a construct containing the hygromycin cassette disrupting the *bW1* locus and the coding region for bE1 in FB6b (Gillissen et al., 1992). FB6b, like FB1, was derived from teliospores resulting from the cross of *Ustilago maydis 521* and *Ustilago maydis 518* (F. Banuett & Herskowitz, 1989). Before modification, at the mating type loci, FB6b is *a1b2*. With the above insertion, RK1725 exhibits *b1* mating type specificity (Gillissen et al., 1992).

Construction of the *ump2* mutant strains

Deletion and overexpression mutants of *ump2* in *U. maydis* were obtained by homologous recombination as described previously (Brachmann et al., 2004). The *ump2* deletion construct was created using a 6 kb PCR product from strain um2h-2, *Δump2 a1 b1* (Smith et al., 2003) generated using primers Ump2KOup5' (GGCAAGACAAGACGAGAAGA) and Ump2_Dn_TapR (TGCGTGTCTCAAACTCCTCT). A detailed description of construction of this vector was described in Chapter 2. The Otef expression vector was linearized using the restriction enzyme *Ssp*I before transforming *U. maydis* to select for recombinants at the *ip* locus, providing carboxin resistance (Brachmann et al.,

2001). The construct for making the *b* deletion in *U. maydis* strain FB1 (*a1 b1*) was obtained from Dr. J. Kämper (Kämper, 2004).

GFP-Tropomyosin construct

The construct for expressing GFP-tagged tropomyosin was graciously provided to us by Dr. Björn Sandrock. The native promoter and coding region for the tropomyosin gene were cloned into the p123 vector, minus the stop codon, in frame with the coding region for GFP. The expression vector was linearized using the restriction enzyme *Ssp*I before transforming *U. maydis* to select for recombinants at the *ip* locus, providing carboxin resistance (Brachmann et al., 2001).

YFP-tagged *ump2* Construct

The YFP-tagged *ump2* construct (Paul et al., 2014) was used to transform FB1 wild-type cells, using hygromyocin resistance as a selectable marker.

RNA Isolation and Expression Analysis

U. maydis cells were grown on AM-glutamine, AM-ammonium and AM-low ammonium plates for 48 hours. RNA isolation for the transcriptional profile was as described previously (Perlin et al., 2015). For Illumina Next Generation Sequencing (RNA-Seq), the total RNAs were subsequently sent to BGI-Americas (Davis, CA) for cDNA library construction, sequencing, and initial bioinformatic analyses. The cDNA library format was a 140-160 bp insert library (Truseq library prep) for each sample, with Read length Paired-end 100 bp and Data output of 4

Gb clean data per sample. RNA-Seq data from different conditions were processed using the Trinity pipeline (Grabherr et al., 2011; Haas et al., 2013) , and RNA-Seq reads from each sample were aligned using bowtie (Langmead et al., 2009) against protein coding sequences extracted based on annotation. Fungal gene expression levels were estimated by RSEM (B. Li & Dewey, 2011), and edgeR with TMM normalization (Kadota et al., 2012; Robinson et al., 2010) was used to identify differentially expressed genes between each pair of conditions with a corrected p-value cutoff of 0.001; for these analyses, RPKM measurements were used to calculate log2-fold changes. To verify differences in expression levels of a subset of genes identified by RNA-Seq, real time quantitative RT-PCR (qRT-PCR) was employed. Primers for the different genes (Table 11) were designed using the ABI Primer Express software version 3.0, ensuring that all the primer sets investigated had the same amplification efficiency, since comparison of gene expression using real-time PCR assay assumes that the efficiency of amplification for all the primer pairs is equal. Differences in expression level were analyzed using the nonparametric Kruskal-Wallis Test (Daniel, 1990) and ANCOVA one directional analysis of covariance (Lowry, 1999-2000).

Microcolonies

To visualize microcolonies of *U. maydis* growing on solid media, either AM-High or AM-Low, cultures were grown overnight and diluted to an Absorbance of 0.500 at 600 nm ($O.D._{600}$). Growth media was spotted onto a

sterile glass slide and allowed to solidify. Cell suspension was then spotted onto cooled agar and the slides were incubated at 30 ^{o}C for 72 hours.

Table 11: Genes and Primers used for qRT-PCR

Gene Name	Primers	Sequences (5' → 3')
guanine nucelotide exchange factor (um04869)	rt-eif-2B-F	CAAATGCGATCCCGAACAG
	rt-eif-2B-R	GGGACACCACTTGTCAAGCA
chitin deacetylease (um01788)	rt-01788-F	TCATCCCTCAAGCGGTCAAC
	rt-01788-R	AGTGCGGGATCCGCTGTA
chitinase (um06190)	rt-06190-F	CGCACGTCCACGAATAAGCT
	rt-06190-R	GAGTCGAGGCTGTCCAATCC
related to YSC84 - protein involved in the organization of actin cytoskeleton (um01671)	um01671 qrt F	GCTGGACGACTGGGAGGAT
	um01671 qrt R	TTGCGGCTCTCGTGTTCAT
related to Thiamine-repressible acid phosphatase precursor (um06428)	um06428 qrt F	CAACAACTCAGGCCAAGTCA
	um06428 qrt R	GAGGCGCTCAGTAAGGTTTG

Microscopy

To induce *ump2* expression, strains were grown in AM-Low broth for 24 hours. Images were acquired using an Olympus Fluoview FV-1000 coupled to an Olympus 1X81 inverted microscope, a PlanApoN 60× objective, and FV-10 ASW 2.1 software. GFP or YFP signal from respective constructs were acquired using the 488 or 514 line of an Argon laser, respectively. A transmitted light image was acquired during scanning for visualization of cell outline, by grouping of the transmitted detector with the argon laser. Optimal brightness setting for each channel was configured by determining the HV setting yielding maximal intensity without saturation. Each of the settings was tested against WT cells to ensure exclusion of non-specific emission. Scanning was performed at a speed of 8µs/pixel. In a subset of studies, cells were grown on agar ----(fill in details as needed). Images of cells on the edge or middle of agar were acquired with a 20x

objective and digital zooming. For quantitation of fluorescence intensity, total sum of intensity (integration value) of the entire image area were used to measure YFP intensity, using FV-10 ASW 2.1 software. Values for multiple images/sample were averaged.

Results

Overexpression of *ump2* from a constitutive promoter does not appear to affect expression level from the native promoter.

Data from RNA-Seq analysis led us to hypothesize that overexpressing *ump2* from a constitutive promoter was able to upregulate expression of this gene from the native locus (Figure 33). However, subsequent qRT-PCR analysis showed that the expression level of the overexpressor strain on low ammonium was more like an additive effect of the normal induction in response to low ammonium from the native promoter plus the constitutive expression level (See chapter 2, Table 3). In order to determine which expression pattern was a more accurate biological representation, we used a fluorescent tag to be able to examine protein level as a result of transcript level. The fluorescent tag was inserted in frame with the native locus, in such a way that all proteins translated from transcripts from the native *ump2* locus would bear the YFP tag. This strain was then transformed with an *ump2* overexpression construct with *ump2* expression driven by the *Potef* promoter. These two strains were then visualized with fluorescent microscopy as described above to determine if constitutive overexpression of *ump2* would result in more Ump2 produced from the native locus.

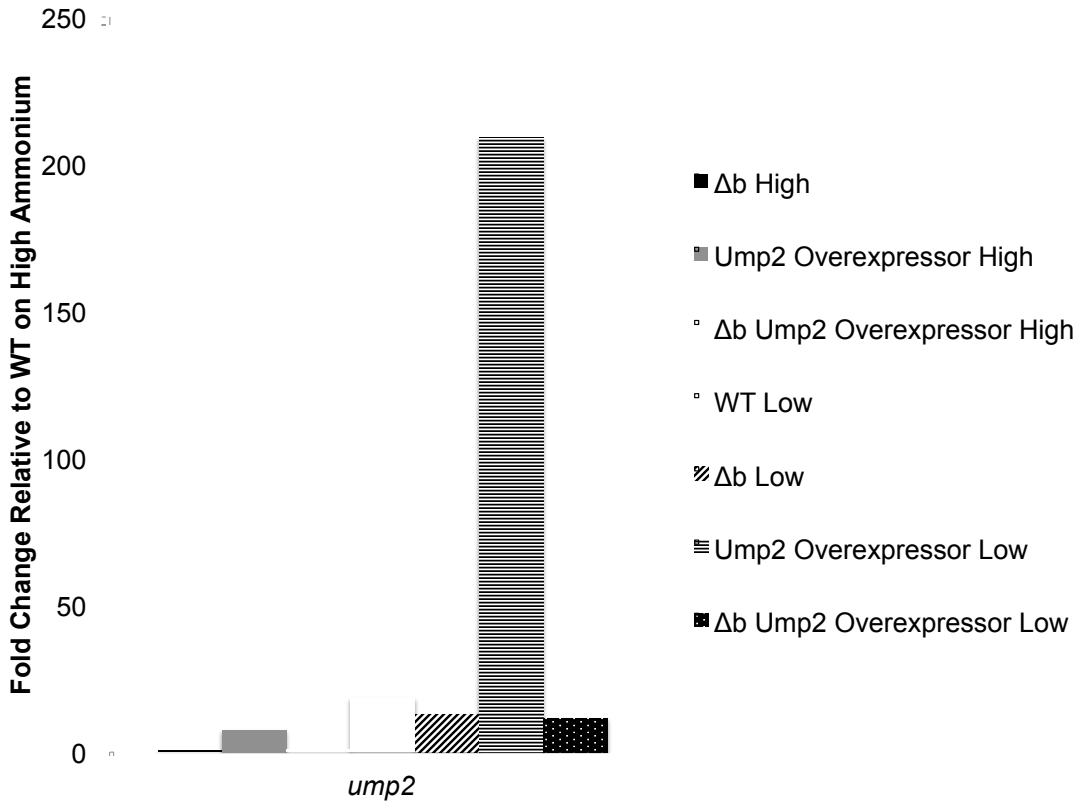

Figure 33: Fold Change of *ump2* Expression relative to FB1 WT on High Ammonium from RNA-Seq Data.
WT, wild-type FB1; *ump2* overexpressor, FB1 with *ump2* over-expressed from constitutive P_{otef} promoter; *Δump2*, FB1 with entire *ump2* gene deleted; *Δb*, FB1 deleted for entire *b* mating-type locus; Δ*b ump2* overexpressior, FB1 deleted for entire *b* mating-type locus with *ump2* over-expressed from constitutive P_{otef} promoter; High, 30 mM NH_4 medium, Low, 50 μM NH_4. Fold changes calculated as log2 of RPKM of strain of interest divided by RPKM for reference strain, FB1 WT on High Ammonium. All fold changes significant at $p<0.001$.

As expected, the expression level of *ump2* in replete media conditions is insufficient to be able to visualize a fluorescent signal (Figure 34a). However, these images were used to set appropriate scan parameters to ensure than any signal detected under low ammonium conditions was a result of expression of *ump2* and not due to background fluorescence. Under these limited nutrient conditions, we were able to detect *ump2*-YFP fusion protein expression (Figure

34b). This protein appeared to localize to the cell membrane, as has been previously reported (Paul et al., 2014). Cells containing the *ump2*-YFP construct and the overxpression construct were also visualized in this manner, and *ump2* localization showed a similar pattern (Figure 34c). Based on the intensity

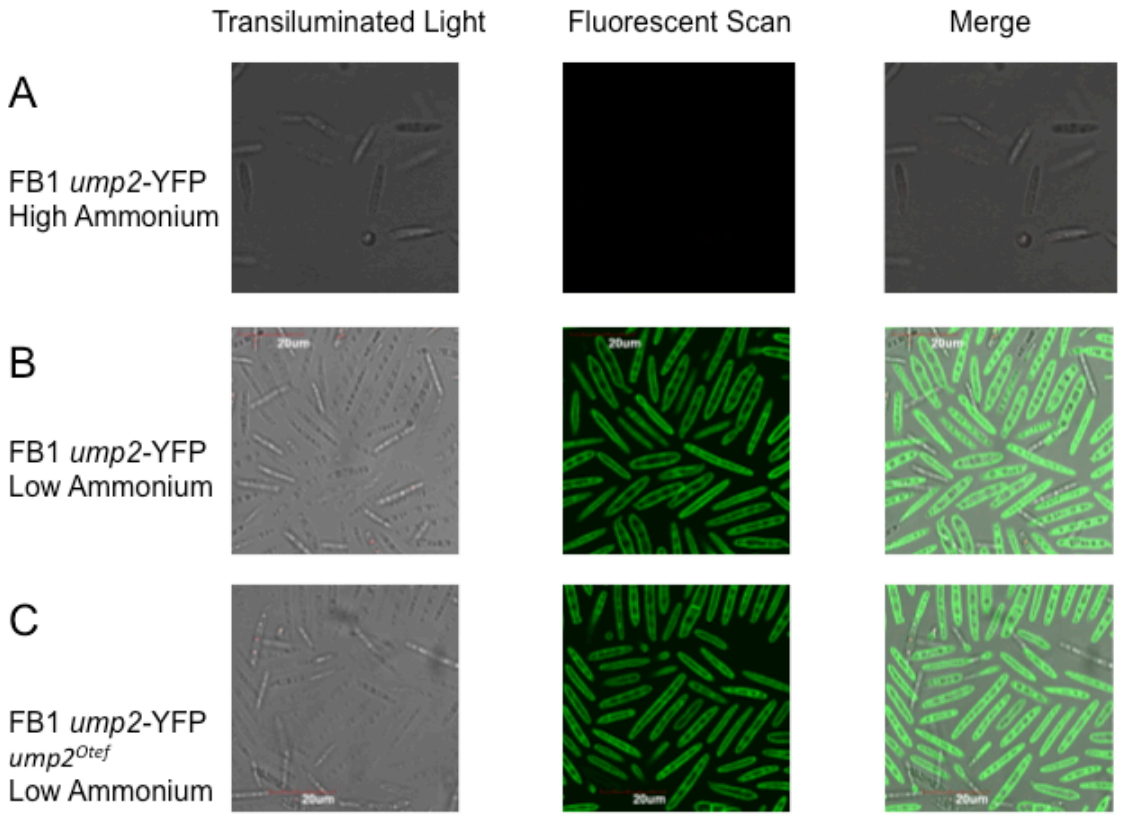

Figure 34: Protein level of *ump2* from native locus as determined by fluorescent microscopy.
FB1 *ump2*-YFP (A) High and (B) Low Ammonium and (C) FB1 *ump2*-YFP *um2*^{Potef} grown in High and Low ammonium broth for 24 hours and visualized as described above. Images are shown for transilluminated light, fluorescent scan, and the merge of the two scans. High, 30 mM NH_4 medium, Low, 50 µM NH_4. Scale bar, 20 µm.

measurements of these two sets of images, we determined that there was no significant difference in the *ump2*-YFP signal from the wild-type strain and that from the *ump2* overexpression strain (Table 12, p=0.847). Contrary to our

hypothesis, these data indicated that overexpression of *ump2* did not increase expression level from the native locus and could not explain the hyperfilamentation phenotype seen in haploid cells of this mutant strain. To further investigate, we sought to explore other targets to determine why various *b* and *ump2* mutants displayed attenuated or exaggerated filamentation phenotypes in response to low ammonium.

Table 12: Average Intensity Measurements[a] of *ump2*-YFP tagged mutants

Strain		Integration from YFP Channel	Area	Average Intensity
FB1 *ump2*-YFP	1	170116447	4827.88	35236.24
	2	220809286	4914.49	44930.20
	3	213547698	4933.92	43281.54
FB1 *ump2*-YFP *ump2*^{Otef}	1	175648958	4818.28	36454.67
	2	216183485	4953.34	43643.94
	3	202740060	4933.92	41091.07

[a] For quantitation of fluorescence intensity, total sum of intensity (integration value) of the entire image area were used to measure YFP intensity, using FV-10 ASW 2.1 software.

Mutants deleted for either the *b* locus or the high affinity ammonium transporter *ump2* show different responses to abiotic stresses.

Osmotic Stress

Both sodium chloride and sorbitol can induce osmotic stress in *U. maydis* at sufficient concentrations. Various mutants were tested for the effect on growth of these two stresses. While both *b* deletion mutants and *ump2* overexpressor strains had a similar response when exposed to 1 M NaCl, the *ump2* deletion mutant seemed to actually grow better under this stress than the FB1 WT. Complementation of the *ump2* deletion strain by *ump2* from a constitutive promotor returned the phenotype more to that of wild-type (Figure 35a).

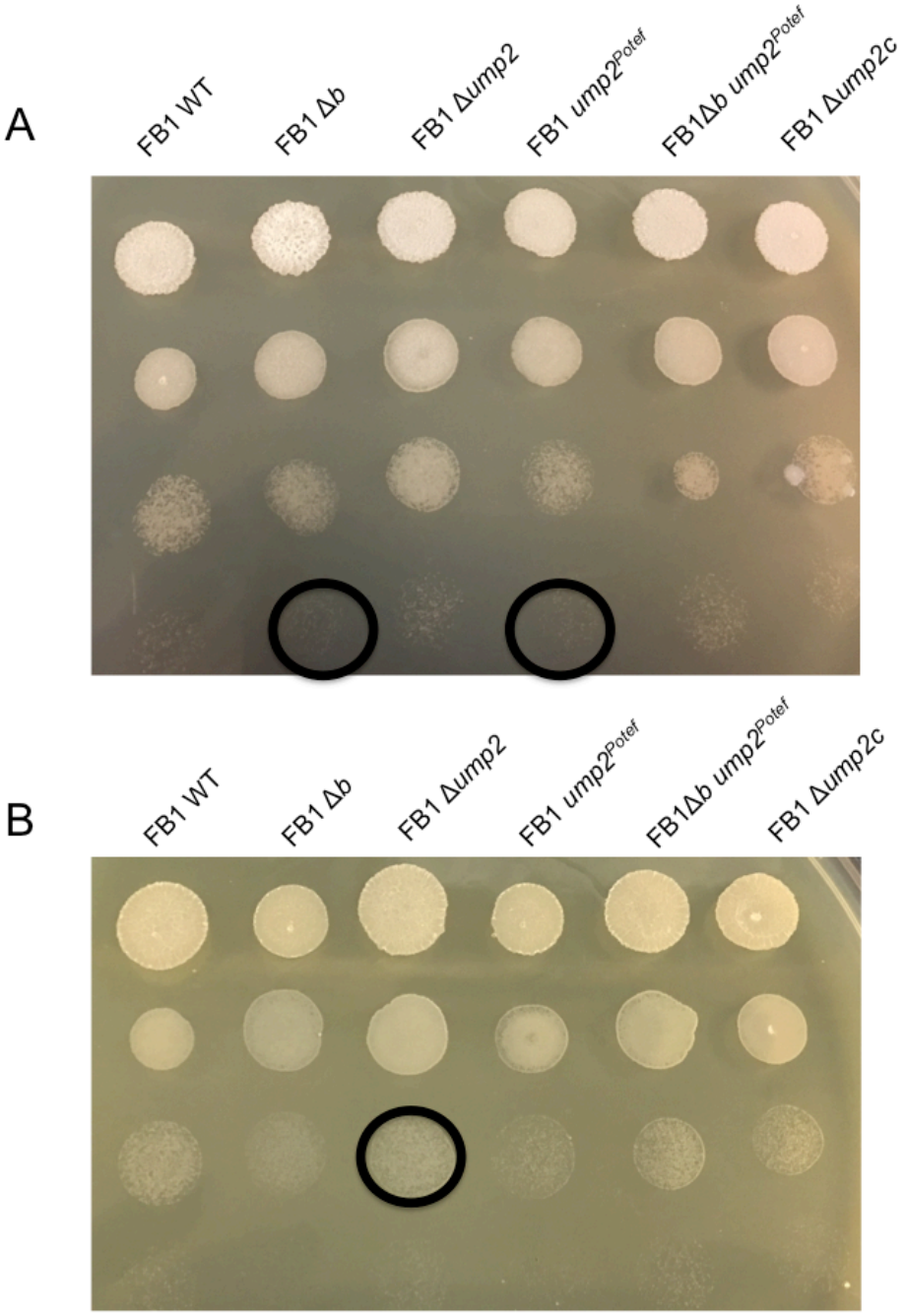

Figure 35: Response of various mutants to abiotic osmotic stress.
Cells grown for 48 hours on (A) 1 M Sorbitol and (B) 1 M NaCl after being serially diluted from overnight culture, full strength, 10^{-1}, 10^{-2}, and 10^{-3}. FB1 *ump2*^{Potef}, FB1 with *ump2* over-expressed from constitutive P_{otef} promoter; FB1*Δump2*, FB1 with entire ump2 gene deleted; FB1*Δb*, FB1 deleted for entire *b* mating-type locus; FB1Δ*b ump2*^{Otef}, FB1 deleted for entire *b* mating-type locus with *ump2* over-expressed from constitutive P_{otef} promoter; FB1*Δump2c*, FB1 with entire *ump2* gene deleted expressing *ump2* from constitutive P_{otef} promoter. Black circles indicate areas of different growth as compared to FB1 WT.

Conversely, when grown in media with 1 M Sorbitol, mutants deleted for the *b* locus showed decreased growth as compared to FB1 wild-type, while *ump2* deletion mutants showed growth similar to the wild-type strain (Figure 35b). Interesting, overexpression of *ump2* in the *b* deletion background rescued the decreased growth phenotype (Figure 35b).

Cell Wall Stress

Congo Red causes stress to fungal cell walls. While deletion mutants lacking either *ump2* or the *b* locus showed little change in their response to this stress compared to the FB1 wild-type strain, overexpression of *ump2* resulted in decreased growth in the presence of Congo Red. Interestingly, a mutant deleted for the native *ump2* locus and expressing *ump2* from a constitutive construct also seemed to show reduced growth under these conditions (Figure 36). The different ability of our mutants to withstand various abiotic stressors led us to investigate the expression level of specific targets related to maintaining cell wall integrity and cell wall modification.

The expression level of *ump2* and/or the presence of the complete or partial *b* locus has different effects on expression of cell wall integrity-related targets.

Because mutants constitutively expressing *ump2* seemed to respond differently to cell wall stress than wild-type cells exposed to the same stress, targets related to cell wall integrity and morphogenesis were examined. Chitin deacetylase converts chitin in the fungal cell wall to chitosan. Although chitosan

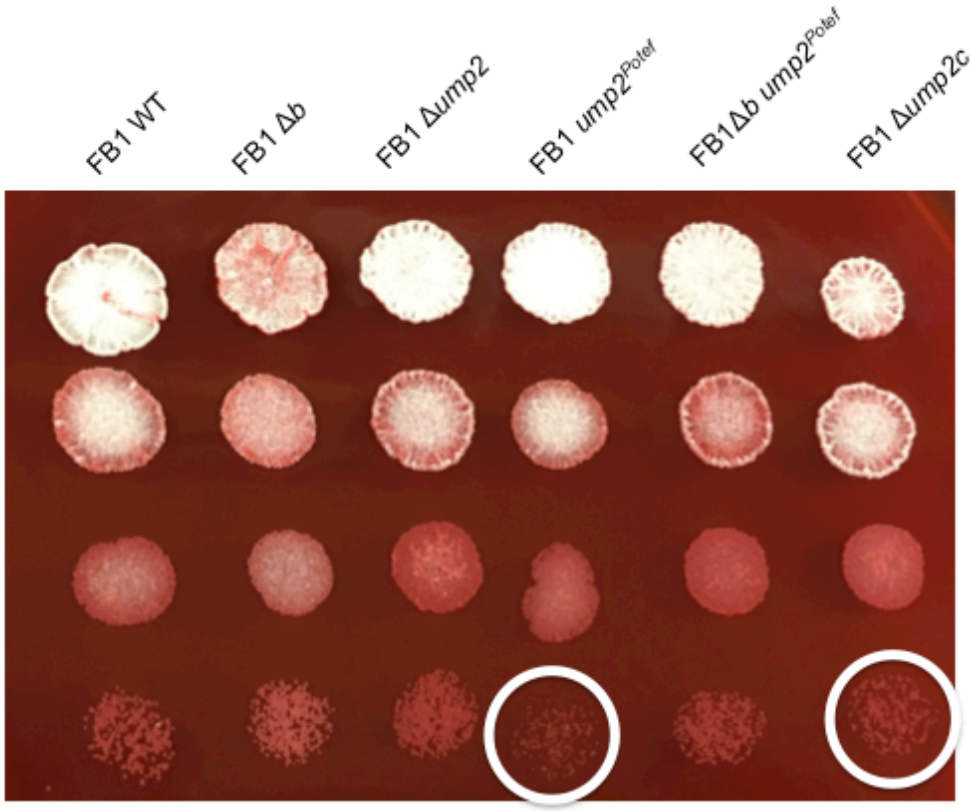

Figure 36: Response of various mutants to cell wall stress.
Cells grown for 48 hours on 1 mM Congo Red after being serially diluted from overnight culture, full strength, 10^{-1}, 10^{-2}, and 10^{-3}. FB1 *ump2*^{Potef}, FB1 with *ump2* over-expressed from constitutive P_{otef} promoter; FB1*Δump2*, FB1 with entire *ump2* gene deleted; FB1*Δb*, FB1 deleted for entire *b* mating-type locus; FB1Δ*b ump2*^{Otef}, FB1 deleted for entire *b* mating-type locus with *ump2* over-expressed from constitutive P_{otef} promoter; FB1*Δump2c*, FB1 with entire ump2 gene deleted expressing *ump2* from constitutive P_{otef} promoter. White circles indicate areas of different growth as compared to FB1 WT.

is not prominent in *U. maydis* cell walls, it is important in pathogenicity for other Basidiomycetes (Ruiz-Herrera, Leon, Carabez-Trejo, & Reyes-Salinas, 1996). The protein encoded by gene um01788 is the putative chitin deacetylase in *U. maydis*. Under replete ammonium conditions, few of the mutants showed differential expression of um1788 relative to FB1 WT on high ammonium (Table 13 and Figure 37 display qRT-PCR as the average of three biological replicates

Table 13: Differentially Expressed Genes of Interest[a] from qRT-PCR Experiments

Target	WT Low[b]	P_{otef} *ump2* High[b]	P_{otef} *ump2* Low[b]	*Δump2* High[b]	*Δump2* Low[b]
chitin deacetylase (um01788)	0.82±0.24	2.50±0.55	-1.99±0.67	-0.17±0.58	0.64±0.20
chitinase (um06190)	-1.54±0.34	-2.72±0.22	-4.62±0.45	-1.63±0.33	-2.91±1.20

Target	*Δb* High[b]	*Δb* Low[b]	FB1Δ*b* $ump2^{Otef}$ High[b]	FB1Δ*b* $ump2^{Otef}$ Low[b]
chitin deacetylase (um01788)	-0.03±0.57	-0.79±0.68	-6.36±0.62	1.99±0.48
chitinase (um06190)	-0.82±0.73	-2.85±0.82	-3.82±1.92	-0.69±0.11

Target	RK1725 High[b]	RK1725 Low[b]	RK1725 *Potef ump2 High*[b]	RK1725 *Potef ump2 Low*[b]
chitin deacetylase (um01788)	-1.00±0.57	1.51±0.17	-0.12±0.79	-0.11±1.28
chitinase (um06190)	-4.23±0.20	-1.27±0.13	-0.82±1.39	0.59±1.14

Target	RK1607 High[b]	RK1607 Low[b]	RK1607 *Potef ump2 High*[b]	RK1607 *Potef ump2 Low*[b]
chitin deacetylase (um01788)	5.86±1.44	3.12±0.19	1.06±0.62	5.66±1.26
chitinase (um06190)	-2.53±0.46	-0.08±0.46	-3.84±1.65	-0.94±0.77

[a]qRT-PCR log2 fold changes, normalized and expressed relative to FB1 WT on rich medium (High) ; negative values reflect decreased expression, whereas positive values represent increased expression

[b]WT, wild-type FB1; P_{otef} *ump2*, FB1 with *ump2* over-expressed from constitutive P_{otef} promoter; *Δump2*, FB1 with entire ump2 gene deleted; *Δb*, FB1 deleted for entire *b* mating-type locus; FB1Δ*b* $ump2^{Otef}$, FB1 deleted for entire *b* mating-type locus with *ump2* over-expressed from constitutive P_{otef} promoter; RK1725, *bE1* deletion in FB1 background; RK1725 $ump2^{Otef}$, RK1725 with *ump2* over-expressed from constitutive P_{otef} promoter; RK1607, *bW1* deletion in FB6b background; RK1607 $ump2^{Otef}$, RK1607 with *ump2* over-expressed from constitutive P_{otef} promoter; High, 30 mM NH_4 medium, Low, 50 µM NH_4

plus or minus standard error). Of note, the *ump2* overexpressor showed increased expression of the putative chitin deacetylase under this condition as did RK1607, the *bW1* deletion strain; however, because the *bW1* deletion strain did not filament under these conditions, expression levels of this target cannot be correlated to the hyperfilamentation phenotype seen in the *ump2* overexpressor

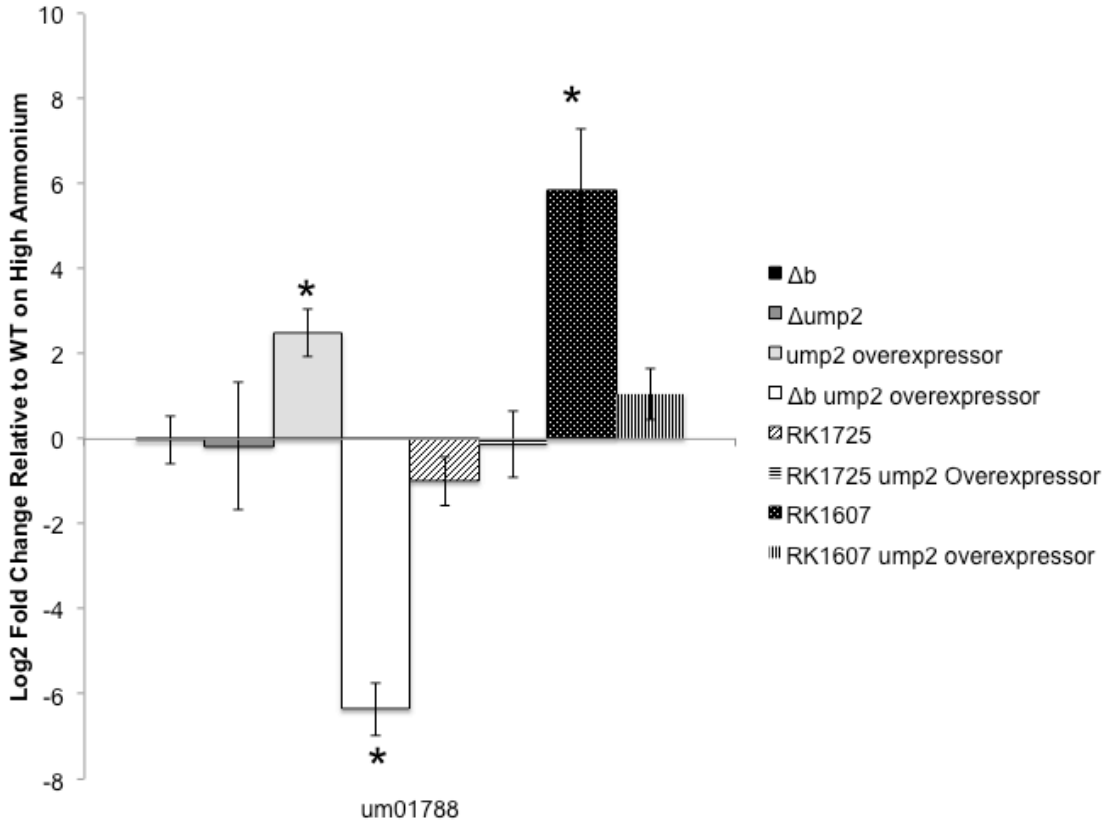

Figure 37: Log2 Fold Change in Expression levels of um01788 of various mutants as compared to FB1 WT on High Ammonium.
ump2 ovexpressor, FB1 with *ump2* over-expressed from constitutive P_{otef} promoter; *Δump2*, FB1 with entire *ump2* gene deleted; *Δb*, FB1 deleted for entire *b* mating-type locus; Δ*b ump2* overexpressor, FB1 deleted for entire *b* mating-type locus with *ump2* over-expressed from constitutive P_{otef} promoter; RK1725, *bE1* deletion in FB1 background; RK1725 *ump2* overexpressor, RK1725 with *ump2* over-expressed from constitutive P_{otef} promoter; RK1607, *bW1* deletion in FB6b background; RK1607 *ump2* overexpressor, RK1607 with *ump2* over-expressed from constitutive P_{otef} promoter; High, 30 mM NH_4 medium, Low, 50 µM NH_4. * significant at p<.05 by Kruskal-Wallis analysis (Daniel, 1990).

on high ammonium. Interesting, the combination of the *b* mating locus deletion and *ump2* overexpression dramatically decreased expression level of this target (Figure 37). These fold changes were analyzed using ANCOVA, and were found to be statistically different compared to FB1 WT on replete media ($p<0.01$).

Analyzing the differences in expression levels of um10788 in each mutant on low versus high ammonium similarly revealed dynamic expression levels but no discernable pattern regarding filamentation (Table 13; Figure 38). The deletion of either the entire *b* mating locus or *ump2* both resulted in changes in expression level on depleted ammonium media as compared to replete ammonium conditions similar to those of the FB1 WT strain. The *ump2* overexpression strain, RK1725 (deleted for only *bE1*) and RK1607 (deleted for only *bW1*) showed decreased expression levels of um01788 on low ammonium as compared to the same mutant on high ammonium, while overexpression of *ump2* in the *b* deletion background or the *bW1* deletion background resulted in increased expression levels comparing the two media conditions. No correlation could be determined between mutants that filament versus those that do not under these conditions based on transcript levels of this target. However, it is of note that *ump2* overexpression in the complete *b* deletion background and RK1607 both demonstrated increased expression levels of this target but not RK1725, indicating a different interplay between *b* regulation and *ump2* regulation in these two mutants (Figure 38). ANCOVA statistical analysis revealed these changes were significant ($p<0.01$).

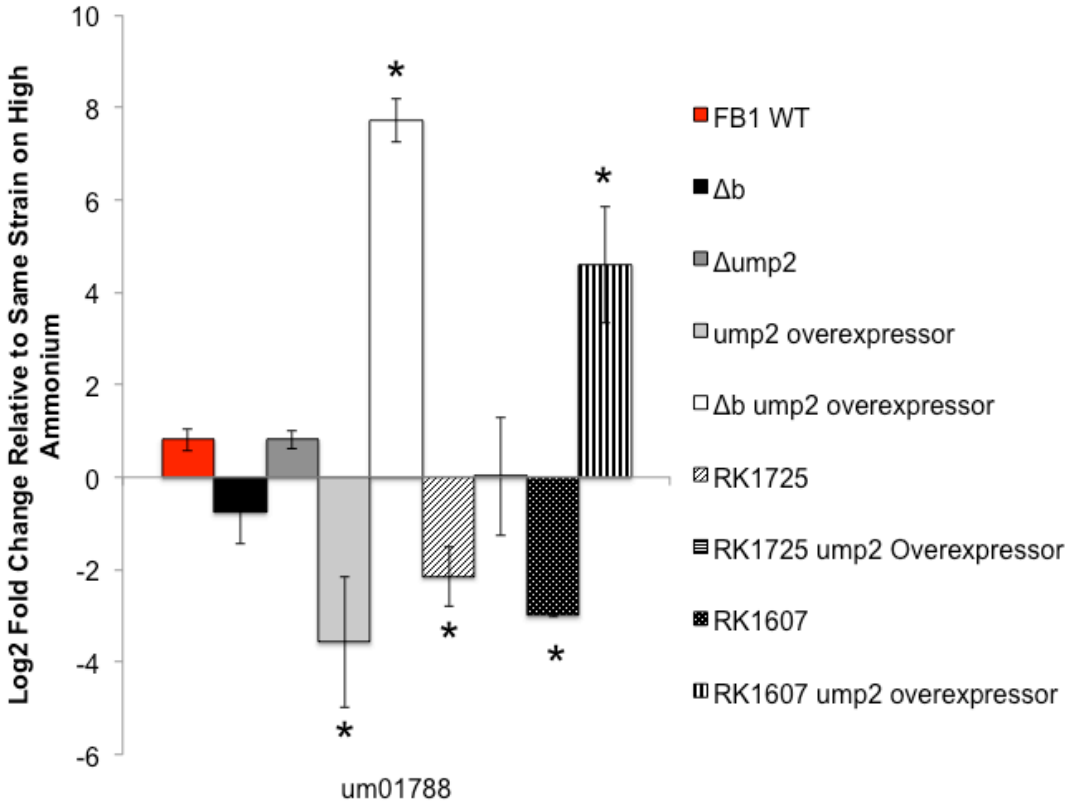

Figure 38: Log2 Fold Change in Expression levels of um01788 on Low Ammonium compared to same strain on High Ammonium.
ump2 ovexpressor, FB1 with *ump2* over-expressed from constitutive P_{otef} promoter; *Δump2*, FB1 with entire *ump2* gene deleted; *Δb*, FB1 deleted for entire *b* mating-type locus; Δ*b ump2* overexpressor, FB1 deleted for entire *b* mating-type locus with *ump2* over-expressed from constitutive P_{otef} promoter; RK1725, *bE1* deletion in FB1 background; RK1725 *ump2* overexpressor, RK1725 with *ump2* over-expressed from constitutive P_{otef} promoter; RK1607, *bW1* deletion in FB6b background; RK1607 *ump2* overexpressor, RK1607 with *ump2* over-expressed from constitutive P_{otef} promoter; High, 30 mM NH_4 medium, Low, 50 µM NH_4. * significant at p<.01 by ANCOVA (Lowry, 1999-2000; Yuan et al., 2006).

Additionally, the various mutants examined in the studies showed different expression levels of um06190, a putative chitinase. Chitinases function in fungi not only to degrade external chitin but also in cell wall remodeling (Hartl, Zach, & Seidl-Seiboth, 2012). As such, we hypothesized that potentially this particular target was differently regulated in our mutants resulting in the various changes in

phenotype on low ammonium, either filamentation or lack thereof. Most of the mutant strains showed decreased expression levels of um06190 on high ammonium as compared to the FB1 WT on the same media conditions, with the exception of the *ump2* overexpressor in the *b* deletion background. This mutant showed significantly higher expression levels of the putative chitinase under replete ammonium conditions (Table 13; Figure 39). ANCOVA analysis revealed that these differences in expression level were significant ($p<0.01$).

Under depleted ammonium conditions, FB1 WT, FB1Δ*b*, FB1Δ*ump2*, and FB1 *ump2*^{potef} all showed decreased levels of um06190 as compared to the same strain under replete conditions. However, either both partial *b* deletion mutants (RK1725 and RK1607) and *ump2* overexpressors in these backgrounds, as well as the *ump2* overexpressor in the complete *b* deletion background show increased expression levels of this target on low ammonium as compared to the same mutant on replete media conditions (Table 13; Figure 40; all differences significant at $p<0.01$ according to ANCOVA). Again, no pattern emerges that correlates with the mutants that filament on low ammonium versus those that do not, but it is interesting that these mutants differentially express targets specific to cell wall modification. Moreover, it did not appear that absolute transcript level of either um01788 or um06190 could explain the filamentation or lack of filamentation in response to low ammonium. As a result, we sought to examine targets specifically related to the actin cytoskeleton which may be involved in the formation of these filaments.

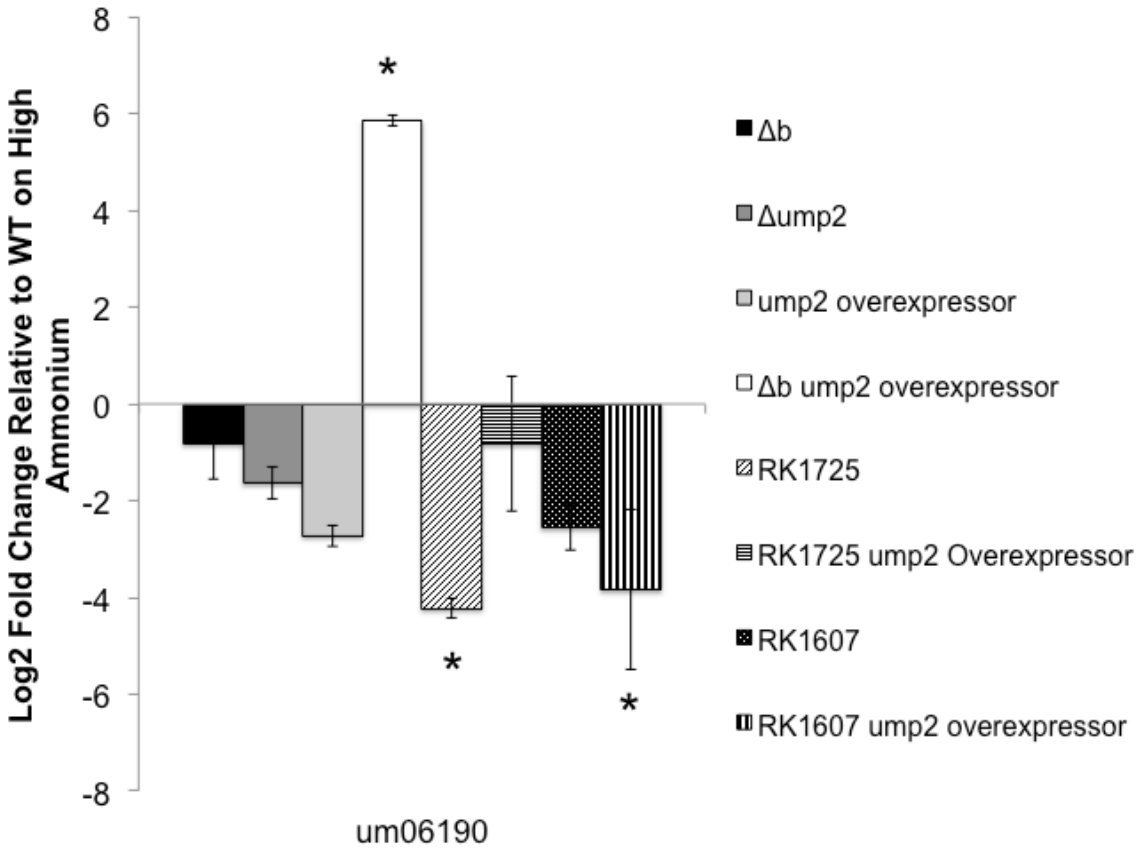

Figure 39: Log2 Fold Change in Expression levels of um06190 of various mutants as compared to FB1 WT on High Ammonium.
ump2 ovexpressor, FB1 with *ump2* over-expressed from constitutive P_{otef} promoter; *Δump2*, FB1 with entire *ump2* gene deleted; *Δb*, FB1 deleted for entire *b* mating-type locus; Δ*b ump2* overexpressor, FB1 deleted for entire *b* mating-type locus with *ump2* over-expressed from constitutive P_{otef} promoter; RK1725, *bE1* deletion in FB1 background; RK1725 *ump2* overexpressor, RK1725 with *ump2* over-expressed from constitutive P_{otef} promoter; RK1607, *bW1* deletion in FB6b background; RK1607 *ump2* overexpressor, RK1607 with *ump2* over-expressed from constitutive P_{otef} promoter; High, 30 mM NH_4 medium, Low, 50 µM NH_4. * significant at $p<.05$ by Kruskal-Wallis analysis (Daniel, 1990).

Exposure of *Ustilago maydis* cells to low ammonium media results in a morphological change of individual cells when grown on solid media.

When grown in broth containing either replete media or low ammonium conditions, morphologically, *U.maydis* cells are indistinguishable across conditions. The filamentous phenotype observed upon exposure to low

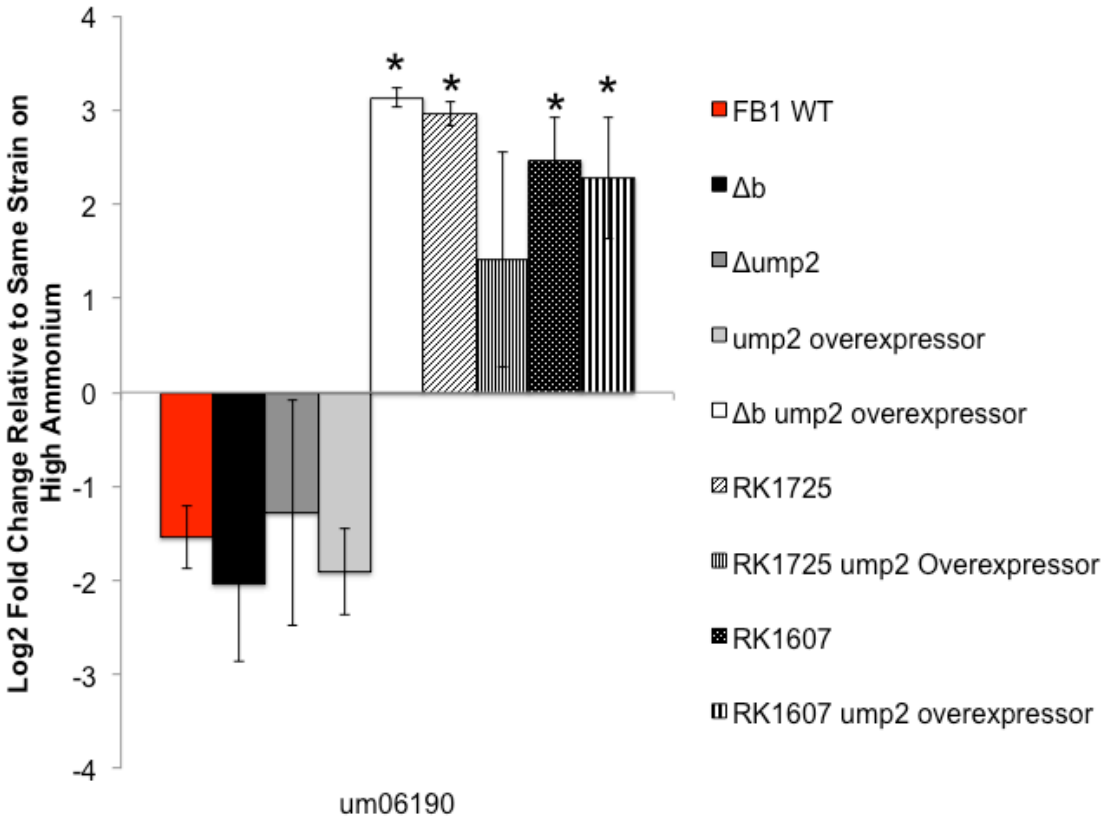

Figure 40: Log2 Fold Change in Expression levels of um06190 on Low Ammonium compared to same strain on High Ammonium.
ump2 ovexpressor, FB1 with *ump2* over-expressed from constitutive P_{otef} promoter; *Δump2*, FB1 with entire *ump2* gene deleted; *Δb*, FB1 deleted for entire *b* mating-type locus; Δ*b ump2* overexpressor, FB1 deleted for entire *b* mating-type locus with *ump2* over-expressed from constitutive P_{otef} promoter; RK1725, *bE1* deletion in FB1 background; RK1725 *ump2* overexpressor, RK1725 with *ump2* over-expressed from constitutive P_{otef} promoter; RK1607, *bW1* deletion in FB6b background; RK1607 *ump2* overexpressor, RK1607 with *ump2* over-expressed from constitutive P_{otef} promoter; High, 30 mM NH_4 medium, Low, 50 µM NH_4. * significant at p<.01 by ANCOVA (Lowry, 1999-2000; Yuan et al., 2006).

ammonium is only visible when the haploid cells are grown on solid media. Examination of magnified cells in microcolonies on solid media reveals that the shape of the cells under low ammonium conditions is actually longer than those grown under replete media conditions (Figure 41a). In the *ump2* overexpression strain on high ammonium, the signs of filamentation on replete media are visible

(although not as profoundly as individual colony morphology, see Chaper 2, Figure 7); in under low ammonium, the tangled mess of hyperfilamentation is visible (Figure 41b).

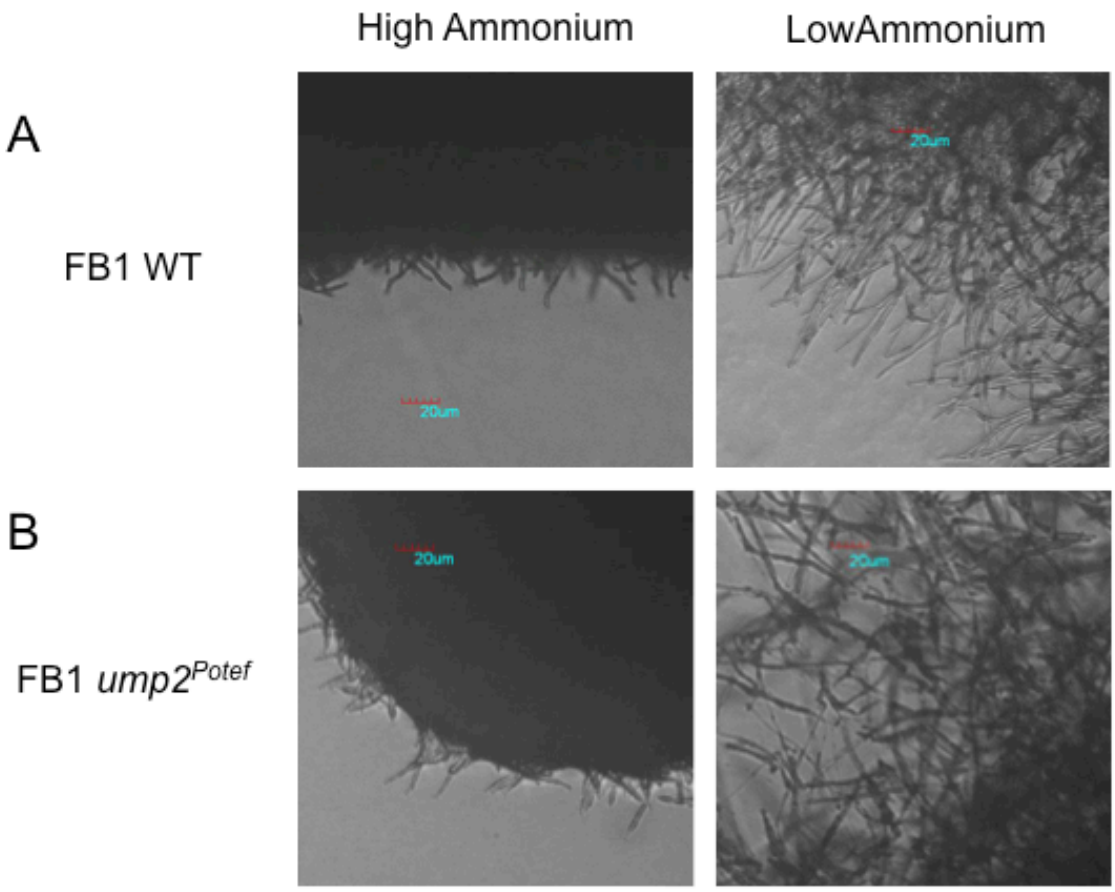

Figure 41: Images of FB1 Wild-type and FB1 *ump2*^{Potef} microcolonies. Cells were grown in liquid media and spotted onto High or Low Ammonium media and allowed to grow for 72 hours at 26 ˚C. Images are taken as described previously. FB1 *ump2*^{Potef}, FB1 with *ump2* over-expressed from constitutive P_{otef} promoter. High, 30 mM NH_4 medium, Low, 50 µM NH_4. Scale bar, 20 µm

In order to try to understand the cytoskeletal dynamics leading to this change in cell morphology in response to low ammonium, we also created mutants carrying YFP fluorescently labeled tropomyosin. Since tropomyosin wraps around the actin microfilaments, we wanted to visualize any differences in

the organization of the cytoskeleton, comparing growth of the microcolonies in low or high ammonium. In the fluorescently labeled strains, the same extension of the overall cell shape was also observed under low ammonium conditions, even when they were not surrounding the edge of the growing mass (Figure 42a). Under replete media conditions, only a few cells within the population examined had high levels of tropomyosin outlining the shape of the cell, while most had lower levels of signal within the cell. On low ammonium media, each cell had several long areas of signal indicating the presence of tropomyosin (Figure 42b and 42c).

The filamentous phenotype seen in haploid cells on low ammonium conditions is seen surrounding the colony, with a dense inner section and finger-like projections extending from the edge. For our microcolonies, we can also visualize this growth by observing around the edge of the spotted cells. Observation of magnified colonies also reveals a size difference in the *U. maydis* cells growing under low ammonium conditions as opposed to those growing under high ammonium (Figure 43a). Again, tropomyosin staining reveals elongated tropomyosin structures more densely visible in the longer cells (Figure 43b and 43c).

Different *b* mutants and *ump2* mutants have dynamic actin expression levels.

Because the actin cytoskeleton seemed to be undergoing change resulting in the filamentous phenotype under low ammonium conditions, various actin related targets were examined using RNA-Seq and qRT-PCR. Although

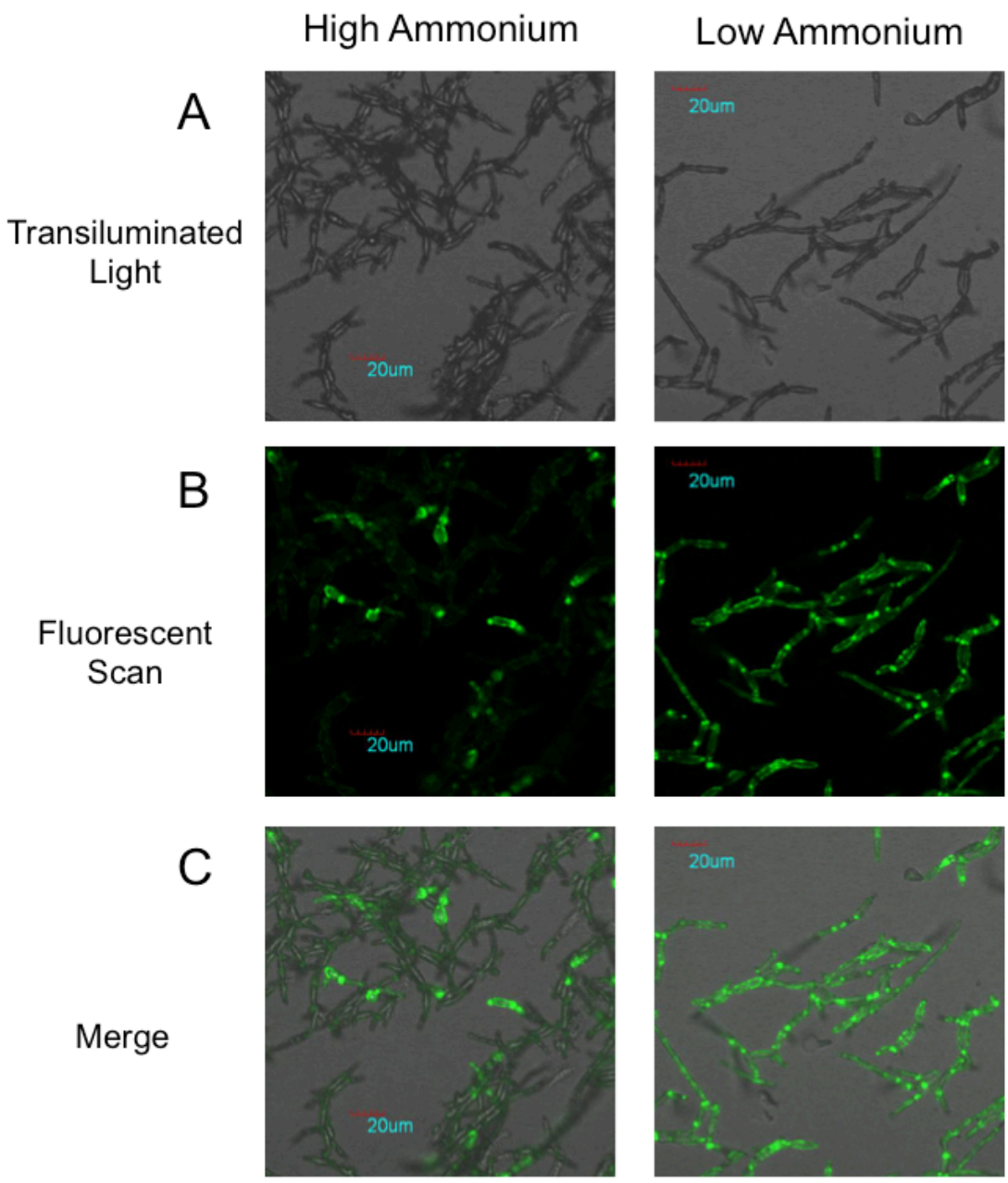

Figure 42: Images of FB1 Wild-type cells expressing biofluorescently tagged tropomyosin grown under high and low ammonium on solid media. Cells were grown in liquid media and spotted onto High or Low Ammonium media and allowed to grow for 72 hours at 26 ˚C. Images were taken as described previously. Transilluminated Light, Fluorescent Scan, and Merged images are shown. High, 30 mM NH_4 medium, Low, 50 µM NH_4. Scale bar, 20 µm.

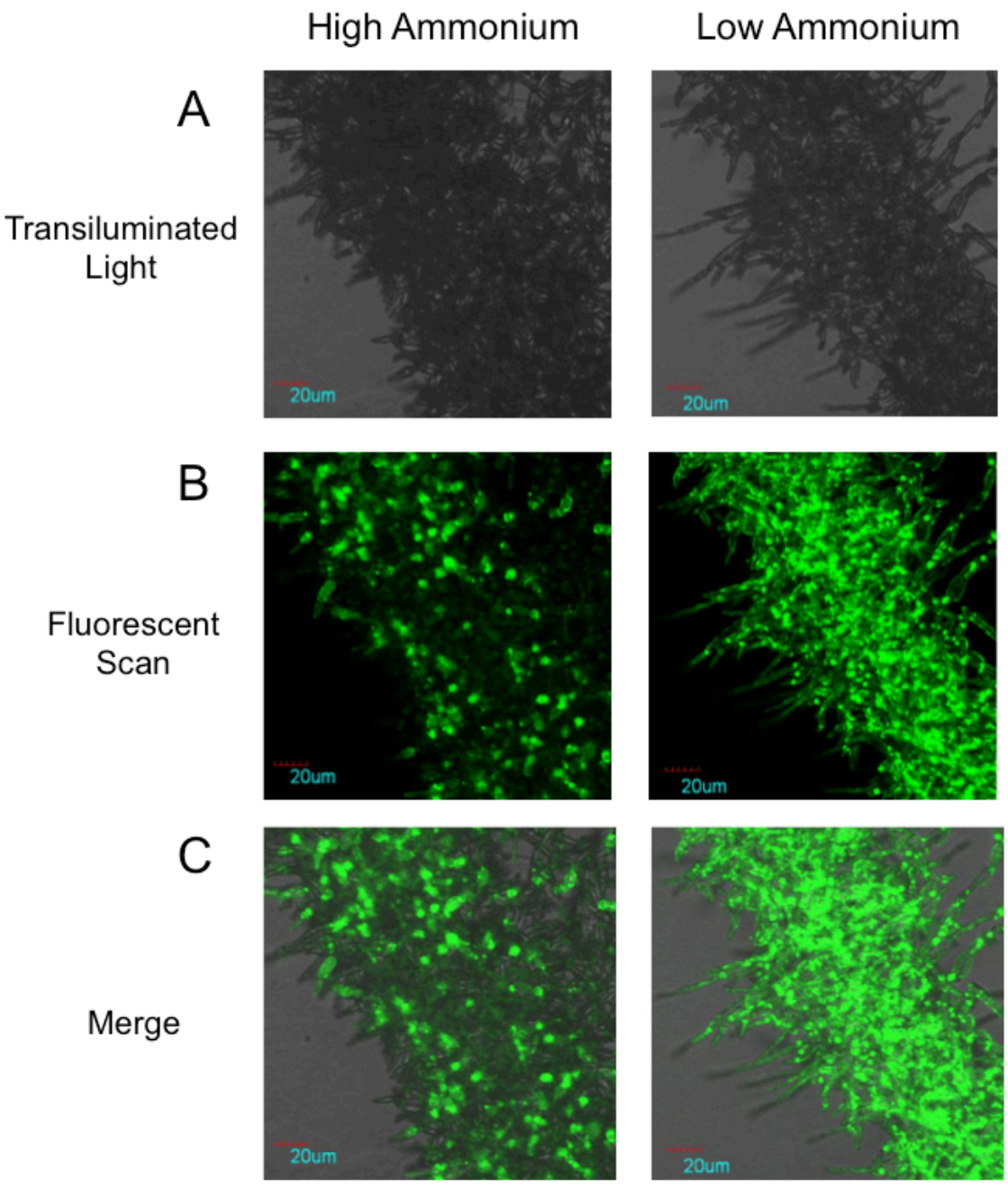

Figure 43: Images of FB1 Wild-type microcolony edges of cells expressing biofluorescently tagged tropomyosin grown under high and low ammonium on solid media.
Cells are grown in liquid media and spotted onto High or Low Ammonium media and allowed to grow for 72 hours at 26 ˚C. Images are taken as described previously. Transilluminated Light, Fluorescent Scan, and Merged images are shown. High, 30 mM NH_4 medium, Low, 50 µM NH_4. Scale bar, 20 µm.

actin is often used as an internal standard for non-differential expression, the group of mutants examined for this study showed dynamic levels of actin transcript dependent upon mutant and ammonium availability. Wild-type FB1 cells had similar levels expression of actin on both high and low ammonium. While there was no obvious phenotype difference between colonies of wild-type FB1 *U. maydis* and the deletion mutants examined within this study, the expression of actin under high ammonium varied greatly (Table 14 lists qRT-PCR data as averages of biological triplicates plus or minus standard deviation; Figure 44). While deletion of either *b* or *ump2* resulted in decreased actin expression on

Table 14: Results of qRT-PCR Analysis of Actin Expression Levels[a]

Strain	High[b] Ammonium	Low[b] Ammonium
FB1 WT[b]		-0.49±1.33
FB1*Δb*[b]	-2.04±0.06	-0.38±0.96
FB1*Δump2*[b]	-1.02±0.52	1.26±1.23
FB1 P_{otef} *ump2*[b]	2.24±0.72	1.16±0.21
FB1Δ*b ump2*$^{Otef\ b}$	1.05±0.43	0.55±0.62
RK1725[b]	1.41±0.90	0.17±0.87
RK1725 *Potef ump2*[b]	2.95±0.63	0.73±1.63
RK1607[b]	-2.78±0.76	-1.78±0.41
RK1607 *Potef ump2*[b]	-2.55±0.46	-0.08±0.46

[a]qRT-PCR log2 fold changes, normalized and expressed relative to FB1 WT on rich medium (High); negative values reflect decreased expression, whereas positive values represent increased expression

[b]WT, wild-type FB1; P_{otef} *ump2*, FB1 with *ump2* over-expressed from constitutive P_{otef} promoter; *Δump2*, FB1 with entire ump2 gene deleted; *Δb*, FB1 deleted for entire *b* mating-type locus; FB1Δ*b ump2*^{Otef}, FB1 deleted for entire *b* mating-type locus with *ump2* over-expressed from constitutive P_{otef} promoter, RK1725, *bE1* deletion in FB1 background; RK1725 *ump2*^{Otef}, RK1725 with *ump2* over-expressed from constitutive P_{otef} promoter ; RK1607, *bW1* deletion in FB6b background; RK1607 *ump2*^{Otef}, RK1607 with *ump2* over-expressed from constitutive *Potef* promoter; High, 30 mM NH_4 medium, Low, 50 µM NH_4

high ammonium medium, overexpression of *ump2* resulted in increased actin expression, even when *ump2* was constitutively overexpressed in the complete or *bE1* deletion background (Figure 44). Deletion of only *bE1* (*i.e.*, in RK1725) did not dramatically change actin expression on high ammonium, while deletion of *bW1* decreased actin expression under the same conditions, as did overexpression of *ump2* in this background (Figure 44). Although Kruskal-Wallis

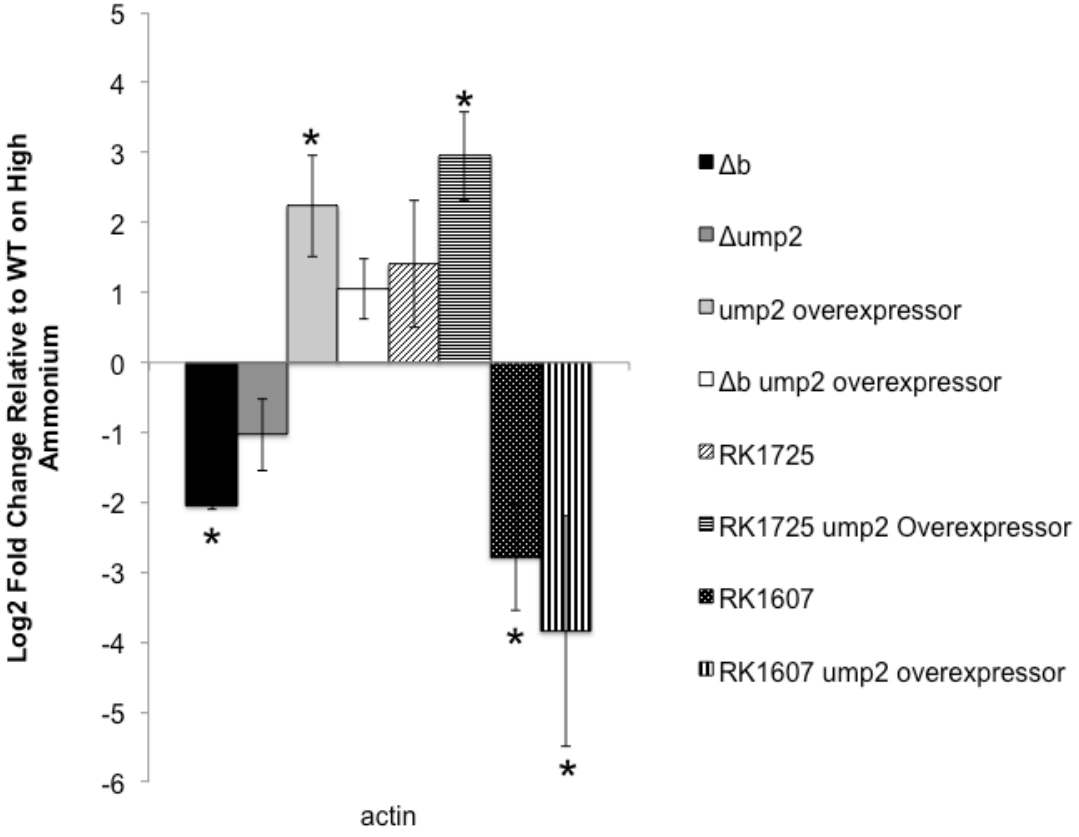

Figure 44: Log2 Fold Change in Expression levels of actin (um11232) of various mutants as compared to FB1 WT on High Ammonium.
ump2 ovexpressor, FB1 with *ump2* over-expressed from constitutive P_{otef} promoter; *Δump2*, FB1 with entire *ump2* gene deleted; *Δb*, FB1 deleted for entire *b* mating-type locus; Δ*b ump2* overexpressor, FB1 deleted for entire *b* mating-type locus with *ump2* over-expressed from constitutive P_{otef} promoter; RK1725, *bE1* deletion in FB1 background; RK1725 *ump2* overexpressor, RK1725 with *ump2* over-expressed from constitutive P_{otef} promoter; RK1607, *bW1* deletion in FB6b background; RK1607 *ump2* overexpressor, RK1607 with *ump2* over-expressed from constitutive P_{otef} promoter; High, 30 mM NH_4 medium, Low, 50 µM NH_4. * significant at p<.05 by Kruskal-Wallis analysis (Daniel, 1990).

analysis did not reveal any significant difference if the group was examined as a whole, when each strain was compared individually to the expression level of FB1 wild-type on High Ammonium, several showed significantly different expression levels, eliminating the use of actin as a viable internal control (Figure 44).

Although actin transcript levels appeared to be downregulated in FB1 wild-type under low ammonium conditions according to RNA-Seq data, this was not supported by subsequent qRT-PCR analysis. The transcript level of actin in FB1 wild-type was essentially the same from high to low ammonium in biological triplicate analysis (Figure 45). However, this was not the case for the mutants in the study. Deletion of either the entire *b* mating locus and deletion of *bE1* alone (RK1725) or deletion of the high affinity ammonium transporter, *ump2*, resulted in increased actin expression on low ammonium when compared within the same strain. Overexpressing *ump2* in all of the backgrounds in this study decreased expression of actin on low ammonium as compared to the same strain on high ammonium (Figure 45).

While the fold changes in expression level were high for actin, the variability of actin expression even within a single mutant in biological triplicate was so great that none of these expression levels were significantly different as analyzed with an analysis of covariance (ANCOVA, (Lowry, 1999-2000; Yuan et al., 2006). Although no specific phenotype can be attributed to these changes in expression levels of actin, it is of note that is most certainly not expressed at a constant level.

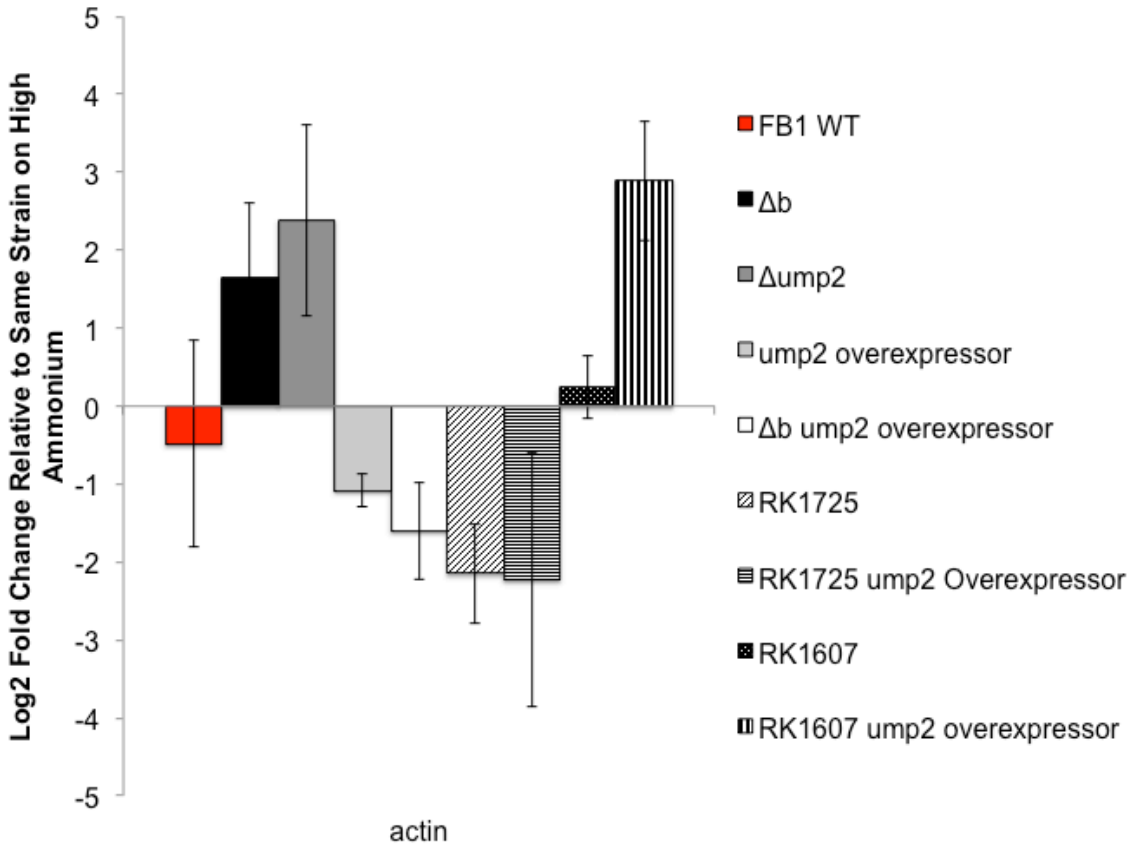

Figure 45: Log2 Fold Change in Expression levels of actin (um11232) on Low Ammonium compared to same strain on High Ammonium.
ump2 ovexpressor, FB1 with *ump2* over-expressed from constitutive P_{otef} promoter; *Δump2*, FB1 with entire *ump2* gene deleted; *Δb*, FB1 deleted for entire *b* mating-type locus; Δ*b ump2* overexpressor, FB1 deleted for entire *b* mating-type locus with *ump2* over-expressed from constitutive P_{otef} promoter; RK1725, *bE1* deletion in FB1 background; RK1725 *ump2* overexpressor, RK1725 with *ump2* over-expressed from constitutive P_{otef} promoter; RK1607, *bW1* deletion in FB6b background; RK1607 *ump2* overexpressor, RK1607 with *ump2* over-expressed from constitutive P_{otef} promoter; High, 30 mM NH_4 medium, Low, 50 µM NH_4. None of these changes were significant as analyzed by ANCOVA (Lowry, 1999-2000; Yuan et al., 2006).

Expression levels of actin regulatory proteins do not seem to be differentially regulated in the mutants tested.

Because actin expression levels were so varied within the group of mutants used in this study, we also examined the expression level of other genes

related to the organization of the actin cytoskeleton to see if they could account for the morphological differences seen in haploid colonies of the mutant strains. We chose two targets, um01671, a protein related to YSC84 involved in actin cytoskeleton rearrangement in *S. cerevisiae*, and um06428, believed to have a role in budding, polarity and filament formation. RNA-Seq data suggested that these two proteins may be differentially regulated in various mutants under low ammonium conditions, so we sought to confirm this through qRT-PCR analysis.

Our qRT-PCR analysis did not confirm what we saw in RNA-Seq data, and no dynamic expression levels of either of these targets could account for the differences in morphologies of wild-type cells under low ammonium conditions or the different colony morphologies seen in the mutants. For the protein putatively related to actin cytoskeleton rearrangement, on replete ammonium conditions, expression levels appeared to be lower than wild-type in the *ump2* overexpressor but higher when *ump2* was overexpressed in the *b* deletion background (Table 15 presents qRT-PCR data as the average of three biological replicates plus or minus standard error; Figure 46). It is again of note that while neither individual mutation (either the deletion of the entire *b* mating locus or overexpression of *ump2*) had a dramatic effect on transcript level of the target in the respective mutant, the combination of these two mutations again had a different effect. On depleted ammonium media, the majority of the mutants showed similar changes in expression level to the same strain on replete ammonium media, as did the FB1 wild-type, with the exception of the *ump2* overexpressor in the complete *b* deletion background (Table 16; Figure 47).

Table 15: Results of qRT-PCR Analysis of um01671 Expression Levels[a]

Strain	High[b] Ammonium	Low[b] Ammonium
FB1 WT[b]		-0.13±0.09
FB1*Δb*[b]	0.34±0.71	0.49±0.51
FB1*Δump2*[b]	0.32±0.13	0.97±0.73
FB1 P_{otef} *ump2*[b]	-1.45±0.99	0.18±0.33
FB1Δ*b ump2*$^{Otef\ b}$	2.56±1.03	-0.86±0.47

[a]qRT-PCR Log2 fold changes, normalized and expressed relative to FB1 WT on rich medium (High); negative values reflect decreased expression, whereas positive values represent increased expression

[b]WT, wild-type FB1; P_{otef} *ump2*, FB1 with *ump2* over-expressed from constitutive P_{otef} promoter; *Δump2*, FB1 with entire ump2 gene deleted; *Δb*, FB1 deleted for entire *b* mating-type locus; FB1Δ*b ump2*^{Otef}, FB1 deleted for entire *b* mating-type locus with *ump2* over-expressed from constitutive P_{otef} promoter; High, 30 mM NH_4 medium, Low, 50 µM NH_4

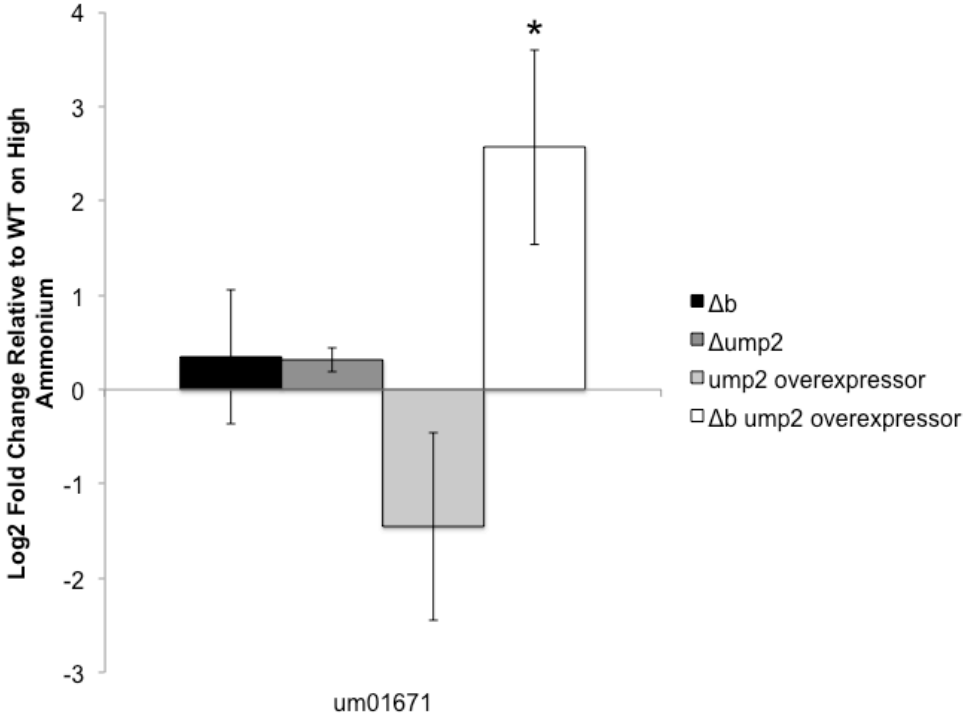

Figure 46: Log2 Fold Change in Expression levels of um01671 of various mutants as compared to FB1 WT on High Ammonium.
ump2 ovexpressor, FB1 with *ump2* over-expressed from constitutive P_{otef} promoter; *Δump2*, FB1 with entire *ump2* gene deleted; *Δb*, FB1 deleted for entire *b* mating-type locus; Δ*b ump2* overexpressor, FB1 deleted for entire *b* mating-type locus with *ump2* over-expressed from constitutive P_{otef} promoter; High, 30 mM NH_4 medium, Low, 50 µM NH_4. * significant at $p<.05$ by Kruskal-Wallis analysis (Daniel, 1990).

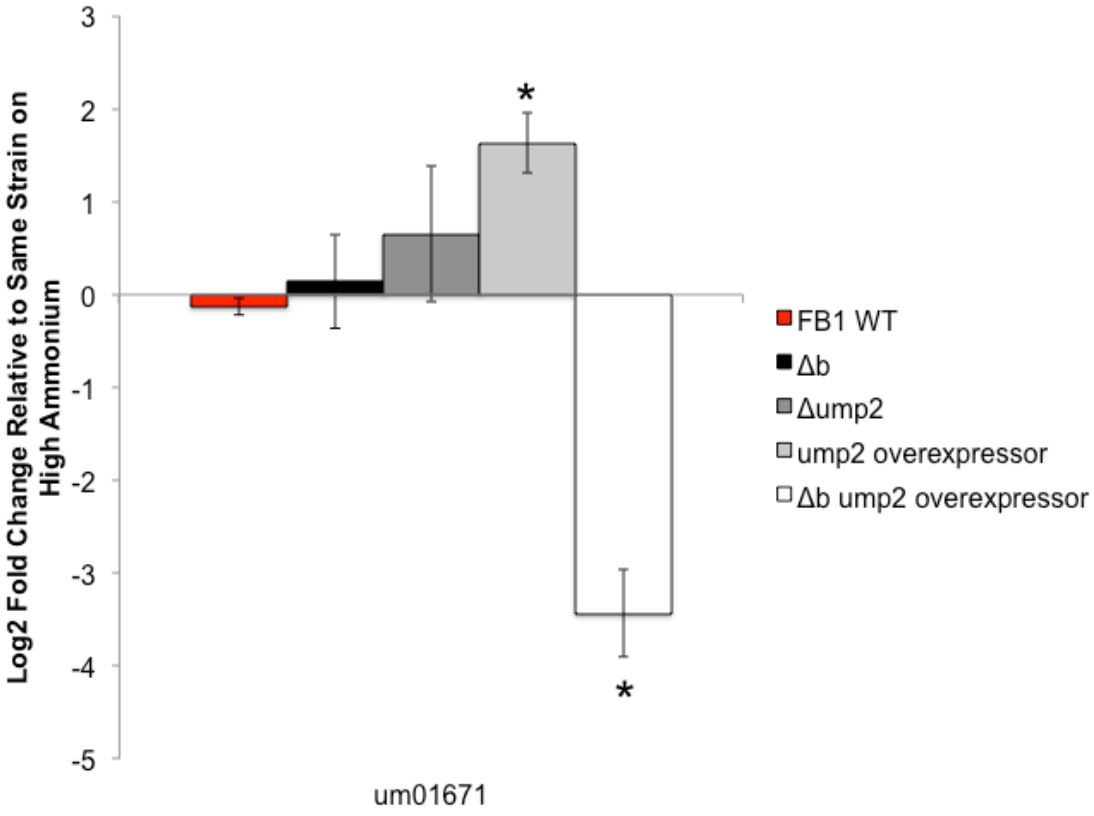

Figure 47: Log2 Fold Change in Expression levels of um01671 on Low Ammonium compared to same strain on High Ammonium.
ump2 ovexpressor, FB1 with *ump2* over-expressed from constitutive P_{otef} promoter; *Δump2*, FB1 with entire *ump2* gene deleted; *Δb*, FB1 deleted for entire *b* mating-type locus; Δ*b ump2* overexpressor, FB1 deleted for entire *b* mating-type locus with *ump2* over-expressed from constitutive P_{otef} promoter; High, 30 mM NH_4 medium, Low, 50 μM NH_4. * significant at $p<0.01$ as analyzed by ANCOVA (Lowry, 1999-2000; Yuan et al., 2006).

For um06428, involved in budding and polarity of the cell, although the *ump2* overexpressor showed decreased expression levels of this target as compared to the FB1 WT on replete media and the other mutants tested under the same conditions, it was not significantly different (Table 16 presents qRT-PCR data as averages of biological triplicates plus or minus standard errors; Figure 48). Under low ammonium conditions, it does appear that this particular target was upregulated in the FB1 wild-type as compared to replete media; this

Table 16: Results of qRT-PCR Analysis of um06428 Expression Levels[a]

Strain	High[b] Ammonium	Low[b] Ammonium
FB1 WT[b]		1.56±0.40
FB1*Δb*[b]	1.54±0.32	0.72±0.77
FB1*Δump2*[b]	1.75±0.81	1.52±0.35
FB1 P_{otef} *ump2*[b]	-0.13±0.61	0.99±0.34
FB1Δ*b ump2*$^{Otef\ b}$	1.40±0.61	0.76±0.10

[a]qRT-PCR log2 fold changes, normalized and expressed relative to FB1 WT on rich medium (High); negative values reflect decreased expression, whereas positive values represent increased expression

[b]WT, wild-type FB1; P_{otef} *ump2*, FB1 with *ump2* over-expressed from constitutive P_{otef} promoter; *Δump2*, FB1 with entire ump2 gene deleted; *Δb*, FB1 deleted for entire *b* mating-type locus; FB1Δ*b ump2*^{Otef}, FB1 deleted for entire *b* mating-type locus with *ump2* over-expressed from constitutive P_{otef} promoter; High, 30 mM NH_4 medium, Low, 50 µM NH_4

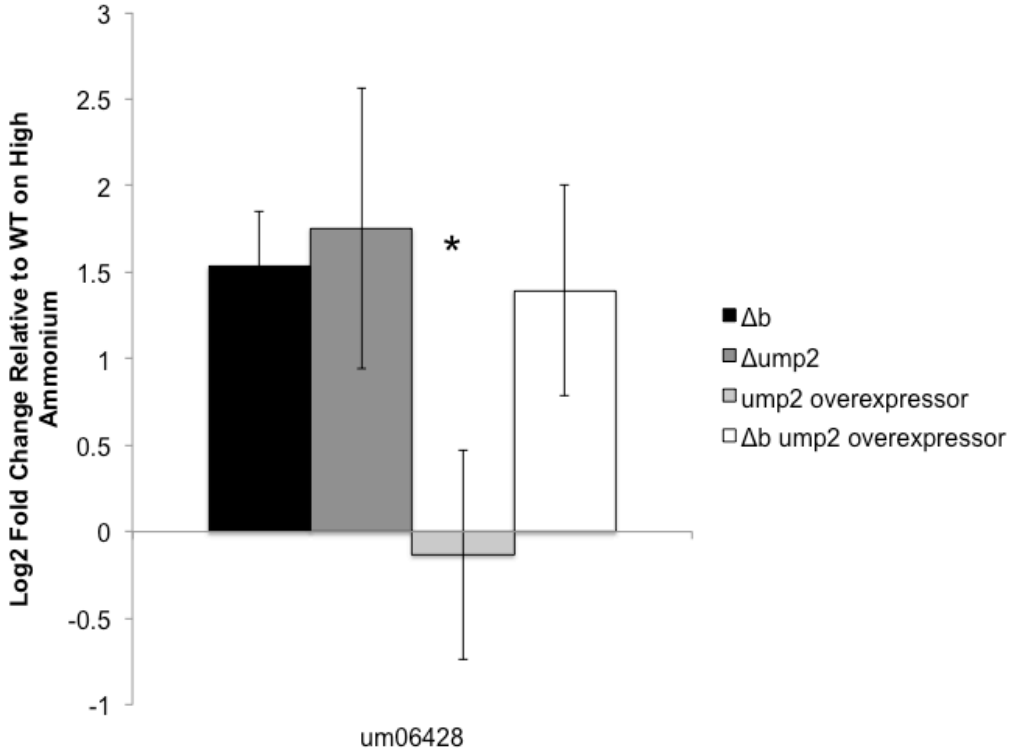

Figure 48: Log2 Fold Change in Expression levels of um06428 of various mutants as compared to FB1 WT on High Ammonium.
ump2 ovexpressor, FB1 with *ump2* over-expressed from constitutive P_{otef} promoter; *Δump2*, FB1 with entire *ump2* gene deleted; *Δb*, FB1 deleted for entire *b* mating-type locus; Δ*b ump2* overexpressor, FB1 deleted for entire *b* mating-type locus with *ump2* over-expressed from constitutive P_{otef} promoter;; High, 30 mM NH_4 medium, Low, 50 µM NH_4. * significant at p<.05 by Kruskal-Wallis analysis (Daniel, 1990).

was also the case with the *ump2* overexpressor (Figure 49). However, because there was not upregulation of this target under low ammonium in the *ump2* overexpressor in the *b* deletion background which also filaments on low ammonium, this difference cannot explain the observed phenotypic phenomena.

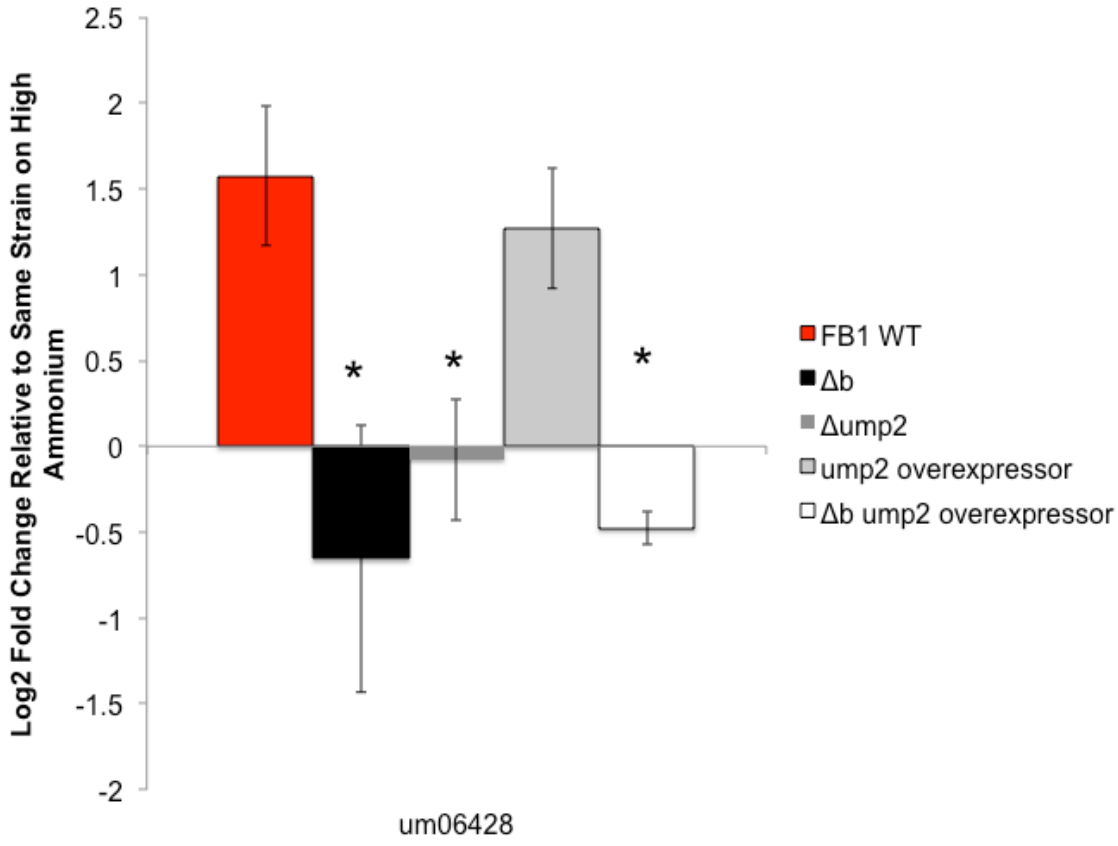

Figure 49: Log2 Fold Change in Expression levels of um06428 on Low Ammonium compared to same strain on High Ammonium.
ump2 ovexpressor, FB1 with *ump2* over-expressed from constitutive P_{otef} promoter; *Δump2*, FB1 with entire *ump2* gene deleted; *Δb*, FB1 deleted for entire *b* mating-type locus; Δ*b ump2* overexpressor, FB1 deleted for entire *b* mating-type locus with *ump2* over-expressed from constitutive P_{otef} promoter; High, 30 mM NH_4 medium, Low, 50 µM NH_4. * significant at $p<0.01$ as analyzed by ANCOVA (Lowry, 1999-2000; Yuan et al., 2006).

Discussion

The goal of the current work was to understand the variation in phenotype of various mutants in terms of filamentous response to low ammonium media conditions. Previous work had determined that while either deleting *ump2* or the entire *b* locus resulted in loss of colony filament formation under low ammonium conditions, overexpression of *ump2* can cause filamentation even under replete ammonium conditions and hyperfilamentation under low ammonium conditions. Both partial *b* deletion mutants, RK1725 and RK1607, showed a similar phenotype as the complete *b* deletion on low ammonium media. Overexpression *ump2* in either the complete *b* deletion background or RK1725 rescued the loss of phenotype, although the same non-filamentous phenotype was observed even if *ump2* was overexpressed in the RK1607 background. Moreover, we had previously found that these various mutations of the *b* mating locus and *ump2* resulted in dynamic changes in transcript level of other mating and pathogencity related genes. Here we investigated the protein level changes of targets we had previously investigated only at a transcript level, as well as the transcriptional regulation of targets more closely related to changes in the cell phentotype.

ump2 does not positively regulate its own expression.

The first examination of protein-level expression tested the hypothesis that *ump2* was able to upregulate its own expression level. Analysis of *ump2* protein level using fluorescent microscopy failed to provide evidence to support this hypothesis. Although the *ump2* overexpressor hyperfilaments on low ammonium

media, it is not as a result of increasing *ump2* expression levels from the native locus and may rather be a phenotype as a result of the additive expression from the native locus and the constitutive construct.

Different expression levels of *ump2* and the *b* mating locus cause changes in stress response to abiotic stress, but not as mediated through differential expression of cell wall integrity proteins.

In addition to the loss of filamentous phenotype in response to low ammonium, we hypothesized that mutants deleted for the entire *b* mating locus or the *ump2* high affinity ammonium transporter may have other defects associated with cell wall integrity and response to stress. The ability to respond to changing environmental conditions is paramount to the organism's ability to establish infection in its host plant, and as *ump2* deletion mutants were also attenuated for virulence, we searched for evidence that this reduced pathogenicity was associated with a lack of response to changing conditions the organism may encounter inside the host. In fact, *ump2* mutants showed decreased growth as compared to FB1 wild-type in response to abiotic stress applied to the cell wall, specifically Congo Red. Conversely, *ump2* deletion mutants seemed to survive better under osmotic stress from NaCl than their wild-type progenitors. Because our goal was broadly to find targets more closely related to changes in cell morphology than the regulatory proteins previously investigated, we attempted to find genes related to cell wall integrity that may explain these differences in growth patterns.

We examined the expression levels of two specific targets, um01788, a putative chitin deacetylase, and um06190, a putative chitinase. Both of these targets are known to be part of the *U. maydis* secretome, indicating they may be vital to infection (Mueller et al., 2008), but their putative function is fungal cell wall modifications which is why we believed they may be important in the filamentous phenotype seen in response to low ammonium. Chitin deacetylase in particular, which converts chitin to chitosan in the fungal cell wall, is vital for cell wall integrity and budding growth in other Basidiomycetes, like *Cryptococcus neoformans* (Baker, Specht, Donlin, & Lodge, 2007). While chitinase activity was not found to be necessary to dikaryon development, it was found to be necessary during saphrophytic growth and separation of nascent daughter cells (Langner et al., 2015), leading us to hypothesize it may play a role in haploid colony phenotype. Moreover, cell wall modification genes have been found to be dependent on products of the *b* mating locus for expression (Heimel et al., 2010).

While the levels of these two targets were dramatically different across the group of mutants tested, there was no discernable pattern of expression relating to ability to filament in response to low ammonium. For example, while the *ump2* overexpressor showed increased levels of chitin deacetylase as compared to the FB1 wild-type on high ammonium, so did the partial *b* deletion mutant, RK1607, although the latter does not filament under replete media conditions. Most of the mutants tested showed decreased levels of chitinase on low ammonium, although not all were able to filament under these conditions. The most interesting observation was the interplay between expression levels of

ump2 and complete or partial deletion of the *b* mating locus. Overexpression of *ump2* in a background with a *b* mutation often led to different expression levels than observed with a single mutation, again providing evidence for the interplay of *ump2* and *b* regulated expression at the transcriptional level.

The actin cytoskeleton is rearranged in response to low ammonium in *U. maydis* cells but the regulation of this process is not at the level of transcription.

By fluorescently labeling parts of the actin cytoskeleton, we were able to visualize changes in the shape of FB1 wild-type cells under low ammonium conditions. To this end, we also examined actin and other actin regulatory proteins to determine if expression level of these targets was responsible for the ability or inability to filament under depleted ammonium conditions. Specifically, we examined expression levels of actin (um11232), um01671 related to rearrangement of the actin cytoskeleton, and um06428 known to be involved in cell polarity and budding. Again, no pattern emerged that coincided with strains that could filament versus those that lacked this phenotype. The most interesting observation from these experiments was again the interplay between regulation by *ump2* expression levels and those from products of the *b* mating locus. In fact, for um06428, putatively involved in cell polarity and budding, while deleting the entire *b* mating locus or overexpressing *ump2* had opposite effects on transcript levels of this target as compared to FB1 wild-type, overexpressing *ump2* in the *b* deletion background resulted in the same effect as just deleting the *b* locus, indicating that the presence of the *b* locus was necessary for normal

expression of this target and the effect of overexpressing *ump2* on this target was dependent on products of the *b* locus.

Although we were unable to find a specific target that was differentially regulated to explain the differences in filamentation phenotype of haploid colonies within the group of mutants tested, the most salient observations, that *ump2* and *b* regulation interact at the transcriptional level, was supported by these findings. It is possible in the case of actin cytoskeleton rearrangement that regulation is not at the level of transcription but our results indicate that changes in the actin cytoskeleton are responsible for the changing morphology of *U. maydis* cells grown under low ammonium conditions and the resulting colonies. Further protein-level investigation will be necessary to fully understand this phenotype.

CHAPTER V

CONCLUSIONS

Ustilago maydis is pathogenic organism that infects its host, maize, upon mating and entering into sexual reproduction; however, it can also exist as a haploid entity, reproducing in an asexual, yeast-like budding manner. Because mating is a crucial precursor to infection, the mating program and its regulatory components have been studied extensively. The goal of this work was to understand the function of these regulatory proteins, canonically involved in mating, in the phenotypes of haploid cells that encounter mating-inducing conditions without a compatible mating partner.

We divided our exploration into two components: the ability to sense nitrogen in the environment and the activity of the *b* mating locus in haploid cells. Ammonium transporters are highly conserved throughout eukaryotes and in other organisms closely related to *U. maydis*, such as *Saccharomyces cerevisiae*, serve as transceptors. That is, they are able to not only physically transport ammonium in the cell but they also are capable of sensing nitrogen availability and causing changes in gene expression as a result. These experiments provide evidence that Ump2*,* the high affinity ammonium transporter in *U. maydis*, also functions as a transceptor. It is necessary for the organism to establish infection

in the host plant and filamentation of haploid cells in response to low ammonium. Moreover, changes in expression level of *ump2* can dramatically alter expression levels of targets related to ammonium assimilation, as well as mating, pathogenicity, and cell structure. Interestingly, some of the regulatory affect *ump2* expression levels can have are dependent on the *b* mating locus, as evidence by the loss of induction of certain targets when the *b* locus is deleted.

The activity of the products of the *b* mating locus has been extensively studied during sexual reproduction. The alleles at the *b* mating locus serve as one component of the organism's ability to recognize self versus non-self and establish infection. In a mated pair of haploid cells, homeodomain protein products from opposite alleles of the *bE* and *bW* form a heterodimer transcription factor that then regulates expression of genes necessary for pathogenicity. In haploid cells, the components of the *b* mating locus are not from compatible alleles to form this heterodimer but our work has found evidence that these two entities function in haploid cells, often by differentially regulating other targets previously considered to only function during the mating process. Perhaps the most important finding of this work is the role of *bE* and *bW* not in their heterodimeric state in haploid cells. Although homeodomain proteins in mating type loci are found in all Basidiomycetes and function in mating in this group of fungi, this work is the first evidence of these proteins functioning in haploid cells independently of each other. Moreover, our analysis provides evidence for the roles of other mating-related genes in phenotypes only observed in haploid cells.

Response to low ammonium availability does seem to evoke a change in the actin cytoskeleton of *U. maydis* cells. Although we were unable to find a specific target that was differentially expressed to explain this phenotype, we did demonstrate that *ump2* and *b* mating locus expression levels are able to change targets not related to ammonium assimilation and sexual reproduction. Moreover, the combination of multiple mutations within a strain resulted in different regulation of selected targets than did a single mutation, again providing evidence for the interplay of these two regulators at the level of transcription. It is possible that regulation of the actin cytoskeleton is post-transcriptional, accounting for our inability to find differential of a specific target explaining the filamentation phenotypes observed in our group of mutants. Further research of changes in the cytoskeleton as a result of exposure to low ammonium will be necessary to fully understand this phenomenon.

REFERENCES

Andrews, D. L., Garcia-Pedrajas, M. D., & Gold, S. E. (2004). Fungal dimorphism regulated gene expression in *Ustilago maydis*: I. Filament up-regulated genes. *Mol Plant Pathol, 5*, 281-293.

Arie, T., Kaneko, I., Yoshida, T., Noguchi, M., Nomura, Y., & Yamaguchi, I. (2000). Mating-Type Genes from Asexual Phytopathogenic Ascomycetes *Fusarium oxysporum* and *Alternaria alternata*. *MPMI, 13*(12), 1330-1339.

Asante-Owusu, R. N., Banham, A. H., Bohnert, H. U., Mellor, E. J. C., & Casselton, L. A. (1996). Heterodimerization between two classes of homeodomain proteins in the muschroom *Coprinus cinereus* brings together potential DNA-binding and activation domains. *Genetic, 172*, 25-31.

Astell, C. R., Ahlstrom-Jonasson, L., & Smith, M. (1981). The Sequence of the DNAs Coding for the Mating-Type Loci of *Saccharomyces cerevisiae*. *Cell, 27*(November 1981 Part 2), 15-23.

Babu, M., Choffe, K., & Saville, B. (2005). Differential gene expression in filamentous cells of *Ustilago maydis*. *Curr Genet, 47*, 316-333.

Badouin, H., Hood, M. E., Gouzy, J., Aguileta, G., Siguenza, S., Perlin, M. H., . . . Giraud, T. (2015). Chaos of Rearrangements in the Mating-Type Chromosomes of the Anther-Smut Fungus *Microbotryum lychnidis-dioicae*. *Genetics, 200*(4), 1275-1284. doi:10.1534/genetics.115.177709

Baker, L. G., Specht, C. A., Donlin, M. J., & Lodge, J. K. (2007). Chitosan, the deacetylated form of chitin, is necessary for cell wall integrity in *Cryptococcus neoformans*. *Eukaryot Cell, 6*(5), 855-867. doi:10.1128/EC.00399-06

Bakkeren, G., Gibbard, A., Yee, E., Froeliger, S., Leong, S., & Kronstad, J. W. (1992). The a and b loci of *U. maydis* hybridize to DNAs from other smut fungi. *Molecular Plant Microbe Interaction, 5*, 347-355.

Bakkeren, G., Jiang, G., Warren, R. L., Butterfield, Y., Shin, H., Chiu, R., . . . Kronstad, J. W. (2006). Mating factor linkage and genome evolution in basidiomycetous pathogens of cereals. *Fungal Genet Biol, 43*(9), 655-666. doi:10.1016/j.fgb.2006.04.002

Bakkeren, G., Kamper, J., & Schirawski, J. (2008). Sex in smut fungi: Structure, function and evolution of mating-type complexes. *Fungal Genet Biol, 45 Suppl 1*, S15-21. doi:10.1016/j.fgb.2008.04.005

Bakkeren, G., & Kronstad, J. W. (1993). Conservation of the b Mating Type Gene Complex among Bipolar and Tetrapolar Smut Fungi. *The Plant Cell, 5*(123-136).

Bakkeren, G., & Kronstad, J. W. (1994). Linkage of mating-type loci distinguishes bipolar from tetrapolar mating in basidiomycetous smut fungi. *PNAS, 91*, 7085-7089.

Bakkeren, G., & Kronstad, J. W. (1996). The Pheremone Cell Signaling Components of the Usilago a Mating-Type Loci Determine Intercompatibility Between Species. *Genetics, 143*, 1601-1613.

Banuett, F., & Herskowitz, I. (1989). Different a alleles of *Ustilago maydis* are necessary for maintenance of filamentous growth but not for meiosis. *PNAS, 86*, 5878-5882.

Banuett, F., & Herskowitz, I. (1994). Morphological Transitions in the Life Cycle of *Ustilago maydis* and Their Genetic Control by the *a* and *b* Loci. *Experimental Mycology, 18*(3), 247-266. doi:10.1006/emyc.1994.1024

Beckerman, J. L., Naider, F., & Ebbole, D. J. (1997). Inhibition of Pathogenicity of the Rice Blast Fungus by *Saccharomyces cerevisiae* alpha-Factor. *Science, 276*, 1116-1119.

Bender, A., & Sprague, G. F. (1989). Pheromones and Pheromone Receptors are the Primary Determinants of Mating Specificity in the Yeast *Saccharomyces cerevisiae*. *Genetics, 121*, 463-476.

Bennett, R. J., Uhl, M. A., Miller, M. G., & Johnson, A. D. (2003). Identification and Characterization of a *Candida albicans* Mating Pheromone. *Molecular and Cellular Biology, 23*(22), 8189-8201. doi:10.1128/mcb.23.22.8189-8201.2003

Berepiki, A., Lichius, A., & Read, N. D. (2011). Actin organization and dynamics in filamentous fungi. *Nat Rev Microbiol, 9*(12), 876-887. doi:10.1038/nrmicro2666

Bernstein, C., & Johns, V. (1989). Sexual Reproduction as a Response to H2O2 Damage in *Schizosaccharomyces pombe*. *Journal of Bacteriology, 171*(4), 1893-1897.

Bistis, G. N. (1981). Chemotropic Interactions between Trichogynes and Conidia of Opposite Mating-Type in *Neurospora crassa*. *Mycologia, 73*(5), 959-975.

Biswas, K., & Morschhauser, J. (2005). The Mep2p ammonium permease controls nitrogen starvation-induced filamentous growth in *Candida albicans*. *Mol Microbiol, 56*(3), 649-669. doi:10.1111/j.1365-2958.2005.04576.x

Biswas, S., Van Dijck, P., & Datta, A. (2007). Environmental Sensing and Signal Transduction Pathways Regulating Morphopathogenic Determinants of *Candida albicans*. *Microbiology and Molecular Biology Reviews, 71*(2), 348-376. doi:10.1128/mmbr.00009-06

Bobrowicz, P., Pawlack, R., Correa, A., Bell-Pedersen, D., & Ebbole, D. J. (2002). The *Neurospora crassa* pheremone precursor genes are regulated by the mating type locus and the circadian clock. *Molecular Microbiology, 45*(3), 795-804.

Bolker, M., Urban, M., & Kahmann, R. (1992). The *a* Mating Type Locus of *U. maydis* Specifies Cell Signaling Components. *Cell, 88*, 441-450.

Bolton, M., & Thomma, B. P. H. J. (2008). The complexity of nitrogen metabolism and nitrogen-regulated gene expression in plant pathogenic fungi. *Physiological and Molecular Plant Pathology, 72*(4-6), 104-110. doi:10.1016/j.pmpp.2008.07.001

Brachmann, A., Konig, J., Julius, C., & Feldbrugge, M. (2004). A reverse genetic approach for generating gene replacement mutants in *Ustilago maydis*. *Molecular Genetics and Genomics, 272*, 216-226.

Brachmann, A., Weinzieri, G., Kamper, J., & Kahmann, R. (2001). Identification of genes in the bW/bE regulatory cascade in *Ustilago maydis*. *Molecular Genetics and Genomics, 271*, 102-110.

Brefort, T., Muller, P., & Kahmann, R. (2005). The high-mobility-group domain transcription factor Rop1 is a direct regulator of prf1 in *Ustilago maydis*. *Eukaryot Cell, 4*(2), 379-391. doi:10.1128/EC.4.2.379-391.2005

Bucking-Throm, E., Duntze, W., Hartwell, L. H., & Manney, T. R. (1973). Reversible arrest of haploid yeast cells at the initiation of DNA synthesis by a diffusible sex factor. *Experimental Cell Research, 76*(1), 99-110.

Burns, C., Stajich, J. E., Rechtsteiner, A., Casselton, L., Hanlon, S. E., Wilke, S. K., . . . Pukkila, P. J. (2010). Analysis of the Basidiomycete *Coprinopsis cinerea* reveals conservation of the core meiotic expression program over half a billion years of evolution. *PLoS Genet, 6*(9), e1001135. doi:10.1371/journal.pgen.1001135

Choi, W., & Dean, R. A. (1997). The Adenylate Cyclase Gene MAC1 of *Magnaporthe grisea* Controls Appressorium Formation and Other Aspects of Growth and Development. *The Plant Cell, 9*, 1973-1993.

Cooper, T. G. (2002). Transmitting the signal of excess nitrogen in *Saccharomyces cerevisiae* from the Tor proteins to the GATA factors: connecting the dots. . *FEMS Microbiol Rev, 26*, 223-238.

Crow, J. F., & Dove, W. F. (1990). The Role of Similarity and Differences in Fungal Mating. *Genetics, 125*(457-462).

Daniel, W. W. (1990). Kruskal–Wallis one-way analysis of variance by ranks. Applied Nonparametric Statistics (2nd ed.). *Boston: PWS-Kent*, 336-234.

Davey, J. (1991). Mating pheromones of the fission yeast *Schizosaccharomyces pombe*: purification and structural characterization of M-factor and isolation and analysis of two genes encoding the pheromone. *EMBO, 11*(3), 951-960.

Day, A. (1979). Mating Type and Morphogenesis in *Ustilago violacea*. *Botanical Gazette, 140*(1), 94-101.

Doehlemann, G., Van der Linde, K., Abmann, D., Schwammback, D., Hof, A., Mohanty, A., . . . Kahmann, R. (2009). Pep1, a Secreted Effector Protein of *Ustilago maydis*, Is Required for Successful Invasion of Plant Cells. *PLoS Pathog, 5*, e1000290.

Donofrio, N. M., Oh, Y., Lundy, R., Pan, H., Brown, D. E., Jeong, J. S., . . . Dean, R. A. (2006). Global gene expression during nitrogen starvation in the rice

blast fungus, *Magnaporthe grisea*. *Fungal Genet Biol, 43*(9), 605-617. doi:10.1016/j.fgb.2006.03.005

Dranginis, A. M. (1990). Binding of Yeast a1 and (alpha)2 as a Heterodimer to the Operator DNA of a Haploid-Specific Gene. *Nature, Oct 18, 1990*, 682-685.

Erdmann, S., Freihorst, D., Raudaskoski, M., Schmidt-Heck, W., Jung, E. M., Senftleben, D., & Kothe, E. (2012). Transcriptome and functional analysis of mating in the basidiomycete *Schizophyllum commune*. *Eukaryot Cell, 11*(5), 571-589. doi:10.1128/EC.05214-11

Farfsing, J. W., Auffarth, K., & Basse, C. (2005). Identification of cis-Active Elements in *Ustilago maydis* mig2 Promoters Conferring High-Level Activity During Pathogenic Growth in Maize. *Mol Plant-Microbe Interact, 18*, 75-87.

Forche, A., Alby, K., Schaefer, D., Johnson, A. D., Berman, J., & Bennett, R. J. (2008). The parasexual cycle in *Candida albicans* provides an alternative pathway to meiosis for the formation of recombinant strains. *PLoS Biol, 6*(5), e110. doi:10.1371/journal.pbio.0060110

Fraser, J. A., Diezmann, S., Subaran, R. L., Allen, A., Lengeler, K. B., Dietrich, F. S., & Heitman, J. (2004). Convergent evolution of chromosomal sex-determining regions in the animal and fungal kingdoms. *PLoS Biol, 2*(12), e384. doi:10.1371/journal.pbio.0020384

Garcia-Pedrajas, M. D., & Gold, S. E. (2004). Fungal dimorphism regulated gene expression in *Ustilago maydis*: II. Filament down-regulated genes. . *Mol Plant Pathol, 5*, 295-307.

Gillissen, B., Bergemann, J., Sandmann, C., Schroeer, B., Bolker, M., & Kahmann, R. (1992). A Two-Component Regulatory System for Self/Non-Self Regulation in *Ustilago maydis*. *Cell, 68*, 647-657.

Gimeno, C. D., Ljungdahl, P. O., Styles, C. A., & Fink, G. R. (1992). Unipolar Cell Divisions in Yeast *S. Cerevisiae* Leads to Filamentous Growth: Regulation by Starvation and RAS. *Cell, 68*, 1077-1090.

Giraud, T., Yockteng, R., Lopez-Villavicencio, M., Refregier, G., & Hood, M. E. (2008). Mating system of the anther smut fungus *Microbotryum violaceum*: selfing under heterothallism. *Eukaryot Cell, 7*(5), 765-775. doi:10.1128/EC.00440-07

Glass, N. L., Grotelueschen, J., & Metzenberg, R. L. (1990). *Neurospora crassa A mating-type region*. *PNAS, 87*, 4912-4916.

Gold, S. E., Brogdon, S. M., Mayorga, M., & Kronstad, J. W. (1997). The *Ustilago maydis* regulatory subunit of a cAMP-dependent protein kinase is required for gall formation in maize. . *Plant Cell, 9*, 1585-1594.

Grabherr, M. G., Haas, B. J., Yassour, M., Levin, J. Z., Thompson, D. A., Amit, I., . . . al., e. (2011). Full-length transcriptome assembly from RNA-Seq data without a reference genome. . *Nat Biotechnol, 29*, 644-652.

Haas, B. J., Papanicolaou, A., Yassour, M., Grabherr, M. G., Blood, P. D., Bowden, J., . . . al., e. (2013). *De novo* transcript sequence reconstruction from RNA-seq using the Trinity platform for reference generation and analysis. . *Nat Protoc, 8*, 1494-1512.

Hagen, D. C., McCaffery, G., & Sprague, G. F. (1986). Evidence the STE3 gene encodes a receptor for the peptide pheremone a factor: Gene sequence and implications for the structure of the presumed receptor. *PNAS, 83*(March 1986), 1418-1422.

Hagen, D. C., & Sprague, G. F. (1984). Induction of the yeast alpha specific STE3 gene by the peptide pheremone a-factor. *Journal of Molecular Biology, 148*(4), 835-852.

Hartl, L., Zach, S., & Seidl-Seiboth, V. (2012). Fungal chitinases: diversity, mechanistic properties and biotechnological potential. *Appl Microbiol Biotechnol, 93*(2), 533-543. doi:10.1007/s00253-011-3723-3

Hartmann, H. A., Kruger, J., Lottspeich, F., & Kahmann, R. (1999). Envrionmental Signals Controlling Sexual Development of the Corn Smut Fungus *Ustilago maydis* through the transcriptional regulator Prf1. *The Plant Cell, 11*, 1293-1305.

Heimel, K., Scherer, M., Schuler, D., & Kamper, J. (2010). The *Ustilago maydis* Clp1 protein orchestrates pheromone and b-dependent signaling pathways to coordinate the cell cycle and pathogenic development. *Plant Cell, 22*(8), 2908-2922. doi:10.1105/tpc.110.076265

Hibbett, D. S., Binder, M., Bischoff, J. F., Blackwell, M., Cannon, P. F., Eriksson, O. E., . . . Zhang, N. (2007). A higher-level phylogenetic classification of the Fungi. *Mycol Res, 111*(Pt 5), 509-547. doi:10.1016/j.mycres.2007.03.004

Hicks, J., Strathern, J. N., & Klar, A. (1979). Transposable mating type genes in *Saccharomyces cerevisiae*. *Nature, 282*, 478-483.

Ho, E., Cahill, M., & Saville, B. (2007). Gene discovery and transcript analyses in the corn smut pathogen *Ustilago maydis*: expressed sequence tag and genome sequence comparison. . *BMC Genomics, 8*, 334.

Holliday, R. (1974). *Ustilago maydis*. *Handbook of Genetics (ed. R.C. King), New York, USA: Plenum Press*, 575-595.

Hood, M. E. (2002). Dimorpic Mating-Type Chromosomes in the Fungus *Microbotryum violaceum*. *Genetics, 160*, 457-461.

Hood, M. E., & Antonovics, J. (1998). Two-Celled Promycelia and Mating-Tye Segregation in *Ustilago violacea* (*Microbotryum violaceum*). *International Journal of Plant Sciences, 159*(2), 199-205.

Hood, M. E., & Antonovics, J. (2000). Intratetrad mating, heterozygosity, and the maintenance of deleterious alleles in *Microbotrum violaceum* (=*Ustilago violacea*). *Heredity, 85*, 231-241.

Hood, M. E., Petit, E., & Giraud, T. (2013). Extensive divergence between mating-type chromosomes of the anther-smut fungus. *Genetics, 193*(1), 309-315. doi:10.1534/genetics.112.146266

Horandl, E. (2009). A combinational theory for maintenance of sex. *Heredity (Edinb), 103*(6), 445-457. doi:10.1038/hdy.2009.85

Horst, R. J., Doehlemann, G., Wahl, R., Hoffman, J., Schmield, A., Kahmann, R., . . . Voll, L. M. (2010). *Ustilago maydis* infection strongly alters organic nitrogen allocation in maize and stimulates productivity of systemic source leaves. *Plant Physiol, 152*, 293-308.

Hull, C. M., & Johnson, A. D. (1999). Identification of a Mating Type-Like Locus in the Asxual Pathogenic Yeast *Candida albicans*. *Science, 285*, 1271-1277.

Imai, Y., & Yamamoto, M. (1994). The fission yeast mating pheromone P-factor: its molecular structure, gene structure, and ability to induce gene expression and G1 arrest in the mating partner. *Genes and Development, 8*, 328-338.

Kadota, K., Nishiyama, T., & Shimizu, K. (2012). A normalization strategy for comparing tag count data. *Algorithms Mol Biol, 7*, 5.

Kaffarnik, F., Muller, P., Leibundgut, M., Kahmann, R., & Feldbrugge, M. (2003). PKA and MAPK phosphorylation of Prf1 allows promoter distinction in *Ustilago maydis*. *EMBO, 22*(21), 5817-5826.

Kahmann, R., Basse, C., & Feldbrugge, M. (1999). Fungal-plant signalling in the *Ustilago maydis*-maize pathosystem. *Curr Opin Microbiol, 2*, 647-650.

Kahmann, R., Basse, C., & Feldbrügge, M. (1999). Fungal-plant signalling in the *Ustilago maydis*-maize pathosystem. *Current opinion in microbiology, 2*(6), 647-650. doi:10.1016/s1369-5274(99)00038-7

Kämper, J. (2004). A PCR-based system for highly efficient generation of gene replacement mutants in *Ustilago maydis*. *Molecular Genetics and Genomics, 271*(1), 103-110. doi:10.1007/s00438-003-0962-8

Kamper, J., Kahmann, R., Bolker, M., Ma, L. J., Brefort, T., Saville, B. J., . . . Birren, B. W. (2006). Insights from the genome of the biotrophic fungal plant pathogen *Ustilago maydis*. *Nature, 444*(7115), 97-101. doi:10.1038/nature05248

Kamper, J., Reichmann, M., Romeis, T., Bolker, M., & Kahmann, R. (1995). Multiallelic Recognition: Nonself-Dependent Dimerization of the bE and bW Homeodomain Proteins in *Ustilago maydis*. *Cell, 81*, 73-83.

Kang, S., Chumley, F. G., & Valent, B. (1994). Isolation of the Mating-Type Genes of the Phytopathogenic Fungus Magnaporthe grisea Using Genomic Subtraction. *Genetics, 138*, 289-296.

Karos, M., Chang, C., McClelland, C. M., Clarke, D. L., Fu, J., Wickes, B., & Kwon-Chung, K. J. (2000). Mapping of the *Cryptococcus neoformans* MATa Locus: Presence of Mating Type Specific Mitogen-Activated Protein Kinase Cascade Homologs. *Journal of Bacteriology, 182*(21), 6222-6227.

Kelly, M., Burke, J., Smith, M., Klar, A., & Beach, D. (1988). Four mating-type genes control sexual differentation in the fission yeast. *EMBO, 7*(5), 1537-1547.

Kim, H., & Borkovich, K. A. (2004). A pheromone receptor gene, pre-1, is essential for mating type-specific directional growth and fusion of trichogynes and female fertility in *Neurospora crassa*. *Mol Microbiol, 52*(6), 1781-1798. doi:10.1111/j.1365-2958.2004.04096.x

Kim, H., Metzenberg, R. L., & Nelson, M. A. (2002). Multiple Functions of mfa-1, a Putative Pheromone Precursor Gene of *Neurospora crassa*. *Eukaryotic Cell, 1*(6), 987-999. doi:10.1128/ec.1.6.987-999.2002

Klosterman, S., Perlin, M. H., Garcia-Pedrajas, M. D., Covert, S., & Gold, S. E. (2007). Genetics of Morphogenesis and Pathogenic Development of *Ustilago maydis*. *Advances in Genetics, 57*, 1-47.

Kronstad, J. W., & Leong, S. (1989). Isolation of two alleles of the *b* locus of *Ustilago maydis*. *PNAS USA, 86*, 978-982.

Kronstad, J. W., & Leong, S. (1990). The *b* mating-type locus of *Ustilago maydis* contains variable and constant regions. *Genes and Development, 4*, 1384-1395.

Kues, U., Richardson, W. V. J., Tymon, A. M., Mutasa, E. S., Gottgens, B., Gaubatz, S., . . . Casselton, L. A. (1992). The combination of dissimilar alleles of the A-alpha and A-Beta gene complexes, whose proteins contain homeo domain motifs, determines sexual development in the mushroom *Coprinus cinereus*. *Genes and Development, 6*, 568-577.

Kwon-Chung, K. J. (1976). Morphogenesis of *Filobasidiella neoformans,* the Sexual State of *Cryptococcus neoformans*. *Mycologia, 68*(4), 821-833.

Langmead, B., Trapnell, C., Pop, M., & Salzberg, S. L. (2009). Ultrafast and memory-efficient alignment of short DNA sequences to the human genome. . *Genome Biology, 10*, R25.

Langner, T., Ozturk, M., Hartmann, S., Cord-Landwehr, S., Moerschbacher, B., Walton, J. D., & Gohre, V. (2015). Chitinases Are Essential for Cell Separation in *Ustilago maydis*. *Eukaryot Cell, 14*(9), 846-857. doi:10.1128/EC.00022-15

Lau, G., & Hamer, J. E. (1996). Regulatory Genes Controlling MPG1 Expression and Pathogenicity in the Rice Blast Fungus *Magnaporthe grisea*. *The Plant Cell Online, 8*, 771-781.

Lengeler, K., Fox, D. S., Fraser, J. A., Allen, A., Forrester, K., Dietrich, F., & Heitman, J. (2002). Mating-Type Locus of *Cryptococcus neoformans*: A Step in the Evolution of Sex Chromosomes. *Eukaryotic Cell, 1*(5), 704-718. doi:10.1128/EC.1.5.704-718.2002

Li, B., & Dewey, C. N. (2011). RSEM: accurate transcript quantification from RNA-Seq data with or without a reference genome. *BMC Bioinformatics, 12*, 323.

Li, J., Lu, L., Jia, Y., Wang, Q., Fukuta, Y., & Li, C. (2016). Characterization of Field Isolates of *Magnaporthe oryzae* with Mating Type, DNA Fingerprinting, and Pathogenicity Assays. *Plant Disease, 100*(2), 298-303. doi:10.1094/pdis-06-15-0660-re

Lin, X., Hull, C. M., & Heitman, J. (2005). Sexual reproduction between partners of the same mating type in *Cryptococcus neoformans*. *Nature, 434*(7036), 1017-1021.

Lindegren, C. C. (1945). Life Cycles, Cytology, Hybridization, Vitamin Synthesis and Adaptive Enzymes. *Bacteriol Rev, 9*(3-4), 111-170.

Lo, H. J., Kohler, J. R., DiDominco, B., Loebenberg, D., Cacciapuoti, A., & Fink, G. R. (1997). Nonfilamentous *C. albicans* mutants are avirulent. *Cell, 90*(939-949).

Lorenz, M. C., & Heitman, J. (1998). The MEP2 ammonium permease regulates pseudohyphal differentiation in *Saccharomyces cerevisiae*. *EMBO Journal, 17*(5), 1236-1247.

Lovely, C. B., Aulakh, K. B., & Perlin, M. H. (2011). Role of Hsl7 in Morphology and Pathogenicity and Its Interaction with Other Signaling Components in the Plant Pathogen *Ustilago maydis*. *Eukaryot Cell, 10*, 869-883.

Lowry, R. (1999-2000). Chapter 17: One-Way Analysis of Covariance for Independent Samples. http://vassarstats.net.

Michaelis, S., & Herskowitz, I. (1988). The a-factor Phermone of *Saccharomyces cerevisiae* is Essential for Mating. *Molecular and Cellular Biology, 8*(3), 1309-1318.

Miller, M. G., & Johnson, A. D. (2002). White-Opaque Switching in *Candida albicans* is controlled by Mating-Type Locus Homeodomain Proteins and Allows Efficient Mating. *Cell, 110*, 293-302.

Mitsuzawa, H. (2006). Ammonium transporter genes in the fission yeast *Schizosaccharomyces pombe*: role in ammonium uptake and a morphological transition. *Genes to Cells, 11*(10), 1183-1195. doi:10.1111/j.1365-2443.2006.01014.x

Mochizuki, N., & Yamamoto, M. (1992). Reduction in the intracellular cAMP level triggers initiation of sexual development in fission yeast. *Molecular and General Genetics, 233*(1), 17-24.

Morrow, C. A., & Fraser, J. A. (2009). Sexual reproduction and dimorphism in the pathogenic basidiomycetes. *FEMS Yeast Res, 9*(2), 161-177. doi:10.1111/j.1567-1364.2008.00475.x

Mueller, O., Kahmann, R., Aguilar, G., Trejo-Aguilar, B., Wu, A., & de Vries, R. P. (2008). The secretome of the maize pathogen *Ustilago maydis*. *Fungal Genet Biol, 45 Suppl 1*, S63-70. doi:10.1016/j.fgb.2008.03.012

O'Shea, S. F., Chaure, P. T., Halsall, J. R., Olesnicky, N. S., Liebbrant, A., Connerton, I. F., & Casselton, L. A. (1998). A Large Pheromone and Receptor Gene Complex Determines Multiple B Mating Type Specificities in *Coprinus cinereus*. *Genetics, 148*, 1081-1090.

Oliveros, J. C. (2007-2015). Venny. An interactive tool for comparing lists with Venn's diagrams. (2.0 edition).

Paul, J. A., Barati, M. T., Cooper, M., & Perlin, M. H. (2014). Physical and Genetic Interaction Between Ammonium Transporters and the Signaling Protein, Rho1, in the Plant Pathogen, *Ustilago maydis*. *Eukaryot Cell, 13*, 1328-1336.

Pellier, A. L., Lauge, R., Veneault-Fourrey, C., & Langin, T. (2003). CLNR1, the AREA/NIT2-like global nitrogen regulator of the plant fungal pathogen *Colletotrichum lindemuthianum* is required for the infection cycle. *Mol Microbiol, 48*, 639-655.

Perkins, D. D., & Berry, E. G. (1977). The Cytogenetics of *Neurospora*. *Advances in Genetics, 19*, 133-285.

Perlin, M. H., Amselem, J. F., E., Toh, S. S., Chen, Z., Goldberg, J., Deplessis, S., . . . Zeng, Q. (2015). Sex and parasites: genomic and transcriptomic analysis of *Microbotryum lychnidis-dioicae*, the biotrophic and plant-castrating anther smut fungus. *BMC Genomics, 16*, 461.

Pham, C. D., Yu, Z., Sandrock, B., Bolker, M., Gold, S. E., & Perlin, M. H. (2009). *Ustilago maydis* Rho1 and 14-3-3 homologues participate in pathways controlling cell separation and cell polarity. *Eukaryot Cell, 8*, 977-989.

Phillips, C. L., Stark, M. R., Johnson, A. D., & Dahlquist, F. W. (1994). Heterodimerization of the yeast homeodomain transcriptional regulators alpha 2 and a1 induces an interfacial helix in alpha 2. . *Biochemistry, 33*(31), 9294-9302.

Radwan, G. L. H. E. (2013). Molecular Comparison and DNA Fingerprinting of *Sporisorium reilianum* and *Peronosclerospora sorghi* Relating to Host Specificity and Host Resistance. *Doctoral dissertation, Texas A&M University. Available electronically from http : / /hdl .handle .net /1969 .1 /149318.*

Ram, A. F., & Klis, F. M. (2006). Identification of fungal cell wall mutants using susceptibility assays based on Calcofluor white and Congo red. *Nat Protoc, 1*(5), 2253-2256. doi:10.1038/nprot.2006.397

Robinson, M. D., McCarthy, D. J., & Smith, G. K. (2010). edgeR: a Bioconductor package for differential expression analysis of digital gene expression data. *Bioinformatics, 26*, 139-140.

Robledo-Briones, M., & Ruiz-Herrera, J. (2013). Regulation of genes involved in cell wall synthesis and structure during *Ustilago maydis* dimorphism. *FEMS Yeast Res, 13*, 74-84.

Romeis, T., Kamper, J., & Kahmann, R. (1997). Single-chain fusions of two unrelated homeodomain proteins trigger pathogenicity in *Ustilago maydis*. *PNAS, 94*, 1230-1234.

Rozen, S., & Skaletskey, H. (2000). Primer3 on the WWW for the general users and for biologist programers. *Methods Mol Biol, 132*, 365-386.

Ruderfer, D. M., Pratt, S. C., Seider, H. S., & Kruglyak, L. (2006). Population genomic analysis of outcrossing and recombination in yeast. *Nat Genet, 38*(9), 1077-1081.

Ruiz-Herrera, J., Leon, C. G., Carabez-Trejo, A., & Reyes-Salinas, E. (1996). Structure and Chemical Composition of the Cell Walls from the Haploid Yeast and Mycelial Forms of *Ustilago maydis*. *Fungal Genet Biol, 20*, 133-142.

Rutherford, J. C., Chua, G., Hughes, T., Cardenas, M. E., & Heitman, J. (2008). A Mep2-dependent Transcriptional Profile Links Permease Function to Gene Expression during Pseudohyphal Growth in *Saccharomyces cerevisiae*. *Molecular Biology of the Cell, 19*(7), 3028-3039. doi:10.1091/mbc.E08-01-0033

Rutherford, J. C., Lin, X., Nielsen, K., & Heitman, J. (2008). Amt2 Permease Is Required To Induce Ammonium-Responsive Invasive Growth and Mating in *Cryptococcus neoformans*. *Eukaryotic Cell, 7*(2), 237-246. doi:10.1128/ec.00079-07

Salmeron-Santiago, K. G., Pardo, J. P., Flores-Herrera, O., Mendoza-Hernandez, G., Miranda-Arango, M., & Guerra-Sanchez, G. (2011). Response to osmotic stress and temperature of the fungus *Ustilago maydis*. *Arch Microbiol, 193*(10), 701-709. doi:10.1007/s00203-011-0706-9

Sánchez-Martínez, C., & Pérez-Martín, J. (2001). Dimorphism in fungal pathogens: *Candida albicans* and *Ustilago maydis*--similar inputs, different outputs. *Current opinion in microbiology, 4*(2), 214-221. doi:10.1016/s1369-5274(00)00191-0

Saunders, C. W., Scheynius, A., & Heitman, J. (2012). Malassezia fungi are specialized to live on skin and associated with dandruff, eczema, and other skin diseases. *PLoS Pathog, 8*(6), e1002701. doi:10.1371/journal.ppat.1002701

Saville, B., Donaldson, M. E., & Doyle, C. E. (2012). Investigation Host Inducted Meiosis in a Fungal Plant Pathogen *Meiosis - Molecular Mechanisms and Cytogenetic Diversity*.

Schauwecker, F., Wanner, G., & Kahmann, R. (1995). Filament-Specific Expression of a Cellulase Gene in the Dimorphic Fungus *Ustilago maydis*. *Biological Chemistry Hoppe-Seyler, 376*, 617-626.

Schirawski, J., Heinze, B., Wagenknecht, M., & Kahmann, R. (2005). Mating type loci of *Sporisorium reilianum*: novel pattern with three a and multiple b specificities. *Eukaryot Cell, 4*(8), 1317-1327. doi:10.1128/EC.4.8.1317-1327.2005

Schlesinger, R., Kahmann, R., & Kamper, J. (1997). The homeodomains of the heterodimeric bE and bW preotins of *Ustilago maydis* are both critical for function. *Mol Gen Genet, 254*, 514-519.

Schulz, B., Banuett, F., Dahl, M., Schlesinger, R., Schafer, W., Martin, T., . . . Kahmann, R. (1990). The b alleles of U. maydis, Whose Combinations Program Pathogenic Development, Code for Polypeptides Containing a Homeodomain Related Motif. *Cell, 60*, 295-306.

Shen, W., Bobrowicz, P., & Ebbole, D. J. (1999). Isolation of Pheromone Precursor Genes of *Magnaporthe grisea*. *Fungal Genet Biol, 27*, 253-263.

Smith, D. G., Garcia-Pedrajas, M. D., Gold, S. E., & Perlin, M. H. (2003). Isolation and characterization from pathogenic fungi of genes encoding ammonium permeases and their roles in dimorphism. *Molecular Microbiology, 50*(1), 259-275. doi:10.1046/j.1365-2958.2003.03680.x

Snoeijers, S. S., Vossen, P., Goosen, T., Van den Broek, H. W., & De Wit, P. J. (1999). Transcription of the avirulence gene Avr9 of the fungal tomato pathogen *Cladosporium fulvum* is regulated by a GATA-type transcription factor in *Aspergillus nidulans*. *Mol Gen Genet, 261*, 653-659.

Specht, C. A. (1995). Isolation of the B alpha and B beta mating type loci of *Schizophyllum commune*. *Curr Genet, 28*, 374-379.

Staben, C., & Yanofsky, C. (1990). *Neurospora crass a* mating type region. *PNAS, 87*, 4917-4921.

Stankis, M. M., Specht, C. A., Yang, H., Giasson, L., Ullrich, R. C., & Novotny, C. P. (1992). The Aa mating locus of *Schizophyllum commune* encodes two dissimilar multiallelic homeodomain proteins. *PNAS, 89*, 7169-7173.

Stetler, G. L., & Thorner, J. (1984). Molecular cloning of hormone response genes from the yeast *Saccharomyces cerevisiae*. *PNAS, 81*(February 1984), 1144-1148.

Sugimoto, A., Iino, Y., Maeda, T., Watanabe, Y., & Yamamoto, M. (1990). *Schizosaccharomyces pombe* ste11+ encodes a transcription factor with an HMG motif that is a critical regulator of sexual development. *Genes and Development, 5*, 1990-1999.

Turra, D., El Ghalid, M., Rossi, F., & Di Pietro, A. (2015). Fungal pathogen uses sex pheromone receptor for chemotropic sensing of host plant signals. *Nature, 527*(7579), 521-524. doi:10.1038/nature15516

Vaillancourt, L. J., Raudaskoski, M., Specht, C. A., & Raper, C. A. (1997). Multiple Genes Encoding Pheromones and a Pheromone Receptor Define the B-beta 1 Mating-Type Specificity in *Schizophyllum commune*. *Genetics, 146*(541-551).

Van Nuland, A., Vandormael, P., Donaton, M., Alenquer, M., Lourenço, A., Quintino, E., . . . Thevelein, J. M. (2006). Ammonium permease-based

sensing mechanism for rapid ammonium activation of the protein kinase A pathway in yeast. *Molecular Microbiology, 59*(5), 1485-1505. doi:10.1111/j.1365-2958.2005.05043.x

Weber, I., Abmann, D., Thines, E., & Steinberg, G. (2006). Polar Localizing Class V Myosin Chitin Synthases Are Essential during Early Plant Infection in the Plant Pathogenic Fungus *Ustilago maydis. Plant Cell Online, 18*, 225-242.

Wendland, J., Vaillancourt, L. J., Hegner, J., Lengeler, K. B., Laddison, K. J., Specht, C. A., . . . Kothe, E. (1995). The mating-type locus Ba1 of *Schizophyllum commune* contains a pheremone receptor gene and putative pheromone genes. *The EMBO Journal, 14*(21), 5271-5278.

Wickes, B., Mayorga, M., Edman, U., & Edman, J. (1996). Dimorphism and haploid fruiting in *Cryptococcus neoformans*: Association with the alpha mating type. *PNAS, 93*, 7327-7331.

Wilkinson, L. E., & Pringle, J. R. (1974). Transient G1 arrest of *S. cerevisiae* cells of mating type alpha by a factor produced by cells of mating type a. *Experimental Cell Research, 89*(1), 175-187.

Wosten, H. A., Bohlmann, R., Eckerskorn, C., Lottspeich, F., Bolker, M., & Kahmann, R. (1996). A novel class of small amphipathic peptides affect aerial hyphal growth and surface hydrophobicity in *Ustilago maydis*. *EMBO, 15*, 4274-4281.

Xu, J., Saunders, C. W., Hu, P., Grant, R. A., Boekhout, T., Kuramae, E. E., & al, e. (2007). Dandruff-associated Malassezia genomes reveal convergent and divergent virulence traits shared with plant and human fungal pathogens. *PNAS, 104*(47), 18730-18735.

Yee, A. R., & Kronstad, J. W. (1993). Construction of chimeric alleels with altered specificity at the *b* incompatibility locus of *Ustilago maydis*. *PNAS, 90*, 664-668.

Yuan, J. S., Reed, A., Chen, F., & Steward, C. N. (2006). Statistical Analysis of real-time PCR data. *BMC Bioinformatics, 7*(85), DOI:10.1186/1471-2105-1187-1185.

Zhao, X., Kim, Y., Park, G., & Xu, J. R. (2005). A mitogen-activated protein kinase cascade regulating infection-related morphogenesis in . *Plant Cell, 17*(4), 1317-1329. doi:10.1105/tpc.104.029116

Zuther, K., Kahnt, J., Utermark, J., Imkampe, J., Uhse, S., & Schirawski, J. (2012). Host Specivicity of *Sporisorium reilianum* is tightly linked to Generation of the Phytoalexin Luteolinidin by *Sorghum bicolor*. *MPMI, 25*(9), 1230-1237.

APPENDIX

RNA Isolation Using Zymo Direct-zol RNA Mini Prep

1. Grow fungal cells on solid media for 48 hours. Scrape cells using metal spatula or plastic inoculating loop.

2. Before moving cells to frozen mortar and pestle, prepare the tubes for the entire extraction. Each extraction requires:

   2 2 mL flat-bottom tubes
   2 collection tubes (from the kit)
   1 column (from the kit)
   1 1.7 mL conical tube
   1 0.6 mL tube for preparation of DNase treatment

   One flat-bottom tube should be placed in the ice before grinding cells.

3. Using mortar and pestle frozen at -80°C, quick freeze cells and homogenize by grinding. For most samples grown on agar, the frozen equipment is capable of freezing the cells. For larger samples or plant tissues, liquid nitrogen may be used. Cells should be ground to a fine powder before water crystals begin to accumulate on the frozen apparatus. This usually requires three rounds of pouring in liquid nitrogen, allowing it to evaporate and grinding.

4. Using a frozen spatula, transfer no more than 100 mg of ground cells to the 2 mL flat bottom tube on ice. Keep the cells frozen until the next reagent is added. Add 600 µL of Trizol and vortex to mix until the Trizol is clear. Vortex time varies. For samples with more cells, it may take up to 5 minutes until the Trizol is clear. For samples with fewer cells, it may take less than 30 seconds. Once the Trizol is clear, avoid vortexing too long. Avoid the appearance of a white milky substance which indicates the sample has already started to degrade.

5. Spin the cell suspension at 12,000 rpm for 1 minute.

6. Remove the supernatant to a clean 2 mL flat bottom tube and avoid disturbing the cellular debris pellet (should be about 600 µL). Immediately add 600 µL 100% ethanol with a wide-bore tip and mix gently by pipetting. The formation of a white precipitate at this point may indicate too many cells were used for extraction and may clog the column.

7. Transfer approximately half (600 µL) of the extract in ethanol to the column inside one of the collection tubes. Spin at 14,000 rpm for 30 seconds.

8. Remove the spin column and carefully pour out the flow through. It is important to get rid of all the flow through so that it does not splash back up through the spin column and contaminate the specimen. This can be accomplished by banging the collection tube upside down on a paper towel. This should be done after every spin in the collection tube. Carefully return the column to the collection tube.

9. Repeat steps 7-8 for the remaining 600 µL of extract in ethanol.

10. After the second extraction, move the spin column to a new collection tube. Add 400 µL of RNA Wash Buffer to the membrane and spin for 30 seconds. Pour off the flow through and carefully return the spin column to the collection tube.

11. Add the DNase Digestion Solution to the column membrane and incubate at room temperate for 15 minutes. The solution should be prepared during the initial spins in a 0.6 mL tube as the enzyme has to be thawed.

    DNase Digestion Solution:

    75 µL DNase Digestion Buffer

    5 µL DNase-I Enzyme

12. Spin for 30 seconds at 14,000 rpm. Carefully remove the spin column from the collection tube and pour off the flow through. Return the spin column to the collection tube.

13. Add 400 µL of RNA Pre-Wash Buffer directly to the column membrane and spin for 30 seconds at 14,000 rpm. Carefully remove the spin column from the collection tube and pour off the flow through. Return the spin column to the collection tube.

14. Repeat step 13.

15. Add 700 µL RNA Wash-Buffer directly to the column membrane and spin for 2 minutes at 14,000 rpm. Carefully remove the spin column from the collection tube and pour off the flow through. Return the spin column to the collection tube.

16. Spin dry (without adding additional reagents) for 1 minute at 14,000 rpm. Remove the spin column from the collection tube, dispose of the collection tube, and move the spin column to the 1.7 mL conical tube. This will be the final storage location for the RNA.

17. Place tubes in hood open for 10 minutes to evaporate any residual ethanol.

18. Add 100 µL RNase/DNase Free Water directly to the column membrane. Incubate at room temperature for 1 minute.

19. Spin at 14,000 rpm for 1 minute. Remove the spin column and dispose. Place the RNA immediate only ice after spin. Keep it on ice as much as possible until it is frozen.

Assessing Quality and Quantity of RNA using NanoDrop

1. The NanoDrop is located in the Running Lab. Approximately 2 µL of RNA extract is necessary for quality and quantity assessment.

2. Blank the machine with sterile water.

3. Load 2 µL of RNA extract of the sample to the pedestal and measure. For RNA-Seq and other more stringent applications, 260/280 and 260/230 ratios must be >1.8. For cDNA synthesis, a similar purity is recommended although 260/230 ratios that are <1.8 are acceptable. 260/280 ratios should still be >1.8.

cDNA synthesis using Superscript III Reverse Transcriptase

1. Approximately 5 µg of RNA is necessary for a whole cDNA synthesis reaction. Depending on the volume of cDNA needed, half reactions can be done with 2.5 mg of RNA. If a half reaction is used, use half of the volumes indicated below.

2. Determine the volume of RNA sample needed to produce 5 µg. Transfer to a clean 0.6 mL thin-walled PCR tube. Dry in the Speed Vac on medium or low heat until all water has evaporated. Longer drying times can result in degraded RNA as can higher temperatures, so choose the combination that is likely to cause less degradation.

3. Resuspend the RNA pellet in 8 µL RNase/DNase Free water. Add 1 µL Oligo-dT. Incubate in the thermal cycler at 65°C for 5 minutes. Immediately after incubation, place on ice for at least one minute.

4. If multiple cDNA synthesis reactions are being done at the same time, a cocktail can be mixed of the following reagents, much like a cocktail for a regular PCR reaction. Accuracy is increased by adding each of the reagents one by one to each synthesis reaction.

10x Reaction Buffer	2 µL
$MgCl_2$	4 µL
DTT	2 µL
RNase Out	1 µL
dNTPs	1 µL

5. If multiple cDNA synthesis reactions are being done at the same time, add 10µL of the mix to each synthesis reaction. Quickspin the cocktail before aliquoting or quickspin each reaction before addition of enzyme. Add 1 µL of Superscript III Reverse Transcriptase to each reaction. AVOID QUICKSPINNING AFTER ENZYME ADDITION.

6. Incubate in a thermal cycler at 50°C for 50 minutes followed by enzyme deactivation by incubating at 85°C for 5 minutes.

7. Add 1 µL of RNase H to each cDNA synthesis reaction. RNASE H CAN BE HARMFUL TO FUTURE EXTRACTIONS SO AVOID ADDING IT IN THE AREA WHERE EXTRACTIONS ARE PERFORMED.

8. Incubate in a thermal cycler at 37°C for 20 minutes.

9. For downstream applications, the original cDNA synthesis reaction can be diluted. For regular PCR to determine if there is any genomic DNA still present, a 20-fold dilution of the synthesis mix is sufficient. For qRT-PCR, depending on expected transcript level of a particular target 6-fold to 12-fold dilution of the synthesis mix is appropriate.

CURRICULUM VITAE

NAME: Rena Margaret Wallen

ADDRESS: 919 Applegate Lane

Clarksville, IN 47129

PHONE: 502-210-0597

EMAIL: r.margaret.wallen@gmail.com

EDUCATION:

Vanderbilt University (1999-2002)

Bachelor of Science: Biology (partial)

Bachelor of Science: Psychology (partial)

University of Louisville (2005 – 2009):

Bachelor of Science: Biology

Bachelor of Science: Psychology

University of Louisville (2010 – 2012):

Master of Science in Biology, Thesis Option

University of Louisville (2012-2017)

Doctor of Philosophy in Biology

PUBLICATION

Wallen, R. M., & Perlin, M. H. (2012). A Tale of 6 Sigmas: How Changing Partners Allows Salmonella to Thrive in the Best of Times and Survive the Worst of Times. INTECH Open Access Publisher.

Agarwal, C., Aulakh, K. B., Edelen, K., Cooper, M., Wallen, R. M., Adams, S., ... & Perlin, M. H. (2013). Ustilago maydis phosphodiesterases play a role in the dimorphic switch and in pathogenicity. *Microbiology*, *159*(5), 857-868.

Paul, Jinny A. Wallen, R.M., Zhao,C, Shi, T, and Perlin, M.H.. Coordinate Regulation by Ammonium Transporters of *Ustilago maydis* Genes Involved in Mating and Pathogenicity (submitted for publication)

NATIONAL MEETING PRESENTATIONS

Wallen, R.M., et al. Transcriptional Regulation by the High Affinity Ammonium Transporter, Ump2, in *Ustilago maydis.* Presentation at the Kentucky Academy of Sciences, November, 2016

Wallen, R.M., Paul, J.A., Zhao, C., Shi, T., and Perlin, M.H. Coordinate Regulation of Ammonium Transporters and the *b* locus of *Ustilago maydis* of Genes Involved in Mating and Pathogenicity. Presentation at Fungal Genetics Conference, Asilomar, CA, March, 2015

TEACHING EXPERIENCE

Graduate Teaching Assistant

Introduction to Microbiology for Non-Majors

Fall 2012
Spring, Summer, Fall 2013
Spring, Summer 2014
Summer 2015
Summer 2016
Summer 2017

Introduction to Microbiology for Biology Majors

Fall 2014
Spring, Fall 2015
Spring, Fall 2016
Spring 2017

VOLUNTEER EXPERIENCE	Louisville Regional Science Fair Judge (March 2012 and March 2016)
AWARDS AND RECOGNTION	University of Louisville, Department of Biology, Furnish Teaching Award for Graduate Teaching Assistant, 2014
	University of Louisville, Department of Biology, Furnish Teaching Award for Graduate Teaching Assistant, 2017